

THE NATURE OF BINOCULAR INTERACTIONS IN DEVELOPMENTAL DISORDERS OF VISION

Thesis submitted to the university of Wales Cardiff by Stuart Faulkner in candidature
for a degree of Philosophiae Doctor

Department of Biological Sciences at University of Wales Cardiff

UMI Number: U203032

All rights reserved

INFORMATION TO ALL USERS

The quality of this reproduction is dependent upon the quality of the copy submitted.

In the unlikely event that the author did not send a complete manuscript and there are missing pages, these will be noted. Also, if material had to be removed, a note will indicate the deletion.



UMI U203032

Published by ProQuest LLC 2013. Copyright in the Dissertation held by the Author.
Microform Edition © ProQuest LLC.

All rights reserved. This work is protected against
unauthorized copying under Title 17, United States Code.



ProQuest LLC
789 East Eisenhower Parkway
P.O. Box 1346
Ann Arbor, MI 48106-1346

DECLARATION

This work has not previously been accepted in substance for any degree and is not being currently submitted in candidature for any degree

Signed Alan Fenton (candidate)

Date 30/11/04

STATEMENT 1

This thesis is the result of my own investigations, except where otherwise stated.

Other sources are acknowledged by footnotes giving explicit references. A bibliography is appended.

Signed Alan Fenton (candidate)

Date 30/11/04

STATEMENT 2

I hereby give consent for my thesis, if accepted, to be available for photocopying and for inter-library loan, and for the title and summary to be made available to outside organisations

Signed Alan Fenton (candidate)

Date 30/11/04

ACKNOWLEDGEMENTS

I would like to extend my deepest gratitude to my supervisor Frank Sengpiel for his never-ending support and enthusiasm, without which I would not have been able to visualise this thesis. My extended gratitude goes to Vasily Vorobyov for his technical expertise, patience and support throughout, in particular with single unit recordings. I thank Christopher Howarth and Laurent Watroba for their assistance with experiments. Extended thanks to all the staff from the animal house for their assistance. Many thanks to Brian Blais for his correspondence and expertise with computer modelling, David Bowker for statistical knowledge and Tim Jacobs for proof reading my thesis. Finally, many thanks and love to my family and close friends who have helped retain at least some of my sanity throughout.

This work was supported by the medical research council.

ABSTRACT

Sensory experience is known to shape the maturation of the cortical circuits during postnatal development. The two studies presented here emphasise the critical role for binocular vision in early cortical development and recovery from instances of early abnormal visual experience. If the prevailing hypothesis of competition between the two eyes for synaptic space in visual cortex (V1) were to stand, competition should be disrupted if geniculocortical afferents from the two eyes are spatially segregated. In kittens, with a strabismus induced in one eye before the onset of the critical period; the effects of a brief period of monocular deprivation (MD) at the height of the critical period and subsequent recovery were assessed in a longitudinal study employing optical imaging of intrinsic signals. Monocular deprivation caused a substantial loss of cortical territory dominated by the deprived eye in all animals. However, in the strabismic animals this loss was smaller than in the control group for the hemisphere contralateral to the deprived eye. When the deprived eye was re-opened, despite a rapid recovery of cortical territory in all kittens, kittens without strabismus prior to MD exhibited a greater rate of recovery from MD. Moreover, recovery of visual acuity, as assessed by visually evoked potential (VEP) measurements, was slower and less complete in animals with strabismus prior to MD than in those without. Therefore, strabismus does not provide lasting protection against the effects of MD. These findings are better explained by associative than by competitive mechanisms of synaptic plasticity.

A second study examined the degree of physiological recovery of the originally non-deprived eye (ONDE) after several reverse occlusion (RO) paradigms, which incorporated a period of binocular vision, was assessed by longitudinal studies of optical imaging of intrinsic signals. Two important physiological links underlying the changes in visual acuity that occurs during RO have been provided here. Firstly, recovery of ONDE ocular dominance (OD) territory was complete during recovery from RO in those animals that received an intermediate period of correlated binocular vision, but was disrupted in those animals that did not. Secondly, the orientation tuning width of single cells was significantly broader in the originally deprived eye (ODE) than the ONDE in animals that did not receive an intermediate period of correlated binocular vision.

Computer simulations accurately predicted the timing of events and outcome of some of the experimental paradigms in this thesis. However, the 'relative simplicity' of computer models highlights the importance of *in vivo* investigations into cortical plasticity.

ABBREVIATIONS

AIR	Automated image registration algorithms
Alpha CaMKII	Alpha Ca ²⁺ /calmodulin-dependent Protein kinase II
APV	2-amino-5-phosphonopentanoic acid
BCM	Bienenstock-Cooper-Munro
BD	Binocular Deprivation
BDNF	Brain Derived Neurotrophic Factor
BI	Binocularity Index
BOLD	Blood-oxygenation level dependent
BV	Binocular vision
CAMP	Cyclic Adenosine Monophosphate
CCD	Charged-coupled device
CO ₂	Carbon Dioxide
CRE	cAMP response element
CREB	cAMP/Ca ²⁺ response element binding protein
DR	Dark Reared
DE	Deprived eye
DOG	Difference of Gaussian
ECG	Electrocardiogram
EEG	Electroencephalogram
ERK	Extracellular-signal-regulated kinase
ERP	Evoked Response Potentials
FMRI	Functional magnetic resonance imaging
GABA	γ aminobutyric acid
HbO ₂	Oxy-haemoglobin
HWHH	Half width Half height
LE	Left eye
LDP	Long Term Depression
LGN	Lateral Geniculate Nucleus
LTP	Long Term Potentiation

MR	Magnetic resonance
MAP2	Microtubule-associated protein 2
mEPSC	Miniature excitatory post-synaptic current
MD	Monocular Deprivation
mRNA	messenger Ribosomal Nucleic Acid
NGF	Nerve Growth Factor
NDE	Non-deprived eye
NMDA	N-methyl-D-aspartate
NMDAR1	N-methyl-D-aspartate receptor 1
NT-3	Neurotrophin 3
NT-4	Neurotrophin 4
N ₂ O	Nitrous oxide
OD	Ocular Dominance
ODE	Originally deprived eye
ONDE	Originally non-deprived eye
OP	Opposite eye (Strabismus + MD)
OSI	Orientation Selectivity Index
O ₂	Oxygen
PCA'	Relative comparison of PCA rule
PET	Positron emission tomography
PKA	cAMP dependent protein kinase
P	Postnatal day
PCA	Principal component analysis
PP1	Protein phosphatase 1
RE	Right eye
rHB	Deoxyheomoglobin component
RO	Reverse Occlusion
ROI	Region of interest
SA	Same eye (Strabismus + MD)
STDP	Spike timing dependent plasticity
SynGAP	Synaptic GTP-ase-activating protein
TrkB	Receptor for BDNF
TTX	Tetrodotoxin

VEP	Visually evoked potential
V1	Visual Cortex
2-DG	2-deoxyglucose
4DBV	4-days binocular vision
4Ddeco	4-days de-correlated vision
θ_M	Modification threshold
τ	Memory constant
η	Learning rate

CONTENTS

Declaration	II
Acknowledgements	III
Abstract	III
Abbreviations	V-VII
List of contents	VIII-XIII
List of figures	XIV-XXV
List of tables	XVI
CHAPTER 1 – Introduction	1-46
<u>1.1 General introduction</u>	1
1.1.1 Anatomy of the visual system	1
1.1.2 Orientation /ocular dominance columns	8
1.1.3 Retinotopy	9
1.1.4 Time line of development of the visual system	12
1.1.5 Plasticity in V1	14
1.1.5.1 Critical period	14
1.1.6 Mechanisms of plasticity in the cortex	16
1.1.6.1 Neural correlates of plasticity	16
1.1.6.2 Molecular correlates of plasticity	24
1.1.7 Animal models of human disorders	26
1.1.7.1 Strabismus	26
1.1.8 Functional imaging of the brain	27
1.1.8.1 fMRI, PET and other techniques	29
1.1.8.2 Optical imaging	31
1.1.8.3 Sources of intrinsic signal	31
<u>1.9 General Methods</u>	37
1.1.9 Preparation	37
1.1.10 Data acquisition	38
1.1.11 Data compression	40
1.1.12 Image analysis	41
1.1.12.1 Mechanical and biological noise	41
1.1.12.2 Data analysis	43
1.1.12.3 Filtering	43

1.1.13 Secondary data analysis	44
1.1.13.1 Ocular dominance	44
1.1.13.2 Orientation selectivity ratio	44
<u>1.1.14 Aims and Objectives</u>	46
CHAPTER 2 – Strabismus and Monocular deprivation	47-124
<u>2.1 Introduction</u>	47
2.1.1 Ocular dominance	47
2.1.2 Orientation selectivity	51
2.1.3 Visually evoked potentials	53
2.1.4 Electrophysiological parameters	54
<u>2.2 Methods</u>	58
2.2.1 Strabismus/Monocular deprivation	58
2.2.2 Optical imaging	59
2.2.3 Electrophysiology	59
2.2.4 Visually evoked potentials	60
<u>2.3 Results</u>	61
2.3.1 Ocular dominance	61
2.3.1.1 Monocular deprivation	61
2.3.1.2 Strabismus prior to monocular deprivation	65
2.3.1.3 Divergent strabismus	73
2.3.1.4 Squint angle and ocular dominance	73
2.3.2 Orientation tuning	78
2.3.2.1 Monocular deprivation	78
2.3.2.2 Strabismus prior to monocular deprivation	82
2.3.2.3 Controls	88
2.3.3 Properties of single cells in V1 of normal, MD and S+MD animals	88
2.3.3.1 Normal rearing	92
2.3.3.2 Monocular deprivation	92
2.3.3.2 Strabismus and MD	96
2.3.4 Effects of monocular deprivation, and strabismus and monocular deprivation on visually evoked potentials	96
2.3.4.1 Effects of MD on acuity	97

2.3.4.2 Effects of strabismus and MD on acuity	97
2.3.4.3 Comparisons between MD and strabismus and MD on acuity	105
<u>2.4 Discussion</u>	108
2.4.1 Methodological considerations	108
2.4.2 Interpretation of results in light of BCM theory	111
2.4.3 Alternative explanations	112
2.4.4 Inter-hemispheric differences and deprivation	113
2.4.5 Recovery from the effects of MD	117
2.4.5 Recovery of responses according to BCM	120
2.4.6 Orientation selectivity: MD effects and recovery	122
CHAPTER 3 - Reverse occlusion	125-179
<u>3.1 Introduction</u>	125
3.1.1 Reverse occlusion and other paradigms	125
<u>3.2 Methods</u>	132
3.2.1 Electrophysiology and visually evoked potentials	133
<u>3.3 Results</u>	134
3.3.1 Ocular dominance	134
3.3.1.1 Immediate reverse occlusion	134
3.3.1.2 Four days binocular vision between the first period of MD and before RO	134
3.3.1.3 Four days of de-correlated vision between the first period of MD and before RO	138
3.3.2 Orientation selectivity	149
3.3.2.1 Immediate reverse occlusion	149
3.3.2.2 Four days binocular vision between the first period of MD and before RO	149
3.3.2.3 Four days of de-correlated vision between the first period of MD and before RO	152
3.3.3 Visual acuity	154
3.3.4 Electrophysiology	158
3.3.4.1 Immediate reverse occlusion	158
3.3.4.2 Four days binocular vision between the first period of MD and before RO	158

3.3.4.3 Four days of de-correlated vision between the first period of MD and before RO	159
<u>3.4 Discussion</u>	162
3.4.1 The effects of RO paradigms on the cortex and recovery from them	163
3.4.2 Anatomical considerations	166
3.4.3 Physiological considerations	169
3.4.4 Behavioural considerations	172
3.4.5 NMDA receptors and LTP	174
3.4.6 Different mechanisms for loss and recovery of cortical binocularity	177
CHAPTER 4 – Computer modelling for MD and S+MD	180-244
<u>4.1 Introduction</u>	180
4.1.1 Model neurone	180
4.1.2 Learning rules	181
4.1.3 Other learning rules	185
4.1.4 Parameters of Learning Rules	186
4.1.4.1 BCM neurone	186
4.1.4.2 PCA neurone	187
4.1.5 Comparing simulation with experiments	190
<u>4.2 Methods</u>	195
4.2.1 ‘Plasticity’ program	195
4.2.1.1 Stabilisation of BCM and PCA models	195
4.2.1.2 Qualitative parameters	196
<u>4.3 Results</u>	199
4.3.1 BCM model	199
4.3.1.1 Normal Rearing	199
4.3.2.1 Monocular Deprivation	203
4.3.3.1 Recovery from MD	205
4.3.4.1 Rearing with an image offset (“strabismus”) in one eye	205
4.3.5.1 Image offset (“strabismus”) and MD in different eyes	208
4.3.6.1 Recovery from MD with a preceding image offset (“strabismus”) in the different eyes	208

4.3.7.1 Image offset (“Strabismus”) and MD in the same eye	209
4.3.8.1 Recovery from image offset (“Strabismus”) and MD in the same eye	214
4.3.2 PCA model	214
4.3.2.1 Normal Rearing	214
4.3.2.2 Monocular Deprivation	217
4.3.2.3 Recovery from MD	217
4.3.2.4 Rearing with an image offset (“strabismus”) in one eye	217
4.3.2.5 Image offset (“strabismus”) and MD in different eyes	221
4.3.2.6 Recovery from MD with a preceding image offset (“strabismus”) in the different eyes	221
4.3.2.7 Image offset (“Strabismus”) and MD in the same eye	221
4.3.2.8 Recovery from Image offset (“Strabismus”) and MD in the same eye	225
4.3.3 Simulations with different offsets	225
4.3.3.1 Simulations with BCM learning	228
4.3.3.2 Simulations with PCA learning	231
4.3.4 Comparisons between BCM and PCA learning rules	232
<u>4.7 Discussion</u>	238
4.7.1 Convergence of responses with PCA and BCM learning during normal rearing	238
4.7.2 PCA and BCM learning rules with input offset	239
4.7.3 PCA and BCM learning with offset (“strabismus”) and MD	241
4.7.4 Biological basis of theoretical models	243
CHAPTER 5 - Computer modelling for RO paradigms	245-273
<u>5.1 Methods</u>	245
<u>5.2 Results</u>	246
5.2.1 BCM learning	246
5.2.1.1 Immediate reverse occlusion	246
5.2.1.2 Recovery from immediate RO	246
5.2.1.3 Four days of binocular vision between the first and second period of MD	251
5.2.1.4 Recovery from RO in 4DBV animals	251

5.2.1.5 Four days of de-correlated vision between first and second period of MD	251
5.2.6.1 Recovery from RO in 4Ddecor animals	257
5.2.2 PCA learning	257
5.2.2.1 Immediate reverse occlusion	257
5.2.2.2 Recovery from immediate RO	261
5.2.2.3 Four days of binocular vision between the first and second period of MD	261
5.2.2.4 Recovery from RO in 4DBV animals	261
5.2.2.5 Four days of de-correlated vision between first and second period of MD	261
5.2.2.6 Recovery from RO in 4Ddecor animals	267
5.2.2.7 Comparisons of 'relative' timing between BCM and PCA learning rules	267
<u>5.3 Discussion</u>	270
5.3.1 Early monocular deprivation	270
5.3.2 Immediate reverse occlusion with BCM and PCA learning	271
5.3.3 Intermediate period of vision between the first period of MD and RO in BCM and PCA learning	271
5.3.4 Comparisons of the relative timing between BCM and PCA learning	272
5.3.5 Limitations of simulations	273
CHAPTER 6 - General discussion	275-279
<u>6.1 General discussion</u>	275
6.1.1 Clinical implications	277
6.1.2 Where next?	278
<u>6.2 Bibliography</u>	280-315
<u>6.3 Appendix I - Figures</u>	316
<u>6.4 Appendix II - Publications</u>	317

LIST OF FIGURES

1.1	Photoreceptors within the retina.	2
1.2	Diagram of the projections from the retina to the lateral geniculate nucleus (LGN) and visual cortex.	3
1.3	Receptive field of retinal ganglion cells.	4
1.4	Representation of the visual field in the optic nerves and tracts.	6
1.5	Macaque ^(A) and Cat ^(A) Lateral Geniculate Nucleus.	7
1.6	Cytochrome Oxidase stain of a coronal section of macaque visual cortex.	7
1.7	Ice cube model of the cortex.	10
1.8	Ocular dominance columns of the macaque ^a and cat ^b visual cortex.	10
1.9	Neighbouring points in the visual cortex represent neighbouring points in visual space.	11
1.10	Timeline of development of the cat visual system.	15
1.11a	Darkfield autoradiographs of visual cortex in kittens aged 2,3,5.5 and 13 weeks of age.	15
1.11b	Ocular dominance distribution of visual cortex in a normal adult cat ^a (left) and a kitten monocularly deprived for 2-3 months ^b (right).	19
1.12	Two contrasting theories of synaptic plasticity in visual	21

cortex.

1.13a	Modification threshold controlling synaptic plasticity	23
1.13b	BCM synaptic modification function. Function $\theta(c, \theta_m)$ as a function of c .	23
1.14	Ocular dominance distribution in cat V1 with strabismus.	28
1.15	The temporal and spatial resolution of methods for the study of brain function.	32
1.16	Time course of the mapping component of the intrinsic signal.	34
1.17	Ocular dominance map (left eye verses right eye) of kitten (842N) visual cortex.	36
1.18	Angle maps of kitten (842) visual cortex.	36
1.19	Polar maps of kitten (842) visual cortex.	36
1.20	Titanium chamber used in optical imaging.	39
1.21	Experimental set-up for optical imaging.	39
1.22	Reference frame recorded from cat visual cortex.	42
1.23	Unfiltered ocular dominance map from visual cortex.	42
1.24	Ocular dominance map of visual cortex.	42
2.1	The ϕ function at 5 values of the modification threshold, θ_m .	50

2.2	Dural VEPs recorded from kitten V1 at P34.	55
2.3	Comparison of contrast sensitivity for normal and strabismic eyes obtained behaviourally (A, B) and electrophysiologically (C, D) for 2 kittens.	56
2.4	VEPs through each eye of a normal and monocularly deprived cat, elicited by 1Hz square wave contrast reversal.	57
2.5a	Cortical ocular dominance and orientation selectivity in the non-deprived (LE) of a kitten before and after monocular deprivation.	62
2.5b	Cortical ocular dominance and orientation selectivity in the deprived (RE) in a kitten before and after monocular deprivation.	63
2.6 a, b	Cortical ocular dominance before in a kitten before and after monocular deprivation.	64
2.6 c	Ratio of DE:NDE of cortical orientation selectivity in a kitten before and after monocular deprivation.	80
2.7a	Effects of strabismus and MD on ocular dominance and orientation selectivity in the non-deprived (LE).	66
2.7b	Effects of strabismus and MD on ocular dominance and orientation selectivity in the deprived (RE).	67
2.7c	Single condition orientation activity maps for NDE and DE of cortex in a strabismic animal immediately after deprivation.	82
2.8 a, b	Cortical ocular dominance before in a strabismic kitten before	68

and after monocular deprivation.

2.8c	Ratio of DE:NDE of cortical orientation selectivity in a strabismic kitten before and after monocular deprivation.	83
2.9a	Cortical ocular dominance and orientation selectivity in the non-deprived (RE) of a strabismic kitten before and after monocular deprivation.	70
2.9b	Cortical ocular dominance and orientation selectivity in the deprived (LE) of a strabismic kitten before and after monocular deprivation.	71
2.10 a, b	Cortical ocular dominance before in a strabismic kitten before and after monocular deprivation.	72
2.10 c	Ratio of DE:NDE of cortical orientation selectivity in a strabismic kitten before and after monocular deprivation.	85
2.11 a, b	Cortical ocular dominance before in a strabismic kitten before and after monocular deprivation.	74
2.12	Summary of cortical area occupied by the deprived eye in each hemisphere imaged in experimental animals.	75-76
2.13	Relationship between ocular dominance and squint angle in kittens made strabismic prior to monocular deprivation.	77
2.14	Examples of an iso- orientation domain and pinwheel centre in kitten V1.	79
2.15	Summary of DE:NDE orientation selectivity index (OSI) in each hemisphere imaged.	86-87

2.16a	Optical imaging maps of ocular dominance and corresponding ocular dominance values over the experimental period in a normal animal.	89
2.16b	Summary of ocular dominance in 3 normal kittens.	90
2.17	Summary LE:RE orientation selectivity index (OSI) for 3 normal kittens.	91
2.18a	Ocular dominance histogram of 93 cells recorded from kitten visual cortex that received normal visual experience.	93
2.18b	Ocular dominance histogram of 77 cells recorded from kitten visual cortex that received a period of monocular deprivation from P35-45 followed by several weeks of binocular recovery.	93
2.18c	Ocular dominance histogram of 60 cells recorded from kitten visual cortex, that received a strabismus prior to a period of monocular deprivation followed by 3 weeks of binocular recovery.	94
2.18d	The binocular indices for normal, MD and S+ MD kittens after an extended period of recovery.	95
2.19	Average visual acuity in both eyes for kittens monocularly deprived for 10 days.	98
2.20	Time series of visually evoked potentials for both eyes before, immediately after MD and during recovery.	99-103
2.21a	Average visual acuity based on VEP cut-offs, in both eyes for kittens made strabismic and monocularly deprived in different eyes.	106

2.21b	Average response amplitude of visually evoked potentials in both eyes for kittens made strabismic and monocularly deprived in different eyes.	107
3.1	Profile of the sensitive period for monocular deprivation (and reverse occlusion) in kittens.	127
3.2a	Changes in visual acuity in 2 kittens after 18 days reverse occlusion, which had previously received monocular deprivation (from natural eye opening) imposed at 5 weeks of age.	128
3.2b	Changes in visual acuity of a monocularly deprived kitten following termination of 12 weeks reverse occlusion, which was imposed at 4 weeks of age.	128
3.3a	Effects of reverse occlusion on ocular dominance and orientation selectivity in the originally non-deprived (LE).	135
3.3b	Effects of reverse occlusion on ocular dominance and orientation selectivity in the originally deprived (RE).	136
3.4 a, b	Cortical ocular dominance in a kitten after reverse occlusion.	137
3.4c	Ratio of ONDE:ODE of cortical orientation selectivity in a kitten after reverse occlusion.	150
3.5a	Effects of a brief period of binocular vision between a period of monocular deprivation and RO on ocular dominance and orientation selectivity in the originally non-deprived (LE).	139
3.5b	Effects of a brief period of vision between a period of monocular deprivation and RO on ocular dominance and	140

orientation selectivity in the originally deprived (RE).

3.5c	Effects of early MD followed by 4DBV on ocular dominance and orientation selectivity in the non-deprived (top) and deprived (bottom) eye.	141
3.6 a, b	Cortical ocular dominance in a kitten with an intermediate period of binocular vision between the first period of monocular deprivation and before reverse occlusion.	142
3.6c	Ratio of ONDE:ODE of cortical orientation selectivity in a kitten with an intermediate period of binocular vision after the first period of monocular deprivation and reverse occlusion.	151
3.7a	Effects of a brief period of de-correlated vision between a period of monocular deprivation and RO on ocular dominance and orientation selectivity in the originally deprived (RE).	143
3.7b	Effects of a brief period of de-correlated vision between a period of monocular deprivation and RO, on ocular dominance and orientation selectivity, in the originally non-deprived (LE).	144
3.8 a, b	Cortical ocular dominance in a kitten with an intermediate period of de-correlated vision between the first period of monocular deprivation and before reverse occlusion.	145
3.8c	Ratio of ONDE:ODE of cortical orientation selectivity in a kitten with an intermediate period of de-correlated vision after the first period of monocular deprivation and before reverse occlusion.	153
3.9	Summary of cortical area occupied by the deprived eye in	147-148

each hemisphere imaged in kittens reared with one of the 3 RO paradigms.

3.10	Summary of ONDE:ODE orientation selectivity index (OSI) in each hemisphere imaged for kittens reared with one of the 3 reverse occlusion paradigms.	155-156
3.11	Summary data of recovery of visual acuity in animals with 4 days of de-correlated vision.	157
3.12	Ocular dominance distribution of single cells recorded from kitten V1 after extended recovery in RO, 4DBV and 4Ddecorr animals.	160
3.13	The binocular indices for Normal, RO, 4DBV and 4Ddecorr kitten after an extended period of recovery.	161
4.1	The sigmoid function of a model neurone.	182
4.2	Effects of parameters on the development of the one-dimensional neurone.	188
4.3	Input environment to retinally processed images.	189
4.4	Examples of PCA simulation of various simulation paradigms.	191
4.5	Examples of BCM simulation of various simulation paradigms.	191
4.6	The effects of noise from the closed eye on the disconnection of the closed eye in MD.	192

4.7 a, b	'Plasticity' programme -example of main screenshot of BCM (top) and PCA (bottom) learning at time (t) = few seconds.	197
4.8a	Example of screenshot from BCM learning at time (t)= 6hrs.	201
4.8b	Example of screenshot from BCM learning at time (t)= P21.	202
4.8c	Example of screenshot from BCM learning at time (t)= P10+MD for 20 iterations.	204
4.8d	Simulation of MD run with 1 iteration per display epoch.	204
4.9a	Example of screenshot from BCM learning at time (t)= P45.	206
4.9b	Example of screenshot from BCM learning (at time (t)= P46) showing 24 hours recovery from MD (RE).	207
4.10a	Example of screenshot from BCM learning (at time (t)= P35) with a 16 pixel offset in RE up to P35.	210
4.10b	Example of screenshot from BCM learning (at time (t)= P45) with a 16 pixel offset in RE followed by MD in LE.	211
4.10c	Example of screenshot from BCM learning (at time (t)= P59) with 14 days of binocular recovery, after an offset in RE and monocular deprivation in LE.	212
4.10d	Example of screenshot from BCM learning (at time (t)= P74) with 29 days of binocular recovery, after an offset in RE and monocular deprivation in LE.	213
4.11a	Example of screenshot from BCM learning (at time (t)= P45) with a 16 pixel offset in RE followed by MD in LE.	215

4.11b	Example of screenshot from BCM learning (at time (t)= P81) with a 16 pixel offset in RE followed by MD in RE.	216
4.12a	Example of screenshot from PCA learning at t=P21.	218
4.12b	Example of screenshot from PCA learning (at time (t)= P45) with MD in the RE.	219
4.12c	Example of screenshot from PCA learning (at time (t)= P45 +12hrs) with MD in the RE P35-P45 then binocular recovery for 12 hrs.	220
4.13a	Example of screenshot from PCA learning (at time (t)= P35) with large offset in the RE.	222
4.13b	Example of screenshot from PCA learning (at time (t)= P45) with large offset in the RE up to P35 then 10 days of deprivation.	223
4.13c	Example of screenshot from PCA learning (at time (t)= P48) with large offset in the RE up to P35, 10 days of deprivation in the LE then 3 days of binocular recovery.	224
4.14a	Example of screenshot from PCA learning (at time (t)= P45) with large offset in the RE up to P35, 10 days of deprivation in the RE.	226
4.14b	Example of screenshot from PCA learning (at time (t)= P48) with large offset in the RE up to P35, 10 days of deprivation in the RE, then 3 days of binocular recovery.	227
5.1a	State of BCM model simulation after MD in RE P14-P35.	247

5.1b	State of BCM model simulation after 3 days (out of 18) of RO.	248
5.1c	State of BCM model simulation after 18 days RO.	249
5.1d	State of BCM model simulation after; 18 days RO, then 24hrs of binocular recovery.	250
5.2a	State of BCM model simulation after; 4DBV followed by 18 days RO.	252
5.2b	State of BCM model simulation after; 4DBV followed by 18 days RO, then 24hrs of recovery.	253
5.3a	State of BCM model simulation after; 4Ddecorr followed by 3 (of 18) days RO.	254
5.3b	Example of screenshot from BCM learning at time (t)= P57 after 4Ddecorr vision, the 18D RO.	255
5.3c	State of BCM model simulation after; 4Ddecorr followed by 18 days RO, then 36hrs binocular recovery.	256
5.4a	State of PCA model simulation after 6hrs of RO.	258
5.4b	State of PCA model simulation after 18 days of RO.	259
5.4c	State of PCA model simulation after; 18 days of RO, then 12hrs of binocular recovery.	260
5.5a	State of PCA model simulation after; 4DBV, then 18 days of RO.	262

5.5b	State of PCA model simulation after; 4DBV, 18 days of RO, then 12hrs of binocular recovery.	263
5.6a	State of PCA model simulation after 4Ddecorrelated vision.	264
5.6b	State of PCA model simulation after; 4Ddecorrelated vision, then 18D RO.	265
5.6c	State of PCA model simulation after; 4Ddecorrelated vision, then 18D RO, then 12hrs of binocular recovery.	266
AppI (i)	Presumed assembly of proteins found in the NMDA receptor complex.	316

LIST OF TABLES

1	Summary of simulations with BCM learning with varying image offsets before and after deprivation in the same or opposite eye.	229
2	Summary of simulations with PCA learning with varying image offsets before and after deprivation in the same or opposite eye.	234
3	Comparison of loss and recovery times of the DE in BCM and PCA learning during simulation and that seen in experiments from the literature.	240
4	Comparison of loss and recovery times of the ODE and ONDE in BCM and PCA learning during simulation and that seen in experiments from the literature (RO)	268

CHAPTER 1

GENERAL INTRODUCTION

The structure and function of the primary visual cortex (area V1) has become one of the most extensively studied areas of the mammalian central nervous system. Much of the early work by Hubel and Wiesel opened the door for a plethora of research into the development of V1 with respect to the segregation of inputs from the two eyes into ocular dominance columns and to orientation selectivity.

Anatomy of the visual system

The visual system is the most complex of all the sensory systems. Visual perception occurs in two stages. Firstly, the cornea and the lens focus light entering the eye. It passes through the eye cavity (the vitreous humor) and projects onto the back of the eye (the retina) where it is transduced into electrical signals by photoreceptors (Fig. 1.1). Secondly, these signals are then sent through the optic nerve to visual centres in the brain for processing further (Fig. 1.2).

More precisely, once light has been converted into an electrical signal at the retina, the signal is propagated (continues away from the retina) via the ganglion cells. Axons of the ganglion cells form the optic nerve, which projects to the lateral geniculate nucleus (LGN) and superior colliculus. Ganglion cells respond continuously (spontaneous activity) with light levels regulating the firing rate. Each cell responds to light falling on a specific area of the retina, the so-called 'receptive field'. Ganglion cell receptive fields are circular, and consist of a centre and an antagonistic surround. There are two different types, allowing for processing of visual information in two parallel pathways. The firing rate of ON-centre cells is enhanced when light falls on the centre of the receptive field and is suppressed when light falls on the surround. Conversely, OFF-centre cells' firing rate is inhibited by light on the centre of the receptive field but enhanced in the surround (Fig. 1.3). These two different processing pathways allow the visual system to detect rapid changes in the visual image and objects that contrast weakly with their backgrounds, i.e. edge detection. The visual system also analyses other aspects of the visual image, such as colour, form and movement. A majority of ganglion cells in the primate retina fall into two main groups, M and P cells. M cells have large receptive fields and are primarily involved in recognition of gross features and movement of a stimulus. The

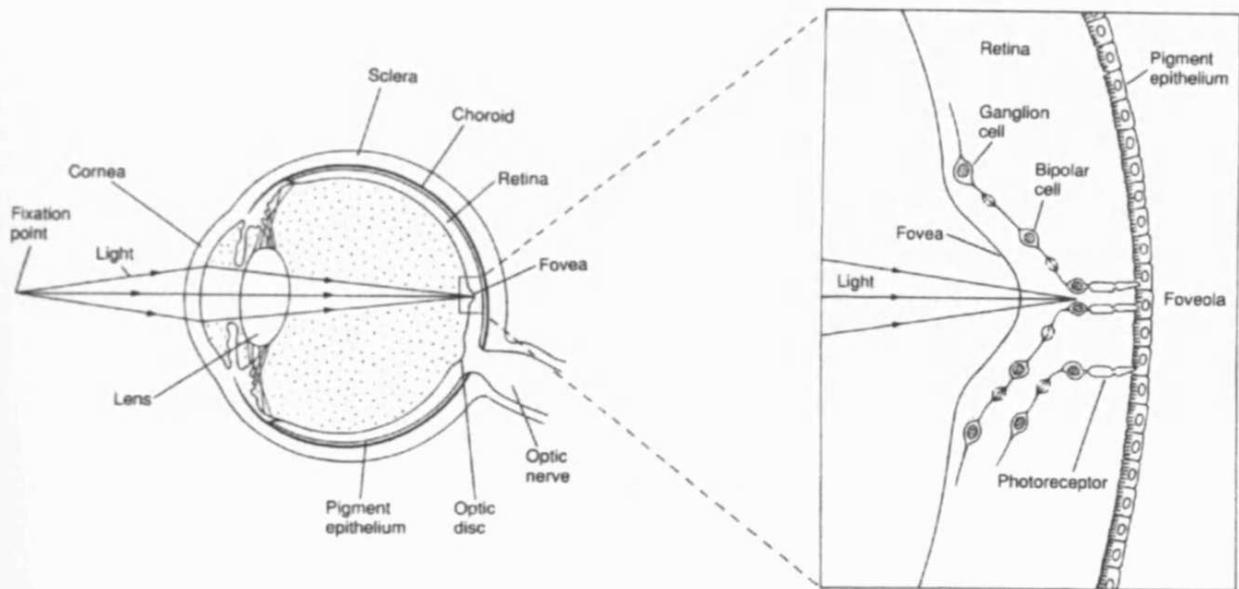


Figure 1.1 Photoreceptors within the retina (From Kandel *et al* 1991)

The passage of light through the eye to reach the retina (left). Detail of the retina at the fovea (right). Light passes through the eye and hits the back of the retina. At the fovea the cell bodies of the proximal retinal neurons are shifted to one side to allow light a direct (least distorted) pathway to the photo receptors.

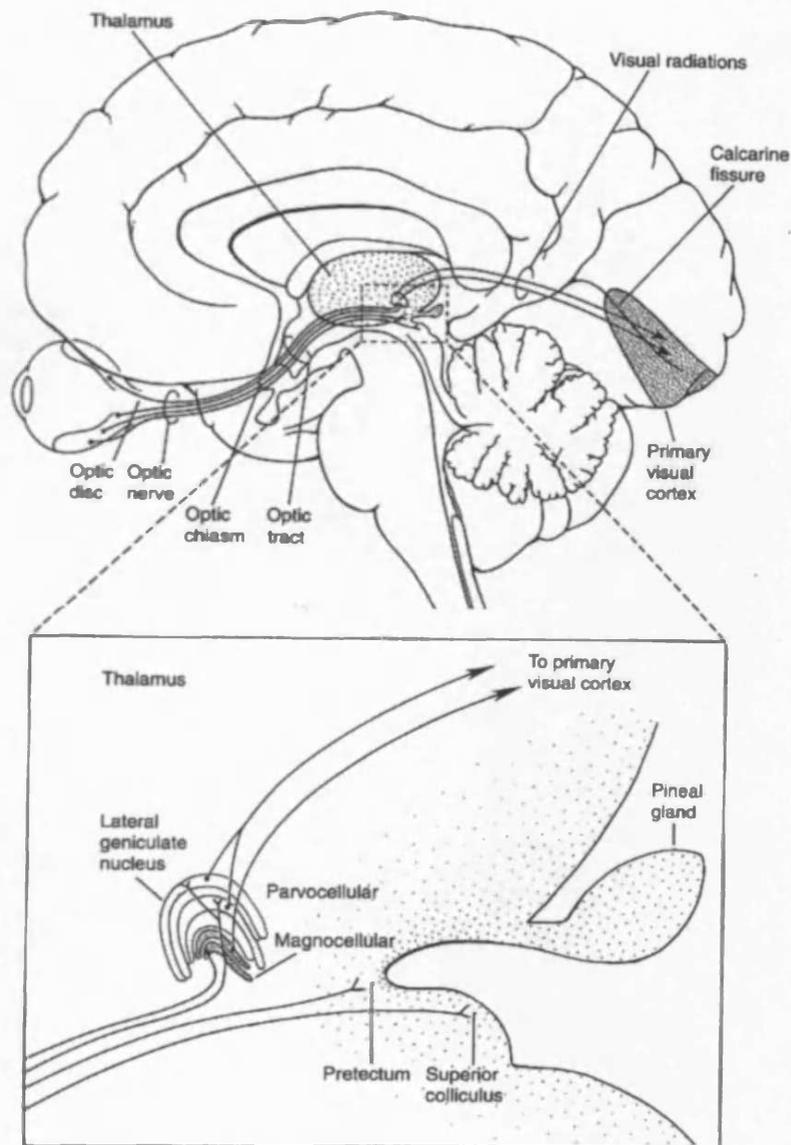


Figure 1.2 Diagram of the projections from the retina to the lateral geniculate nucleus (LGN) and visual cortex (Adapted from Kandel *et al* 1991)

Axons from retinal ganglion cells converge in the optic disk and form the optic nerve. This projects to the optic chiasm where fibers from each eye form into optic tracts. The optic tracts project to the lateral geniculate nucleus (LGN) and from there to the visual cortex.

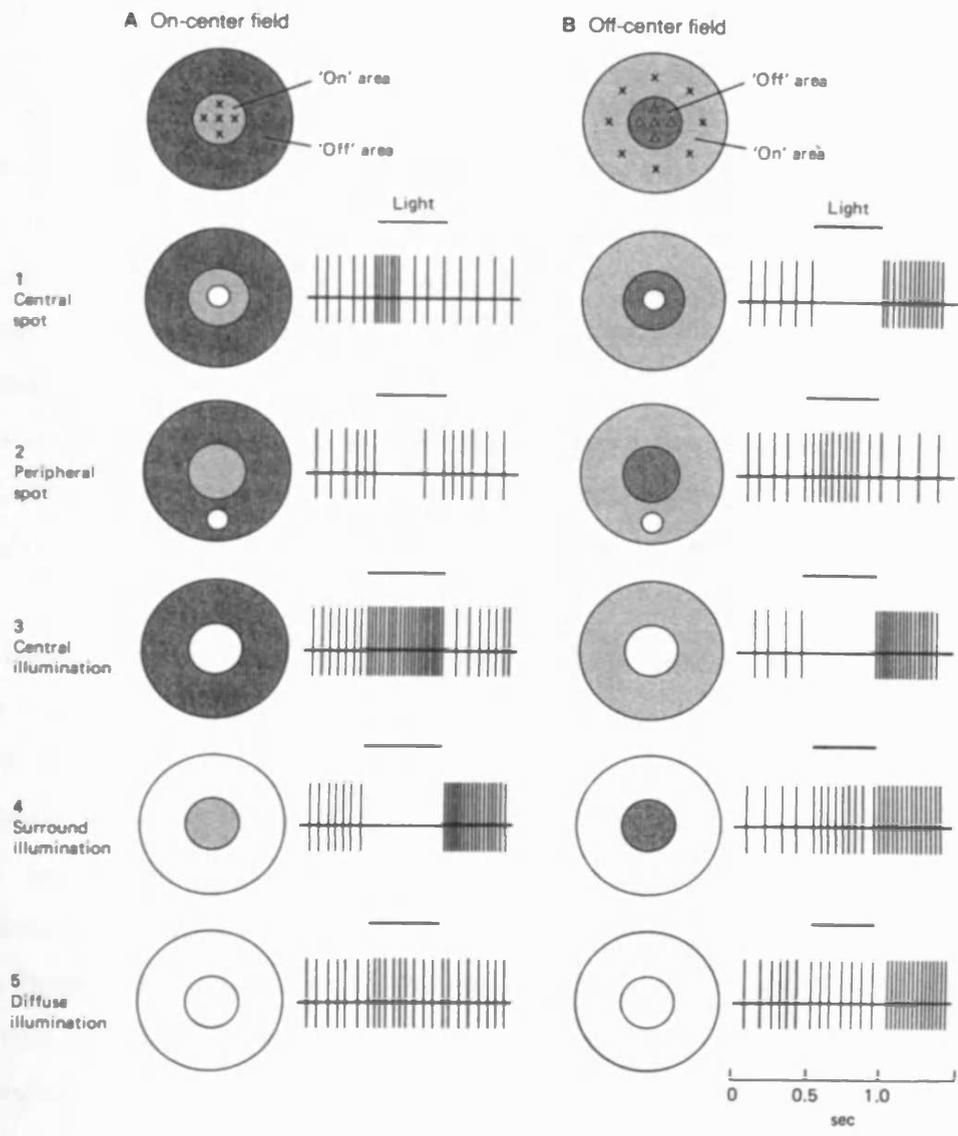


Figure 1.3. Receptive field of retinal ganglion cells (adapted from Kandel *et al* 1991)

Responses of both types of cells to different stimuli (white portion of the receptive field). Grey area is 'ON' area and black is 'OFF' area. The pattern of action potentials in response to each stimulus is shown in extracellular recording.

●**ON-center cell**

These type of cells are excited when stimulated by light in their centre and inhibited when stimulated in their surround.

●**OFF-center cell**

These cells are excited when stimulated by light in the surround and inhibited when simulated in their center.

smaller and more numerous P cells have smaller receptive fields and are wavelength selective, therefore, are involved in resolving finer detail and colour vision.

The optic disk is the exit point for retinal ganglion cell axons, which combine to form the optic nerve. The optic nerves from the left and right eyes meet anterior to the pituitary gland to form the optic chiasm. Here, axons from the nasal half of each retina cross over to the opposite side of the brain, whereas axons from the temporal hemiretina do not (Fig. 1.4). The optic tracts on each side finally project to three subcortical regions (Fig. 1.1). The pretectal area of the midbrain controls pupillary reflexes and the superior colliculus controls saccadic eye movements. However, the lateral geniculate nucleus (LGN) is the major target of retinal axons; the projection to the LGN and on to the primary visual cortex (V1) constitutes the so-called *primary visual pathway*.

The lateral geniculate nucleus of macaques and humans is arranged in six layers. Input from the two eyes is kept separate. Ipsilateral eye axons synapse on layers 2, 3, and 5, while contralateral eye axons synapse on layers 1, 4, and 6 (Fig. 1.5a). Furthermore, P-type retinal ganglion cells project to the dorsal (3-6) parvocellular LGN layers, while M-type ganglion cells project to the ventral (1 and 2) magnocellular LGN layers. The LGN of the cat has only 3 laminae, A, A1 and C (Fig. 1.5b). Input from the contralateral eye terminates in laminae A and C, while ipsilateral eye input terminates predominately in A1, with some 'patchy' input in C. A majority of ganglion cells in the cat retina fall into two main groups, X and Y cells. The X and Y cell pathways in cats form parallel systems from the retina to the visual cortex. Axons of the small, X-cells innervate lamina A or A1. Y-cells innervate laminae C and A - from the contralateral retina and laminae A1 - from the ipsilateral retina (Sur *et al* 1982). In response to flashed stimulus, the larger, Y cells exhibit larger, more transient responses than X cells. Higher spatial frequency stimuli preferentially stimulate X cells, where as Y cells respond better to lower spatial frequencies (Derrington and Fuchs 1979). Due to their response properties, X cells are likely to be involved in analysis of detailed vision, while Y cells involved in more basic analysis of form vision and detection of motion (Sherman 1979).

In the 1960's Hubel and Wiesel discovered that neurons in the LGN have very similar receptive fields as those found in the retina. They also consist of ON-centre and OFF-centre cells.

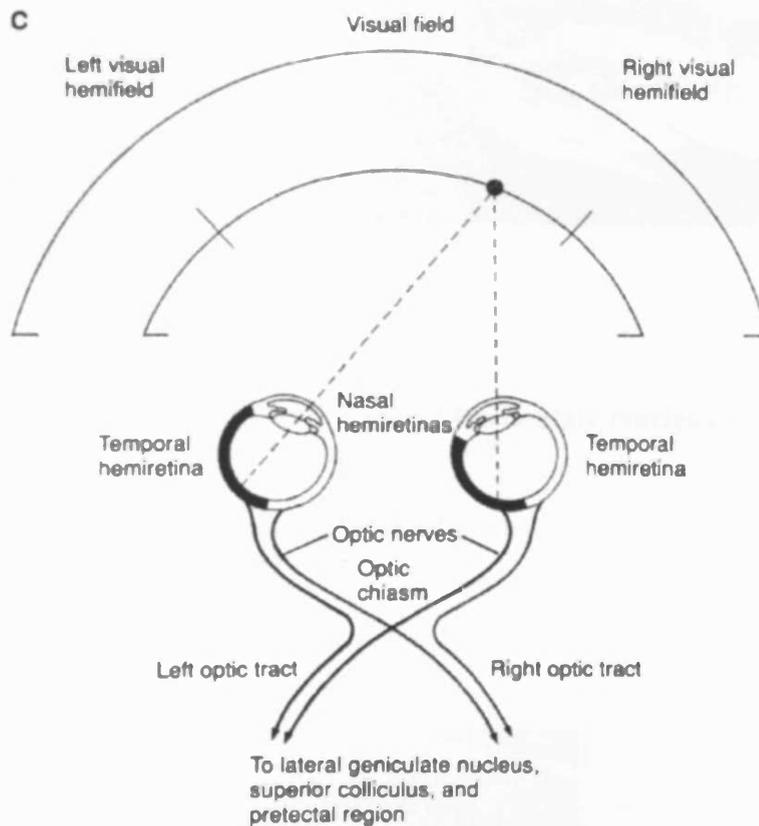


Figure 1.4 Representation of the visual field in the optic nerves and tracts (Adapted from Kandel *et al* 1991)

Fibers from the nasal hemiretina of each eye cross to the opposite side of the optic chiasm, whereas fibers from the temporal hemiretina do not cross.

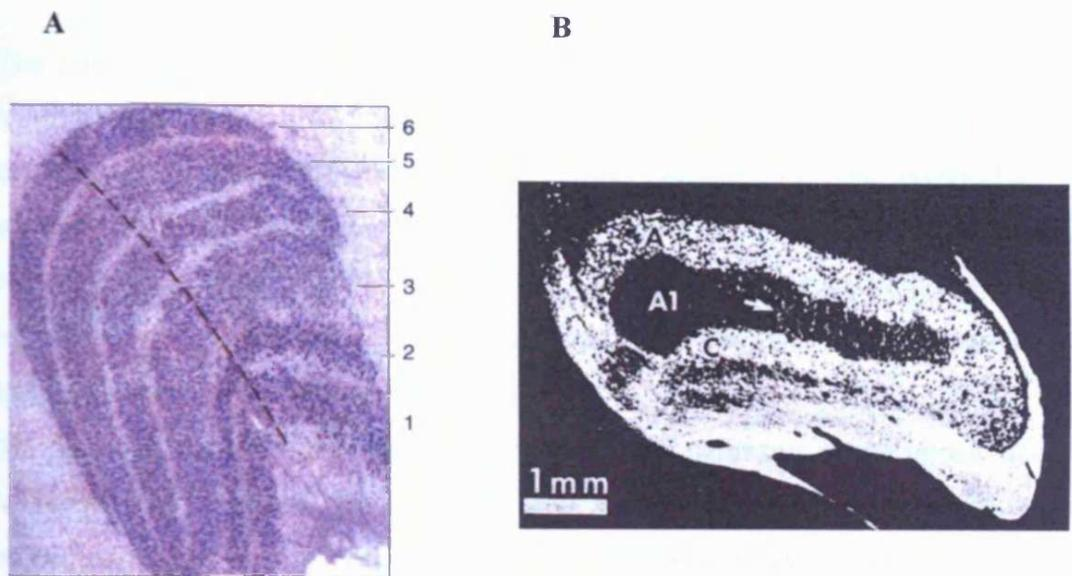


Figure 1.5 Macaque ^(A) and Cat ^(B) Lateral Geniculate Nucleus (LGN) (in Bear *et al* 1996:Adapted from Hubel 1988^A, Shatz *et al* 1977^B)

A The macaque LGN has 6 clearly segregated layers.
B The feline LGN has just 3 layers.

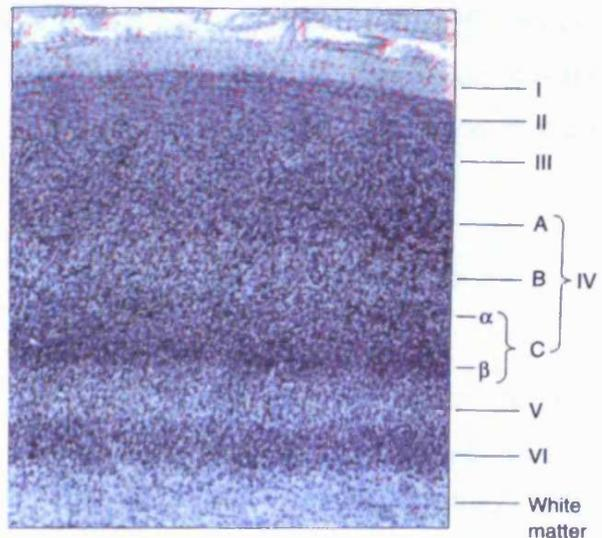


Figure 1. 6 Cytochrome Oxidase stain of a coronal section of macaque visual cortex (in Bear *et al* 1996 (Adapted from Hubel 1988))

The primary visual cortex has 6 distinct layers. Most LGN afferents terminate in layer IV. Axons from parvocellular layers terminate in layer IV β while axons from magnocellular layers terminate in IV α .

The primary visual cortex (V1) is located in the occipital lobe of the mammalian brain. Most of primate V1 lies on the medial surface of the hemisphere surrounding the calcarine fissure (Fig. 1.2). Macaque V1 consists of 6 main layers (Fig. 1.6) with further distinct sub-layers in layer IV (IVA, IVB and IVC). Axons from the LGN terminate in several different layers of the primary visual cortex, with a majority in layer IVC. Parvocellular LGN neurones project to layer IVC β , while magnocellular LGN neurones project to layer IVC α .

The parvocellular pathway splits into two separate pathways in the upper layers of V1: blobs and inter-blobs (aptly named after staining with the mitochondrial enzyme cytochrome oxidase in superficial layers of V1, which shows up as dark patches or 'blobs'). These blobs are more sensitive to colour and brightness, whereas the surrounding 'interblob' regions respond to stimuli of a particular orientation.

In the primary visual cortex receptive field properties change considerably (compared to retina and LGN). Whereas before cells had circular receptive fields, cells in V1 respond best to bars of light and therefore have approximately rectangular receptive fields. The cells fall into two categories, simple and complex cells. Simple cells have spatially separate, antagonistic ON/OFF zones. Complex cells have larger receptive fields than simple cells with overlapping ON/OFF zones, so the position of the bar within the field is less important for the magnitude of response (Hubel 1959; Hubel and Wiesel 1962). However, the axis of orientation of the stimulus is critical just like for simple cells.

Orientation /ocular dominance columns

There are two key properties that characterise neurons in the primary visual cortex: binocularity and orientation selectivity. Single cell recordings by Hubel and Wiesel (1962) found that groups of cells responded preferentially or solely to one eye, and quickly changed to responding to the other eye when the recording electrode was advanced tangentially through the cortex. This led to the hypothesis that groups of cells responding preferentially to one eye or the other formed a regular columnar pattern – ocular dominance columns. Hubel and Wiesel (1962) made a similar observation for the orientation preference of cells, which also appeared to change

gradually from cell to cell, suggesting a columnar fashion. These results set up the next decade of research in which anatomical data, using horseradish peroxidase and de-oxyglucose uptake into V1 cells, showed clear OD columns in macaque layer 4 (Hubel and Wiesel 1972). Labelling of geniculocortical afferents using eye injection of ^3H -proline showed a similar, but more patch-like network of label in layer 4 of cat visual cortex, corresponding to OD columns (LeVay *et al* 1978). Neurones with similar specificity with respect to ocular dominance (OD) and preferred orientation are grouped into columns, running perpendicular to the cortical surface through all six layers (Fig. 1.7).

Prior to the development of optical imaging techniques, the hypothesis of a perpendicular relationship between ocular dominance columns and orientation columns (Hubel & Wiesel 1972, 1974, 1977; Hubel *et al* 1978; Löwel *et al* 1988; Blasdel 1992) could not be verified with certainty. Optical imaging allowed the orientation preference and ocular dominance maps to be visualised in their entirety (within the accessible part of V1). In the monkey striate cortex, ocular dominance columns are spatially related with orientation domains, with iso-orientation lines intersecting OD column borders at close to right angles (Obermayer and Blasdel 1993; Blasdel 1995). Studies by Hubener *et al* (1997) show a very similar architecture in the cat's visual cortex despite a more irregular layout of ocular dominance columns. (Fig.1.8). Several studies have shown that there is also a weak relationship between ocular dominance columns and spatial frequency domains (blobs) in cats (Dyck and Cynader 1993; Murphy *et al* 1995; Shoham *et al* 1997), although in macaques this relationship is stronger (Hendrickson *et al* 1981; Horton & Hubel 1981; Horton 1984).

Retinotopy

Since the primary visual cortex receives orderly input from the LGN, a retinotopic organisation of V1 follows, i.e. neighbouring points on the cortex represent neighbouring points in visual space (Fig. 1.9). However, this is only true on a global scale. There are many local distortions in the retinotopic map. The fovea contains the highest proportion of neurones. Although a very small region of the visual field (~ 4 deg.), it has the largest proportion of cortical surface dedicated to it, hence visual

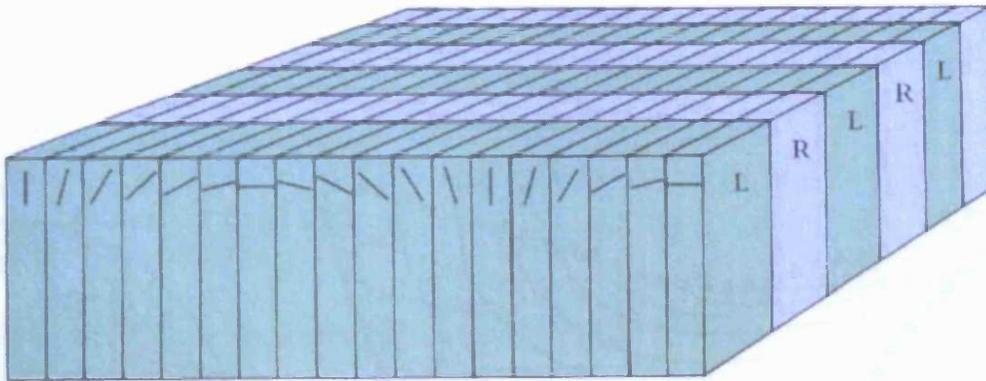
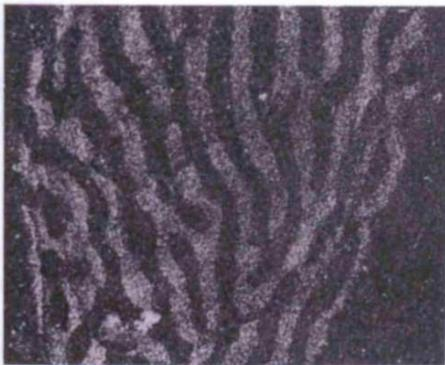


Figure 1.7 Ice cube model of the cortex (Adapted from Hubel, 1988)

Neurons with similar receptive fields are organized into columns of cells running perpendicular to the cortical surface. Each column contains cells with identical axis of orientation. Sequential *orientation columns* change in axis of orientation in an orderly fashion across the cortical surface. Groups of cells preferentially responding to either eye form into *ocular dominance columns*. Eye preference changes in an orderly fashion over the surface of the cortex. A complete cycle of orientations is present within each ocular dominance column.

A



B



Figure 1.8 Ocular dominance columns of the macaque^A and cat visual cortex^B
 ((in Bear *et al* 1996: Adapted from LeVay *et al* (1980)^A Kitten 513^B)

A Autoradiograph of macaque visual cortex. The animal was injected with ³H-proline into vitreous of one eye 1-2 weeks before the brains were perfused, tangential sections taken and developed for several months to allow visualization of OD columns. In macaque these form a stripy appearance.

B Optical imaging of intrinsic signals from cat visual cortex. *In vivo* visualization of neuronal activity due to changes in metabolic activity of neurons in response to visual stimulation of oriented gratings. Combined activity maps for all orientations tested through one eye are divided by the combination of activity maps through the other eye to give an ocular dominance map. Ocular dominance columns in cats appear 'patch-like'.

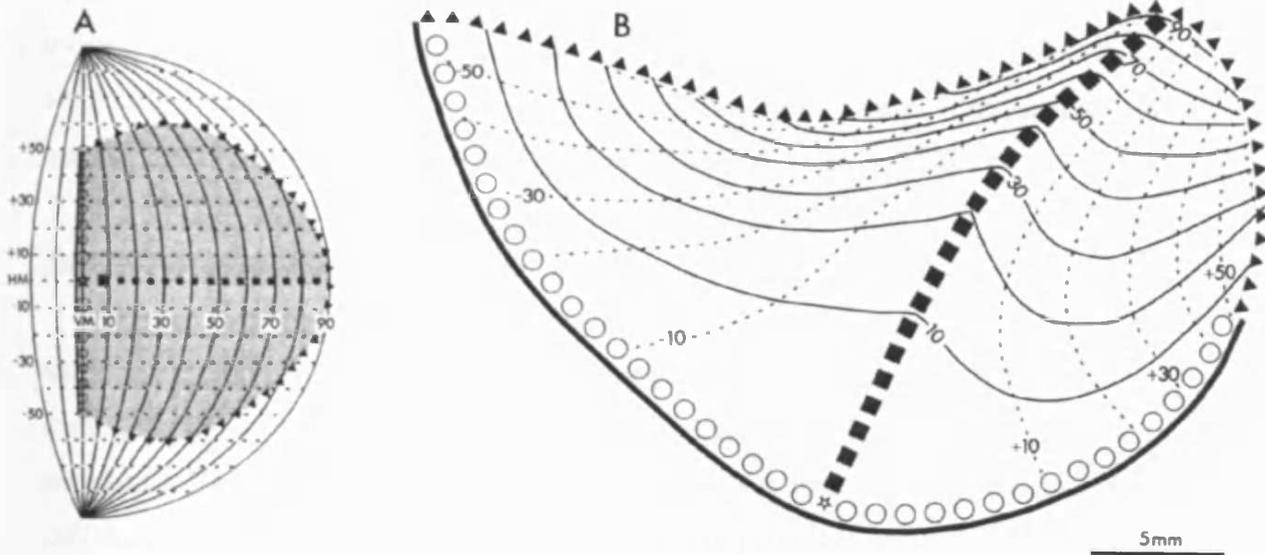


Figure 1. 9 Neighbouring points in the visual cortex represent neighbouring points in visual space (Daniel and Whitteridge 1961)

A Representation of degrees of visual space on the retina of one eye.

B Representation of visual space on the visual cortex.

Thick dotted line on both pictures represents the horizontal meridian (HM).

Thick continuous line on both pictures represents vertical meridian (VM).

Although a fairly linear representation of visual space on the retina, the corresponding points in the visual cortex follow an eccentric nature. A large area of cortex is devoted to the corresponding 10 degrees of visual space at the point of HM and VM convergence (area centralis).

acuity is at its highest. In the cat, 50% of the total area of V1 is dedicated to just 20 degrees of the contralateral hemifield (Tusa *et al* 1978). These distortions can be accounted for by the magnification factor (millimetres of cortical surface/degrees of visual field) devised by Daniel and Whitteridge (1961). The magnification factor is greatest at the area centralis and decreases exponentially with eccentricity (Daniel and Whitteridge 1961). Other such distortions arise from ocular dominance and orientation columns and at the V1/V2 border (Blasdel and Campell 2001).

Time line of development of the visual system

Most studies have been performed on carnivores, especially in cats and ferrets. The maturation of cortical cell responses of the visual system in both cases is dependent on intrinsic factors (experience independent) before the time of eye opening, and in cats occurs mostly prenatally. Experience dependent processes set in shortly after eye opening. Due to the ferret being born relatively immature (6 weeks gestation as opposed to 9 weeks for cats), they have lent themselves to the study of the early stages of development of the visual system. For example, it has been shown that retinal waves (patterns of retinally generated bursting activity that spread across the retina in waves) play a role in the lamination of the LGN: when intracellular levels of cyclic adenosine monophosphate (cAMP) were increased (with forskolin, cholera toxin or an analogue of cAMP), activity in the eye that was injected increased and that eye's corresponding layer in the LGN was larger, despite the other eye having normal levels of activity. But when both eyes were injected (increasing retinal activity binocularly) the area of LGN occupied by both eyes was similar to normal control levels (Stellwagen and Shatz 2002). This finding is important in itself. However, (combined with the knowledge that functional retinogeniculate synapses precede that of LGN maturation) the coincidence of correlated retinal waves being recorded and LGN laminar segregation occurring around the same time (E49-63 in cats – Fig. 1.10), indicates that activity plays an instructive role in the development of the LGN. In other words, 'instructive' activity (i.e. retinal waves) provides the information required to fashion development, as opposed to 'permissive' activity which is required only to allow axons to process intrinsic information.

Eye opening in cats occurs between postnatal day (P) 7-10. It originally seemed that ocular dominance columns formed with the beginning of the critical period - about P21 (LeVay *et al* 1978. See Fig 1.11b). Since this was much later than eye opening, it was thought that visual experience was responsible for driving the formation of ocular dominance columns. However, it was found (using transsynaptically transported label injected into one eye – Horton and Hocking 1996) that segregation of thalamocortical afferents into stripes occurs before birth in macaque monkeys (Rakic 1976; Horton and Hocking 1996). More recently it has been shown by Crair *et al* (2001), that in cats ocular dominance columns are distinguishable at P14, one week before the onset of the critical period. An even clearer distinction between the establishment of ocular dominance columns and the critical period has recently been shown in the ferret (Crowley and Katz 2000). Direct injections of anterograde tracers into ferret LGN has shown that ocular dominance segregation is visible within one week of LGN axons arriving in layer IV (P16) – at least 3 weeks before transneuronal tracing reveals columns (Finney and Shatz 1998, Ruthazer *et al* 1999) and some time before the onset of the critical period in ferret (P33). In addition, in ferrets, LGN axons in V1 enter the cortical plate at P10 and in less than 7 days clear eye-specific patches are visible (Crowley and Katz 1999, 2002). The timeline of ocular dominance formation challenges the original view from transneuronal transport data (i.e. LeVay *et al* 1978) that development of the geniculocortical projection consists of overlapping populations of axons which must retract and sprout in new locations in order to establish an adult pattern. The more recent data from direct LGN injections (Crowley and Katz 2000) suggests that selective elaboration of arbours occur directly into appropriate columns. Therefore, ocular dominance development appears (in the ferret at least) to be considerably more rapid and precise than once thought.

As with ocular dominance column formation, it appears that orientation preference is also present to some extent at birth. Electrophysiological recordings from neonatal kittens show approximately one quarter of neurones have orientation selectivity (Blakemore and Van Sluyters 1975; Fregnac and Imbert 1978). Recent work using optical imaging of V1 in kittens, binocularly deprived from birth, reveal orientation preference maps of a mature layout (Godecke 1997; Crair *et al* 1998). Visual deprivation by either lid suture or enucleation before the critical period does not prevent the formation of orientation maps or formation of ocular dominance bands (Crair *et al* 1998, 2001; Crowley and Katz 1999, 2000).

This points to spontaneous activity having a role in the formation of cortical specificity and maps independent to some extent of visual input or retinal waves. In short, although maps of orientation preference and ocular dominance have been shown to be present to some extent before eye opening, their formation follows a seemingly “passive” process, independent of visual input, until P21, where approximately the critical period for ocular dominance and orientation preference begins (Fig. 1.10).

Plasticity in V1

Plasticity

Adj. The quality of being plastic; capacity for being moulded or undergoing a permanent change in shape.

Biol. Adaptability of an organism to changes in its environment (Oxford English Dictionary)

Critical Period

The critical period for plasticity within layer 4 of the visual cortex begins around P21 in cats (Fig. 1.10). It peaks at P35 and starts to tail off after P49, and although significant effects of monocular deprivation (MD) can only be seen up to 4 months of age, some plasticity can be seen up to 1 year of age (Daw 1994). The initial estimates of the vulnerable period of the cortex to monocular deprivation were misleading due to the unequal periods of occlusion used by Hubel and Wiesel (1968). Fixed periods of deprivation used by Olson and Freeman (1980) showed that the sensitive period for visual manipulation starts as early as 2 weeks (kittens deprived in one eye between the ages of P8-19 showed disruption to cortical binocularity, but no large shift in dominance of cells to favour the open eye).

An earlier study by Olson and Freeman (1978) showed that kittens deprived after P13 exhibited a breakdown in cortical binocularity and a shift of dominance towards the open eye) which persists longer than 4 months of age (later verified by Cynader *et al* 1980). Blakemore and Van Sluyters (1974b) studied the susceptible period to manipulation in an alternative way.

Figure 1.10 Time line of development of the cat visual system (from Crair *et al* 2001).

At birth in the cat, retinogeniculate axons have already formed laminar specific connections. LGN axons reach layer IV just before birth. Some orientation selective cells can be detected by postnatal day (P) 7. Functional ocular dominance columns and clear orientation maps appear by P14.

Figure 1.11a Dark-field autoradiographs of visual cortex in kittens aged 2, 3, 5.5 and 13 weeks of age (Autoradiographs from Le Vay *et al* (1978). Diagram courteous of Sengpiel)

At 2 weeks of age the label is uniform in layer IV.

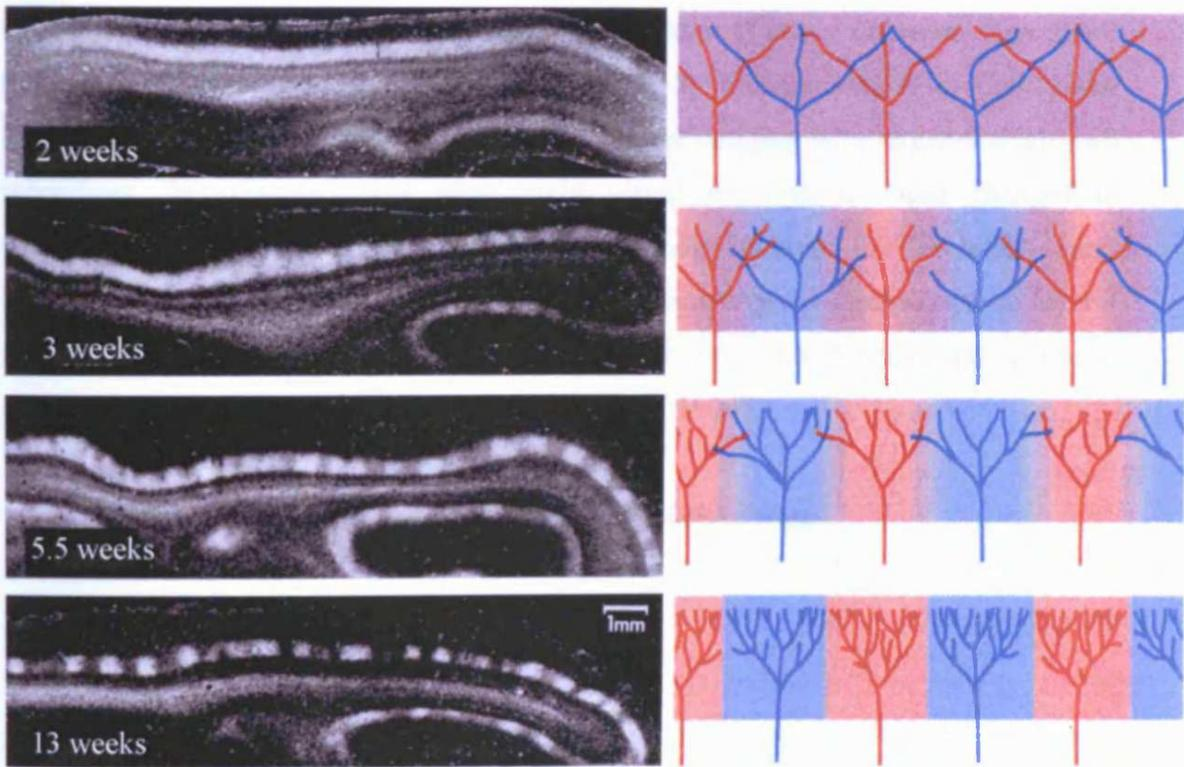
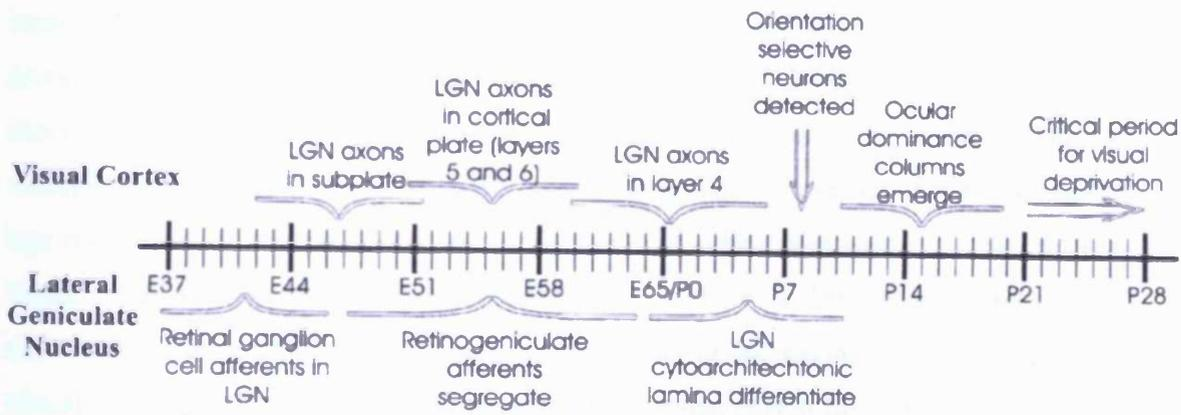
At 3 weeks a mild periodic fluctuation in the density of the labeling is visible.

At 5.5 to 13 weeks of age an adult-like pattern is similar is seen at 5.5 weeks and is robust at 13 weeks.

Pictorial representation of geniculocortical afferent from each eye.

At 2 weeks afferents from each eye are sparse and intermingled. By adulthood they have formed distinct left and right eye columns with increased afferentation within each column.

A second model has more recently come to light from work by Crowley and Katz (2000, 2002). Consistent with direct LGN injections in ferret, despite a similar sparse geniculocortical innervation early on, segregation into OD columns follows a selective elaboration into appropriate regions.



They studied the degree of the reversal of ocular dominance in kittens that had been occluded in one eye, followed by reopening that eye and occluding the other eye (reverse occlusion). The 'reversal index' as it was called was the proportion of recorded cortical cells dominated by the initially deprived eye. Animals reverse sutured early at 5 or 6 weeks showed an almost complete reversal. After 6 weeks of age the degree of reversal decreases until week 14 where almost no reversal occurs. Work by Blakemore & Van Sluyters (1974b), Berman & Daw (1977), Daw *et al* (1978) and Daw (1994) strengthened a hypothesis of increasing plasticity along the visual processing hierarchy by showing that the critical period for changes in direction selectivity ends prior to that for ocular dominance changes. It is known that a high percentage of simple cells found in (the first level of) layer IV are direction selective, whereas the signals from the two eyes are still separate in layer IV and combine in higher areas. In other words direction selectivity is almost completely 'set' before stereopsis begins.

However, the 'critical period' (for visual manipulations) is not universal throughout the layers of the cortex. Studies including those by Trachtenberg *et al* (2000) and Trachtenberg and Stryker (2001), combining optical imaging with targeted single-cell recordings, demonstrated that after early visual deprivation, rapid changes in connections in layers II/III occur before those seen in layer IV. Therefore, early changes in the supragranular layers may guide the slower later changes seen in layer 4 (Trachtenberg *et al* 2000; Trachtenberg and Stryker 2001). Furthermore, extragranular plasticity has been found adulthood (Diamond *et al* 1994).

Mechanisms of plasticity in the cortex

Neural correlates of plasticity

According to Hebb's postulate, 'When an axon of cell A excites cell B and repeatedly or persistently takes part in firing it, some growth process or metabolic change takes places between one or both cells so that A's efficiency as one of the cells firing B is increased' (Hebb 1949). Stent (1973) added to Hebb's original postulate by stating that post-synaptic activation was necessary not just for LTP but for all synaptic modifications (LTP and LTD) and post-synaptic activity was dependent on the level of pre-synaptic activity.

Ocular dominance plasticity is thought to require neural activity in the visual cortex (Hata *et al* 1999). Monocular deprivation studies have shown not to give rise to a shift in cortical response towards the open eye when the activity of cortical cells (and their inputs) are blocked by infusion of Tetrodotoxin (Reiter *et al* 1986). The importance of activity of cortical (post-synaptic) cells in OD plasticity was highlighted further by Reiter and Stryker (1988). Cortical cells were pharmacologically silenced by γ -aminobutyric acid (GABA_A) receptor agonist, muscimol, however activity of the geniculate afferents was not affected. The resulting inhibition of cortical cells resulted in activity in the open eye being less effective than that of the closed eye and its territory shrunken while that of the deprived eye expanded (Hata and Stryker 1994). It is now accepted that the developing visual system of many species is influenced dramatically by the extent and nature of early visual experience. Much of this understanding has come about due to experiments that manipulate the early visual experience through one or both eyes.

One extreme manipulation of normal binocular vision is through monocular deprivation. This leads to a breakdown of cortical binocularity and a shift in ocular dominance almost completely towards the non-deprived eye (Fig. 1.11b).

However, with binocular deprivation, there was at least initially very little change in ocular dominance between the two eyes, in particular no loss of binocularity (Hubel and Wiesel 1964). Binocular deprivation for extended periods of time led to a generally unresponsive cortex. These striking differences between the two paradigms led to the idea that the inputs subserving each eye compete for synaptic space on visual cortical neurones. Under normal binocular vision, left and right retinal cells project to left and right LGN cells on a one-to-one basis. The left and right LGN cells converge onto one cortical cell. Since the two eyes are being activated together, their input strengths are 'equal' and neither eye has a competitive advantage, resulting in the strengthening of binocularity. In the absence of patterned activity in one of the two eyes (monocular deprivation, reverse occlusion) the other eye is placed at a competitive advantage. This results in an increase in the open eye's effectiveness at driving the cortical cell, in turn leading to greater control of post-synaptic space in the cortex at the expense of the other eye. In effect, the deprived eye's corresponding

columns shrink first and are subsequently taken over by the non-deprived eye (Antonini and Stryker 1993, 1996).

This *spatial* competition between two sets of synapses is called **heterosynaptic competition** (Fig. 1.12). As ocular dominance plasticity involves morphological changes in pre-synaptic terminals, LTP induction (at the post-synaptic site) must be retrogradely signalled to the pre-synaptic cell. One candidate 'retrograde messenger' is brain derived neurotrophic factor (BDNF). According to competition-based theories, inputs from the two eyes compete for limiting amount of BDNF (see Cabeli *et al* 1995). It has been hypothesised that the induction of LTP in synapses made by axons from the non-deprived (more active) eye led to LTD in the deprived (less active) eye (see Kind 1999). Guillery and Stelzner (1970) strengthened this hypothesis by showing that geniculate laminae representing the deprived eye of kittens grew less than normal. Antonini and Stryker (1998) further backed up this idea more recently; by comparing geniculocortical arbors of binocularly deprived kittens to those of normally reared and monocularly reared. Arbours of binocularly deprived kittens were very similar to those of normally reared kittens. Reiter and Stryker (1988) inhibited post-synaptic activity with muscimol infusion.

This resulted in a shift of cortical responses towards the less active deprived eye, unlike the normal shift towards the open eye. Heterosynaptic mechanisms could not readily explain this result. It could be explained however by the postsynaptic blockage having a relatively greater effect on synapses made by the more active non-deprived eye afferents, than on the less active deprived eye afferents.

Anatomical studies by Hata *et al* (1999) showed that silencing the cortex of monocularly deprived kittens with muscimol resulted in a shrinkage of non-deprived eye arbors and an almost normal size of arbours representing the deprived eye. From these results it appeared that it is not the *amount* of afferent activity but the *correlation* between pre- and post-synaptic neurones that leads to synaptic modification.

Dews and Wiesel (1970) and Hubel and Wiesel (1970) reported very little physiological recovery when monocular deprivation was followed by a period of binocular vision. This result was attributed to the lack of a competitive advantage over the experience eye when the deprived eye had simply been re-opened. However, the extent of physiological and behavioural recovery was considerably higher in similar experiments by Giffin & Mitchell (1978), Mitchell *et al* (1977), and Mitchell and

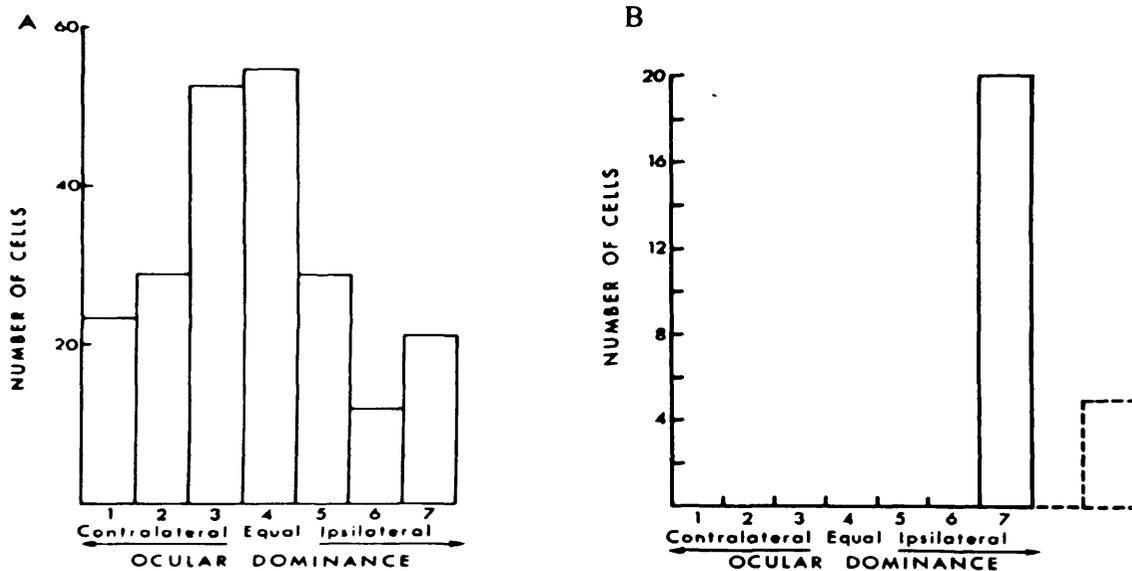


Figure 1.11b Ocular dominance distribution of visual cortex in a normal adult cat^A (left) and a kitten monocularly deprived for 2-3 months^B (right) (Hubel and Wiesel 1962^A, Wiesel and Hubel 1963)^B

Responses from single cells recorded from cat visual cortex to orientated stimuli. Each cell is categorized depending on its relative response to each eye. Cells in category 1 and 7 respond solely to one eye or the other. Those in category 4 respond equally to both eyes. Dotted line bar 4 = unresponsive cells.

Gingras (1998). A majority of units recorded possessed qualitatively normal orientation selective receptive fields (Mitchell *et al* 1977). Re-opening of the deprived eye to allow normal binocular vision resulted in the initially deprived eye re-establishing control of 37% and 31% (45 and 60 days monocular deprivation, respectively) of cortical neurones (Mitchell *et al* 1977).

Again, heterosynaptic (competitive) mechanisms could not explain the recovery seen by Mitchell and colleagues after monocular deprivation. Competitive mechanisms would predict that upon opening the deprived eye the non-deprived eye would maintain its competitive advantage and little or no recovery would be seen in the deprived eye.

It was therefore suggested that it is not competition *between* synapses (based on absolute levels of activity between both eyes) that determines neuronal responses and synaptic strength. A contrasting view- exemplified by the Bienenstock-Cooper-Munro (BCM) theory is based upon pre- and post-synaptic activity levels at each synapse *individually*. Patterns of input activity compete in the *temporal domain*. This competition is known as **homosynaptic plasticity** and does not require a conserved resource (Fig. 1.12).

This homosynaptic model of plasticity conjectures that the direction or sign of a change in synaptic efficacy is dependent on a 'modification threshold' (θ_m). This threshold itself is dependent on the average level of cortical activity. Cooper *et al* (1979) first introduced the 'modification threshold' by which, when depolarisation of a cortical neurone passes the modification threshold, synaptic potentiation occurs in Hebbian fashion (LTP). But when the post-synaptic activity falls below this threshold then synaptic strength decreases (LTD) (Fig. 1.13a).

Further analysis gave rise to the problem that if the post-synaptic response to all patterns fell below the modification threshold, then the efficacy of all synapses would drop to '0'. This situation would be expected to occur during binocular deprivation.

Bienenstock *et al* (1982) therefore modified Cooper *et al* 's (1979) theory further, by allowing the modification threshold to slide as a non-linear function of the *averaged post-synaptic activity* of the cell. During normal binocular experience LTP and LTD can be elicited and postsynaptic activity is relatively high. During binocular deprivation, post-synaptic activity is low so the modification threshold decreases and t

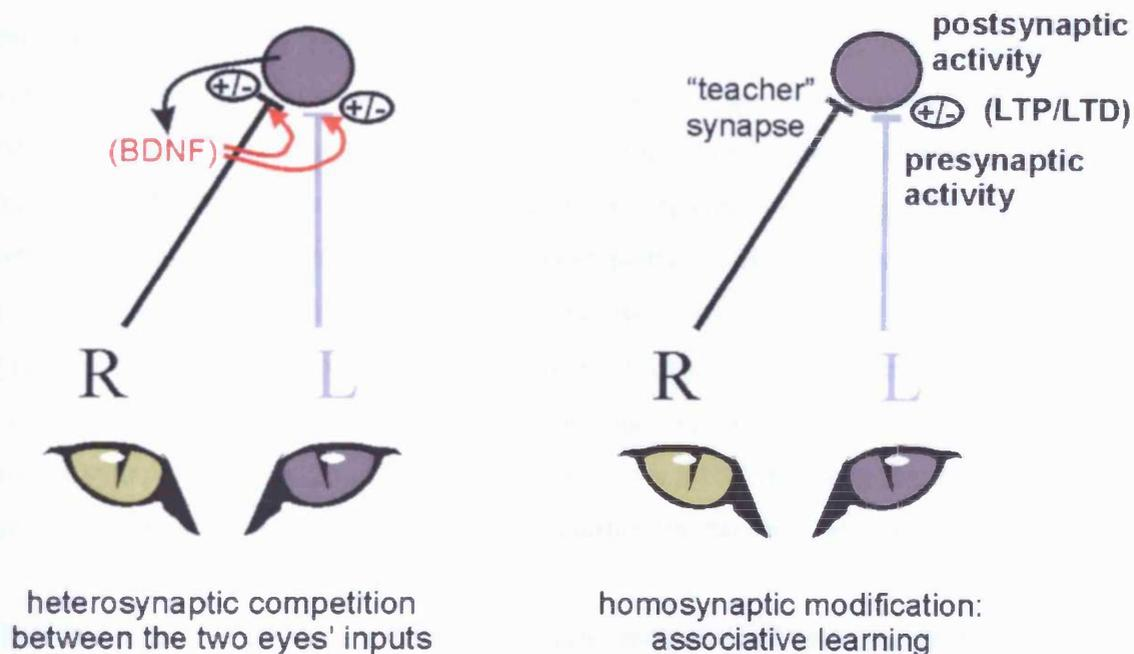


Figure 1.12 Two contrasting theories of synaptic plasticity in visual cortex (Courtesy of Sengpiel)

Heterosynaptic 'Competitive':

Competition between inputs from the two eyes, maybe for limiting amounts of a neurotrophin (e.g. BDNF) released by post-synaptic neurons. In the absence of activity in one eye [monocular deprivation (MD), reverse occlusion(RO)], the other eye is placed at a competitive advantage. Binocular deprivation (BD) has comparably milder effects.

Homosynaptic 'Associative':

Bienenstock-Cooper-Munro (BCM) model (Bienenstock *et al* 1982) - Direction or sign of a change in synaptic efficacy is dependent on a 'modification threshold' (θ_m), which itself depends on average levels of post-synaptic (cortical) activity. LTP occurs when pre-synaptic activity coincides with post-synaptic activity above θ_m , and LTD when pre-synaptic activity coincides with post-synaptic activity below θ_m . Absence of activity in one or both eyes results in θ_m being reduced to an extent which biases towards LTP induction, although in case of MD, LTD induction is not eliminated.

he 'system' becomes biased towards LTP induction. The possibility of induction of LTD is almost eliminated. During monocular deprivation, the threshold is reduced to a lesser extent due to there still being post-synaptic activity driven through the open eye. Although the bias towards LTP induction still occurs, the possibility of LTD induction is not eliminated (Fig. 1.13b).

Inter-ocular injection of Tetrodotoxin blocks pre-synaptic activity in the visual cortex, which leads to postsynaptic activity being close to zero too. Rittenhouse *et al* (1999) used this to show that a greater shift of ocular dominance occurred towards the non-deprived eye during monocular deprivation as opposed to silencing the eye with Tetrodotoxin. Lid suture leaves the retina spontaneously active, whereas Tetrodotoxin eliminates activity completely. Homosynaptic depression will only occur at active synapses. With Tetrodotoxin, synapses are effectively inactive and neither LTP nor LTD can occur. However, with lid suture retinal activity is still present, therefore driving synaptic depression. This result confirms the BCM theory in that pre-synaptic activity is necessary to generate LTD that underlies the ocular dominance shifts seen.

There are several aspects of the heterosynaptic competition-based theory that cannot explain results obtained from behavioural studies either. In the heterosynaptic theory, the extent of recovery of the deprived eye from monocular deprivation would be minimal after re-opening, unless the non-deprived eye was reverse lid-sutured (giving the originally deprived eye a competitive advantage). In BCM, correlated input between the two eyes would give rise to the visual recovery observed. Mitchell and Gingras (1998) and Kind *et al* (2002) have showed substantial visual recovery during a binocular period after MD. More importantly, when input was de-correlated after a period of MD, physiological and behavioural recovery was disrupted (Kind *et al* 2002).

Whichever is the case, it is clear that there is not a single system or form of synaptic modification that can account for complex plastic changes in the visual cortex that occur due to altered visual experience. One possibility is that, homosynaptic mechanisms could dominate initially, followed by heterosynaptic modification.

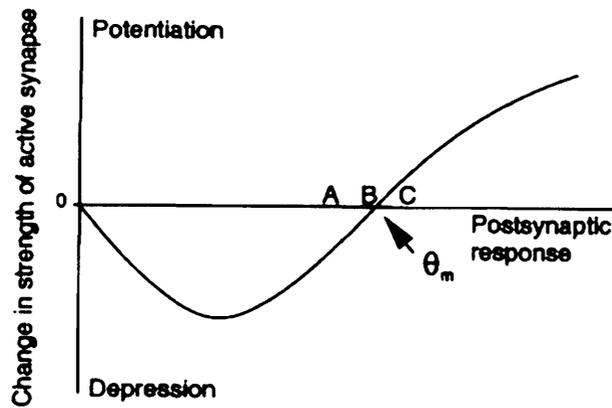
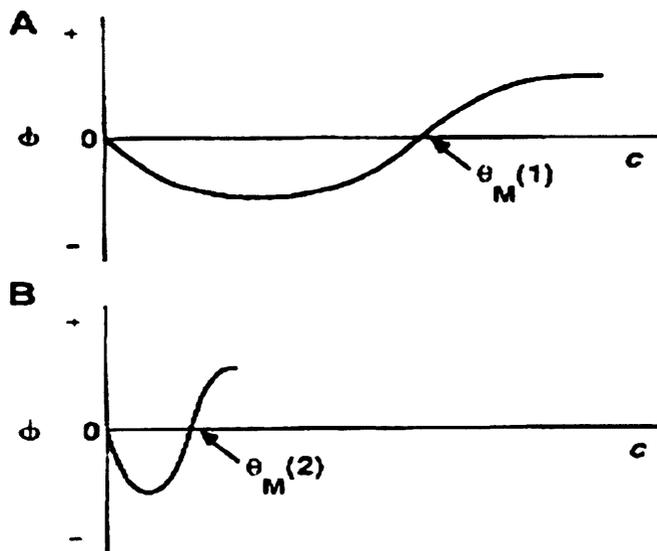


Figure 1.13 a Modification threshold controlling synaptic plasticity (Bear 1996)

Cooper *et al* (1979) proposed that active synapses are potentiated when the total post-synaptic response exceeds a critical value, the modification threshold (θ_m). Post-synaptic responses to stimuli A-C are considered. Stimuli C is above θ_m therefore active synapses during presentation of C potentiate. Stimuli A and B are below θ_m , therefore synapses active during presentation of A and B depress.



BCM modification function: $dm/dt = \phi(c, \theta_m)d$

m is vector of synaptic weights
 d is pre synaptic activity of cell
 c is post-synaptic activity of cell
 θ_m is modification threshold
 ϕ is function of post-synaptic response

Figure 1.13 b BCM synaptic modification function. Function $\theta(c, \theta_m)$ as a function of c (Bear *et al* 1987)

The moving threshold stabilizes synaptic weights. **A** When the post-synaptic response is above θ_m (as with normal rearing), the ϕ function is positive, potentiation occurs, θ_m moves to the right and the response function now becomes biased towards LTD induction. **B** When the post-synaptic response is below θ_m , the ϕ function is negative, depression occurs, and θ_m resets to a new lower level and the response function becomes biased towards LTP induction (as with binocular deprivation).

Molecular correlates of plasticity

Until fairly recently understanding of the underlying mechanisms of the maturation of cortical circuits has lagged behind the physiology. Neurotrophins have been suggested as a possible candidate for retrograde messengers in synaptic modification (LTP, LTD). Snider & Lichtman (1996) suggested that these neurotrophins may act as 'synaptotrophins' which influence synaptic strength and maintenance. The classical mechanism of neurotrophic actions is that neurotrophins are released continuously and influence the development and survival of populations of neurones occurring throughout the nervous system. Increasing evidence indicates that these neurotrophins could be released in an activity dependent way, influencing neuronal differentiation and survival in an activity dependent manner (see Thoenen 1995). Brain derived neurotrophic factor and nerve growth factor (NGF) are both present in the neocortex (Ernfors *et al* 1990, Maisonpierre *et al* 1990, Phillips *et al* 1990). There is mounting evidence that the addition of exogenous neurotrophins can interfere with activity dependent organisation and re-organisation of synaptic connections in the developing cortex. Galuske and colleagues (2000) carried out a comprehensive study of the effects of neurotrophins on ocular dominance plasticity in the developing and adult cat visual cortex. Continuous application of exogenous brain derived neurotrophic factor (BDNF) into the visual cortex of monocularly deprived kittens reversed the normal OD shift towards the open eye to favour the closed eye. Even when activity was equal through both eyes (binocular deprivation or normal rearing) BDNF shifted the natural cortical bias in favour of the contralateral eye to that of the ipsilateral eye. However, in adult cats BDNF had no effect on OD distribution. In stark contrast, NGF had no effect on the OD shift in monocularly deprived kittens but did cause a reverse OD shift to favour the closed eye in monocularly deprived adult cats. Neurotrophic factor 4/5 (NT 4/5) inhibits the segregation of thalamocortical afferents into OD columns (Cabelli *et al* 1995, 1997). Infusion of NT4 has been shown to prevent the retrograde degeneration of geniculocortical terminals normally observed after MD (Riddle *et al* 1995).

Huang *et al* (1999) used a mouse over expressing BDNF to show the link between BDNF and the critical period. It was found that BDNF accelerates the development of visual acuity, the time period of ocular dominance plasticity development and

synaptic activity. The above experiments suggest that neurotrophins have profound effects on the activity-dependent and age-dependent functioning of the visual cortex.

Other molecular correlates of cortical plasticity focus on proteins and receptor channels. One main candidate protein is the transcription factor cAMP/Ca²⁺ response element binding protein (CREB). Neuronal activity and neurotrophins regulate CREB function, hence it is inherently linked with adaptive neuronal responses. It has been shown that CREB is induced during MD in mouse cortex (Pham *et al* 1999). In ferrets, a mutated form of CREB (containing a single point mutation that prevents its activation) expressed during monocular deprivation prevented the loss of responses to the deprived eye (Mower *et al* 2002). A follow up study (using the same mutated form of CREB) looked at CREB activation during recovery of cortical function from MD. In a reverse deprivation paradigm, during binocular recovery, inhibition of CREB function prevented the loss of responses to the newly deprived eye. However, recovery of responses to the previously deprived eye did occur (Liao *et al* 2002). These two studies show that CREB function is required for the loss but not recovery of deprived eye responses.

An increasing number of studies indicate that N-methyl D-aspartate (NMDA) receptors play a major role in ocular dominance during MD plasticity (Bear *et al* 1990, Rauschecker *et al* 1990, Roberts *et al* 1998). Blocking NMDA receptors prevents the effects of MD being seen (Bear *et al* 1990). N-methyl D-aspartate receptors are developmentally regulated and their expression is modified by electrical activity (Berardi *et al* 2003). Over the course of development of the visual cortex the subunit composition of these receptors change. There are two main subunits, NR1 and NR2. The latter can have one of four forms forms, NR2A, B, C or D. The most extensively studied are the forms NR2A and NR2B. At birth the subunit NR2B is highly expressed. Over the next few weeks a rise in NR2A is seen. This change in ratios is thought to be activity related. Several studies using dark rearing support this hypothesis. The change in ratios between NR2A and B is delayed during dark rearing (Nase *et al* 1999; Quinlan *et al* 1999). NR2A is rapidly upregulated when the animals are then exposed to light (Quinlan *et al* 1999b). A later study by Philpot *et al* (2001) demonstrated bi-directional experience dependent regulation of NMDA receptors. Visual experience of only 2 hours induced detectable changes in synaptic transmission, while binocular deprivation induced changes took several days.

These sub-unit changes correlate well with the critical period, suggesting that both are inherently linked. However, mice that have had the NMDA sub-unit 2A deleted, show a sensitivity to MD restricted to the normal critical period (Fagiolini *et al* 2003) suggesting the 2A sub-unit does not control the duration of the critical period. It could be that the subunits affect plasticity independently of changes in current kinetics, i.e. intracellular signalling pathways.

Animal models of human disorders

Strabismus

Despite monocular deprivation being a successful model for studying cortical plasticity, the incidence of this type of form deprivation is quite rare in humans. The condition that comes closest is a dense unilateral cataract, either congenital or of very early onset. A more common visual disorder in humans is strabismus. This is defined as a deviation of the visual axis of the eye with respect to the direction of fixation. The vision through that eye often becomes less effective, particularly in discriminating detail (Crewther and Crewther 1990). The commonest form of strabismus is esotropia (convergent squint) which is generally associated with unilateral fixation and strabismic amblyopia (central loss of visual acuity) in the non-fixating eye. This condition is most prevalent in infants with an incidence rate of about 6%.

While during normal binocular vision afferents from the two eyes converge onto the same cortical cell, in strabismus a majority of afferents from the two eyes contact separate cortical cells. By mis-aligning the visual axes to produce a divergent strabismus (exotropia) during development in kittens, Hubel and Wiesel (1965) were able to show that there was a decrease in the proportion of binocularly driven cortical cells from approximately 80% to approximately 20% (Fig. 1.14).

More recent data including optical imaging show that segregation of geniculocortical afferents is enhanced in strabismic cats (Shatz *et al* 1977; Löwel and Singer 1993; Löwel 1994; Löwel *et al* 1998) with activity maps of the two eyes in strabismic cats being clearly complementary and clearly segregated, more so than in normal adult cats (Löwel *et al* 1998).

Electrophysiological and anatomical data indicate that the contralateral eye occupies more cortical territory than the ipsilateral eye (Hubel and Wiesel 1962; Shatz and Stryker 1978; Tieman and Tumosa 1983; Löwel and Singer 1987; Löwel 1994; Löwel *et al* 1998). This bias remains with strabismus regardless of whether the contralateral eye is deviated or not (Hubel and Wiesel 1965; Löwel and Singer 1992; Löwel *et al* 1998).

Despite the physiological and anatomical cortical deficits in strabismic cats much of the gross functional architecture of the cortical maps remain intact. Ocular dominance patterns remain consistent (Sengpiel *et al* 1998), pinwheel organisation in iso-orientation domains resembles that of normal cats (Löwel *et al* 1998). Receptive field size and spatial frequency tuning of neurones is no different from normal animals (Chino *et al* 1988). Recovery of deprived eye (DE) cortical maps and visual acuity has been shown to be affected by the presence of a strabismus. Experiments by Kind *et al* (2002) studied recovery from 10 days of monocular deprivation, induced near the height of the critical period. One group of kittens experienced normal binocular vision during the recovery period, in the other group strabismus was induced in the previously non-deprived eye. Results showed that the area of cortex responding to deprived eye stimulation was smaller in strabismic kittens than those with normal recovery. Visual acuity in the formerly deprived eye was lower in strabismic recovery compared to normal recovery, paralleling what was reported physiologically.

Functional imaging of the brain

Until fairly recently, tools for visualising complex brain activities such as reading, memory and spatial visualization have been limited. One of the main limitations has been spatial resolution. This has been severely limited in procedures such as electrical recordings or by positron emission tomography (PET), where only moderate spatial resolutions of ~ 5-10mm have been achieved.

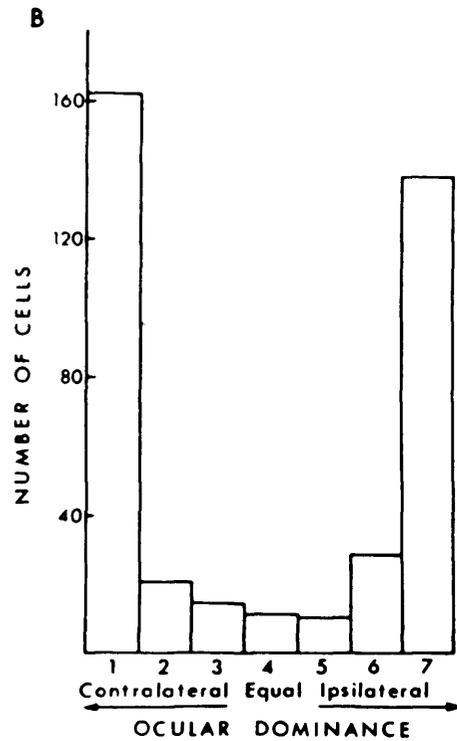


Figure 1.14 Ocular dominance distribution in cat V1 with strabismus
 (from Hubel and Wiesel 1965)

Responses from single cells recorded from cat visual cortex to orientated stimuli. Each cell is categorized depending on its relative response to each eye. Cells in category 1 and 7 respond solely to one eye or the other. Those in category 4 respond equally to both eyes.

fMRI, PET and other techniques

Early anatomical studies, including that done by Hubel and Wiesel (1977) used various staining techniques to visualise the architecture of visual cortex; in particular ocular dominance columns. One method visualizes metabolic activity: The subject is injected with a radioactively labelled chemical, ^{14}C 2-deoxyglucose (2-DG). The subject is visually stimulated and the metabolically active neurones take up the 2-DG. The brain is removed and uptake is visualised using autoradiography. The spatial resolution is better than that of functional magnetic resonance imaging (fMRI) and optical dyes (Fig. 1.15). However, the animal must be sacrificed after brief stimulation and the brain processed before results can be seen, so the technique is not suitable for *in vivo* work. Alternatively, the geniculocortical afferents can be labelled by injecting into one eye a dye such as WGA-HRP (wheat germ agglutinin associated with horseradish peroxidase) which is taken up by the retinal ganglion cells and transported transneuronally across the retinogeniculate synapse and on to V1.

Extracellular recordings can record at the level of small clusters or even single neurones and so the spatial resolution is very good. However, since the cortical responses involve large numbers of neurones, a representative sample is difficult to obtain and time-consuming.

Electroencephalogram (EEG) and evoked response potentials (ERP) can look at patterns of brain activity and brief changes in brain activity respectively. They are both capable of distinguishing excitation and inhibition, and have excellent temporal resolution. However, recordings are usually taken from the scalp, so despite the advantage of the non-invasive nature of these techniques, their very poor spatial resolution renders them less useful.

Positron emission tomography (PET) was developed in the 1970's to visualise brain activity. It uses a positron-emitting isotope attached to 2-deoxyglucose injected into the blood stream. The location of these positrons is detected and activity can be calculated. However, it does have limited spatial and temporal resolution, is costly and it is not possible to run many repetitions on single subjects (because of the radioactive substances involved).

In 1936 Pauling and Coryell noted a difference in the magnetic susceptibility of oxy-haemoglobin and deoxy-haemoglobin. It was not until much later that Thulborn *et al* (1982) showed that the signal decay rate of deoxy-haemoglobin is more rapid than that of oxy-haemoglobin.

Activated areas of the brain are characterised by localised de-oxygenation of the blood, which is followed by recruitment of capillaries in surrounding tissue and increased blood flow and volume. Local variations in the magnetic field strength due to increased oxygen content of the blood results in increased intensity of the magnetic resonance (MR) signal.

The fMRI signal takes several seconds (4.4 sec according to Kwong *et al* 1992) to reach its peak following the onset of the stimulus presentation (Cohen and Bookheimer 1994). This is much slower than neuronal responses, therefore the temporal resolution falls between electrical (EEG) and PET recordings (Fig 1.15).

Oxygen delivery is more localised to the site of electrical neuronal activity than blood flow and blood volume changes are. Nevertheless, the spatial resolution remains fairly low (2000-4000 μm).

Functional MRI responses to (visual) stimuli have been reported in primary sensory areas (Kwong *et al* 1992; Blamire *et al* 1992; Bandettini *et al* 1992; Frahm *et al* 1992; Menon *et al* 1992). Despite its relatively poor temporal resolution, more recently (using the early negative portion of the in blood-oxygenation level dependent (BOLD) signal) the technique has even been used to visualise iso-orientation columns in the primary visual cortex (Kim *et al* 2000).

Using the deoxy-haemoglobin as an endogenous contrast agent (as in BOLD fMRI) bypasses the need for an extrinsic contrast agent (as with PET). Most importantly this allows *in vivo* visualisation in a non-invasive way, posing no harm to the subject. Results from functional imaging in awake and anaesthetised animals have proved to be non-comparable. While the intrinsic signal in anaesthetised and awake monkeys (at 630nm) is very similar, PET imaging results in a strong signal from awake subjects but very weak signal from anaesthetised ones. A similar problem is seen with fMRI.

This could be related to what component of the cortical signal is measured in optical imaging and in PET/fMRI. Positron emission topography imaging is most sensitive to changes in blood flow whereas optical imaging detects changes in oxygenation delivery and light. Activity dependent changes in the oxidation level of blood in

awake animals are slower relative to anaesthetised animals. The poor temporal resolution of PET and fMRI compared to optical imaging could account for the lack of signal seen in awake subjects (Grinvald *et al* 1991, and in Bonhoeffer and Grinvald 1996).

Optical imaging

The existence of intrinsic signals coupled with metabolic or electrical activity has been known for over 50 years (Hill & Keynes 1949, Chance *et al* 1962, Jobis *et al* 1977). It was not until Grinvald *et al* (1986), that these signals were used to map cortical activity. Intrinsic signal imaging offers the highest spatial resolution of any *in vivo* imaging technique currently available (Bonhoeffer & Grinvald, 1996). It has the added advantage of not using extrinsic operations (dyes, labels) which may alter or damage the function of the brain.

Sources of intrinsic signal

“The brain possesses an intrinsic mechanism by which vascular supply can be varied locally in correspondence with local variations of functional activity”

(Roy and Sherrington 1890)

The concept of electrical activity linked to changes in micro-vasculature is not new. However, more recent studies have identified three components to the signal.

- 1) Changes in blood volume due to local capillary recruitment or dilation of venules in areas of active neurones. The increase in blood volume is primarily made up of oxy-haemoglobin, with an absorption max near 580 nm
- 2) Activity dependent changes in oxygen saturation level of haemoglobin. Firstly, an increase in deoxy-haemoglobin due to enhanced oxygen consumption; secondly, a decrease in deoxy-haemoglobin due to blood entering active tissue contains high levels of oxy-haemoglobin.

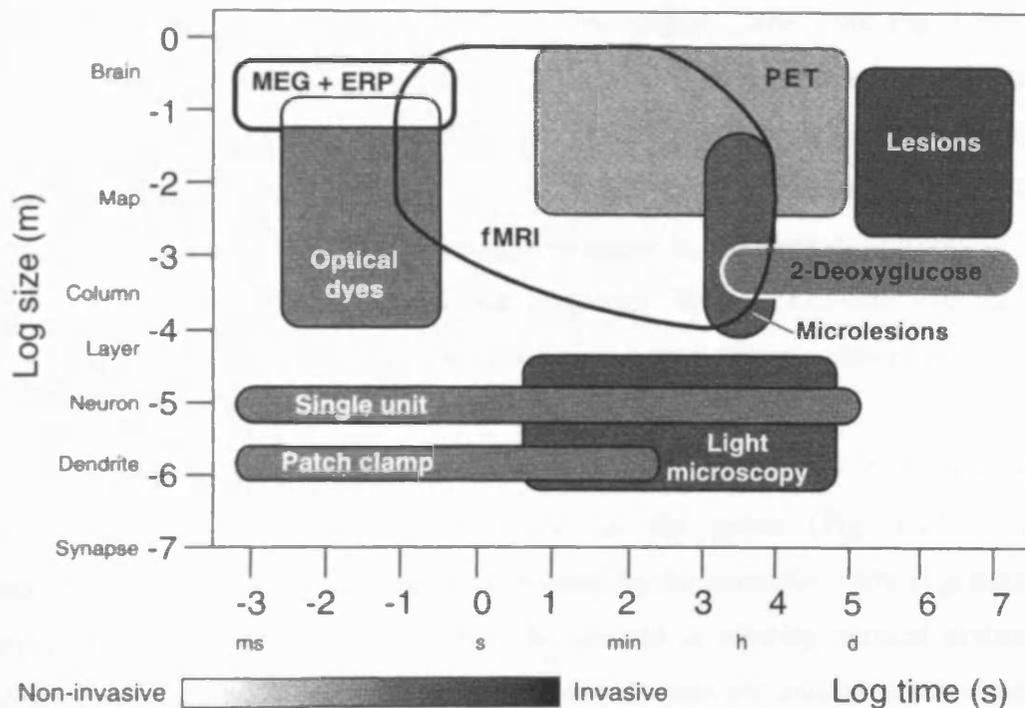


Figure 1.15 The temporal and spatial resolution of methods for the study of brain function (Cohen and Bookheimer 1994)

The y and x-axis represent the spatial and temporal resolution of each method respectively. The greyscale key represents the relative invasiveness of each technique. The darker the shade the more invasive it is. Abbreviations: MEG: magnet-encephalographic, ERP: event related potentials, fMRI: functional magnetic resonance imaging, PET: positron emission topography.

3) Light scattering changes (increase in absorption) occurring due to water and ion movement, capillary expansion and neurotransmitter release.

The various components of the intrinsic signal yield different spatial resolution with the signal from the micro-vasculature mostly reflects the changes in the concentration of the haemoglobin molecules within the cortex (points 2 and 3 see Fig. 1.16). More active neurones have a higher metabolic demand, which is reflected in an increase in blood flow in the surrounding vasculature. The light scattering component probably yields the best spatial resolution followed by the oxy-haemoglobin vs deoxy-haemoglobin component. Changes in light intensity due to neuronal activity at 700nm constitute less than 0.1% of the total light reflected. This can't be seen with the naked eye, so the change in signal needs to be extracted from images (described in detail in Methods).

Images are taken from the exposed cortex of an animal while it is viewing (e.g. moving) gratings of different orientations on the screen (Fig. 1.21 – General methods). To map the cortical regions activated by for example. vertical gratings, one simply takes the image captured while the animal is viewing vertical gratings and divides this image by the sum of images obtained when the animal is stimulated with gratings of all orientations (Bonhoeffer & Grinvald 1996).

The mapping of ocular dominance domains can also be achieved (Fig. 1.17). This can be done simply by dividing all the images taken for one eye viewing a stimulus set, by all the images taken for the other eye. Blasdel & Salama (1986) first introduced angle maps, a pseudo-colour representation of orientation preferences (Fig. 1.18). In these maps, the colour hues correspond to different preferred orientations.

Polar maps additionally show the relative strength of the orientation selective signal over the entire cortex (Fig. 1.19) as brightness of colour.

Several other areas including V2 have been studied using this procedure. Separate pathways of the thick, thin and pale stripes have been imaged by Ts'o and colleagues (1990, 1991, and 1993). Some of the higher visual areas once thought too deep to visualise such as V4 (Ghose *et al* 1994) and the infero-temporal area (Wang *et al* 1994) have been mapped. A few studies have been carried out on human cortex (Toga *et al* 1995; Canestra *et al* 1998, 2000; Sato 2002; Pouratian *et al* 2000; Shoam and Grinvald 2001). The greatest problem with human studies is minimising cortical

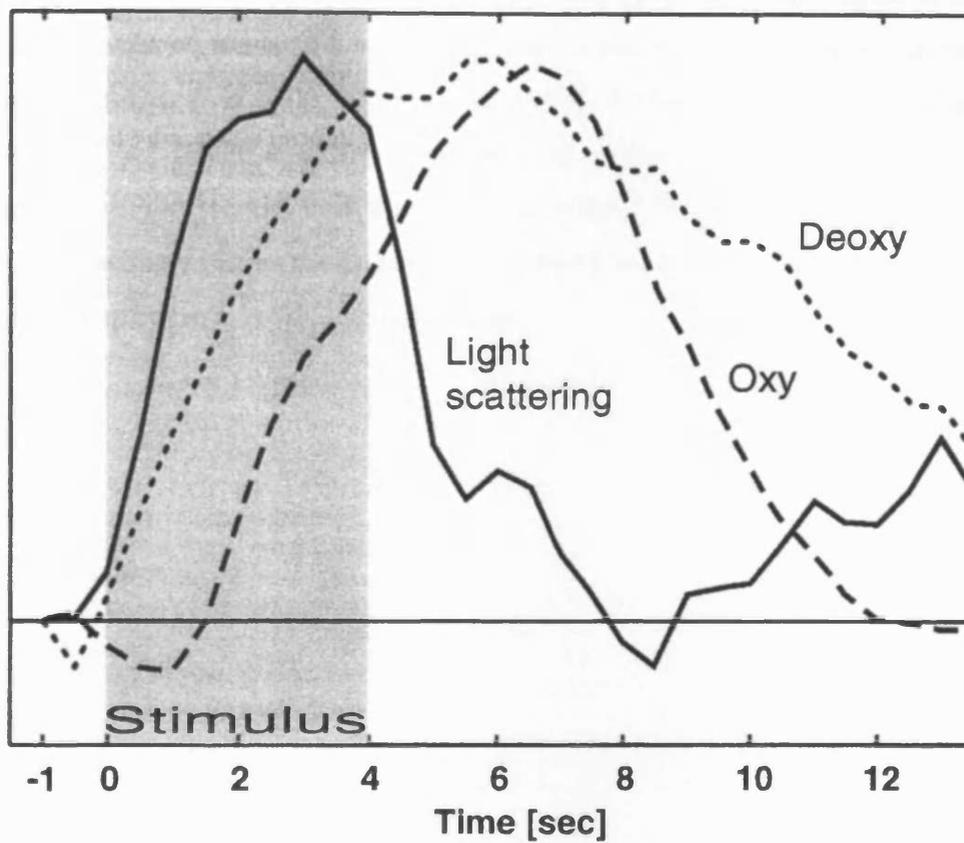


Figure 1.16 Time course of the mapping components of the intrinsic signal (in Bonhoeffer and Grinvald 1996)

The y and x-axis represent absorbency and time respectively. The light scattering component of the signal peaks during stimulus presentation while the blood components (Oxy- and De-oxy-haemoglobin) peak several seconds afterwards.

movement. A glass plate is placed on top of the cortex to reduce motion and flatten the cortex (as in animal studies). Synchronisation of image acquisition can be paired with respiratory and cardiac cycles. Thirdly, post-acquisition image registration using automated image registration algorithms (AIR) is used to align images (Cannestra *et al* 2000; Pouratian *et al* 2000; Woods *et al* 1992). All images in a trail are aligned to an initial control image and direct comparisons between ‘trial’ images and control images are made to identify active areas of the brain relating to the implemented task. These improvements in methods have only now allowed human studies using optical imaging to expand into more detailed studies.

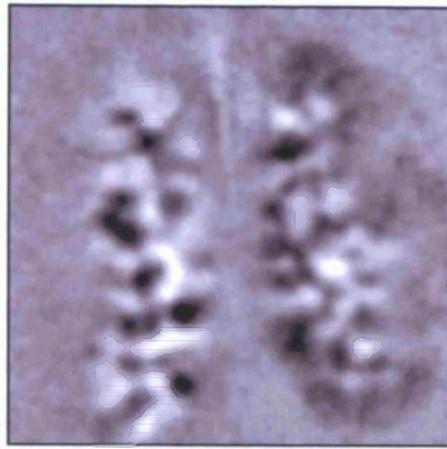


Figure 1.17 Ocular dominance map (left eye verses right eye) of kitten (842) visual cortex

The sum of responses to all orientations through one eye are divided by the sum of responses to all orientations through the other eye. A patch-like formation of ocular dominance patches can be seen. Black represents high neuronal activity, and white, low neuronal activity. With respects to the left vs right eye map here, dark areas represent neurons responding preferentially to the left eye and light areas responding preferentially to the right eye. The vertical meridian (stripe of uniform grey) separates the two hemispheres. Areas of responsive/visible cortex are clearly distinguishable from the uniform background.

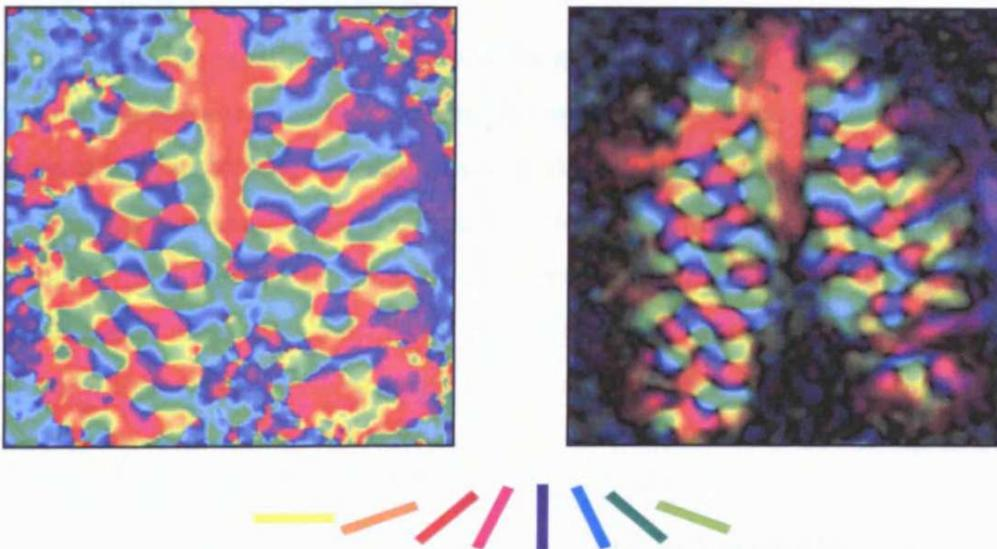


Figure 1.18 Angle map of kitten (842) visual cortex

The resulting vector of responses to all orientations tested is allocated a colour to represent preferred orientation. The angle of this colour is seen in the colour key. Orientation preference changes smoothly over the cortical surface. The vertical meridian separates the two hemispheres and appears as a red stipe down the middle of the image. A large blood vessel artifact can also be seen as a thick red line in the top portion of the left hemisphere.

Figure 1.19 Polar map form kitten (842) visual cortex

The relative strength of the oriented response is represented on a scale of brightness. The brighter the response, the stronger the oriented response. The area(s) of responsive cortex can easily be distinguished from the dark background. Again, the vertical meridian and large blood vessel on the left hemisphere appear as artifacts in the image.

GENERAL METHODS

Preparation

All surgery and optical imaging was performed under sterile conditions and in accordance with UK Home Office regulations on animal experimentation [Animals (Scientific Procedures) Act 1986] and European Community Council Directive 86/609/EEC. Effort was made to minimise animal suffering and reduce the number of subjects used.

Anaesthesia was induced with Ketamine (20-40mg kg⁻¹) and Xylazine (2-4mg kg⁻¹). Animals were intubated and placed in a stereotactic frame and ventilated with nitrous oxide/oxygen (3:2) supplemented with isoflurane (2-2.5% - decreased to 1.5% during imaging). End tidal volume, carbon dioxide, electrocardiogram, and rectal temperature were monitored constantly. A 4% glucose saline solution was infused i.v. at 3ml/kg/hr throughout the experiment.

In the initial imaging session the scalp was incised and retracted. A craniotomy was performed to expose area 17 in both hemispheres of visual cortex. A circular titanium chamber was implanted onto the skull, held in place with two bone screws and dental cement. A screw was implanted in the cement in front of the chamber to allow extra cranial support and ease of fixation in repeat experiments. The cortical surface was carefully cleared and kept free from traces of blood using Sugi sterile swabs (Kettenbach, Eschenburg, Germany). The chamber was filled with silicon oil (dimethylpolysiloxane, Sigma-Aldrich, Poole, UK), sealed with a cover slip pressed into a silicon inner ring by an outer threaded ring (Fig. 1.20).

In all cases the dura was left intact as long as possible and removed only in the last experiment or when imaging through the dura became impossible due to over-growth of tissue.

Using an ophthalmoscope, the animal's eyes were refracted with gas permeable contact lenses to focus their eyes onto a 21inch monitor at a distance of 33cm.

Following each, but the final session, the dura was covered with a layer of agar containing an anti-inflammatory steroid (Dexafort, Intervet UK Ltd, Milton Keynes, UK). The chamber filled with silicon oil and resealed. Systemic antibiotics (Betamox, Norbrook Laboratories, Carlisle, UK; or Metacam, Boehringer-Ingelheim, Ingelheim, Germany) and analgesic (Ketofen, Merial, Harlow, UK) were injected

prophylactically for 5 days after each experiment. After a period of recovery the animal was allowed to return to littermates. At the end of the terminal imaging session, the animal was euthanized with an overdose of barbituates (Euthatal) via intravenous injection.

Data Acquisition

Visual stimuli were produced by a visual stimulus generator (VSG, Cambridge Research Systems, Rochester, UK). Sixteen out of 20 stimuli consisted of low frequency (0.1-0.2cy/deg) and high (0.45-0.6cy/deg) frequency, high contrast, sinusoidal gratings (Frequency increasing with age; ~ 0.2 and 0.4 for an animal at 5 weeks of age, up to 0.3 and 0.6 for animals >10 weeks of age) drifting back and forth at 2 cycles/second and presented at four different orientations (0, 45, 90 or 135 degrees). Four blank stimuli (including one also used for reference image calculation) consisted of a blank screen of the same mean luminance as the grating (~40cd/m²). Computer controlled occluders in front of both eyes were used for monocular stimulation.

The cortex was illuminated with red light of 700nm. This is achieved using a halogen light and a number of bandpass filters to achieve the desired wavelength used for imaging. Two light guides allow the light to be directed accurately and achieve an even illumination of the cortex. Wavelengths of 540 –750 (up to 900nm in some cases) are used to achieve intrinsic images. Shorter wavelengths are closer to the absorption maxima for oxy-haemoglobin. At this end of the light spectrum a large proportion of the signal measured comes from the change in the oxygenation state of the blood. At longer wavelengths, a much smaller proportion of the oxy-haemoglobin component is measured and a larger proportion of the signal comes from light scattering changes due to capillary expansion and ion movement. Although using light of a higher wavelength reduces the absolute signal that can be measured, it greatly reduces blood vessel noise from changes in the volume of oxygenated blood (which follow the initial de-oxygenation caused by 'normal' activity). Also higher wavelengths allow deeper penetration of the tissue.

Images of the intrinsic signals were captured using an enhanced differential imaging system (Imager 2001, Optical Imaging Inc., Mountainside, NJ) with the CCD camera focused ~500µm below the cortical surface (Fig. 1.21). A macroscope tandem- lens

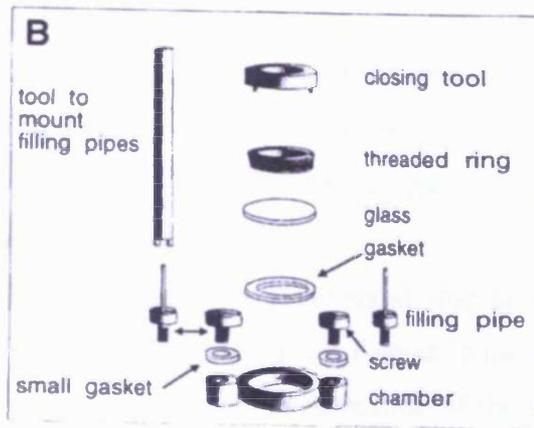


Figure 1.20 Titanium chamber used in optical imaging (Adapted from Bonhoeffer and Grinvald 1996)

Then chamber is filled with silicon oil via the filling pipe. The rubber gasket and glass plate are held in place with a threaded ring.

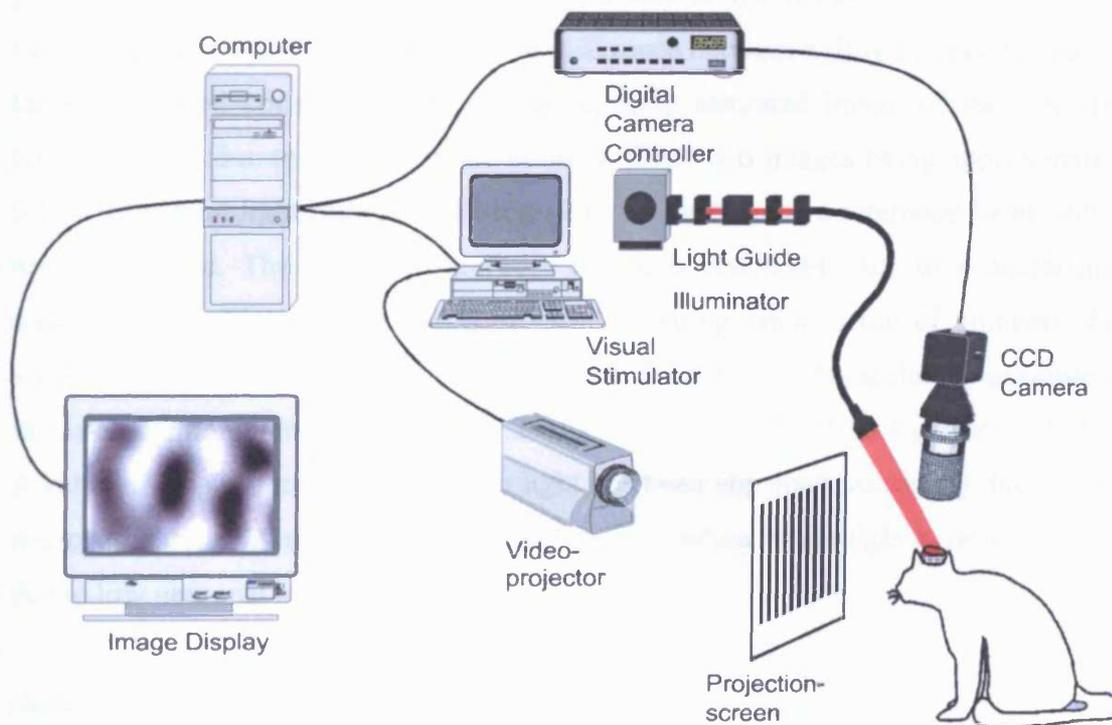


Figure 1.21 Experimental set-up for optical imaging (Adapted from Bonhoeffer and Grinvald 1996)

Images are taken from the exposed cortex of an animal while it views gratings of different orientations. The signal obtained from the cortex is captured using a CCD camera. In the computer a reference frame is subtracted. The resulting data series is visualized on a greyscale. Black represents high neuronal activity and white, low neuronal activity.

arrangement is used, made up of two front-to-front photographic lenses (50mm, f 1.2). This provides a very high numerical aperture and gives a very low depth of field. Therefore when focused (i.e. 500 μ m) below the cortical surface, the surface vasculature is sufficiently blurred.

Seven frames of 600ms duration were collected during 4.2 seconds of stimulus presentation, preceded by an additional 3 frames collected (600 ms each) for (baseline) 'first frame' analysis with the presentation of the stationary stimulus on the screen. Each stimulus was followed by a 7 second, inter-stimulus interval during which the next stimulus was presented stationary.

The signal obtained from the cortex is in the form of a charge. Photons reflected from the cortex hit the CCD chip liberating electrons that accumulate in wells (A 'well' is where electrons accumulate onto one pixel on the CCD chip). This 'charge' is digitised in the 8-bit camera. In the Imager 2001 box, this 8 bit data is subtracted from an 8 bit reference frame, after conversion back to analogue data. This reference frame pictures the overall light reflection (modulation) of the cortex (Fig. 1.22). To the naked eye there would be no discernible difference between a fully saturated image of the un-activated cortex and the, not quite, fully saturated image of the activated cortex. This is due to the difference between these two images being approximately 0.1% of the total light reflected. With a 12 or 16 bit camera, a reference frame would not be required. The resulting reference image is converted back to a digital data series. The resulting file format is a 16 bit 'floating point' array of numbers. For visualisation purposes, the 16 bit data is compressed to an 8-bit scale. An example of this is ocular dominance maps (Fig. 1.23). These are visualised on a greyscale, 0-255. A value of '0' appears as black, when light has been absorbed maximally due to high neuronal activity. A value of '255' value appears white, when light is reflected back due to low neuronal activity.

Data Compression

To maximise data quality, it would be ideal to keep every frame of every trial. This however leads to vast amounts of data. The amount of storage space needed for a typical experiment lasting one hour, with a data acquisition of 3 seconds and inter-stimulus interval of 10 seconds would amount to 30 Gigabytes (Bonhoeffer and

Grinvald 1996). Apart from the obvious storage problems, data transfer time would also become unmanageable.

So data reduction needs to occur at several stages during data acquisition. Firstly, video frames are accumulated into data frames. Data is averaged over identical stimulus conditions, averaged over time, and trials added together to form 'blocks'.

'On chip' binning is another way of data compression. A 2x2 or 3x3 'on chip' binning occurs on the CCD chip. The value (charge) for several adjacent pixels is combined. All these combined reduce the amount of data by over 1000-fold.

Image analysis

Mechanical and Biological Noise

Small magnitude of light intensity changes (<0.1%), difficulties in obtaining even illumination over the cortex, and biological noise all contribute to poor image quality. Mechanical noise and the stochastic nature of light absorption by the CCD chip ('shot noise') contribute to high spatial frequency noise. Low spatial frequency noise is dominated by biological noise such as slow overall changes in the saturation levels of blood, heartbeat and respiration artefacts. Since the high frequency noise is normally at a much higher frequency than the periodicity of the functional domains, filtering it out will not significantly effect the image. Biological noise presents a greater problem since it is often similar or smaller in periodicity than the functional domains. To combat this, in all cases a 'first frame' analysis is used. If the periodicity of the noise is slower than the duration of the trial, it will appear to some extent in all subsequent frames in the trial. Therefore, the image aquired from the first three frames (containing the slow noise) is subtracted from subsequent images. Data aquisition can also be synchronised to coincide with respiration and hearbeat.

To correct for the uneven illumination, a baseline image needs to be subtracted from the stimulus-related images. In other words, one needs to subtract the activity maps by a cortical stimulus independent image. This can be done in one of two ways. The use of a 'blank' image obtained from an un-stimulated cortex is subtracted from all activity maps. This type of blank is based on no assumptions being made about the complete set of stimuli required to make the cortex respond uniformly. Although this

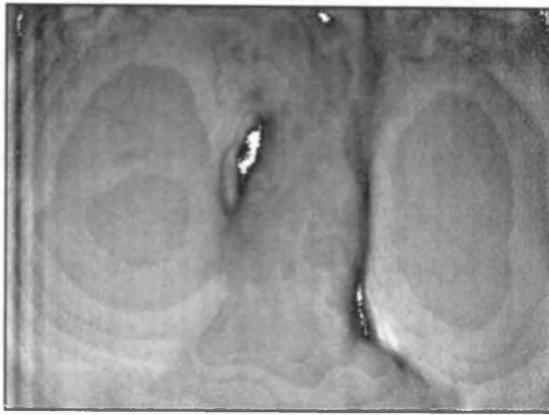


Figure 1.22. Reference frame recorded from cat visual cortex

This image shows the overall light reflection (modulation) of the cortex. The reference frame is subtracted from all subsequent images.

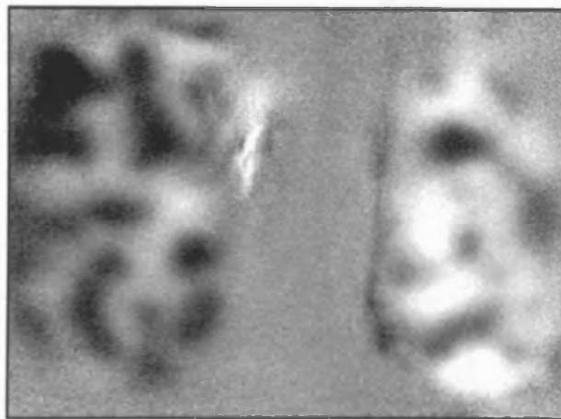


Figure 1.23 Unfiltered ocular dominance map from visual cortex

For illustrations, signals were clipped at 1.5% and 98.5% so that the most responsive pixels were set to black, the least responsive set to white and the signal amplitude displayed on an 8-bit grey-scale.

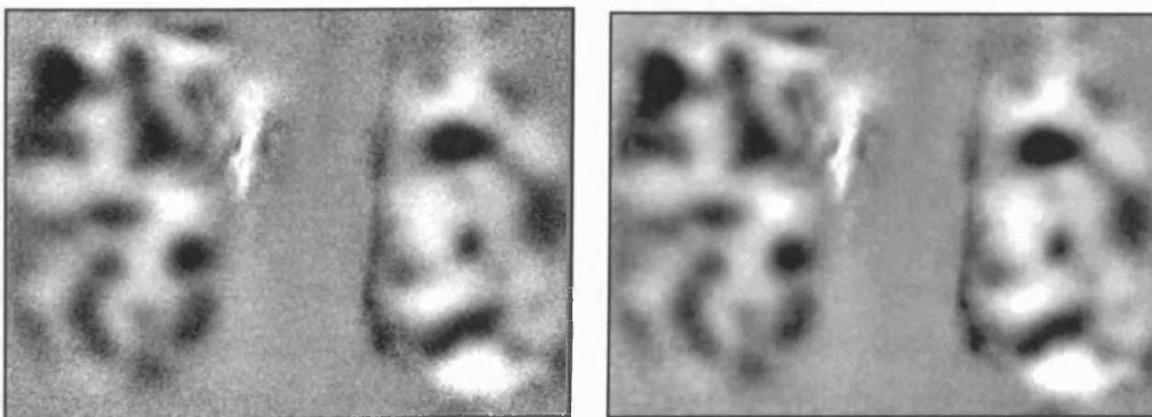


Figure. 1.24 Ocular dominance map of visual cortex

With high pass filter (100 pixels) - left side, and with high pass (100 pixels) and low pass (5 pixels) filtering applied - right side. Within each hemisphere, black represents high neuronal activity, and white, low neuronal activity. With respects to the left vs right eye map here, dark areas represent neurons responding preferentially to the left eye and light areas responding preferentially to the right eye.

is an advantage, the disadvantage of this type of subtraction stems from gross changes in blood flow when the cortex is stimulated. These activity-related changes are strong and can often lead to distortion of some structures.

The other option is to use a 'cocktail blank'. This blank is obtained from a uniformly activated cortex. In other words, the cortex has been presented with a set of stimuli that should uniformly activate the cortex and the combined data can then be used as the 'cocktail blank'. This type of blank is more useful for obtaining orientation preference maps, because the only difference between a single activity map and the baseline image is the orientation of the stimulus. However, the disadvantage it has is that it makes assumptions about the architecture of the cortex. Stimulating the cortex with a complete set of orientations does not always result in all areas being stimulated uniformly.

Data analysis

Activity maps were analysed using IDL software (RSI, Boulder, CO). Ocular dominance maps were obtained by dividing the sum of responses to all 4 orientations through one eye by the similar sum of responses through the other eye.

Single condition maps responses were divided (a) by responses to the blank screen and (b) by the sum of responses to all four orientations to obtain orientation preference maps (pseudo-color coded). Polar maps add another dimension. The colour here represents information about both the preferred angle and brightness as the magnitude of preference.

Filtering

The resulting bitmaps were clipped and filtered to improve the resolution (as detailed above). The clipping range was set at 1.5%, 98.5%. Since the pixel greyscale is approximately normally distributed, clipping the image removes the upper and lower percentile (very high and very low) values. The resulting pixel range is re-scaled to fit to 256 greyscale. (Fig. 1.23) High pass filtering was essential to remove the global DC signal component, which is superimposed on the spatially restricted stimulus selective ("mapping") signal (Bonhoeffer and Grinvald 1996). With the tandem macro-lens set-up, (i.e. no additional lenses) the maximum area that can be recorded is approximately

6x8mm. At this magnification each pixel is approximately 22µm in size. With the high pass filter, for example, set to 100, every signal over 100 pixels wide is filtered out of the image. A 100 pixel high pass means that anything over 2200µm in size will be subtracted from the image. Ocular dominance domains are in the order of 600-1000µm in size so a high pass filter of 100 pixels is well outside that range hence doesn't remove any signal of interest (Fig. 1.24 - left map). In many cases an extra lens was used to give a 0.67 magnification. The resulting maximum area available was 9x12mm, with each pixel approximately 32µm in size. Without the use of a low pass filter the picture appears 'grainy' due to neighbouring pixels representing a different value on the grey scale. These values also include noise both biological and physical. A low pass filter averages over the set number of pixels using a Gaussian weighting factor (Fig. 1.24 - right map). This results in effectively smoothing the image and allowing better definition.

Secondary data analysis

Ocular dominance

A region of interest, taking care to exclude blood vessel artefacts, was defined by the visually responsive part of the image. Within this, pixels are assigned to the left and right eye depending on whether their value was greater or less than 1. From this the resulting percentage of cortex responding to each eye was obtained.

Orientation selectivity ratio

A quantitative measure of orientation selectivity (index) (OSI) was generated from the responses of each pixel as:

$$OSI = \frac{\sqrt{(R_0 - R_{90})^2 + (R_{45} - R_{135})^2}}{R_0 + R_{45} + R_{90} + R_{135}},$$

where R_0 , R_{45} , R_{90} and R_{135} represent the responses in each of the four iso-orientation maps (Bonhoeffer *et al* 1995). This value was calculated from 'blank' corrected data as this makes no assumptions about the overall activation of the cortex. The OSI represents the magnitude of the orientation preference vector divided by the sum of all responses; it is therefore normalised to values between 0 and 1. A ratio of deprived eye to non-deprived eye (DE: NDE) was then used for comparisons between the two eyes.

AIMS and OBJECTIVES

A

It is predicted that if the amount of synaptic space in V1 occupied by afferents from the two eyes depended on competition between the afferents, then prior strabismus should serve to 'protect' to a large extent, against the effects of monocular deprivation.

By comparison, according to the BCM theory, strabismus should have a 'partial protective' effect on the effects of MD. Strabismus should result in 2 populations of cells forming with no connections for between eye interactions, and only one type of input per cell. Cells dominated by the open eye would remain unaffected by deprivation (Ref. Fig 2.1). However, in those cells dominated by the eye that is being deprived, the modification threshold falls quickly, LTD becomes difficult to induce, and changes take much longer. Therefore, the deprivation effect as a whole would be 'reduced'. This conclusion would be strengthened if orientation selectivity through the deprived eye was affected similarly. Recovery from MD (with or without prior strabismus) should be complete.

B

Binocular vision intercalated into reverse occlusion paradigms appears to improve considerably the recovery of visual acuity after RO (Murphy *et al* 2002). Work aims at providing physiological correlates that underlie some of the behavioural (and anatomical) changes seen during RO with and without binocular vision, and recovery afterwards. It is predicted that a brief period of binocular vision between MD and RO should permit swift and substantial physiological recovery of the DE. However, if the two eyes' inputs were de-correlated during that brief period of binocular vision between MD and RO, little recovery of the DE should be seen. Upon termination of RO, recovery of the recently deprived eye should be minimal, as with immediate RO.

C

Computer simulations will be employed to test the time course and final outcome for the experimental paradigms used in this thesis. It is predicted that BCM learning will most accurately predict the outcomes from the data presented here, while correlation-based models like PCA, will only account for some of the experimental outcomes.

CHAPTER 2

INTRODUCTION

Ocular dominance plasticity

As outlined in the general introduction, two candidate models of ocular dominance plasticity have been fiercely debated. Are the interactions between the two eyes competitive or associative? The substantial visual recovery seen after MD following the reopening of the deprived eye (Mitchell *et al* 1977; Griffin and Mitchell 1978; Mitchell and Gingras 1998) called into question inter-ocular competitive mechanisms of visual cortical plasticity, but is in agreement with associative mechanisms such as the BCM theory. The BCM theory is broadly speaking an extension of Hebb's rule. It allows synaptic change to be bi-directional. The modification of one set of synapses in one direction (LTP) does not need to be matched by an equal and opposite modification (LTD) in a second group of synapses. Instead of absolute levels of pre-synaptic and post-synaptic activity governing change, as in competitive models, the BCM theory achieves stability by allowing the modification threshold to shift as a function of time-averaged post-synaptic activity (for reviews see Kirkwood *et al* 1996; Rittenhouse *et al* 1999; Blais *et al* 1999).

However, the BCM theory only predicts recovery from monocular deprivation if the inputs from the two eyes are correlated during the recovery period – that is, if pre-synaptic (geniculocortical) activity coincides with post-synaptic (cortical) activity above the modification threshold. De-correlation of left-and right-eye pre-synaptic activity, caused by a strabismus, largely eliminates correlation between deprived-eye afferent activity and post-synaptic activity and should therefore disrupt recovery from monocular deprivation. This idea was tested in a recent study by Kind *et al* (2002). They studied concordant binocular recovery from 10 days of monocular deprivation, induced at the height of the critical period, and strabismic recovery (with a squint induced in the non-deprived eye upon termination of the period of MD). Results showed that the area of cortex responding to deprived-eye stimulation was smaller in strabismic kittens than in those with normal binocular vision during recovery. Orientation selectivity in deprived-eye regions was reduced in strabismic kittens also. Visual acuity in the formerly deprived eye was lower following strabismic recovery compared to normal binocular recovery, paralleling what was reported

physiologically. The disruption of recovery from MD by induced strabismus lends strong support to the BCM theory.

An earlier study carried out by Malach and Van Sluyters (1989) reported that strabismus had no effect on recovery from monocular deprivation. However, the angle of squint in those kittens was small, which may well account for greater recovery, since the residual correlation between the two eyes would have been considerable. In addition, the kittens were kept in the dark during the period prior to MD. Susceptibility to LTP induction coincides with the critical period and, like the critical period, can be prolonged by rearing animals in darkness (Kirkwood *et al* 1995). Hence, the predisposition of neurones in these animals to subsequent recovery would have been increased.

From birth (in cats) the geniculocortical afferents from the two eyes are overlapping in layer IV (LeVay and Gilbert; 1976, LeVay *et al* 1978) and segregate into OD columns from the second week onwards (Crair *et al* 2001). In monkeys, periodic labelling of geniculocortical afferents is evident from birth (Horton and Hocking 1996). In cats, functional OD columns can be visualised from as early as the second postnatal week (Crair *et al* 1998; Crair *et al* 2001). In strabismic cats (induced within the first few postnatal weeks), the segregation of OD columns is greater than in non-strabismic cats (Shatz *et al* 1977; Löwel and Singer 1993; Löwel 1994; Löwel *et al* 1998) when ascertained several months later. In tandem, a breakdown in cortical binocularity occurs. If cortical territory occupied by afferents from the two eyes depended on competition between these afferents, then a prior strabismus should 'protect' against the effects of monocular deprivation, since geniculate terminals would have a greatly reduced number of binocular neurones to compete for. This hypothesis was put forward by Mustari & Cynader (1981). They gave two possible outcomes. First, the much greater separation of ocular dominance bands in strabismic animals might reduce the amount of competitive interaction between right and left eye geniculocortical afferents, since very few of them would contact the same post-synaptic neurones. The decreased competition might protect cortical neurones from the ocular dominance shift normally observed after monocular deprivation. Second, it had been reported that binocularly driven neurones were the first to be lost during monocular deprivation (Hubel and Wiesel 1970; Olson and Freeman 1980). The loss of binocularity caused by strabismus produces effects that resemble the initial stages

of monocular deprivation. Hence strabismus could facilitate these changes and an enhanced susceptibility to monocular deprivation might be seen.

From natural eye opening (~P10) kittens were made strabismic in one eye prior to a period of monocular deprivation (in the same eye), and compared to kittens with just monocular deprivation. In control kittens with the same MD regime, a pronounced ocular dominance shift towards the non-deprived eye was seen in both hemispheres. In strabismic kittens, a similar shift was seen in the hemisphere ipsilateral to the deprived eye. However, in the hemisphere contralateral to the deprived eye the shift was much reduced, suggesting a protective effect of the prior strabismus. It had been noted previously that ocular dominance bands representing the contralateral eye were larger than those of the ipsilateral eye in both normal and strabismic cats (Wiesel and Hubel 1963; Shatz and Stryker 1978). Therefore, Mustari and Cynader (1981) suggested the competing LGN terminals representing the non-deprived eye are closer to the cells being influenced by the deprived eye in the hemisphere contralateral to the deprived eye. This distance is probably increased in the cortex of strabismic cats, hence the deprived-eye dominated neurones may be less susceptible to an ocular dominance shift.

Although this study is not conclusive (not least because of very small sample sizes of cells per animal, and the lack of data regarding the orientation selectivity of single cells), it raises interesting questions about the mechanisms governing cortical plasticity, particularly since the BCM theory was not put forward until after this study was done.

As mentioned above, if competitive mechanisms between the two eyes for cortical space governed cortical plasticity, a strong 'protective' effect of a prior strabismus on the effects of monocular deprivation might be expected. Strabismus leads to a breakdown of binocular interactions between left- and right-eye afferents, hence a loss of competition. In contrast, the BCM theory predicts a 'partial protective' effect of a prior strabismus. After induction of strabismus de-correlating the inputs to the two eyes means that pre-synaptic activity would not coincide with post-synaptic activity above the modification threshold (θ_M). Therefore θ_M would initially left-shift on a similar time scale as with MD (Figure 2.1a). However, after several days of strabismus, two separate cell populations will develop – each one solely driven by one

Figure 2.1. The ϕ function with different values of the modification threshold θ_m at various time points under visual manipulation

According to the BCM theory, at active synapses LTP occurs when ϕ is positive and LTD occurs when ϕ is negative. When C , the post-synaptic activity is greater than θ_m , the ϕ function is positive.

Continuous black line in all diagrams represents expected θ_m with normal visual experience

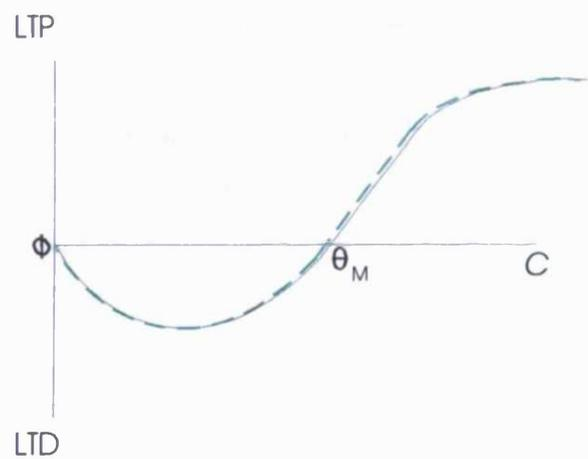
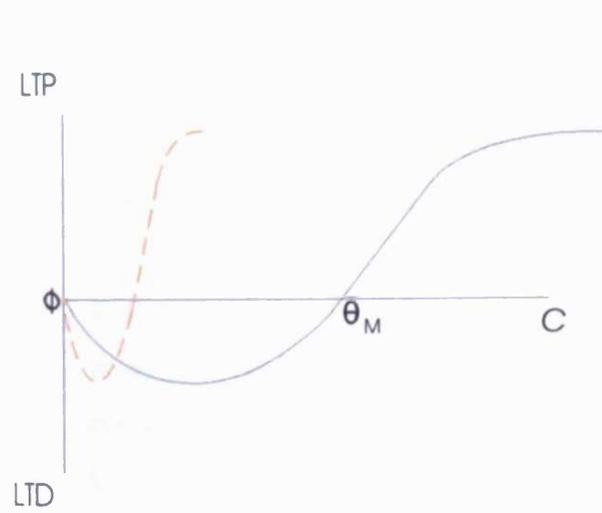
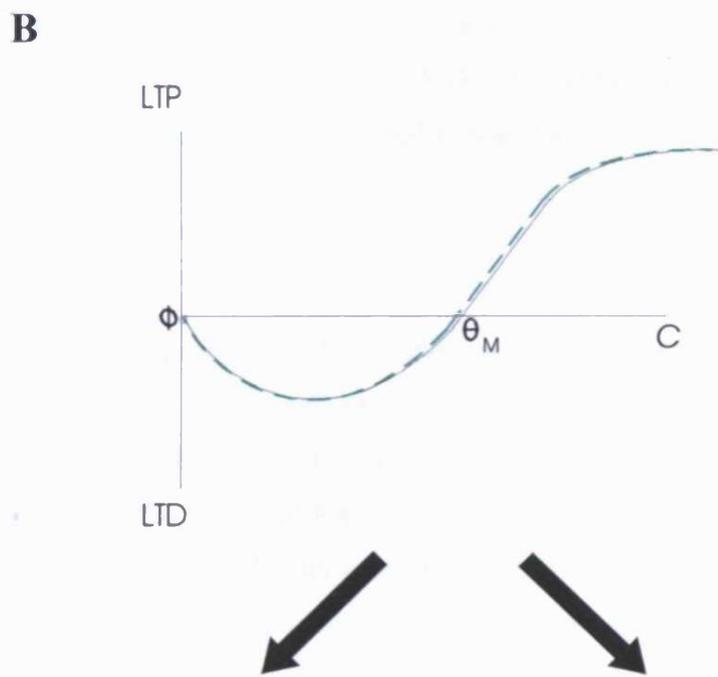
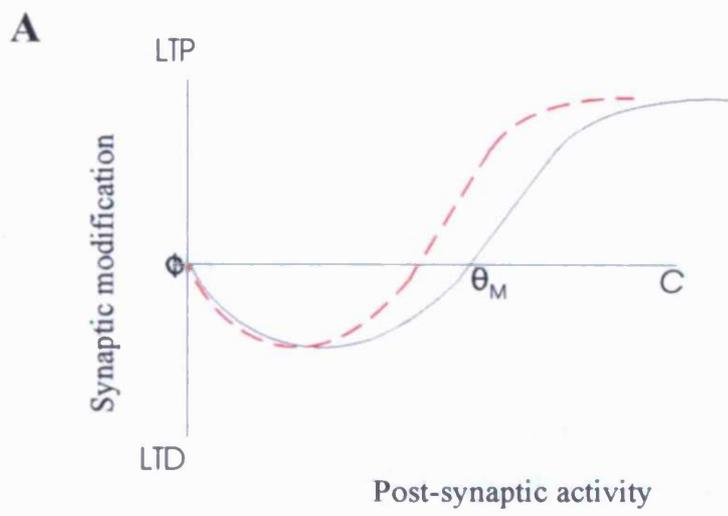
Expected θ_m after:

A) Strabismus of 1-2 days

B) Immediately prior to MD.

C and D) Monocular deprivation in deprived (C) and non-deprived (D) dominated cells.

In (A) de-correlating the inputs initially causes a leftward shift in θ_m similar to MD. However, once binocular connections (and inter-eye correlations) have been lost intra-eye correlations within the two populations of monocular cells would drive θ_m back up to normal or near normal levels (B). Closing one eye would remove all input from DE dominated cells and θ_m would fall very quickly - similar to BD (C), but in NDE dominated cells θ_m would not change (D). The result would be a limited deprivation effect.



eye. By the time monocular deprivation is initiated (P35), θ_M would have returned to a 'normal' or 'near normal' level (Fig. 2.1b), with each eye retaining a separate population of cells with only one type of input. Upon initiating MD, in those cells controlled by the eye that is deprived, *all* input is lost, therefore θ_M would left-shift very quickly and to a great extent (as with binocular deprivation). Long-term depression would occur, but it would be limited, and would occur at a much slower rate compared to a 'normal' MD effect. Cells dominated by the open eye prior to deprivation, independent of any influence from DE cells, would remain unaffected by the deprivation (Fig 21.c). A question also arises whether a prior strabismus offers a lasting protection against the effects of MD; i.e. during recovery from MD. Would recovery of OD from MD proceed normally in animals with a strabismus?

Orientation selectivity

It is apparent that spontaneous activity, independent of geniculate input, in the visual cortex, has some role in the generation of orientation selectivity. Direct electrical stimulation of the optic nerve (in ferrets) was used to synchronously activate retinal ganglion cell axons (Weliky and Katz 1997). This meant that the degree of correlated activity between ON and OFF ganglion cells was above normal levels. The result was reduced orientation selectivity of cortical cells. ON and OFF responses of cells within the LGN were unaffected, adding to the suggestion that altering the structure of correlated activity within the visual pathway disrupts cortical orientation tuning and this disruption can occur without direct LGN disruption. Correlated patterns of spontaneous activity in the developing ferret retina, that sweep across the retina in 'waves' of ganglion cell activity has been shown by Meister *et al* (1991). Retinal spontaneous activity appears crucial for the development (Penn *et al* 1998; Cook *et al* 1999) and maintenance (Chapman 2000) of LGN specific layers. Much less is known about the degree to which spontaneous activity in the LGN is involved in cortical map development. Electrophysiological recordings from ferrets prior to eye opening show synchronous bursts of action potentials within LGN layers (Weliky and Katz 1999). Correlations in firing patterns between neurones within eye specific layers were high while those between eye specific layers were weak. However, significant binocular correlations were present even when retinal activity was removed but was abolished

when cortical feedback was removed. It appears that the LGN does not simply relay patterns of retinal activity to the cortex but this activity is transformed by corticothalamic interactions (see review Weliky 2000). Since the patterns of spontaneous activity within the cortex are not yet known it is difficult to know how reliably this activity is connected to LGN activity or to what extent it guides the underlying scaffold of connections for cortical map development.

Optical imaging of kittens that have been binocularly deprived from birth revealed orientation maps of a normal layout (Godecke 1997; Crair *et al* 1998). In young ferrets, two weeks prior to natural eye opening, orientation selective responses have been recorded through the closed eye-lids (Krug *et al* 2001) and in neonatal kittens about one quarter of neurones have some orientation selectivity (Blakemore and Van Sluyters 1975; Fregnac and Imbert 1978). The layout of the orientation maps appears to change little in the first few weeks after eye opening regardless of visual experience (Chapman *et al* 1996; Godecke *et al* 1997; Crair *et al* 1998). Indeed orientation maps in cat V1 appear identical for the two eyes even if they have had no common visual experience (Kim and Bonhoeffer 1994; Godecke and Bonhoeffer 1996). Is this further evidence for a role of spontaneous activity, independent of visual experience, in orientation map development, or perhaps an underlying genetic determinant of basic cortical map structure?

Although the ocular dominance domains have greater separation in kittens reared with strabismus, little effect of squint is seen on the layout of orientation preference maps. Iso-orientation maps appear to be continuous across the borders of adjacent ocular dominance columns and iso-orientation lines and OD column borders tend to intersect at right angles to each other, like in normal cats (Hubener *et al* 1997). Mean pinwheel densities between normal and strabismic animals was also the same (Löwel *et al* 1998; Engelmann *et al* 2002). Orientation selectivity appears to be lower in deprived eye regions of kittens made strabismic after deprivation (Kind *et al* 2002).

It seems likely that orientation plasticity obeys the same Hebbian learning rules as ocular dominance.

Since it is predicted that a strabismus prior to a period of MD should protect against the changes in ocular dominance, this hypothesis would be strengthened if orientation selectivity were also preserved in the deprived eye. Recovery of these parameters should also be effected by the prior strabismus. As predicted and shown in the BCM

model, reopening the deprived eye and allowing correlated vision to both eyes allows the deprived eye to recover almost fully. If however the two eyes are de-correlated during recovery, post-synaptic activity is kept below θ_M and LTP can not be initiated. However, this may not apply to the animals with prior strabismus. Here, one effectively has two separate populations of cells, each with its own θ_M , and recovery of the DE might be expected to proceed normally.

Visually Evoked potentials

The technique of recording visually evoked potentials has been applied successfully for 30 years for assessing the visual system both, experimentally and clinically (Spekreijse *et al* 1972; Arden *et al* 1974; Bornsterin 1976; Levi and Harwerth 1978; Snyder and Shapley 1979; Kraut *et al* 1985; Schroeder *et al* 1991; Aminoff and Goodin 1994). The visually evoked potential (VEP) is the electrical representation of the mass action of all cortical neurones around a site of recording, to a visual stimulus (Padnick and Linsenmeier 1999).

Behaviourally (in human subjects) strabismic related deficits include: reduced visual acuity in accordance with reduced contrast sensitivity, spatial resolution, vernier acuity (Levi and Klein 1985) and spatial distortion of images (Hess and Holiday 1992; Hess *et al* 1978).

In animals, the use of VEPs as a measure of visual acuity has, in some instances been preferred over other methods. For instance, discrepancies in results from single cell recordings (Ikeda and Tremain 1979; Cleland *et al* 1982), the advantage that the VEP data is quantitative (both absolute levels of response and the ratio between the two eyes and hemispheres), is less subject to sample bias (as can be the case with electrophysiological data) and can be recorded chronically to assess the dynamics of cortical plasticity, has made it a useful tool.

Visually evoked potentials are typically elicited using square wave gratings that are phase reversed (at 1Hz) on a monitor screen. Recordings are often taken intracortically in chronic experimental conditions and have been shown to alter with depth (Pizzorusso *et al* 1997). However, they can also be recorded from the cortical surface and in humans through the skull.

The VEP is commonly quantified by measurement of the peak-to-trough heights of the main response component (Insert in Fig. 2.2). Note that the VEP waveform changes with spatial frequency (Fig 2.2).

Results from behavioural and electrophysiological measurements of visual responses have been shown to be similar and comparable. Figure 2.3 (From Von Grunau and Singer 1980) show a deficit in the strabismic eye of kittens tested for contrast sensitivity tested both electrophysiologically and behaviourally. The amplitude of the response is reduced over a range of spatial frequencies in the strabismic eye. Although the maximum cut off points in many cases were very similar in the same study by (Freeman *et al* 1983), a number of other studies have shown a reduction in grating acuity in the strabismic eye of cats (Jacobson and Ikeda 1979; Cleland *et al* 1982) and in monkeys (Baker *et al* 1974; Harwerth *et al* 1983). The effects are expectedly more pronounced in monocularly deprived kittens (Fig. 2.4 a and b) where severe deficits are seen in the deprived eye (Synder and Shapley 1979; Freeman *et al* 1983; Speed 1991).

Electrophysiological parameters

More subtle deficits in strabismic animals can be detected with single unit recordings. As mentioned earlier, with strabismus, binocular cells are lost and neurones generally respond solely to one eye or the other (Hubel and Wiesel (1965) although the absolute number driven through each eye is very similar (Chino *et al* 1983; Mower *et al* 1982; Singer *et al* 1980). The proportion of orientation selective cells does not appear to differ between the deviated and non-deviated eye (Kalil *et al* 1984). Receptive field size (Chino *et al* 1988) and spatial response properties of neurones was reported to be no different from normal animals (Singer *et al* 1979, 1980; Chino *et al* 1983, 1988; Freeman and Tsumoto 1983; Crewther and Crewther 1990; Blakemore and Vital-Durand 1992; Eschweiler and Rauschecker 1993; Roelfsema *et al* 1994; Kiopes *et al* 1998), however, deficits in contrast sensitivity through the deviated eye have been shown (Von Grunau and Singer 1980). Regions of the cortex representing the temporal retina are most poorly activated by cortical neurones from the deviated eye (Kalil *et al* 1984). The visual deficits of the deviated eye appear to be related to the functional suppression of that eye when concurrent activation of the non-deviated eye occurs (Freeman and Tsumoto 1983).

Figure 2.2 Dural VEP's recorded from kitten V1 at P34

Raw traces from the right hemisphere of kitten 280 made strabismic in the RE at P23. VEP's were recorded from a medial posterior position on the dura. VEP's were elicited with horizontal gratings phase reversed at 1Hz over a range of spatial frequencies 0.2 -1.6 cyc/deg.

Insert box shows peak-to-trough measurement used for the amplitude of the VEP response.

Right eye

Cycles/degree

Left eye



0.2



0.28



0.4



0.56



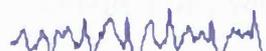
0.8



1.13



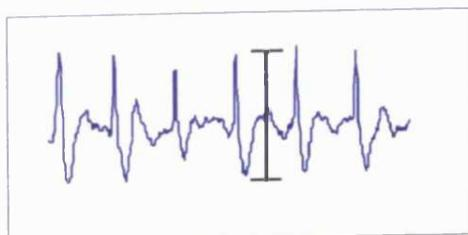
1.6



Blank



500 μ V
500ms



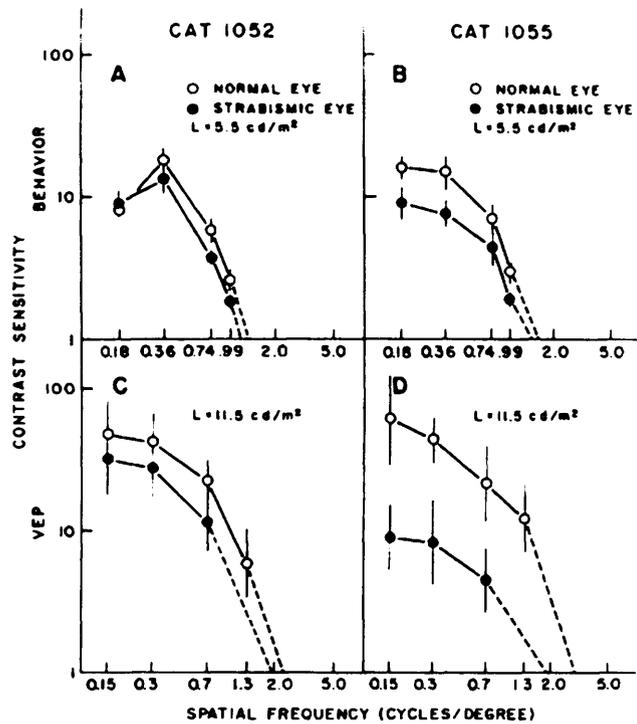


Figure 2.3 Comparison of contrast sensitivity for normal and strabismic eyes obtained behaviourally (A, B) and electrophysiologically (C, D) for 2 kittens (From Von Gruau and Singer 1980)

The deficit of the strabismic eye compared to the normal eye can be appreciated both behaviourally and electrophysiologically.

Dotted line represents extrapolation to obtain spatial frequency cut-offs.

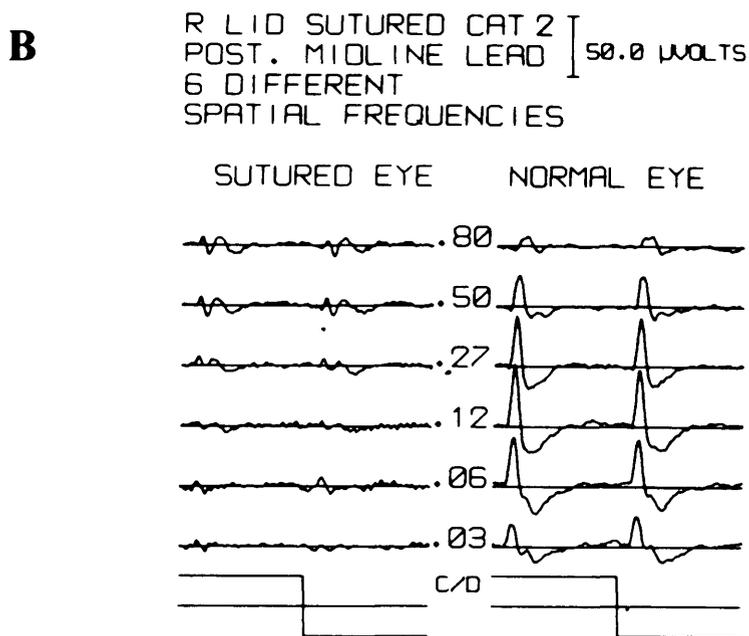
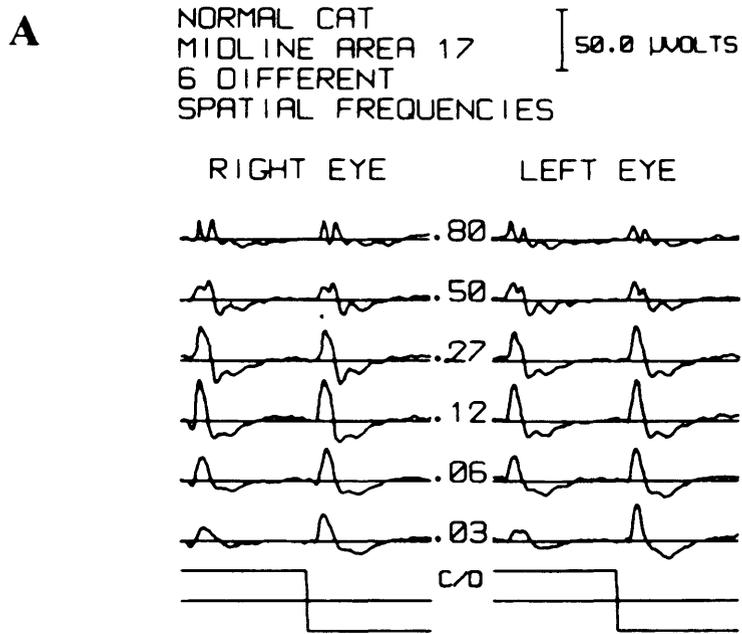


Figure 2.4 VEPs through each eye of a normal and monocularly deprived cat, elicited by 1 Hz square wave contrast reversal (From Snyder and Shapley 1979)

A Normal cat.

B Monocularly deprived cat - only residual VEP responses are seen at the lowest spatial frequencies of the sutured eye.

METHODS

Strabismus monocular deprivation

In six kittens a convergent squint was induced surgically between postnatal day P19-23. This was done to coincide with the beginning of the critical period, during which strabismus been shown to cause OD segregation within only a few days (Trachtenburg and Stryker 2001).

The lateral rectus muscle of the right eye was severed and surrounding connective tissue removed. In two other animals a divergent squint was achieved by severing the lateral medial muscle of the right eye. The animals were allowed to recover and returned to the litter.

From P35-45 these 8 animals were monocularly deprived - five in the eye that had been made strabismic and 3 in the opposite eye. The conjunctiva was dissected from the inside of the eyelids and sutured shut using no.5 vicryl (absorbable); the outer lid margins were sutured using no.4 silk (non-absorbable). The eye was treated with antibiotic ointment and surveyed every day for signs of infection or reopening.

In 5 additional kittens (with no prior strabismus) P35-45 one eye was monocularly deprived from P35-45. In all kittens at P45, the sutured eye was reopened, cleaned, treated with sterile eye drops and allowed to recover.

The angle of squint in strabismic cats was assessed on the day of the final imaging session. The animal was paralysed (using i.v. infusion of Gallamine) to arrest eye movement. An ophthalmoscope was used to find the position of the optic disk and area centralis in each eye. These were then back-projected onto a screen and the relative position in the strabismic eye compared to the normal eye. The angle of squint was hence calculated.

Convergent squint angles ranged from 7-15° in four animals. Two kittens had barely detectable squints (3-4°). In the two divergent squinting kittens, one measured 10° and the other was approximately 45°.

Optical imaging

Animals were implanted with a chamber and imaged, if possible, on the day of eye closure (P35), and again (all subjects) on the day of eye opening (P45). Subsequent imaging sessions were generally 3-5 days, 11-13 days and 21-24 days after eye opening. This is the first longitudinal study of the effects of MD and subsequent recovery. Such an approach overcomes the uncertainties inherent to inter-individual comparisons and greatly increases statistical power. Animals and even more so, littermates can vary widely with respect to the layout of OD columns, their periodicity and their contralateral bias (Kaschube *et al* 2002, 2003), and starting conditions differing between animals can therefore compound or obscure developmental changes. In contrast, in an individual animal, maps remain remarkably consistent in the absence of manipulation of visual input (Chapman *et al* 1996; Godecke *et al* 1997).

Optical imaging was carried out as described in General methods. On the final imaging session the dura was removed and an extended optical imaging session was carried out, followed in some animals by single-cell recordings.

Electrophysiology

Single cell recordings were carried out throughout V1. A number of electrode penetrations were made based on left and right eye OD columns identified with optical imaging superimposed on the blood vessel pattern. Effort was made to ensure that the chosen electrode penetrations were within or near to the area of V1 corresponding to the area centralis. Single cells were recorded quantitatively for orientation and spatial frequency tuning, discriminated by their spike shapes (Brainware, TDT, Alachua, FL).

Responses to drifting gratings of 16 different orientations were averaged over 5 trials. Preferred orientation and half width of tuning at half height, as well as ocular dominance was later determined.

Visually Evoked potentials

In four kittens, 2 strabismus and MD (934 and 280) and two just MD (070 and 370), after each optical imaging session, dural VEP's were recorded from V1 in each hemisphere and for each eye.

A silver ball-tip electrode was placed at a medial posterior position on the dura, i.e. close to the representation of the centre of the visual field. Visual stimuli were produced by a visual stimulus generator (VSG series three Cambridge systems) placed 57cm from the animal. This was done for ease of calculation for acuity (at 57cm, 1cm = cyc/deg) and to allow higher spatial frequencies to be accurately displayed. Stimuli consisted of high contrast square wave horizontal gratings phase reversed at 1Hz, with a drift velocity of 0.1 cyc/deg. Preliminary testing showed that a slowly drifting grating elicited a stronger response than a stationary grating. Signals were amplified at 10k and low pass filtered at 300Hz. Each spatial frequency was presented and repeated 20 times before the next was presented pseudo-randomly. Potentials were recorded at a frequency of 200Hz with the sweep length of 3000 milliseconds (containing 6 contrast reversals), with an inter-stimulus interval of 6000 milliseconds, using software written in Labview (National instruments, Austin, UK). A range of 7 spatial frequencies (and one blank) were tested for each eye and hemisphere separately: Low range: 0.05-0.4cy/deg or Mid range: 0.2 -3.2cy/deg. These results were later analysed to determine amplitude ratios and maximum frequency cut-off points, using IDL software (RSI, Boulder, CO).

In the case of the first session where time was limited, an abbreviated subset of spatial frequencies was used (0.2 -1.6 cyc/deg). For all subsequent sessions a full range of spatial frequencies was used (0.05-3.2cy/deg). For each stimulus, VEPs were averaged over 20 trials with 6 contrast reversals per trial. The peak-to-trough amplitude of each potential was obtained and plotted against spatial frequency into a graph. Cut-off spatial frequencies were obtained from extrapolating the last 4 descending data points to the intercept of with the blank response (spontaneous potential modulation).

RESULTS

All maps were filtered as described in General methods. For quantitative analysis a mask was applied to the maps to exclude blood vessel artefacts, which if included would have distorted the values obtained for each eye. An example of such masks is shown in Figure 2.5 as a white dotted line.

Ocular dominance

Monocular Deprivation

At five weeks of age (prior to monocular deprivation), the ocular dominance (OD) maps for all experimental animals without strabismus, appear fairly balanced with respect to the two eyes. This is illustrated for kitten 282 in Figure. 2.5a and 2.5b: column A, row A. Closer inspection of single condition maps in response to gratings of 0° (Figure 2.5a and b; row A, column B) shows slightly stronger responses from the contralateral eye in each hemisphere. Quantitative analysis (Fig. 2.6) highlights a slight OD bias towards the eye contralateral to the hemisphere imaged, as the left eye dominated 63.8% of the right hemisphere and the right eye dominated 58.6% of the left.

After a 10-day period of MD an ocular dominance shift to favour the NDE is seen in figure 2.5b; row B, column A and B. The DE responses are restricted to a number of dark 'islands', while the response to the NDE are enhanced (light regions). Single condition maps in column B confirm this with responses to the DE (Fig. 2.5a) being very weak and NDE responses prominent (Fig. 2.5b). Despite the original contralateral bias, the effects of MD are identical in each hemisphere. This is confirmed quantitatively. The DE now occupies approximately 19% of cortical territory in both hemispheres. A short period (3-4 days) of binocular recovery led to a rapid return of responses in the DE, with DE patches more prominent and enlarged (Fig. 2.5b; row C, column A and B). The DE occupies slightly less cortical territory than it did before MD (54.3% compared to 58.6 % and 32.3% compared to 36.2% for contralateral and ipsilateral hemispheres, respectively). The OD maps change little with further binocular recovery, with final values for both eyes being almost identical

Figure 2.5 a Cortical ocular dominance and orientation selectivity in the non-deprived (LE) of a kitten before and after monocular deprivation

Data is from kitten 282 which was monocularly deprived of vision in the RE for 10 days.

Column A - Ocular dominance (left eye/right eye): Patches of black represents high neuronal activity, and white, low neuronal activity. With respects to the left vs right eye map here, dark areas represent neurons responding preferentially to the left eye and light areas responding preferentially to the right eye.

Column B - Single condition (0deg/blank): The relative strength of the response is represented on the level of darkness. The darker the patch the greater the response.

Column C -Angle map: The resulting vector of responses to all orientations tested is allocated a colour to represent preferred orientation.

Column D - Polar map: The relative strength of the oriented response is represented on a scale of brightness.

Rows A-E represent time course: Immediately before closing the RE (P33), Immediately upon reopening of deprived eye (P43), then P47, P54, P65.

In Row C an example of a mask is shown by a white dotted line. It is used to exclude large blood vessels or other unwanted artifacts which could bias the result. Only the area within the mask is used for subsequent analysis.

Colour key represents preferred orientation in angle maps. Line arrows represent relative orientation of the head.

Of note: A blood- related artifact is present on the right hemisphere at P43. This was unavoidable as it developed during the course of imaging session. Despite this, it can be seen from the angle and polar maps in particular, that it did not effect the quality of the signal in the maps.

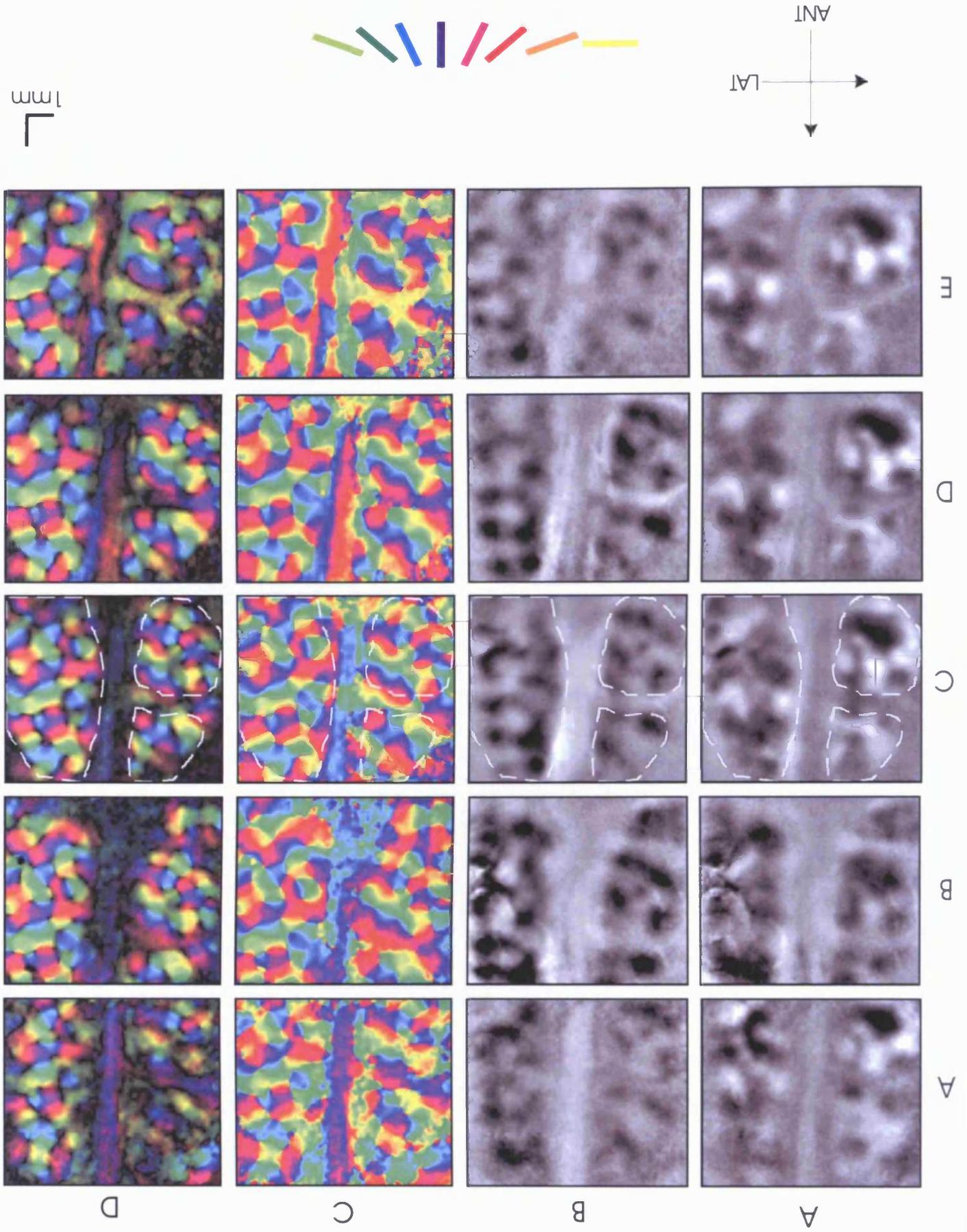


Figure 2.5 b Cortical ocular dominance and orientation selectivity in the deprived (RE) in a kitten before and after monocular deprivation

Data is from kitten 282 which was monocularly deprived in the RE for 10 days.

Column A - Ocular dominance (right eye/left eye): Patches of black represents high neuronal activity, and white, low neuronal activity. With respects to the right vs left eye map here, dark areas represent neurons responding preferentially to the right eye and light areas responding preferentially to the left eye.

Column B - Single condition(0deg/blank): The relative strength of the response is represented on the level of darkness. The darker the patch the greater the response.

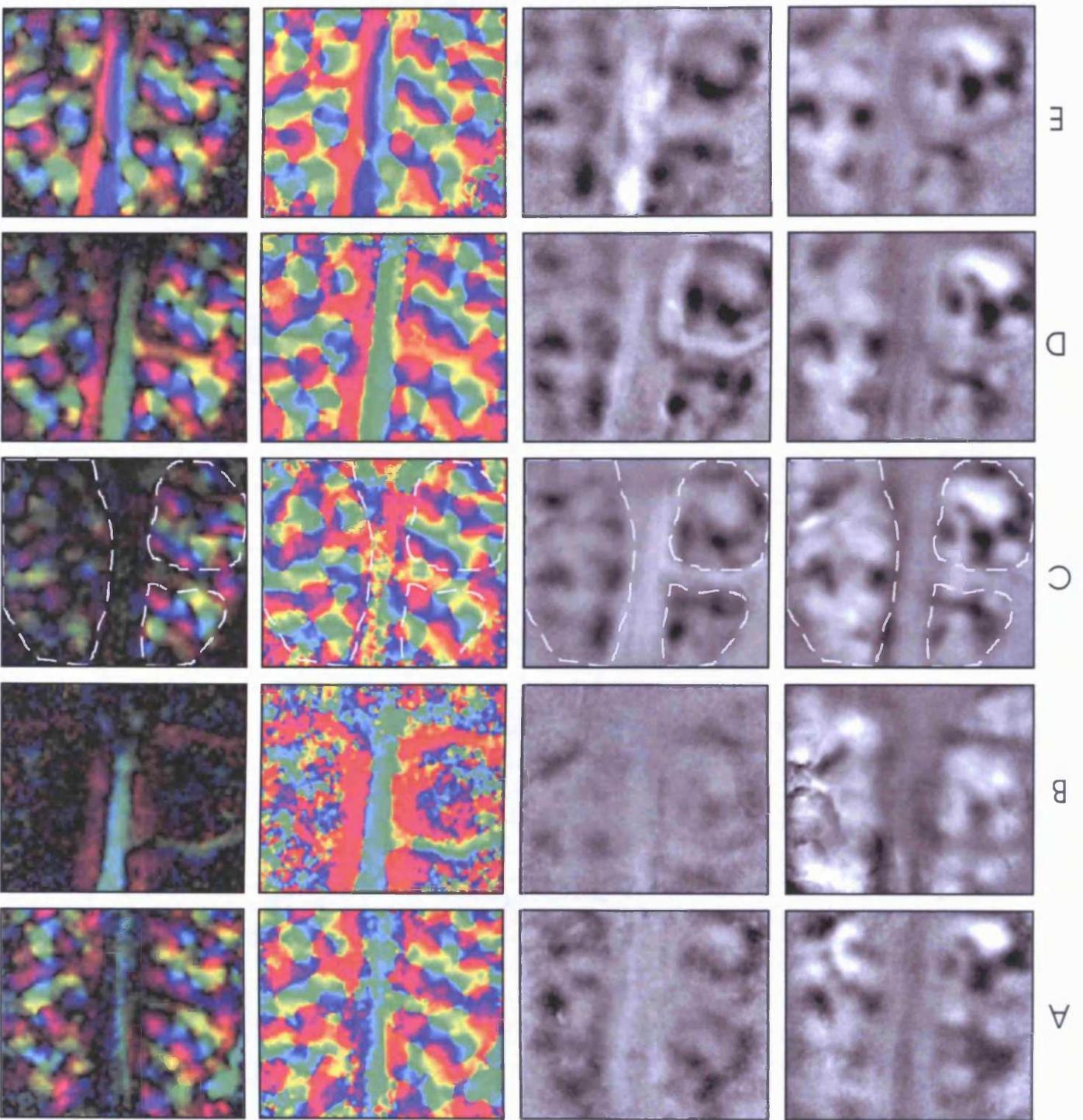
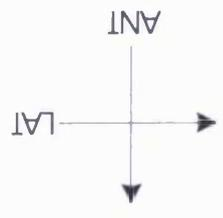
Column C - Angle map: The resulting vector of responses to all orientations tested is allocated a colour to represent preferred orientation.

Column D - Polar map: The relative strength of the oriented response is represented on a scale of brightness

Rows A-E represent time course: Immediately before closing the RE (P33), Immediately upon reopening of deprived eye (P43), then P47, P54, P65.

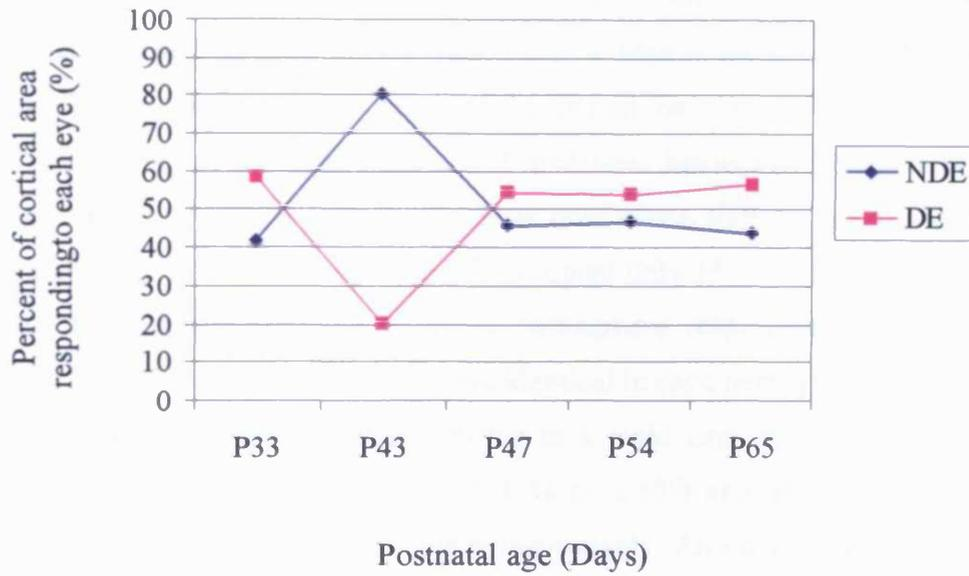
In Row C an example of a mask is shown by a white dotted line. It is used to exclude large blood vessels or other unwanted artifacts which could bias the result. Only the area within the mask is used for subsequent analysis.

Colour key represents preferred orientation in angle maps. Line arrows represent relative orientation of the head.



A B C D

A



B

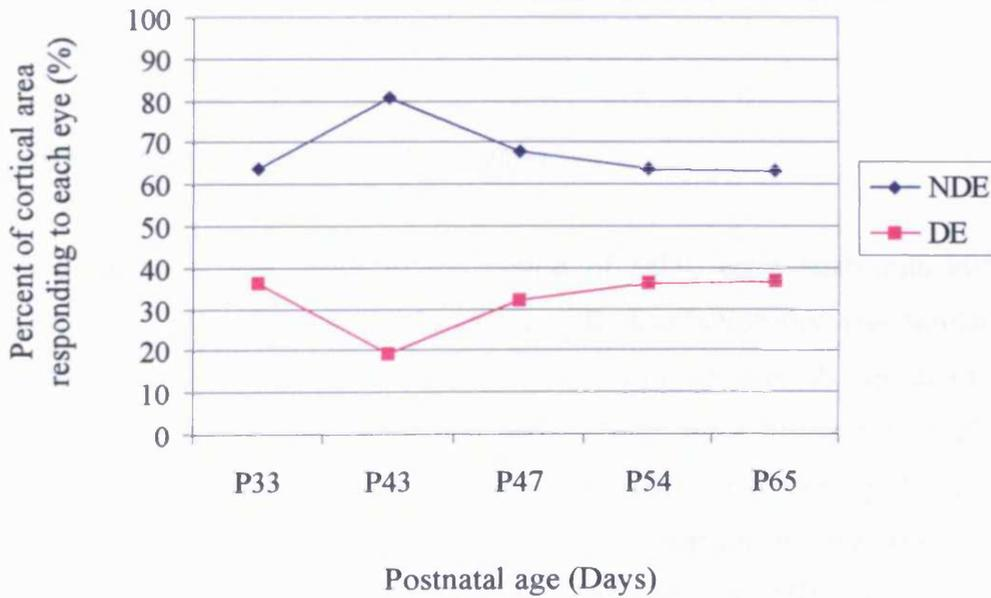


Figure 2.6 a and b Cortical ocular dominance before in a kitten before and after monocular deprivation

Data is from kitten 282 which was monocularly deprived for 10 days (P33-43).

NDE is represented by the blue line.

DE is represented by the pink line.

A) Data for the hemisphere contralateral to the DE.

B) Data for the hemisphere ipsilateral to the DE.

to those present before MD (56.3% and 63.4% for the DE in the hemispheres contralateral and ipsilateral to the DE respectively).

A summary of results from all 5 animals is shown in figure 2.12. The normal contralateral-eye bias prior to deprivation can be seen in the summary diagram; figure 2.12a. The eye that was to be deprived dominated, on average, 61.7% ($\pm 1.91\%$) and 38.2% ($\pm 3.4\%$) of the contralateral and ipsilateral hemisphere respectively. After a 10-day period of MD, a 'classical' ocular dominance shift to favour the NDE was observed (Fig. 2.12b, red bar). The DE occupied only 15.1% ($\pm 1.6\%$) and 15.5% ($\pm 1.5\%$) of the contralateral and ipsilateral hemisphere, respectively. Despite the initial cortical bias, the effects of the MD were identical in each hemisphere.

A short period of binocular recovery led to a rapid gain of deprived eye territory. Within 3-5 days, the DE occupied 60.4 % ($\pm 2.6\%$) and 44.1 % ($\pm 5.1\%$) of the contralateral and ipsilateral hemisphere, respectively. An extended period of binocular recovery resulted in minimal further change in OD distribution with final values being very similar to those before MD (Fig. 2.12d). Territory occupied by the DE was 61.7% ($\pm 3.8\%$) for the contralateral and 38.2% ($\pm 2.2\%$) for the ipsilateral hemisphere.

Strabismus prior to Monocular Deprivation

At five weeks of age (prior to the period of MD), eight strabismic kittens (six convergent and two divergent), showed an OD distribution that was similar in both hemispheres to that of other strabismic or normal animals. A typical example is shown in figures 2.7 and 2.8 (Kitten 065). Again, prior to the period of MD the distribution of left- and right-eye patches appears fairly uniform (Fig. 2.7a and b; row A). Quantitatively, a slight bias towards the contralateral eye was present in both hemispheres (around 54%). Notably, after a 9-day period of MD a full-scale OD shift to favour the NDE is not seen in this animal. Figure 2.7a and b; row B show that the DE has lost some cortical territory to the NDE, however DE patches are more numerous and prominent than typically seen after MD (Fig. 2.7b, row B, column A and B, compare with Fig. 2.5). The 'reduced shift' in favour of the NDE is confirmed quantitatively in figure 2.8. The DE still occupies 36.6% and 29.6% of the cortex in the contralateral and ipsilateral hemisphere, respectively. After a period of 6 days of recovery, DE patches appeared similar in distribution and size to pre-MD levels, in

Figure 2.7 a Effects of strabismus and MD on ocular dominance and orientation selectivity in the non-deprived (LE)

Kitten 065 - A strabismus was imposed in the RE at P21 followed by a 9 day period of monocular deprivation in RE (P35-44).

Column A - Ocular dominance (left eye/right eye): Patches of black represents high neuronal activity, and white, low neuronal activity. With respects to the left vs right eye map here, dark areas represent neurons responding preferentially to the left eye and light areas responding preferentially to the right eye.

Column B -Single condition (0deg/blank): The relative strength of the response is represented on the level of darkness. The darker the patch the greater the response.

Column C - Angle map: The resulting vector of responses to all orientations tested is allocated a colour to represent preferred orientation.

Column D - Polar map: The relative strength of the oriented response is represented on a scale of brightness

Rows A-E represent time course: Immediately before MD (P35) Immediately upon reopening of deprived eye (P44), then P50, P57, P64.

Row A images differ in size from subsequent images due to the original maps being acquired with the camera rotated 90 degrees. The images have been rotated for ease of comparison with other images.

Colour key represents preferred orientation in angle maps. Line arrows represent relative orientation of the head.

It should be noted that an artifact does appear on the left hemisphere at P64. The artifacts was excluded from the analysis of the maps by using a mask (see also Fig 2.5).

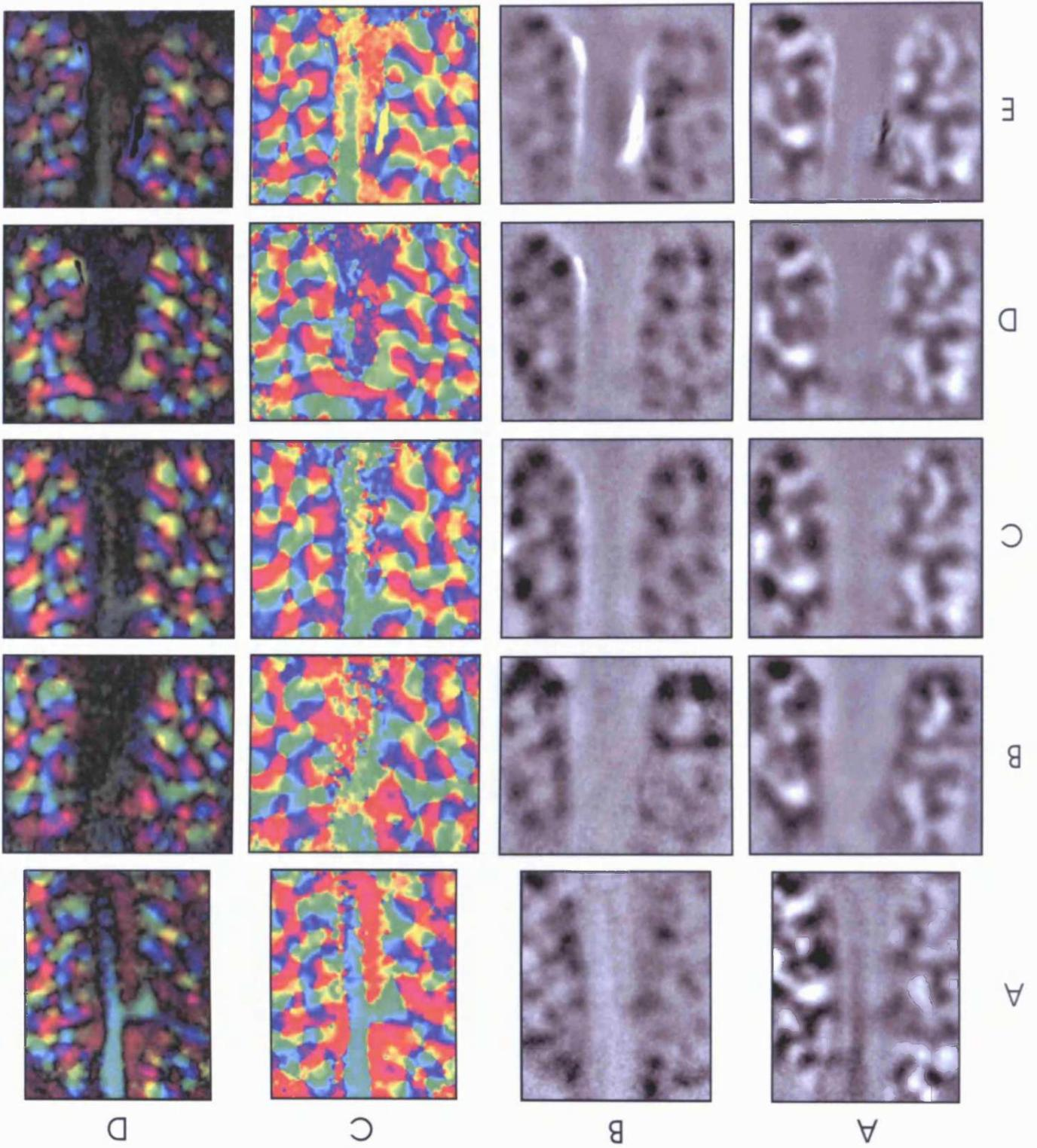
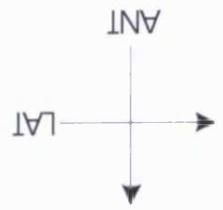


Figure 2.7 b Effects of strabismus and MD on ocular dominance and orientation selectivity in the deprived (RE)

Kitten 065 where a strabismus was imposed in the RE at P21 followed by a 9-day period of monocular deprivation in RE (P35-44).

Column A - Ocular dominance (right eye/left eye): Patches of black represents high neuronal activity, and white, low neuronal activity. With respects to the right vs left eye map here, dark areas represent neurons responding preferentially to the right eye and light areas responding preferentially to the left eye.

Column B -Single condition (0deg/blank) angle: The relative strength of the response is represented on the level of darkness. The darker the patch the greater the response.

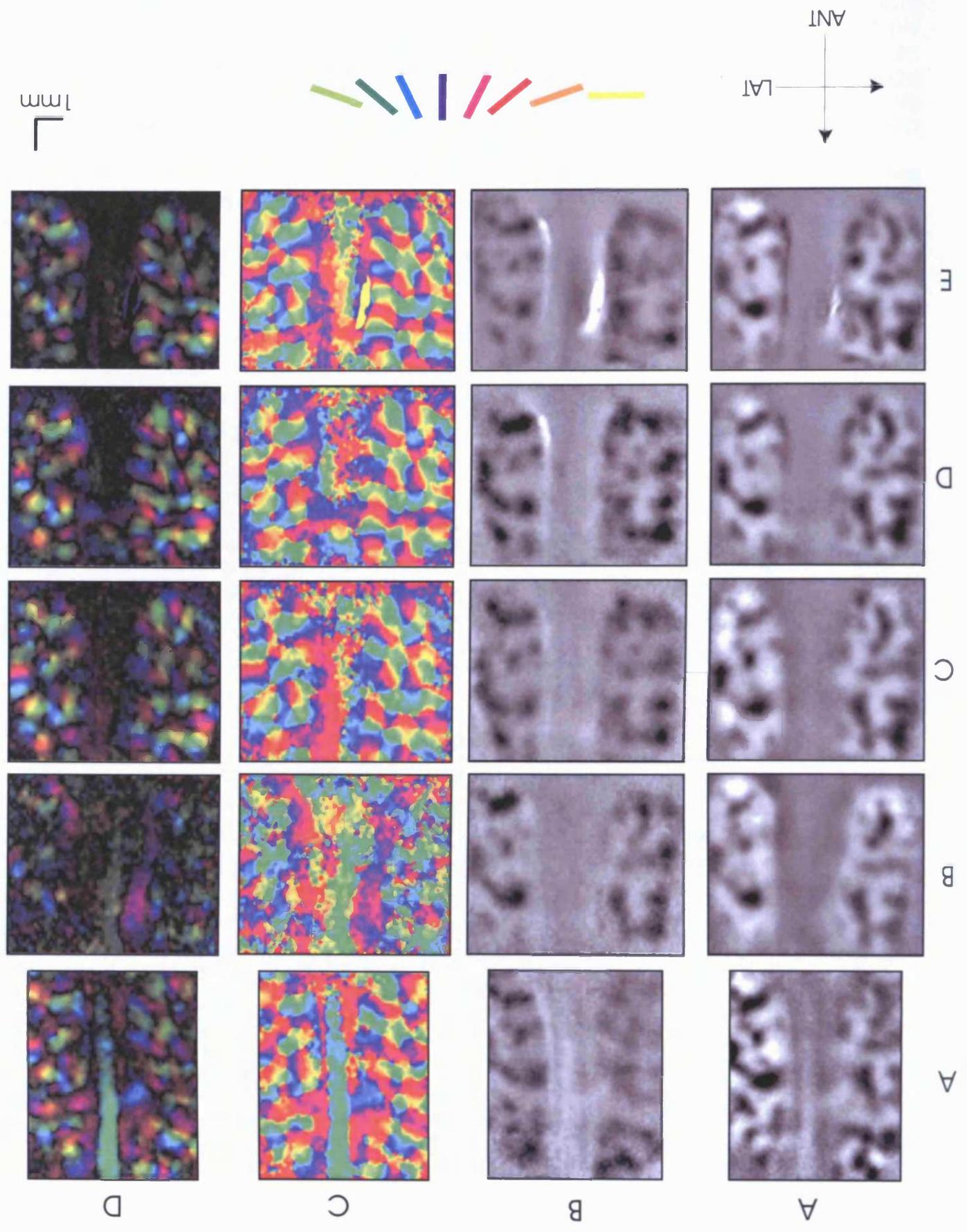
Column C -Angle map: The resulting vector of responses to all orientations tested is allocated a colour to represent preferred orientation.

Column D - Polar map: The relative strength of the oriented response is represented on a scale of brightness

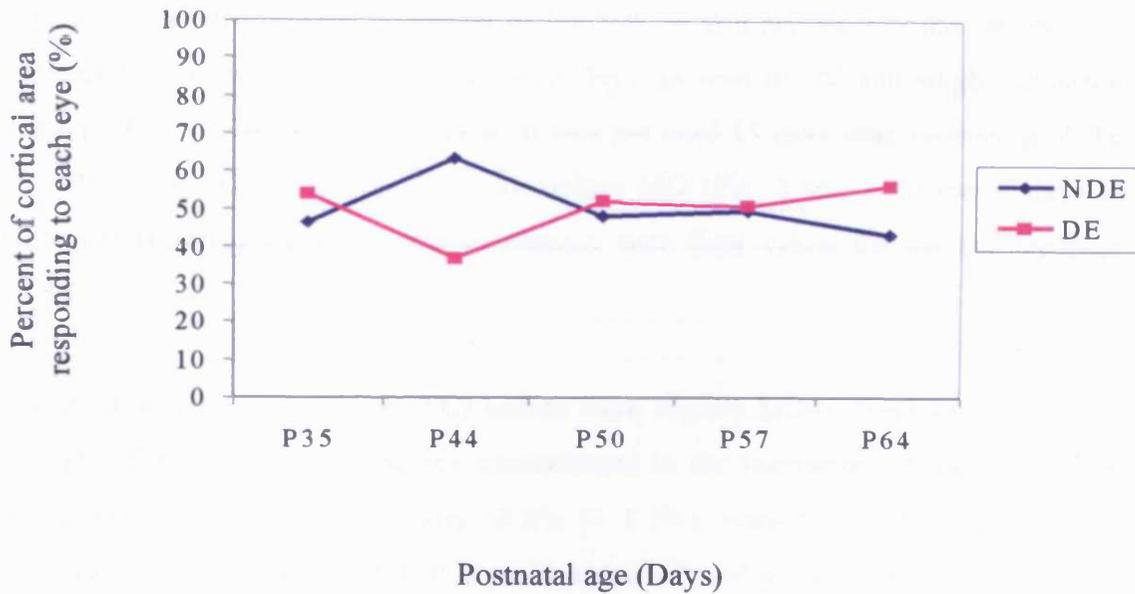
Rows A-E represent time course: Immediately before MD (P35). Immediately upon reopening of deprived eye (P44), then P50, P57, P64.

Row A images differ in size from subsequent images due to the original maps being acquired with the camera rotated 90 degrees. The images have been rotated for ease of comparison with other images.

Colour key represents preferred orientation in angle maps. Line arrows represent relative orientation of the head.



A



B

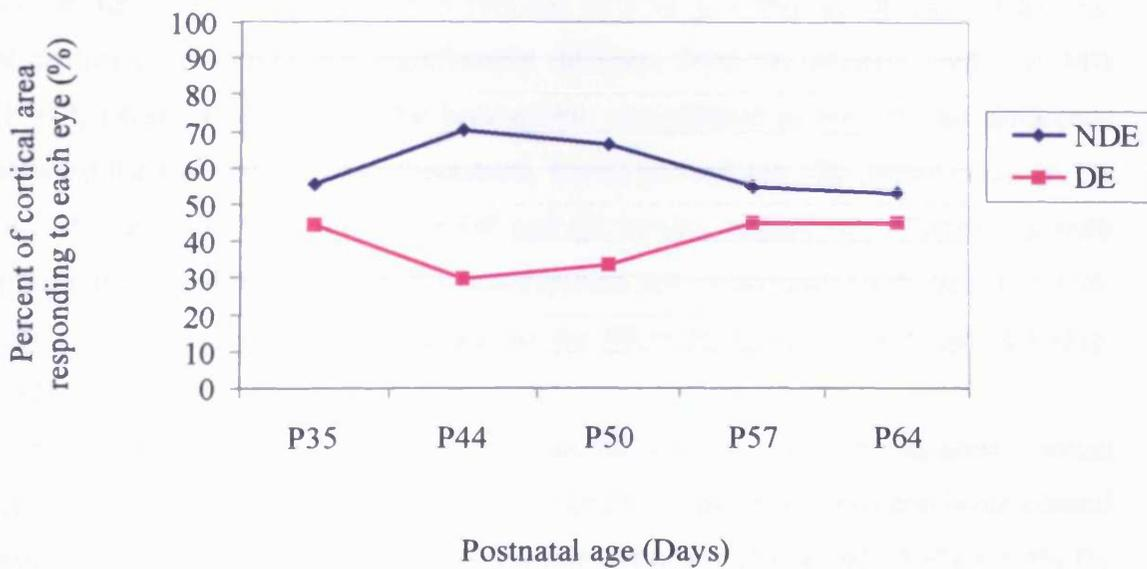


Figure 2.8 a and b Cortical ocular dominance before in a strabismic kitten before and after monocular deprivation

Data is from kitten 065 which was made strabismic in the RE (P21) followed by 9 days of MD in the RE (P35-44).

NDE is represented by the blue line.

DE is represented by the pink line.

A) Data for the hemisphere contralateral to the DE.

B) Data for the hemisphere ipsilateral to the DE.

the hemisphere contralateral to the DE. Values were similar to those prior to MD (52.1%) and changed little with further binocular recovery. Final values for the DE were 56.2% for the hemisphere contralateral to the DE. Recovery was somewhat delayed in the hemisphere ipsilateral to the DE. In this hemisphere the DE patches expanded more gradually in the following days, as seen in OD and single condition maps in figure 2.7b, column A and B. It was not until 13 days after reopening of the DE (P57) that values returned to those before MD (Fig. 2.8b). A further 7 days of binocular recovery led to no further change, with final values for the DE reaching 44.8%.

For all strabismic animals, pre-MD values were slightly below those for the control animals. The bias towards the eye contralateral to the hemisphere imaged was less prominent at 52.9% ($\pm 3.6\%$) and 56.2% ($\pm 1.2\%$), respectively, for animals with convergent strabismus and MD in opposite eyes (OP) and in the same eye (SA).

The summary in figure 2.12 highlights the 'reduced' shift after MD in squinting animals. After the period of MD, in the hemisphere ipsilateral to the DE, values for the DE territory were 16.4 % ($\pm 3.7\%$) and 21.3 % ($\pm 3.5\%$) for OP and SA kittens, respectively. This was not significantly different from the animals with just MD ($P=0.4$, t-test). However, in the hemisphere contralateral to the DE the difference between the two groups was pronounced. In this hemisphere, DE territory was 26.1% ($\pm 5.2\%$) and 30.7% ($\pm 4.8\%$) for OP and SA kittens, respectively. Combining both groups, the OD shift (to favour the non-deprived eye) was significantly less ($P=0.008$, t-test) in the hemisphere contralateral to the DE than in kittens with just MD (Fig. 2.12b).

In most cases, after a brief period of binocular recovery, the DE regained cortical territory in the contralateral hemisphere to the DE to match the non-strabismic control group, and to levels just above pre-MD levels (59.6% $\pm 10.6\%$ and 55.9% $\pm 5.4\%$ for OP and SA kittens respectively). However, in three kittens: 065 - SA (Fig. 2.8), 280 - OP (Fig. 2.9 and 2.10) and 307 - SA (Fig. 2.11), recovery of the DE took longer in the hemisphere ipsilateral to the DE (14, 9 and 19 days for kittens 065, 280 and 307 respectively) to return to pre-MD values. Hence, in SA kittens (065 and 307 included), after a brief recovery period, the DE occupied less territory in the ipsilateral hemisphere than in the non-strabismic animals, namely only 31.6% ($\pm 2.2\%$) of the cortex.

Figure 2.9 a Cortical ocular dominance and orientation selectivity in the non-deprived (RE) of a strabismic kitten before and after monocular deprivation

Data is from kitten 934 which was made strabismic in the RE (P21) followed by 10 days of monocular deprivation in the LE (P35-45)

Column A - Ocular dominance (right eye/left eye): Patches of black represents high neuronal activity, and white, low neuronal activity. With respects to the right vs left eye map here, dark areas represent neurons responding preferentially to the right eye and light areas responding preferentially to the left eye.

Column B -Single condition(0deg/blank): The relative strength of the response is represented on the level of darkness. The darker the patch the greater the response.

Column C -Angle map: The resulting vector of responses to all orientations tested is allocated a colour to represent preferred orientation.

Column D - Polar map: The relative strength of the oriented response is represented on a scale of brightness

Rows A-E represent time course: Immediately before closing the RE (P35),Immediately upon reopening of deprived eye (P45), then P48, P54, P61

Colour key represents preferred orientation in angle maps. Line arrows represent relative orientation of the head.

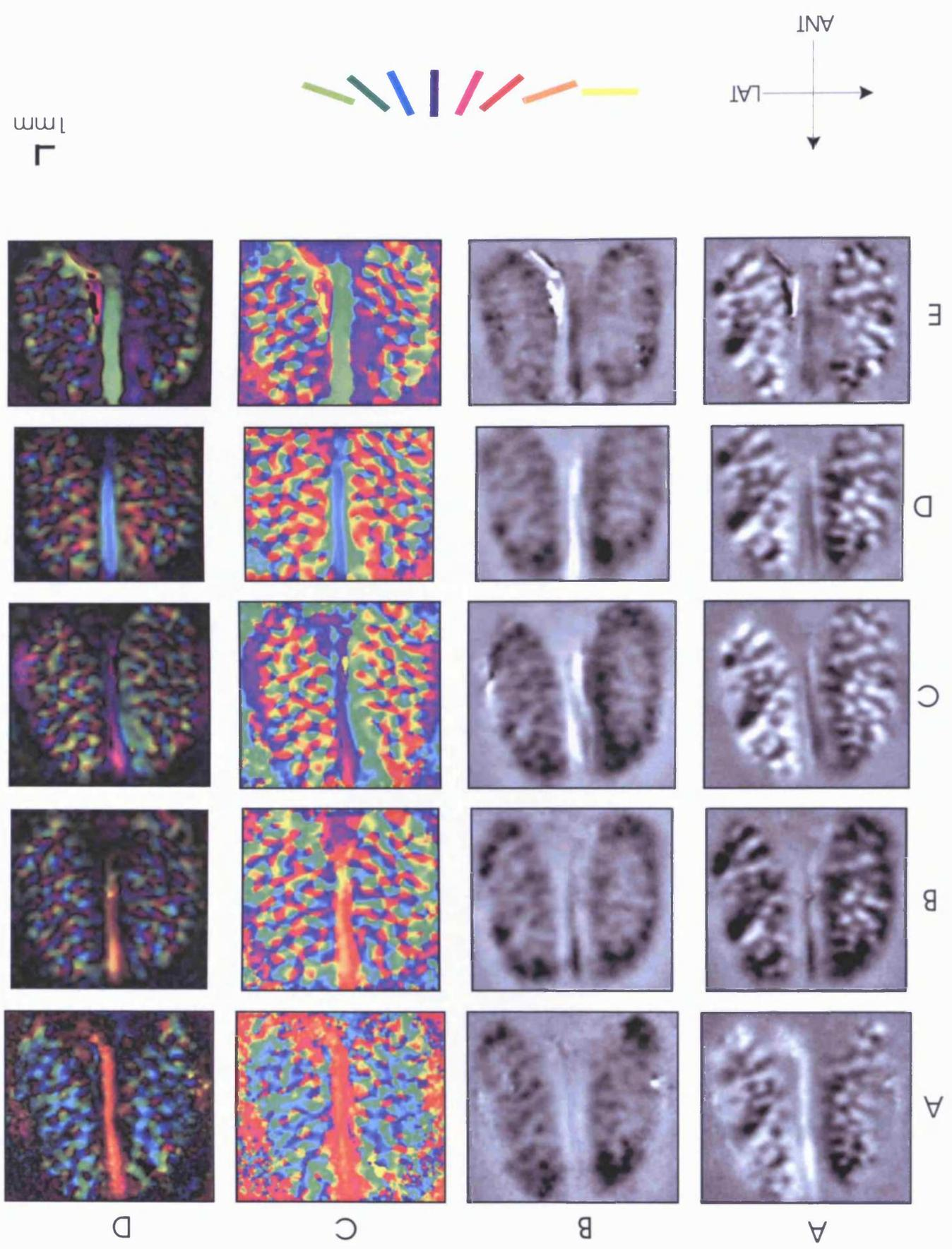


Figure 2.9 b Cortical ocular dominance and orientation selectivity in the deprived (LE) of a strabismic kitten before and after monocular deprivation

Data is from kitten 934 which was made strabismic in the RE (P21) followed by 10 days of monocular deprivation in the LE (P35-45)

Column A - Ocular dominance (left eye/right eye): Patches of black represents high neuronal activity, and white, low neuronal activity. With respects to the left vs right eye map here, dark areas represent neurons responding preferentially to the left eye and light areas responding preferentially to the right eye.

Column B - Single condition(0deg/blank):The relative strength of the response is represented on the level of darkness. The darker the patch the greater the response.

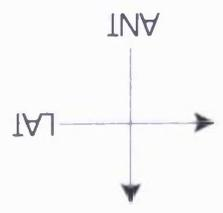
Column C - Angle map: The resulting vector of responses to all orientations tested is allocated a colour to represent preferred orientation.

Column D - Polar map: The relative strength of the oriented response is represented on a scale of brightness

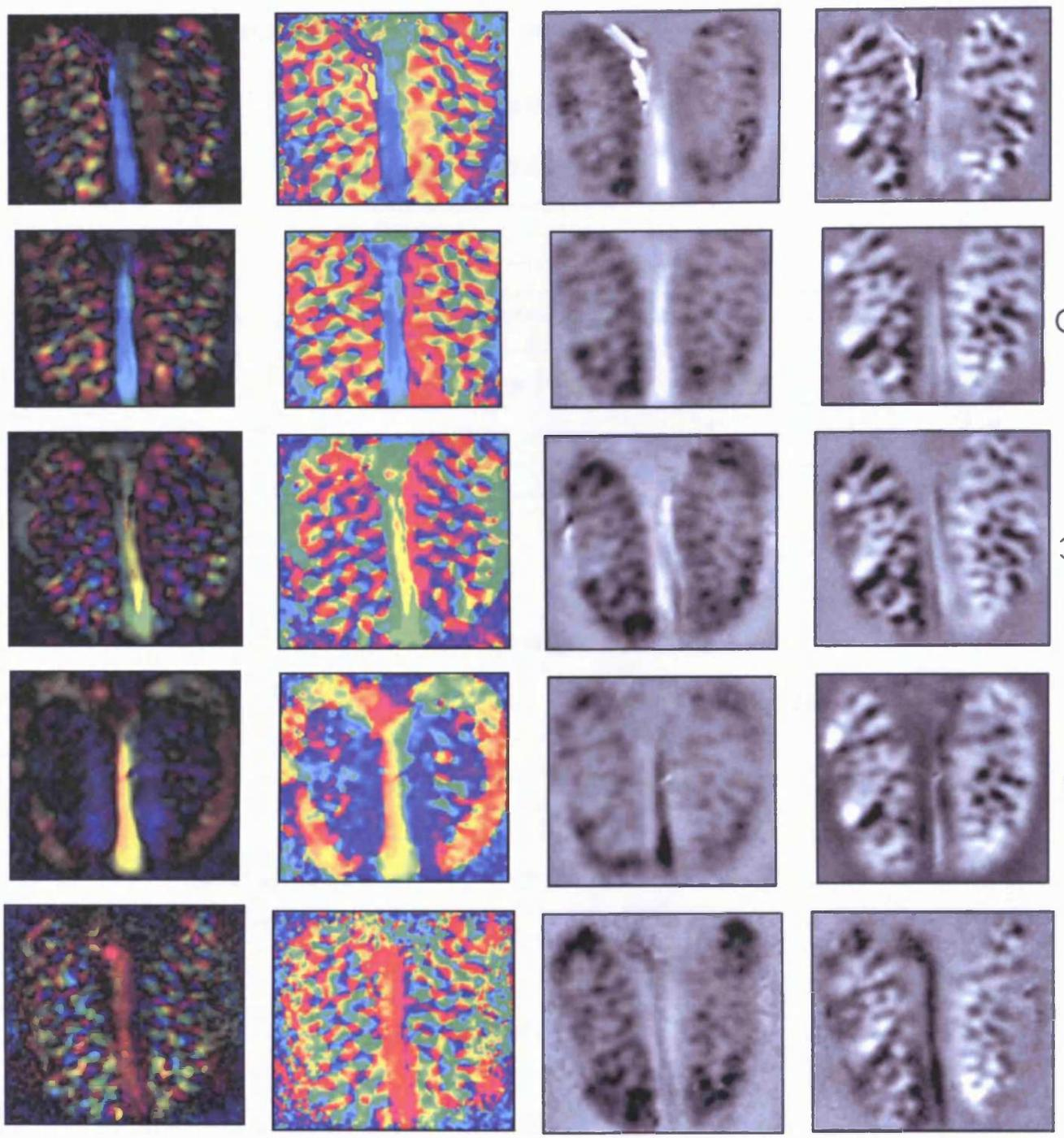
Rows A-E represent time course: Immediately before closing the RE (P35),Immediately upon reopening of deprived eye (P45), then P48, P54, P61

Colour key represents preferred orientation in angle maps. Line arrows represent relative orientation of the head.

A
B
C
D
E



1mm
└┘



A
B
C
D

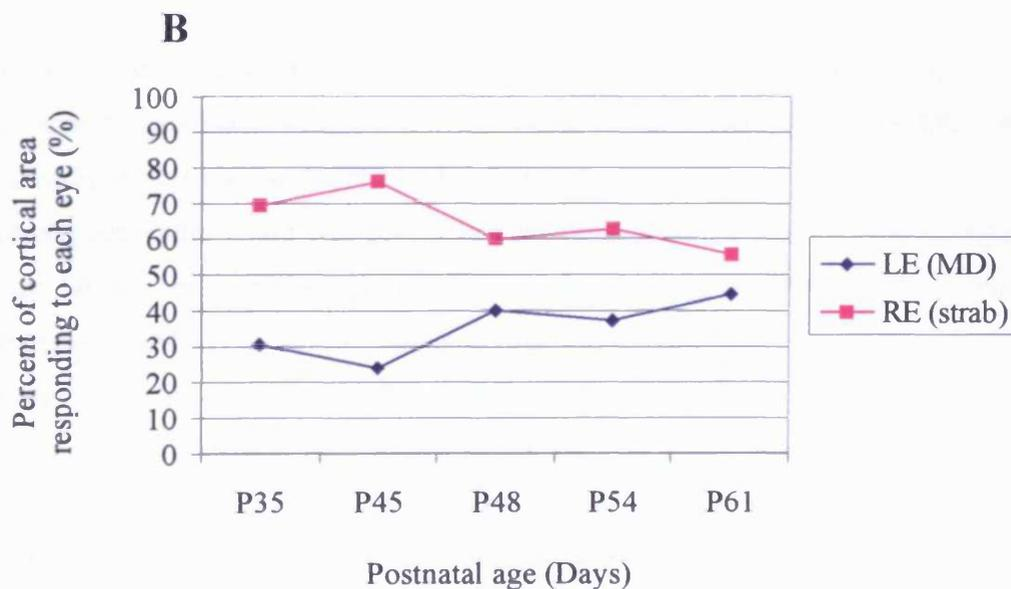
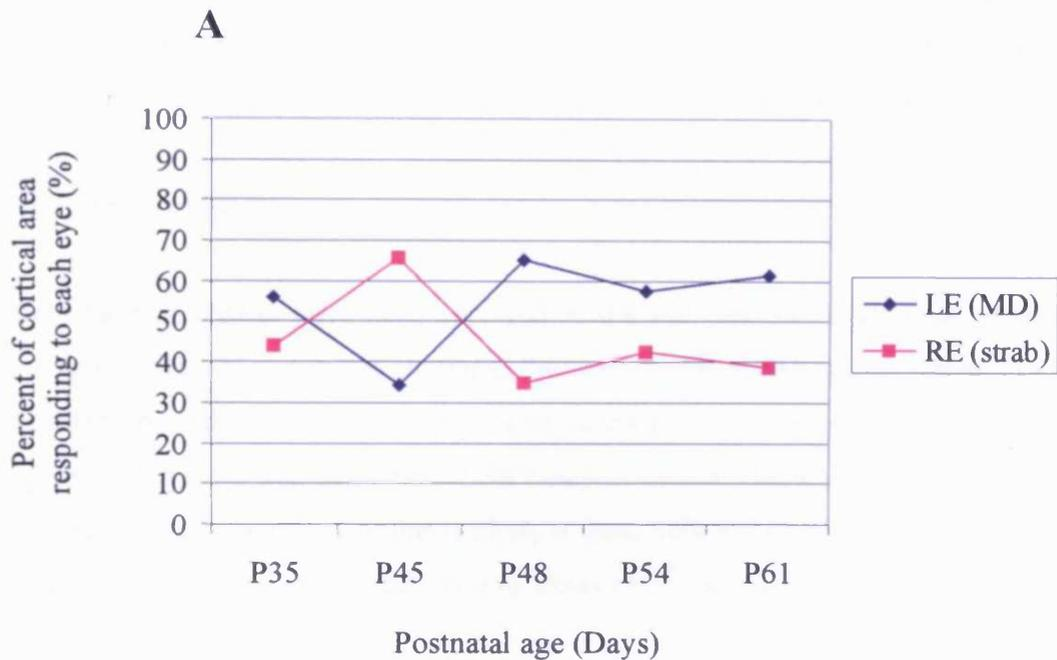


Figure 2.10 a and b Cortical ocular dominance before in a strabismic kitten before and after monocular deprivation

Data is from kitten 934 which was made strabismic in the RE (P21) followed by 10 days of MD in LE (P35-45).

NDE (Strabismic) is represented by the pink line.

DE is represented by the blue line.

A) Data for the hemisphere contralateral to the DE.

B) Data for the hemisphere ipsilateral to the DE.

After an extended period of recovery, the DE in strabismic kittens overall occupied a very similar amount of cortical territory to that seen prior to MD. One exception was the hemisphere ipsilateral to the DE in SA kittens, where DE territory remained somewhat, but not significantly, below that of pre-MD values ($35.1\% \pm 4.3\%$).

Divergent strabismus

The divergent kittens were both deprived in the eye that had been made strabismic (SA group) with one example shown in figure 2.11. The other animal, kitten 334, was excluded from the analysis. It was found to have a very large divergent squint of approximately 45° , well in excess of the range of squints obtained in other animals (7-15°). Such a large angle of squint is likely to have affected the motility of the eye and made it impossible to ensure that the eye always saw the stimulus screen fully.

Squint angle and Ocular dominance

As stated earlier, convergent squint angles measured 7-15 degrees. Notably, two of the three kittens made strabismic in the NDE became esotropic in the DE, with the originally strabismic eye (NDE) looking straight.

Convergent squint angle was inversely correlated with the area of cortex responding to the DE (in the contralateral hemisphere where a reduced OD shift was seen) after the period of MD (Fig. 2.13a), however this relationship was very weak ($r = -0.16$). It appeared that the magnitude of the squint had no significant effect on the OD shift seen in the contralateral hemisphere to the DE. As noted above, in several animals, recovery of the DE was slightly delayed. Squint angle was then correlated with the percentage of cortical territory recovered after a brief period of binocular recovery, with respect to the initial values before MD (Fig. 2.13b). An inverse correlation was seen within both hemispheres. Correlation for both hemispheres was $r = -0.79$. Therefore the magnitude of the squint did affect recovery of cortical territory of the DE (although not significantly: $P=0.43$, Pearson's test).

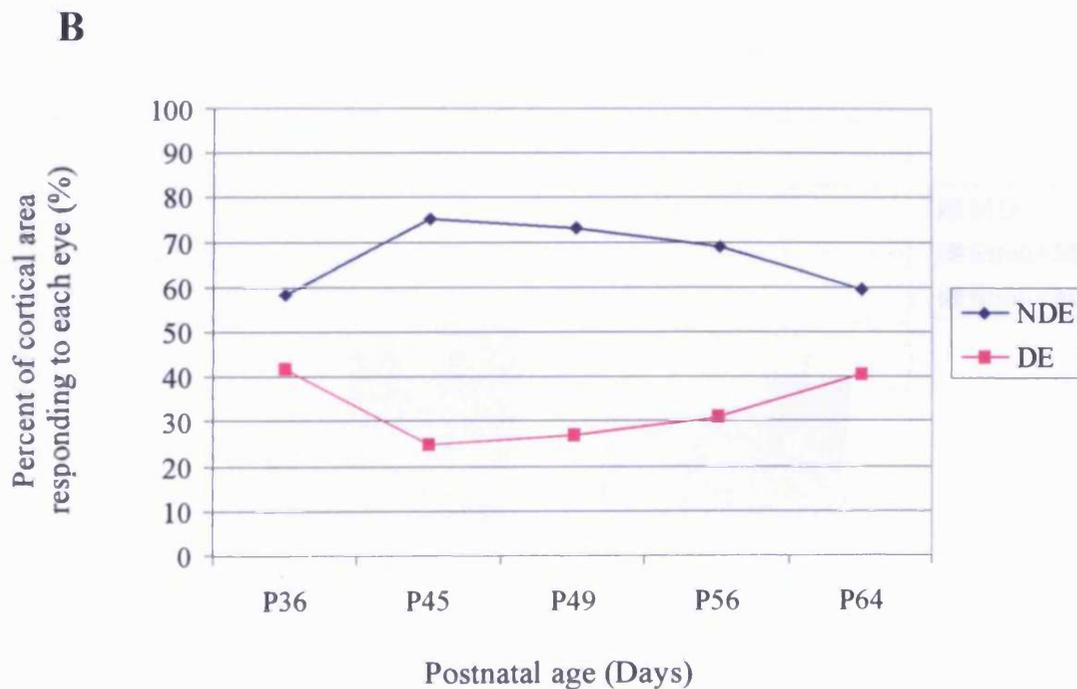
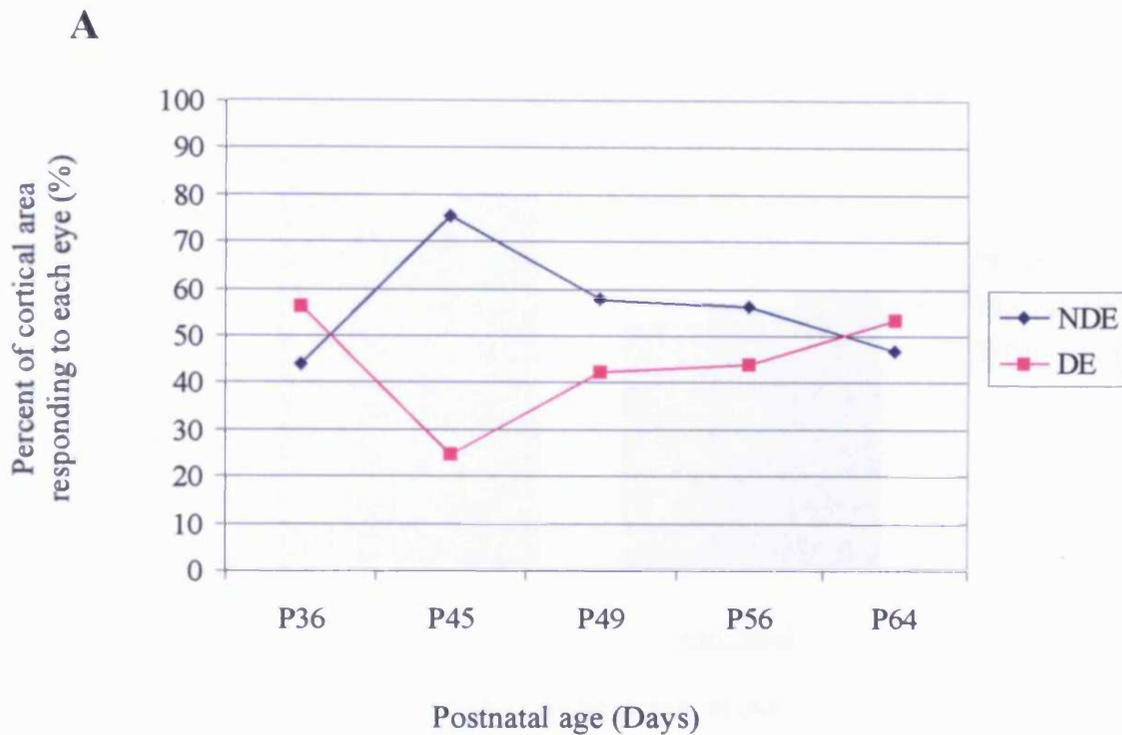


Figure 2.11 a and b Cortical ocular dominance in a strabismic kitten before and after monocular deprivation

Data is from kitten 307 which was made strabismic (divergent) in the RE (P23) followed by 9 days of MD in RE (P36-45).

NDE is represented by the blue line.

DE is represented by the pink line.

A) Data for the hemisphere contralateral to the DE.

B) Data for the hemisphere ipsilateral to the DE.

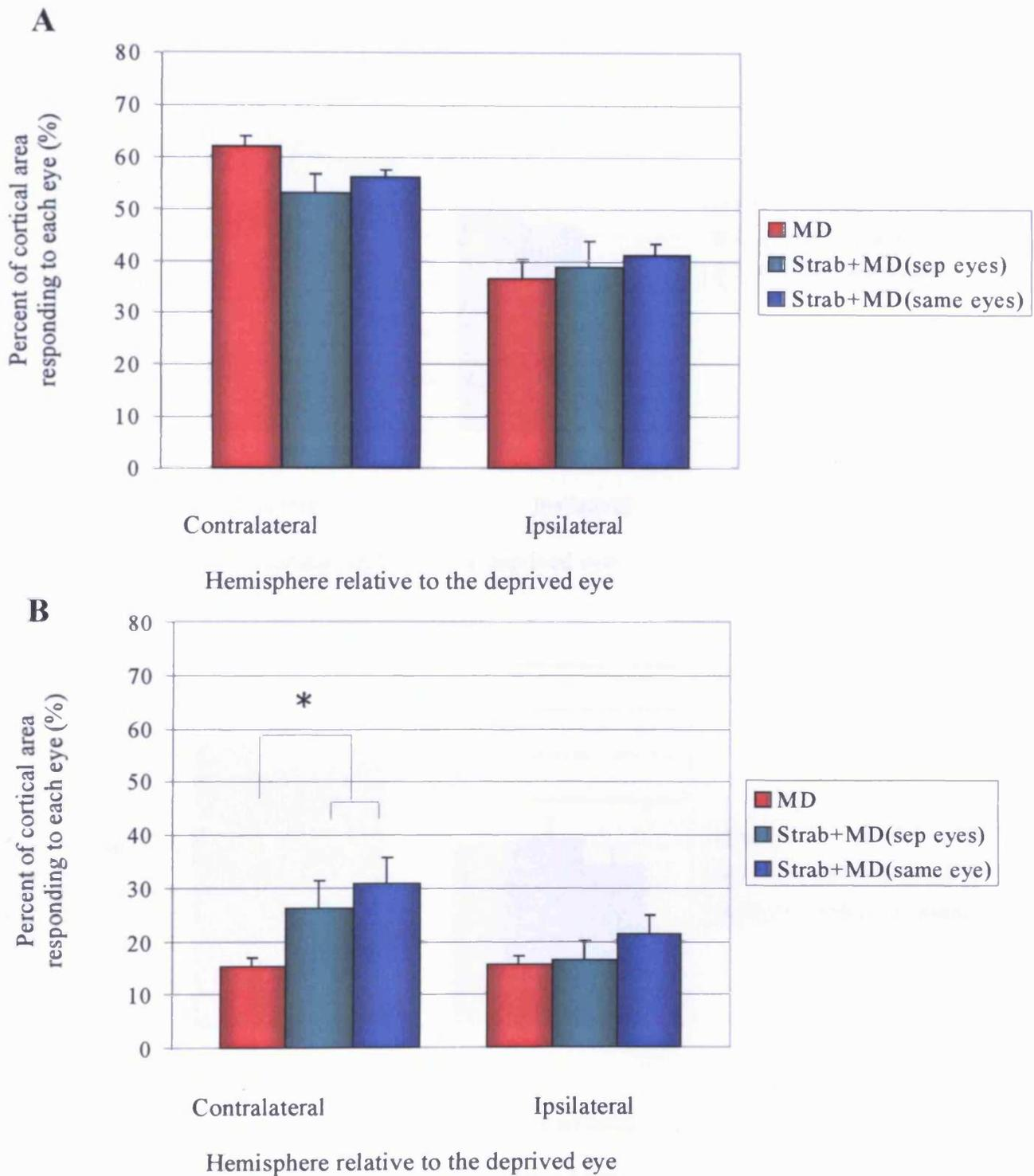


Figure 2.12 a-d Summary of cortical area occupied by the deprived eye in each hemisphere imaged in experimental animals

A) Before MD.

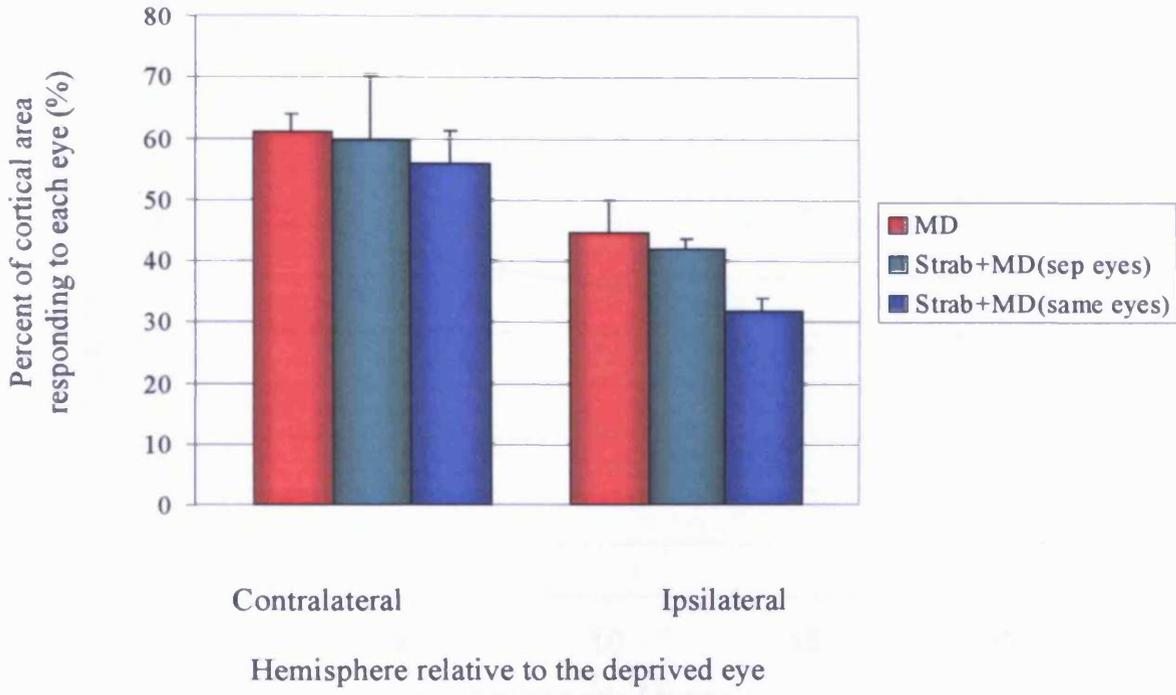
B) Immediately after MD.

C) Brief period of binocular recovery.

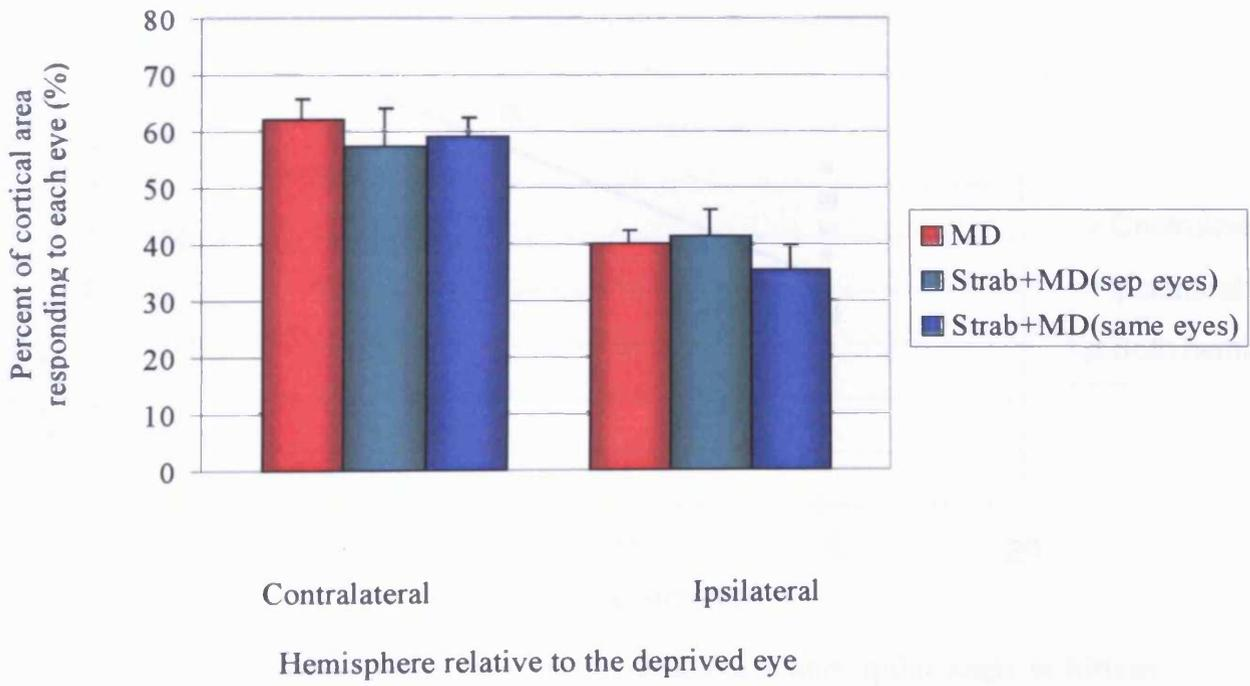
D) Extended period of binocular recovery.

Star depicts significant difference (*) between MD and S+MD animals ($P=0.08$, t-test).

C



D



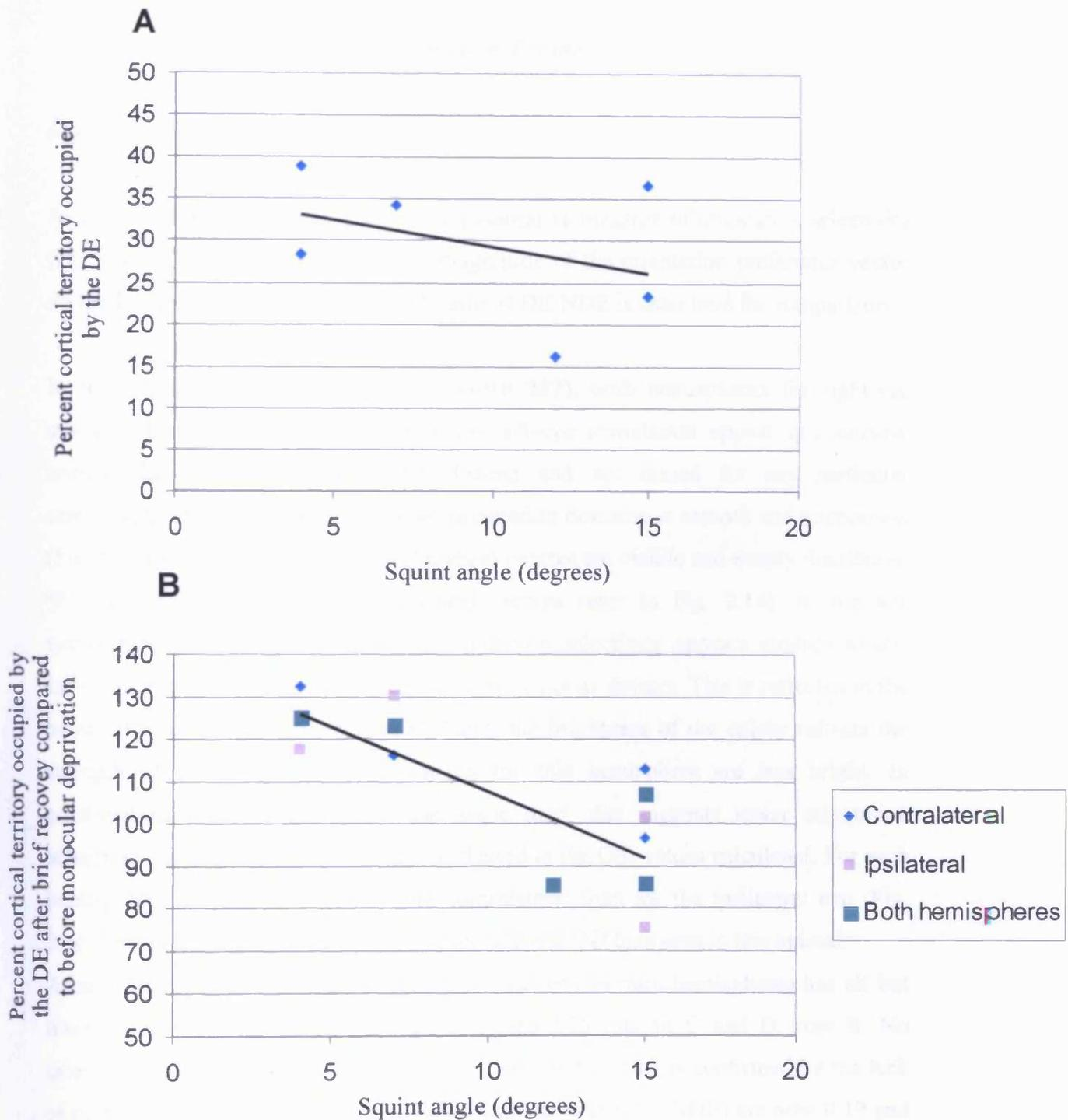


Figure 2.13 Relationship between ocular dominance and squint angle in kittens made strabismic prior to monocular deprivation

A) Percent cortical territory occupied by the DE immediately after monocular deprivation in relation to squint angle
 Regression line given for values for contralateral hemisphere
 $r = -0.16$

B) Percent change in cortical territory occupied by the DE after brief recovery compared to before monocular deprivation.
 Regression line given for values for average of both hemispheres
 $r = -0.79$
 Variables in graph **B** did not show significant relationship ($P = 0.43$, Pearson's test).

Orientation Tuning

Monocular Deprivation

As described in the General methods, a quantitative measure of orientation selectivity (OS index, OSI) was generated from magnitude of the orientation preference vector divided by the sum of all responses. A ratio of DE:NDE is used here for comparison.

In the example shown in figure 2.5 (kitten 282), both hemispheres for right-eye stimulation and the right hemisphere for left-eye stimulation appear qualitatively normal. Iso-orientation patches are distinct and not biased for any particular orientation. The transition between iso-orientation domains is smooth and continuous (Fig. 2.5a and b; column C row A). Pinwheel centres are visible and evenly distributed (For a more detailed look at pinwheel centres refer to Fig. 2.14). In the left hemisphere, for left-eye stimulation, orientation selectivity appears slightly lower. Iso-orientation patches and pinwheel centres are not as distinct. This is reflected in the polar maps in figure 2.6a; column D. Here, the brightness of the colour reflects the strength of the signal. The polar maps for this hemisphere are less bright. In combination with the deficits in the angle map, this suggests lower orientation selectivity for this hemisphere. This is reflected in the OSI values calculated. For each hemisphere, the OSI is larger for the contralateral than for the ipsilateral eye (Fig. 2.6c. This is in parallel with the strong contralateral OD bias seen in this animal.

After a 10-day period of MD, orientation selectivity in both hemispheres has all but disappeared. This can easily be seen in figure 2.5b; column C and D, row B. No orientation patches or pinwheel singularities are visible. This is confirmed by the lack of response seen in the polar maps. Values for the OSI (DE: NDE) are now 0.19 and 0.11 (for the hemispheres contralateral and ipsilateral to the DE, respectively). Responses for the NDE improve slightly (Fig. 2.5a column C+D). With a 7-day period of binocular recovery, orientation selectivity improved visibly in the DE, with a return of iso-orientation patches. Transition between iso-orientation patches was smooth and the typical pinwheel organisation had returned. A return of orientation selective responses is also visible in polar maps. Orientation selectivity in the DE continued to improve with further binocular recovery. This is most noticeable as an

A



B

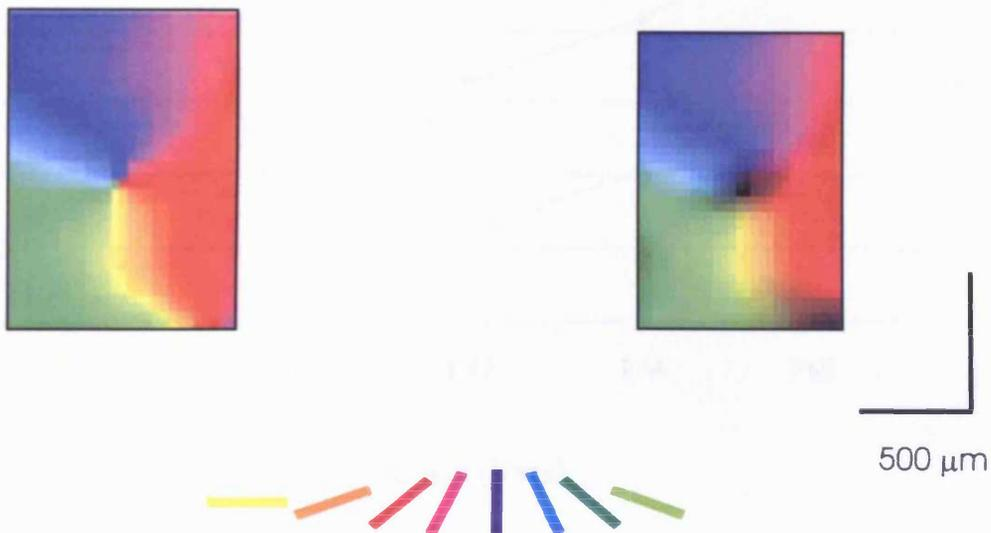


Figure 2.14. Examples of an iso-orientation domain and pinwheel centre in kitten V1

Images are taken from angle and polar maps of kitten V1 and enlarged
Left column is from the angle map and right column is from the polar map

A) Typical iso-orientation domain(s) responding to a single orientation (45°) - green. Towards the borders of the domain orientation changes gradually and in a linear fashion. Reading from top left to bottom right orientation changes from; 135° (red) through 0° (yellow) to 45° (green) and into 90° (blue)

B) Typical pinwheel center. Orientation changes rapidly with iso-orientation domains radiating out from the center. Polar maps also shows that there is little or no orientation selective response at this singularity.

C

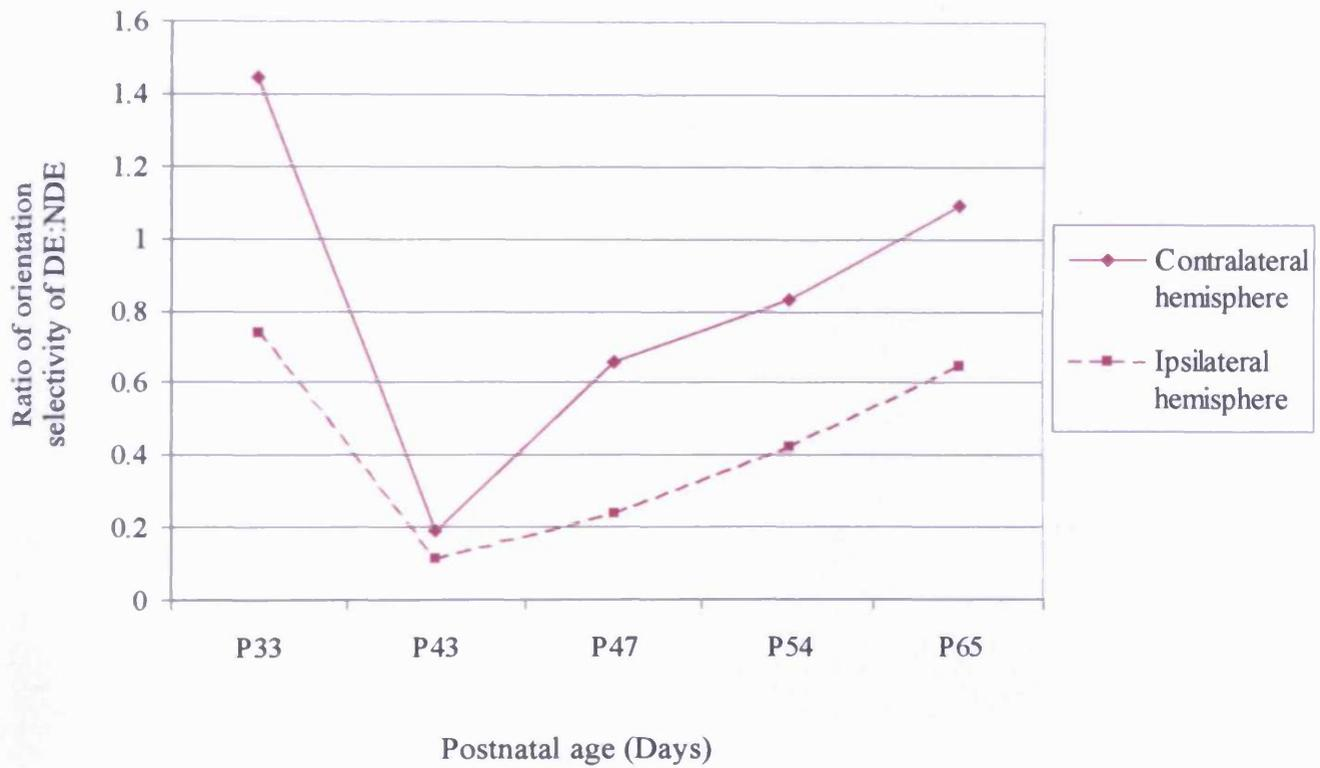


Figure 2.6 c Ratio of DE:NDE of cortical orientation selectivity in a kitten before and after monocular deprivation

Data is from kitten 282 which was monocularly deprived for 10 days (P33-43). Contralateral hemisphere to the DE is represented by the continuous line. Ipsilateral hemisphere to the DE is represented by the dotted line.

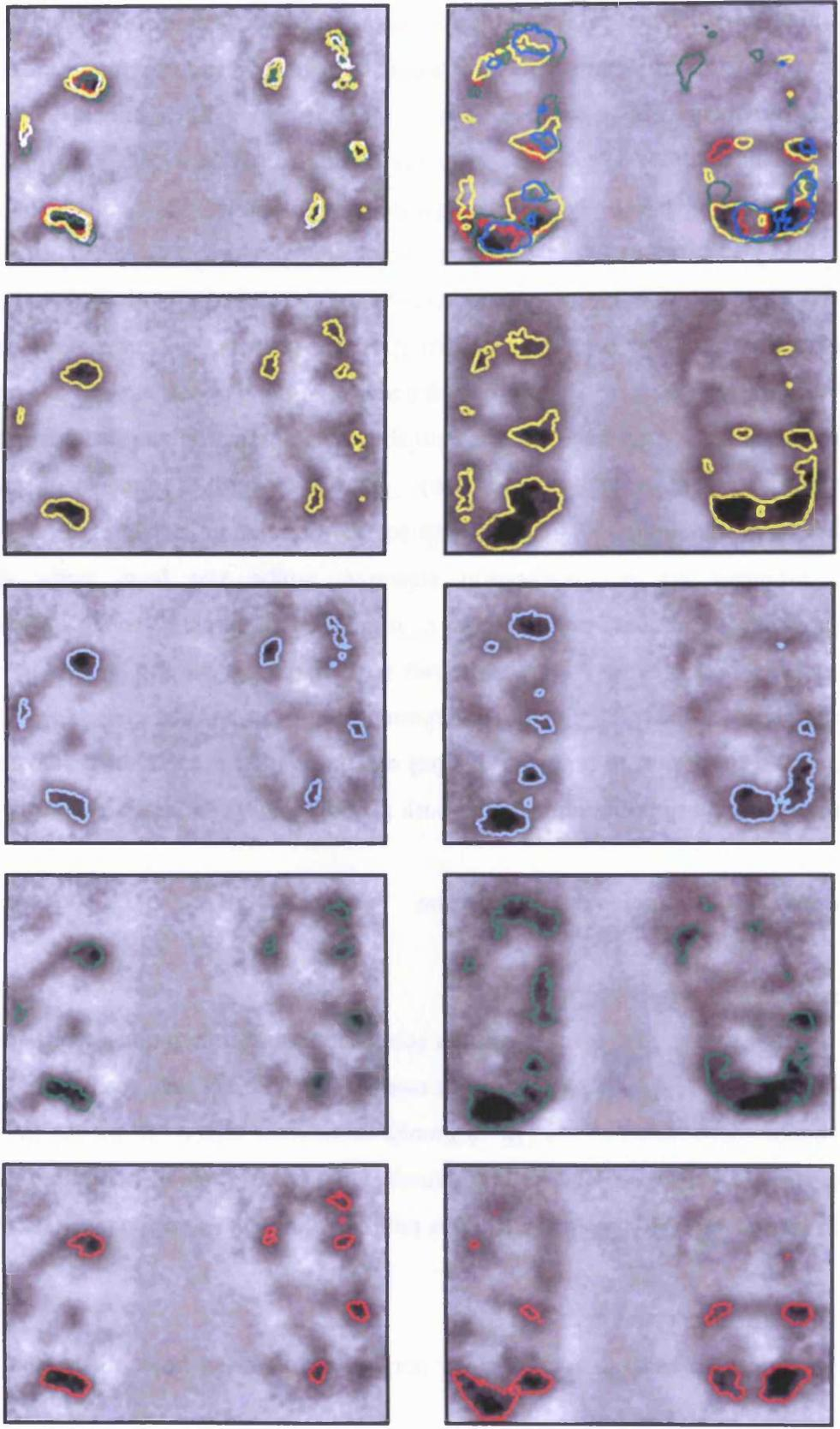
Figure 2.7 c Single condition orientation activity maps for NDE and DE of cortex in a strabismic animal immediately after deprivation

Single condition maps of 0° (red), 45° (green), 90° (blue) and 135° (yellow) from the NDE (left column) and DE (right column) of kitten 065 made strabismic in the RE prior to deprivation in the RE.

The threshold of single orientation response was set to the equivalent of $\sim 25\%$ of the total response level.

The fifth row shows all 4 maps overlaid. The NDE dominates more numerous and larger areas of the cortex than the DE. Overlap in responsive regions to each orientation are apparent in both eyes, however this overlap is much less pronounced in the NDE, resulting in greater orientation selectivity through the NDE.

Colour key represents the 4 of the orientations tested. Line arrows represent relative orientation of the head.



increase in the strength of the signal in both hemispheres in polar maps (Fig. 2.5b column D, rows C, D and E).

Values for the OSI (DE: NDE) reflect this improvement. However the OSI ration does not reach pre-MD levels in either hemisphere. This is most noticeable in the hemisphere contralateral to the DE. Although orientation selectivity for the two eyes was almost equal (OSI = 1.09), it was, in relative terms, lower than the pre-MD value (OSI = 1.44; Fig. 2.5c). Throughout the recovery period, orientation selectivity was qualitatively stable in the NDE.

Strabismus prior to monocular deprivation

Before MD, again the orientation selectivity for both eyes is qualitatively similar. For kitten 065, a slight bias in favour of the left eye in the right hemisphere is apparent in angle and polar maps (Fig. 2.7a and b; column C and D, row A and Fig. 2.8b).

After a 9-day period of MD, clear responses through the DE can still be seen in single condition maps (responses to gratings of 0° in Fig. 2.7b; column B, row B). However, these responses are not orientation selective. Angle and polar maps appear disorganised and grainy with no defined iso-orientation patches or pinwheel singularities. The polar map is very weak. This observation is reflected in the OSI values, which were 0.36 and 0.26 for hemispheres contralateral and ipsilateral to the DE, respectively (Fig. 2.8c). This seeming paradox of good iso-orientation patches but no angle/polar map is resolved through the fact that the iso-orientation patches obtained for 0, 45, 90 and 135 degrees all look more or less the same for the DE (see Fig. 2.7c). Therefore, the pixel-by-pixel vector sum is close to 0. In contrast (Fig. 2.7c), for the NDE it can be seen that the iso-orientation patches obtained for the 4 angles are much more distinct for each orientation (but still a degree of overlap), therefore the pixel-by-pixel vector sum is closer to '1'. Six days of binocular recovery resulted in only small increases in DE responses in single condition maps. However, angle and polar maps in both hemispheres improved noticeably qualitatively. Orientation selectivity improved with a return of defined orientation patches and obvious pinwheel singularities, but was not as good as in the NDE.

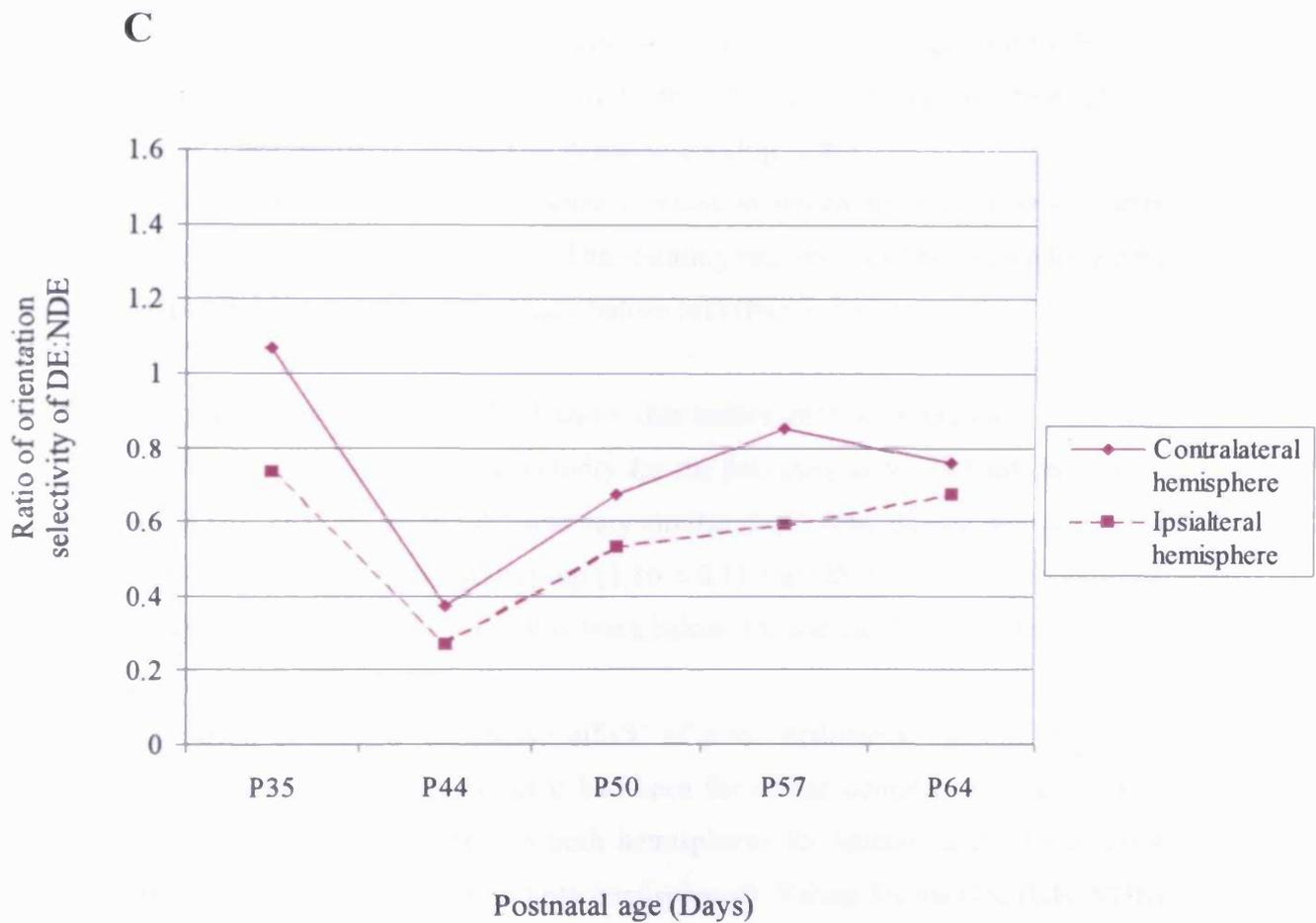


Figure 2.8 c Ratio of DE:NDE of cortical orientation selectivity in a strabismic kitten before and after monocular deprivation

Data is from kitten 065 Kitten 065 - A strabismus was imposed in RE at P21 followed by a 9 day period of monocular deprivation in RE (P35-44)

Contralateral hemisphere to the DE is represented by the continuous line

Ipsilateral hemisphere to the DE is represented by the dotted line

Quantitatively, OSIs (DE: NDE) were 0.67 and 0.53 for the hemispheres contralateral and ipsilateral to the DE (Fig. 2.8c). Orientation selectivity continued to improve with further binocular recovery. Although good orientation selectivity returned to the DE, it remained below that seen before MD, at 0.75 and 0.66 for the hemispheres contralateral and ipsilateral to the DE, respectively (Fig. 2.8c).

In contrast, in another kitten, 934, some orientation selectivity was preserved after MD (Fig. 2.9b; column C and row B). The resulting recovery was more complete with OSI values finishing very close to those before MD (Fig. 2.10c).

The summary graphs in figure 2.15 show that before MD, a contralateral bias was present for ratios of orientation selectivity for the two eyes as for OD (as with OD - see Fig. 2.12). The DE: NDE OSI was very similar in the contralateral hemisphere to the deprived eye-to-be in the MD group (1.16 ± 0.1), the OP group (1.09 ± 0.06) and the SA group (1.06 ± 0.06). The ratios were below 1.0 and again similar for all three groups for the other hemisphere.

After a period of MD, a 'protective effect' of prior strabismus was not seen with respect to orientation selectivity, as it had been for ocular dominance. Overall, MD had an equally deleterious effect in both hemispheres for animals with and without prior strabismus ($P > 0.05$, t-test, in both hemispheres). Values for the OSI (DE: NDE) ranged from 0.33-0.38 and 0.37-0.41 for the hemisphere contralateral and ipsilateral to the DE respectively (Fig. 2.15b).

After a brief period of binocular recovery, orientation selectivity improved to similar extents in both hemispheres. In the hemisphere contralateral to the DE, OSIs were close to 1.0, but just below 0.8 for the ipsilateral hemisphere. In all cases, however the differences between control and strabismic kittens were negligible. Extended recovery led to only minor changes in OSI values for both hemispheres. In all cases the orientation selectivity in the DE was at best equal to, or lower than in the NDE (Fig. 2.15d). Moreover, orientation selectivity in the DE finished below that before MD for both hemispheres and all groups of kittens (Fig. 2.15a and d).

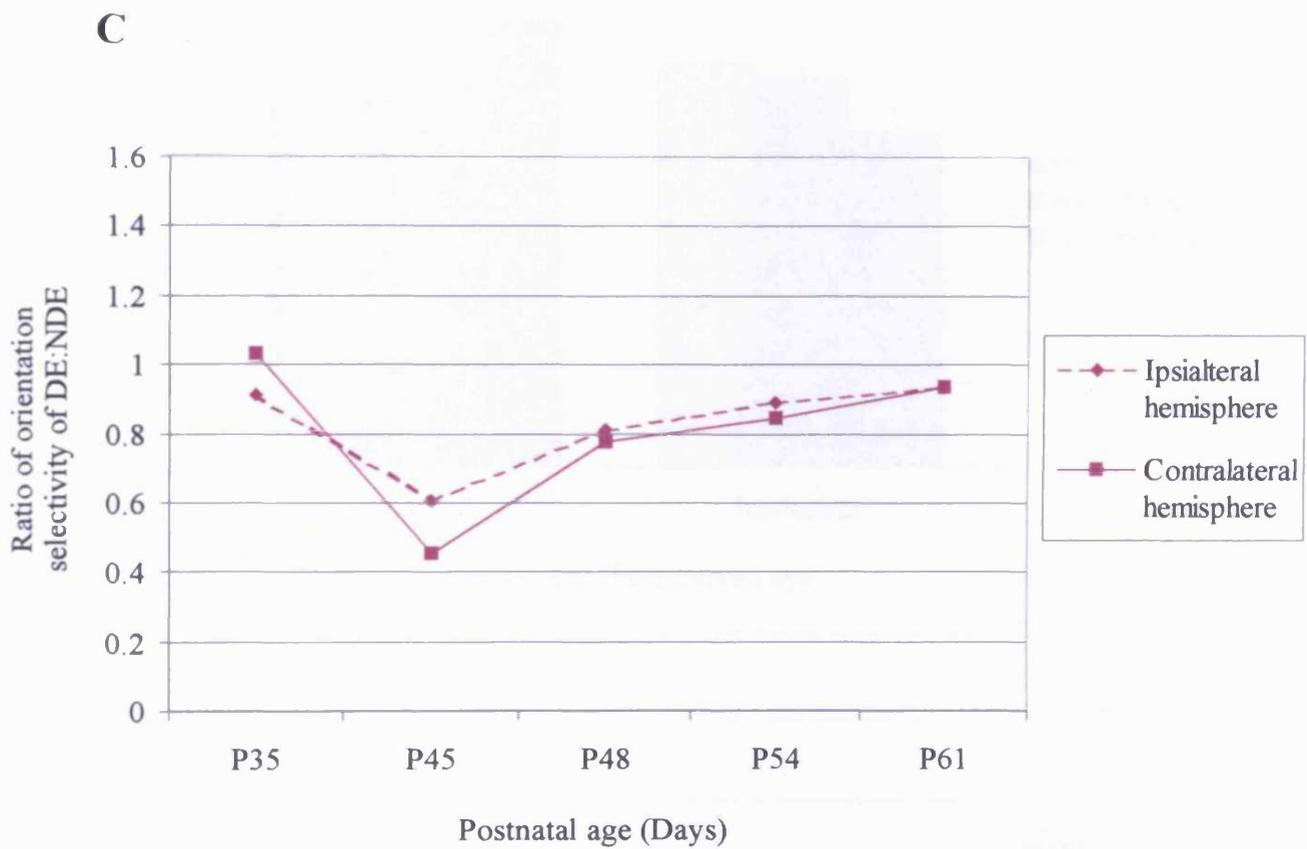


Figure 2.10 c Ratio of DE:NDE of cortical orientation selectivity in a strabismic kitten before and after monocular deprivation

Data is from kitten 934 which was made strabismic in the RE (P21) followed by 10 days of MD in LE (P35-45).

Contralateral hemisphere to the DE is represented by the continuous line.

Ipsilateral hemisphere to the DE is represented by the dotted line.

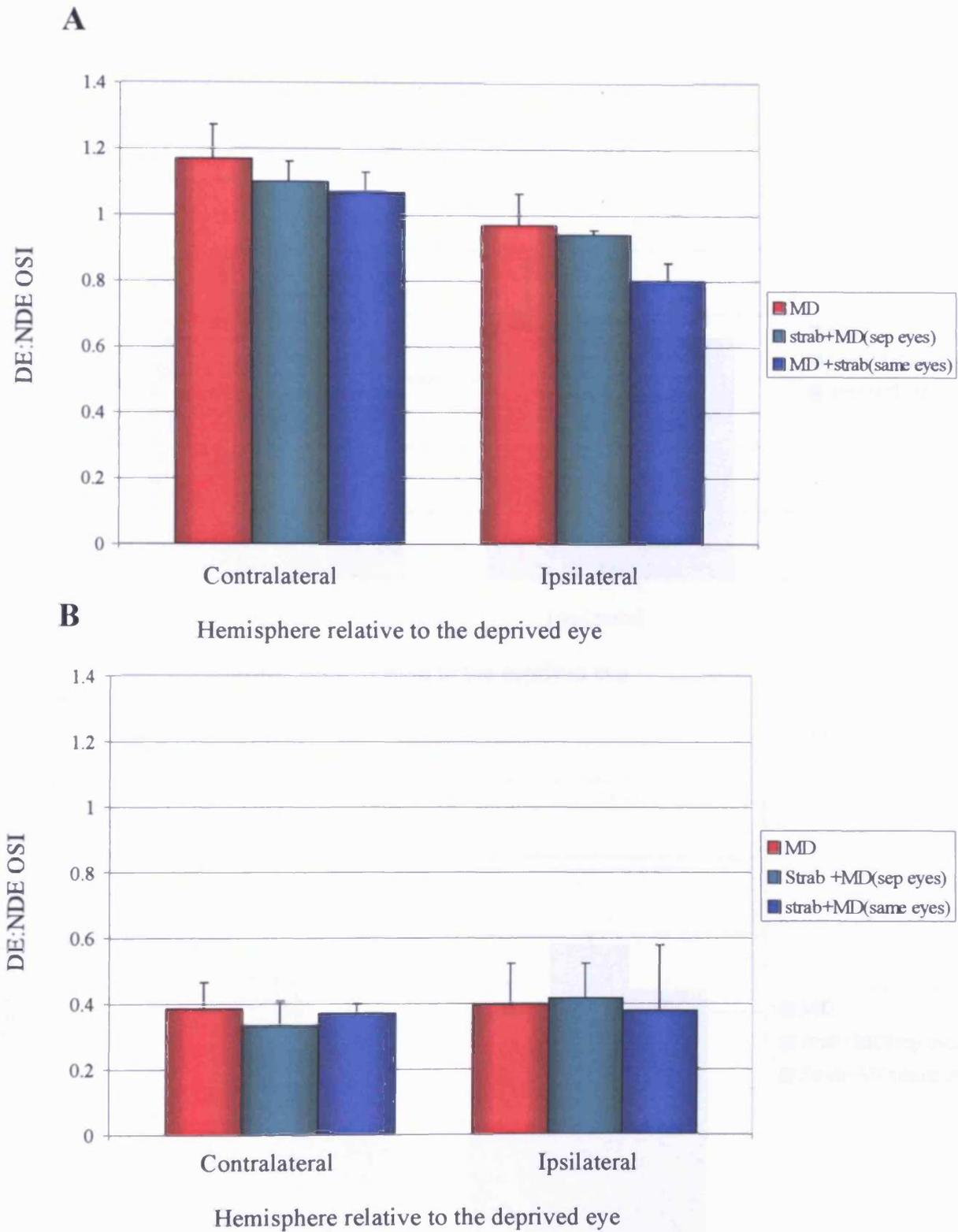
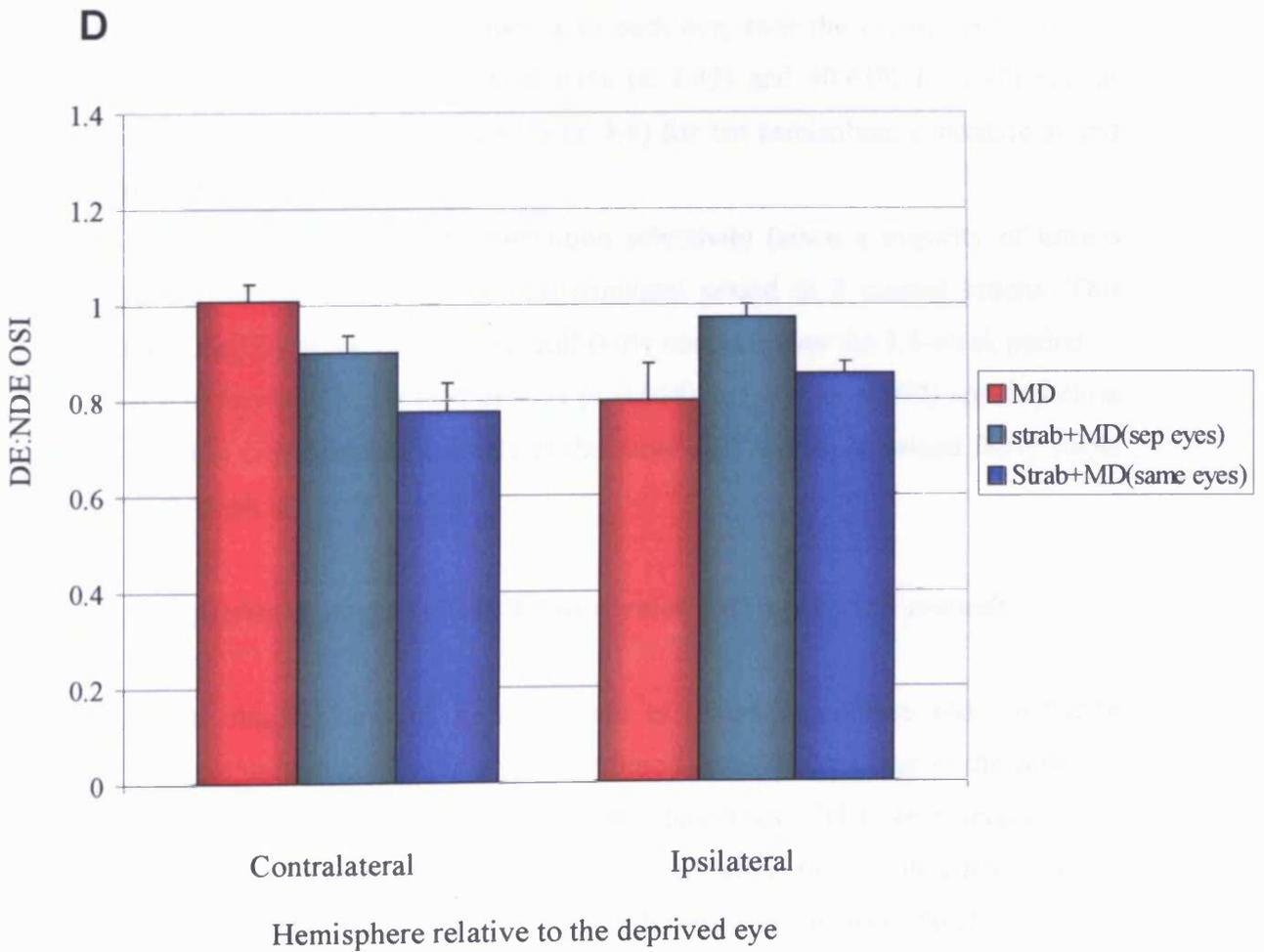
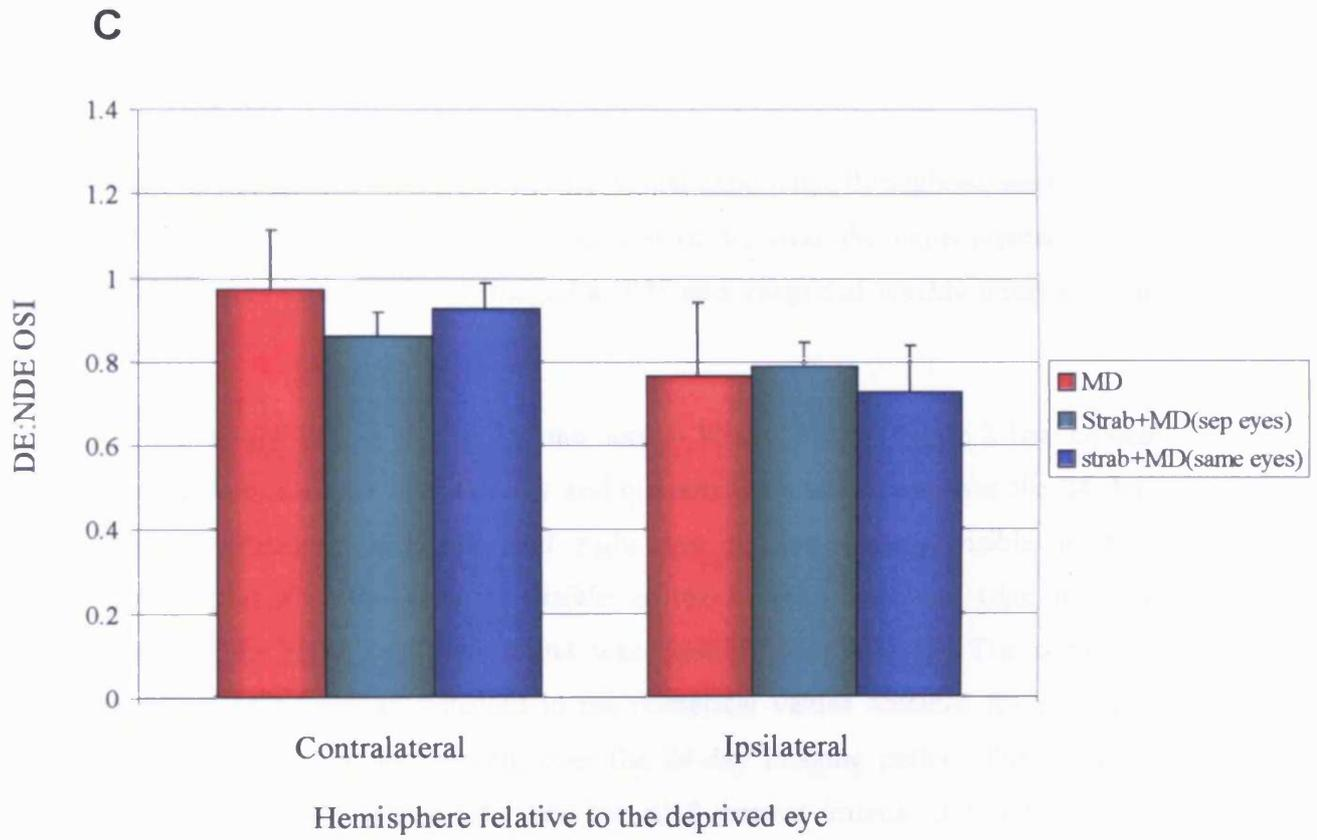


Figure 2.15 a-d Summary of DE:NDE orientation selectivity index (OSI) in each hemisphere imaged

- A) Before MD.
 - B) Immediately after MD.
 - C) Brief period of binocular recovery.
 - D) Extended period of binocular recovery.
- SE bars shown.

No significant difference between MD and S+MD animals was found at any time point ($P > 0.05$, t-test).



Controls

Three additional kittens, which had normal visual experience throughout, were used to study the natural time course of development of V1 over the experimental period. Each animal was implanted and imaged at P35 and imaged at weekly intervals from P35-P56/57.

Ocular dominance data is shown for one normal kitten (842) in figure 2.16a. Optical imaging maps of OD are qualitatively and quantitatively consistent over the 24 days of imaging sessions, with left and right eye patches clearly visible in both hemispheres; at P57 the area of visible cortex became restricted (due to dural regrowth) in the right hemisphere and was omitted from analysis. The consistent nature of the OD maps is reflected in the numerical values obtained for each eye. Values vary only by a few percent over the 24-day imaging period. The summary graph in figure 2.16b shows OD data for all 3 normal kittens. It is immediately obvious that the cortical area responding to each eye, over the experimental period, remains constant. Values at P35 were 61% (± 1.43) and 40.61% (± 1.43) and at P56/57 were 58.1% (± 3.8) and 41.85% (± 3.8) for the hemisphere contralateral and ipsilateral to the reference (left) eye.

Figure 2.17 summarises RE: LE orientation selectivity (since a majority of kittens were deprived in the RE), over the experimental period in 3 control kittens. This parameter is slightly more variable but still fairly constant over the 3.5-week period. Values at P35 for the RE: LE OSI of 1.03 (± 0.038) and 0.99 (± 0.072) are very close to those seen in experimental animals of the same age. Values remained fairly stable thereafter through to P56/57.

Properties of single cells in V1 of normal, MD and S+MD animals

After the last imaging session, cortical maps of ocular dominance and orientation preference were used in conjunction with the blood vessel pattern map of the cortex to target electrode penetrations for extracellular recordings. Cells were recorded for ocular dominance, orientation preference and orientation tuning. Post-hoc analysis allocated each cell the OD category 1-7. Smooth tuning curves were fitted to the data points on the basis of Fourier analysis and preferred orientation and half-width half-

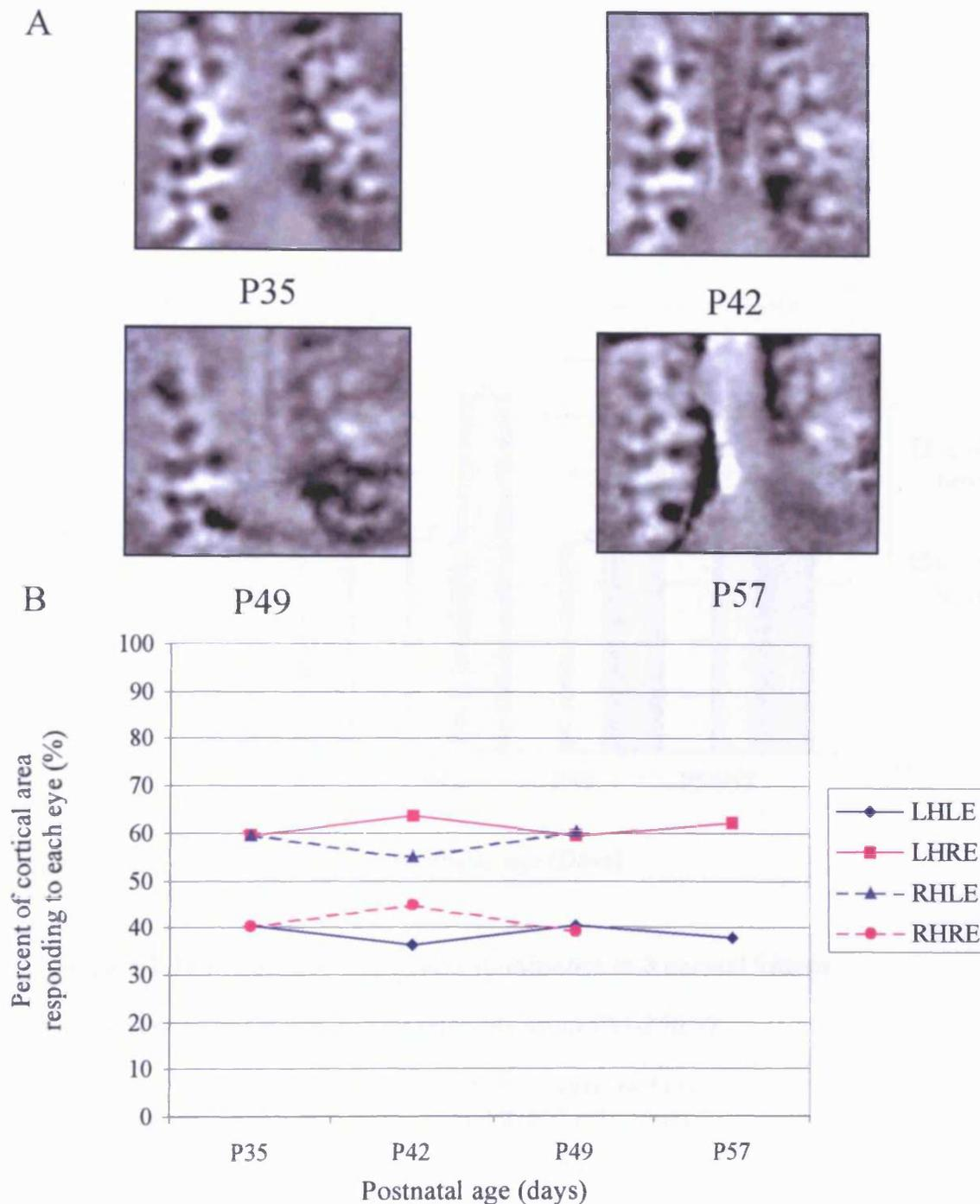


Figure 2.16 a Optical imaging maps of ocular dominance and corresponding ocular dominance values over the experimental period in a normal animal

A Maps are from normal kitten 842 which was imaged at weekly intervals from P35 to P57.

B Percent cortical territory occupied by each eye in each hemisphere. Continuous line is data from the left hemisphere. Dashed line is data from the right hemisphere.

The quality of ocular dominance maps remain consistent over the experiential period and cortical territory varies but only a few percent. At P57 the signal in the right hemisphere became restricted due to dural regrowth, hence analysis was omitted.

Map sizes vary slightly between imaging sessions.

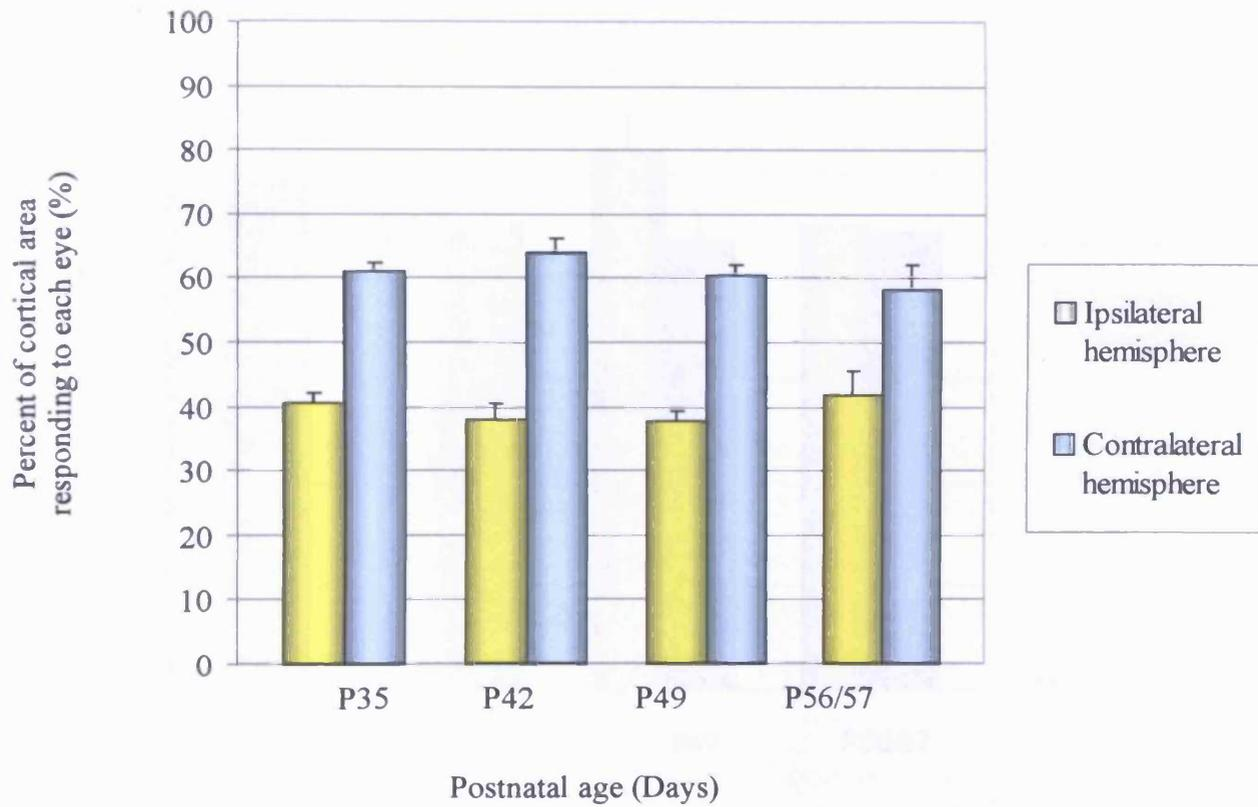


Figure 2.16 b Summary of ocular dominance in 3 normal kittens

Kittens were imaged at weekly intervals from P35-P56/57

Ipsilateral hemisphere to the stimulated eye (yellow bar)
 Contralateral hemisphere to the stimulated eye (blue bar)

SE bars shown

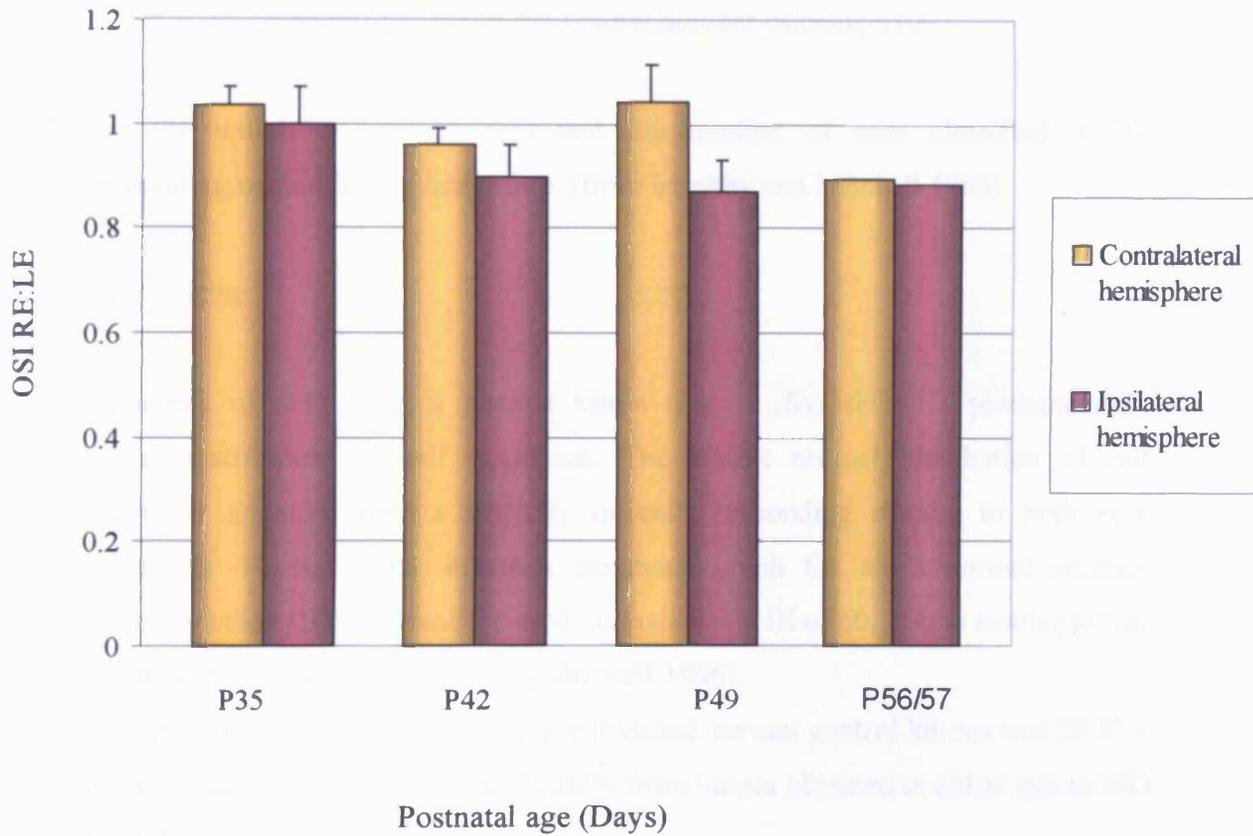


Figure 2.17 Summary LE:RE orientation selectivity index (OSI) for 3 normal kittens

Kittens were imaged at weekly intervals from P35-P56/57.

Ipsilateral hemisphere to the stimulated eye (orange bar).

Contralateral hemisphere to the stimulated eye (purple bar) normal kittens.

SE bars shown.

At P57 only one data point is used so no error bar is applied.

height values were calculated. A binocularity index was calculated to allow quantitative comparisons between cells distributions between different animals. The index was calculated as follows:

$$[(4+2/3(3+5)+1/3(2+6) / \text{total number of cells}] \times 100$$

Where the italicised numbers represent the number of cells classified in the corresponding ocular dominance group. (from Murphy and Mitchell 1986).

Normal rearing

An example of data from a normal kitten (Fig. 2.18a) shows a predominantly binocular distribution of cell responses. The classic normal distribution of cell responses is apparent with a majority of cells responding equally to both eyes (category 4). Figure 2.18d shows a summary graph for all 3 normal animals binocularity index (BI). Normally reared animals had a BI of 60. This is similar to that reported in the literature (Murphy and Mitchell 1986).

The mean half width half height in 2 age matched normal control kittens was $28.9^\circ \pm 1.45^\circ$. This value did not differ significantly from values obtained in either eye in MD or S+MD animals ($P > 0.05$, t-test).

Monocular deprivation

Figure 2.18b shows the OD distribution for 3 kittens after extended recovery from MD. Again the cells follow a predominantly normal binocular distribution, with a majority of cells falling into categories 3,4,5, similar to that of normal animals.

The binocular index of 56.7 (Fig. 2.18d) is only just below that of normal animals (BI 60), suggesting extensive recovery of binocular responses of cells. Recovery from MD ascertained by single cells recordings is widely reported in the literature (Dews and Wiesel 1970; Movshon 1976; Mitchell *et al* 1977a; Olson and Freeman 1978; Liao *et al* 2004). The half width half height for the NDE was $26.8^\circ \pm 1.6^\circ$, but was greater (although not significantly, $P = 0.2$, t-test) for the DE at $30.0^\circ \pm 2.0^\circ$, suggesting a broader tuning of responses through this eye.

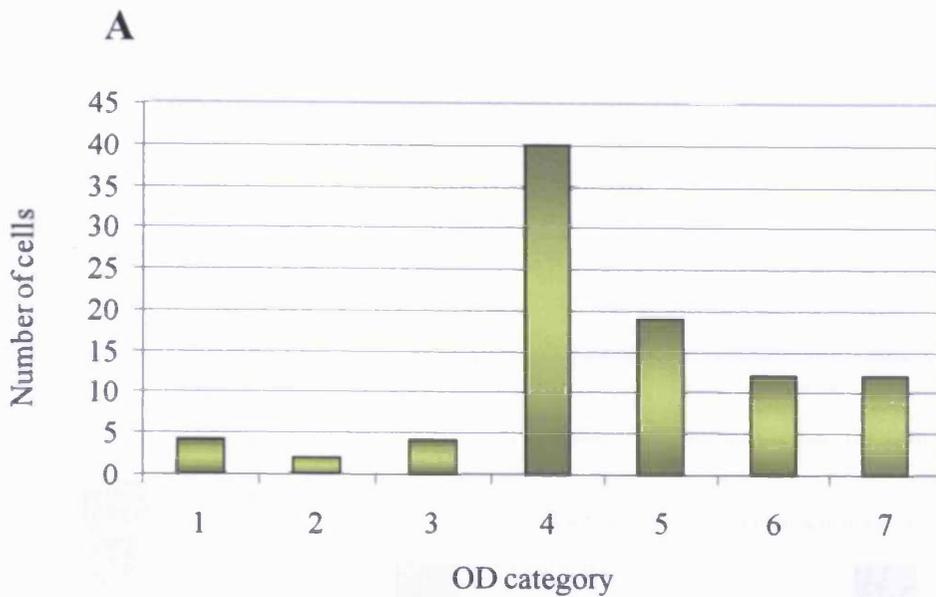


Figure 2.18 a Ocular dominance histogram of 93 cells recorded from kitten visual cortex that received normal visual experience

Category 1 cells respond solely to the RE.
 Category 7 cells respond solely to the LE.
 Category 4 cells respond equally to both eyes.

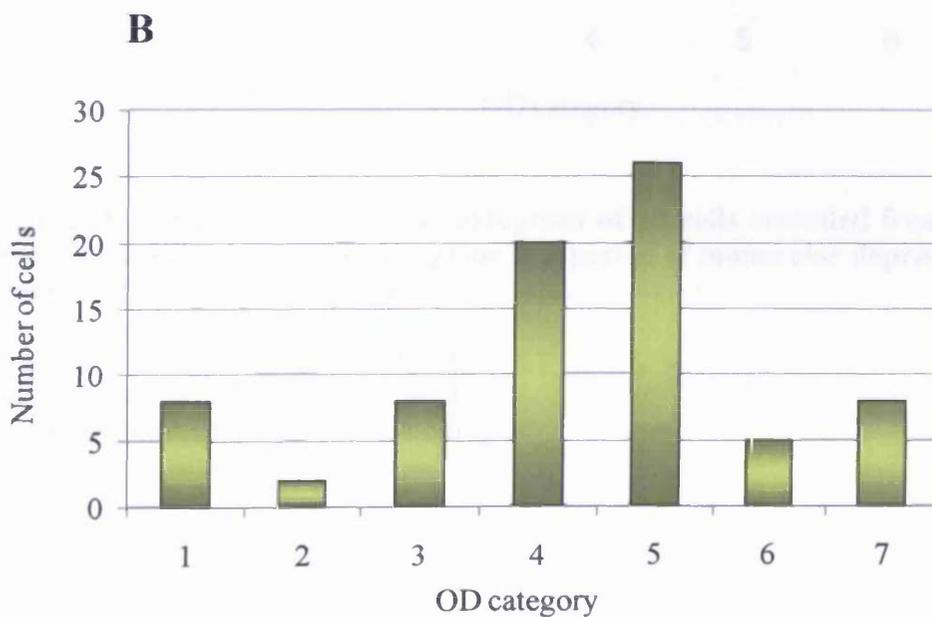


Figure 2.18 b Ocular dominance histogram of 77 cells recorded from kitten visual cortex that received a period of monocular deprivation from P35-45 followed by several weeks of binocular recovery

Category 1 cells respond solely to the RE.
 Category 7 cells respond solely to the LE.
 Category 4 cells respond equally to both eyes.

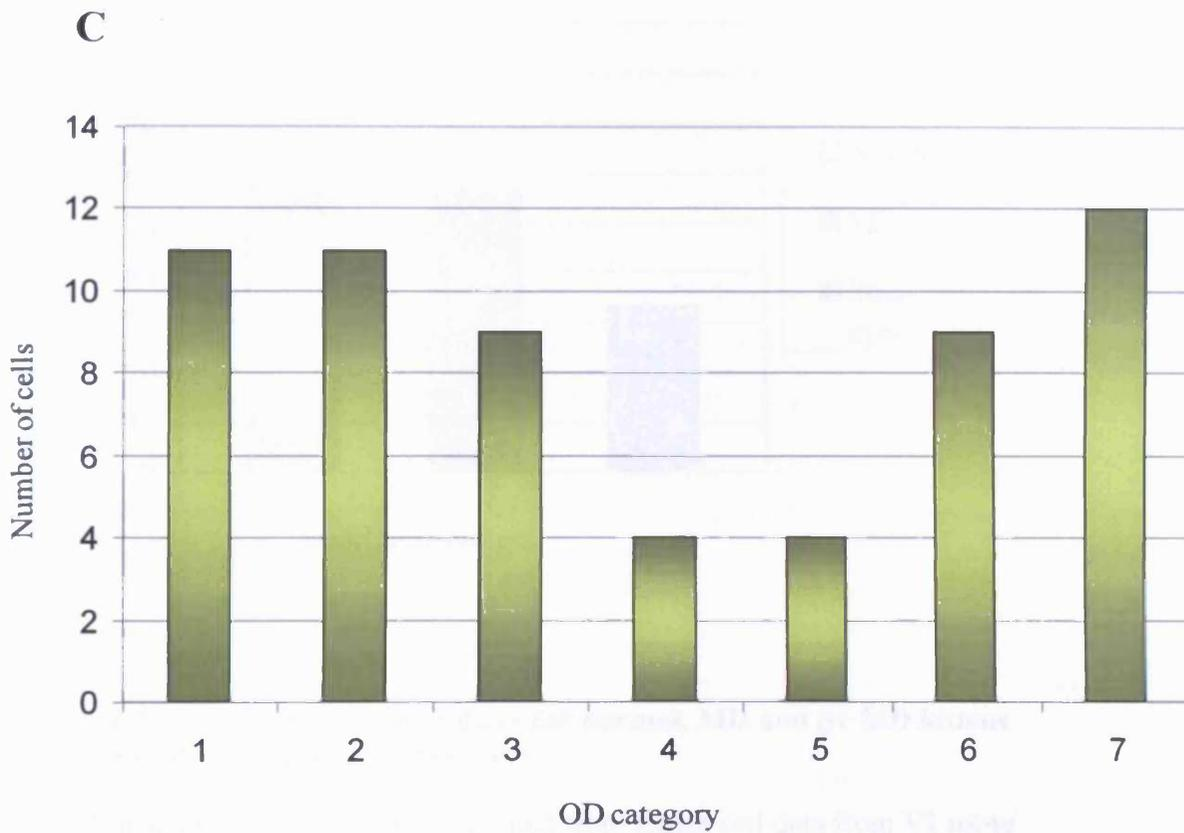


Figure 2.18 c Ocular dominance histogram of 60 cells recorded from kitten visual cortex, that received a strabismus prior to a period of monocular deprivation followed by 3 weeks of binocular recovery

Category 1 cells respond solely to the RE.

Category 7 cells respond solely to the LE.

Category 4 cells respond equally to both eyes.

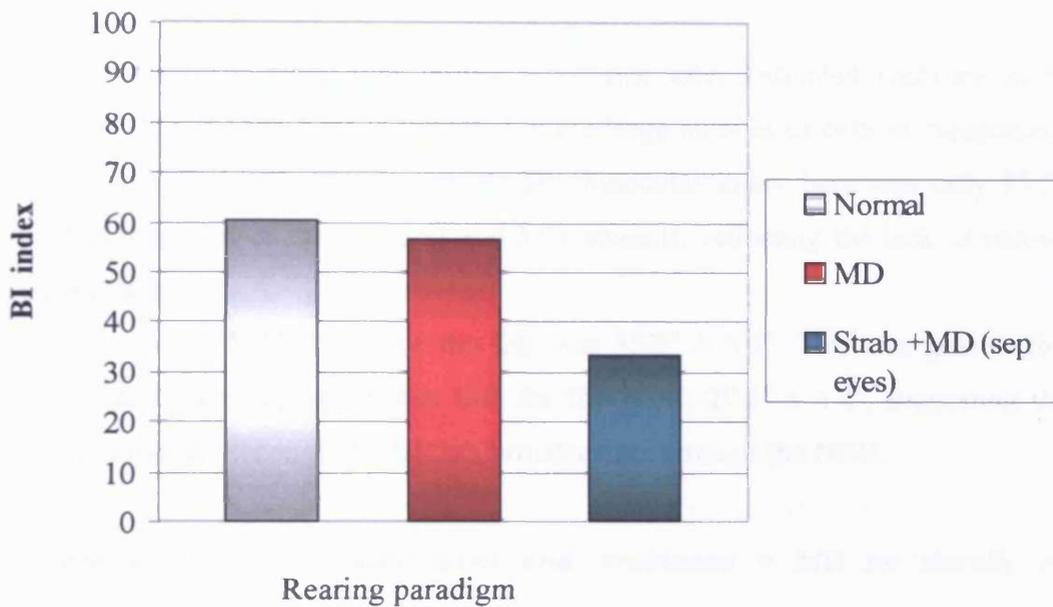


Figure 2.18 d The binocular indices for normal, MD and S+ MD kittens after an extended period of recovery

The binocular index (BI) was calculated from single cell data from V1 using the calculation below:

$$[(4 + 2/3 (3+5) + 1/3 (2+6) / \text{total number of cells}] \times 100$$

Italicized numbers represent the number of cells classified in the corresponding ocular dominance category (from Murphy and Mitchell 1986).

A binocular index of 100 would mean that all cells respond equally to both eyes. A value of 0 would mean all cells respond solely to one eye or the other.

Strabismus and MD

A predominantly monocular cortex is present after extended recovery in S+MD animals (Fig. 2.18c). This is reflected in the large number of cells in categories 1 and 7 and very few cells in category 4. The binocular index here was only 33.2 (Fig. 2.18b), much lower than normal and MD animals, reflecting the lack of recovery of binocular cells.

The half width half height for the DE was $35.5^\circ \pm 3.5^\circ$. This was greater (but not significantly, $P=0.2$, t-test) than that for the NDE; $29.1^\circ \pm 4.4^\circ$, suggesting that the tuned responses through the DE are broader than through the NDE.

Effects of monocular deprivation and strabismus + MD on visually evoked potentials

An example of raw VEPs (averaged over 20 trials) is shown in figure 2.2. These are at P35 taken from kitten 280, which was made strabismic in the RE and later monocularly deprived in the LE. Horizontal gratings were phase reversed at 1Hz over a 3-second period, resulting in 6 VEPs (3 for an ON response and 3 for an OFF response of the cells).

These are most clearly seen in both eyes at the lower spatial frequencies. Although data acquisition is synchronised with stimulus presentation, there is a variable phase relationship, which occasionally leads to the first potential being obscured by the stimulus offset artefact (first trace RE). However, generally 6 clear responses can be seen qualitatively even up to some of the highest spatial frequencies used.

In the strabismic RE it can be seen that the response with the biggest amplitude is at 0.2 cyc/deg. As the spatial frequency of the gratings increase, the amplitude of the response decreases up to 1.13 cyc/deg. Beyond that no clear VEPs are distinguishable and the trace differs little from that seen in response to a blank screen.

In the non-strabismic LE, the amplitude of the corresponding responses to those seen in the strabismic eye are greater. Again the response is strongest at 0.2 cyc/deg. As the spatial frequencies increase, the amplitude of the response decreases. Although at spatial frequencies above 0.56 cyc/deg, the VEPs become less distinct, VEPs are still

visible beyond the maximum of 1.13 cyc/deg of the strabismic eye. A weak response is present at 1.6 cyc/deg, which is still discernible from the response to a blank screen.

Effects of MD on acuity

Figure 2.19 shows the combined data from two MD animals. Acuity for both eyes are very similar (LE - 2.7cyc/deg and RE - 2.5 cyc/deg (± 0.2 cyc/deg for both)). The acuity of the NDE varies over the experimental period. It decreased slightly upon immediate termination of MD and after 2 days of recovery, before returning to the original level, finishing slightly below that seen before MD (2.2 cyc/deg, ± 0.3 cyc/deg). Immediately after MD the acuity of the DE decreased dramatically to 0.6cyc/deg ± 0.14 cyc/deg). Despite a slight decrease in acuity of the NDE at this point also, by far the most important relationship is the ratio of DE to NDE response. From a ratio of just below '1' before MD, after MD that had fallen to just over 0.5. In short, the acuity of the NDE was twice that of the DE. Just two days of recovery after MD and the acuity of the DE had improved considerably but had not yet returned to its pre-MD value or match that of the NDE. The deprived eye had reached an acuity of 1.5cyc/deg (± 0.39 cyc/deg), approximately 2/3 that of the NDE. However, between 2-9 days recovery of acuity of the DE continued, returning to pre-MD levels and matching that of the NDE (~ 2.5 cyc/deg for both eyes ± 0.14 - 0.18 cyc/deg).

Effects of strabismus and MD on acuity

Figure 2.20 shows graphs of VEP responses recorded from kitten 934 over the experimental period (strabismus and MD in separate eyes). Before MD, the acuity of the non-strabismic eye (to be deprived) was 2.35 cyc/deg. The acuity of the strabismic eye was only 68% of that value, at 1.6 cyc/deg (Fig. 2.20 a and b). Maximum amplitudes for each eye were very similar in both eyes (Fig. 2.20 a and b and Fig. 2.21b). Immediately after a ten-day period of MD the acuity of the DE decreased dramatically (Fig. 2.20 c and d). It is only just above the level of the noise. The acuity of the NDE had increased. The amplitude of the VEPs is only just above the level of noise. Acuity of the DE is only 0.38 cyc/deg while that of the NDE had reached a maximum acuity 3.8 cyc/deg. Orientation tuning at this point was broader than previous.

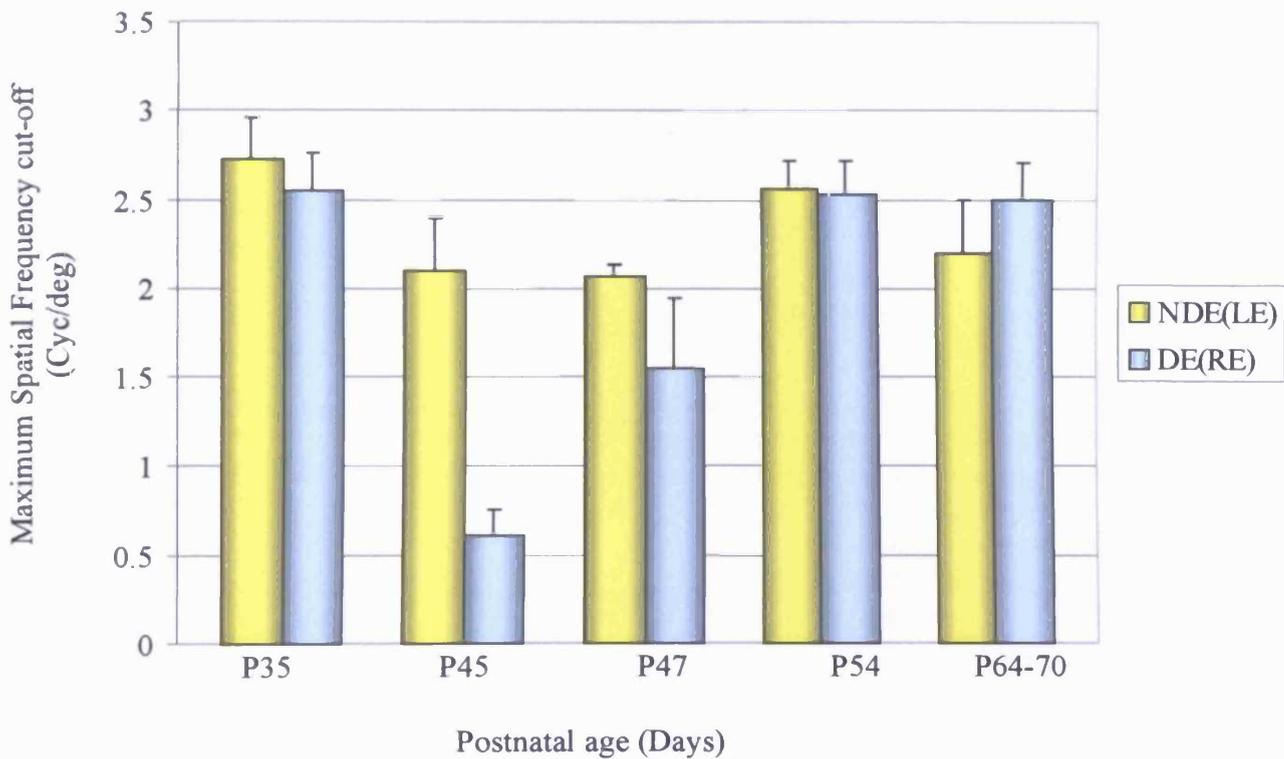


Figure 2.19 Average visual acuity in both eyes for kittens monocularly deprived for 10 days

Kittens were monocularly deprived in the RE at P35-P45.

Values are the average of each hemisphere and each animal.

Blue bar represents the deprived eye.
 Yellow bar represents the non-deprived eye.
 Standard error bars shown.

Figure 2.20 a-j Time series of visually evoked potentials for both eyes before, immediately after MD and during recovery

Data from kitten 934 where strabismus was imposed in the RE at P21 followed by 10 day period of monocular deprivation in the LE from P35-45

Filled circles represent the RE.

Open circles represent the LE.

Filled triangles represent response to a blank screen.

Top figure - VEPs for the hemisphere contralateral to the DE.

Bottom figure - VEPs for the hemisphere ipsilateral to the DE.

Before MD - A and B.

Immediately after MD - C and D.

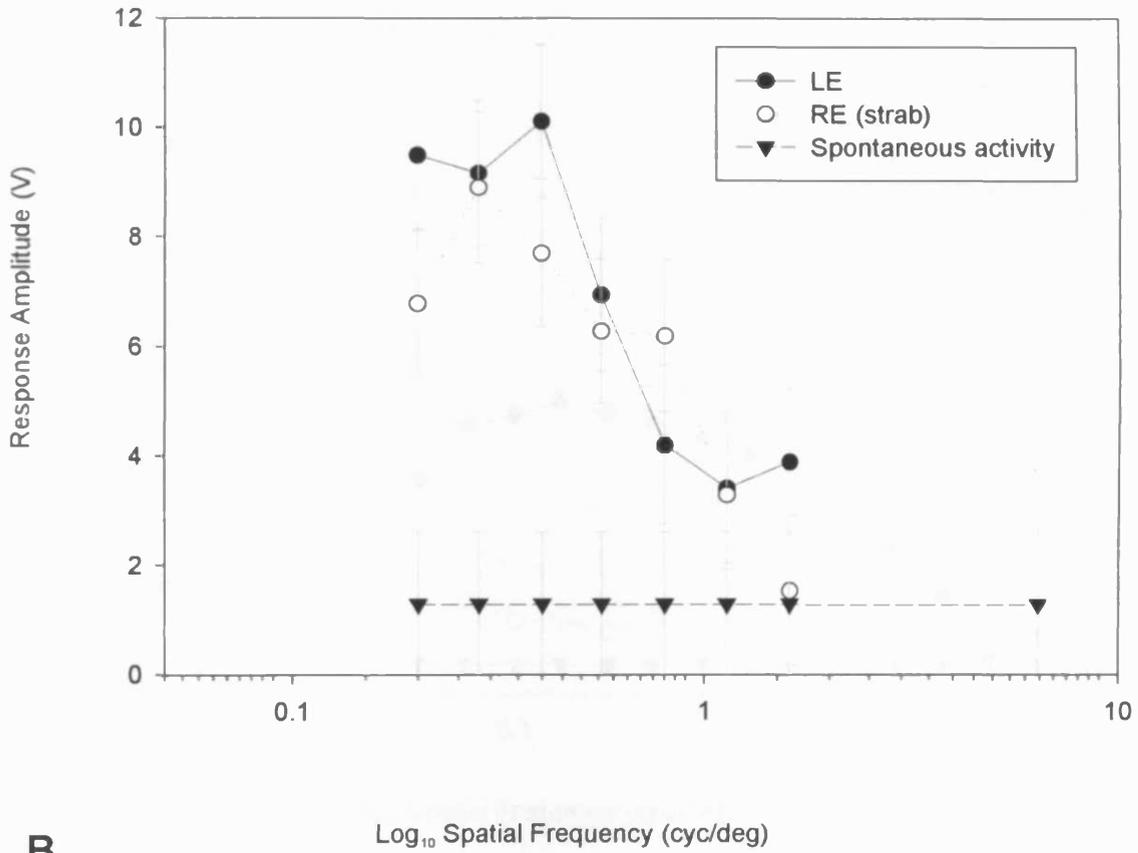
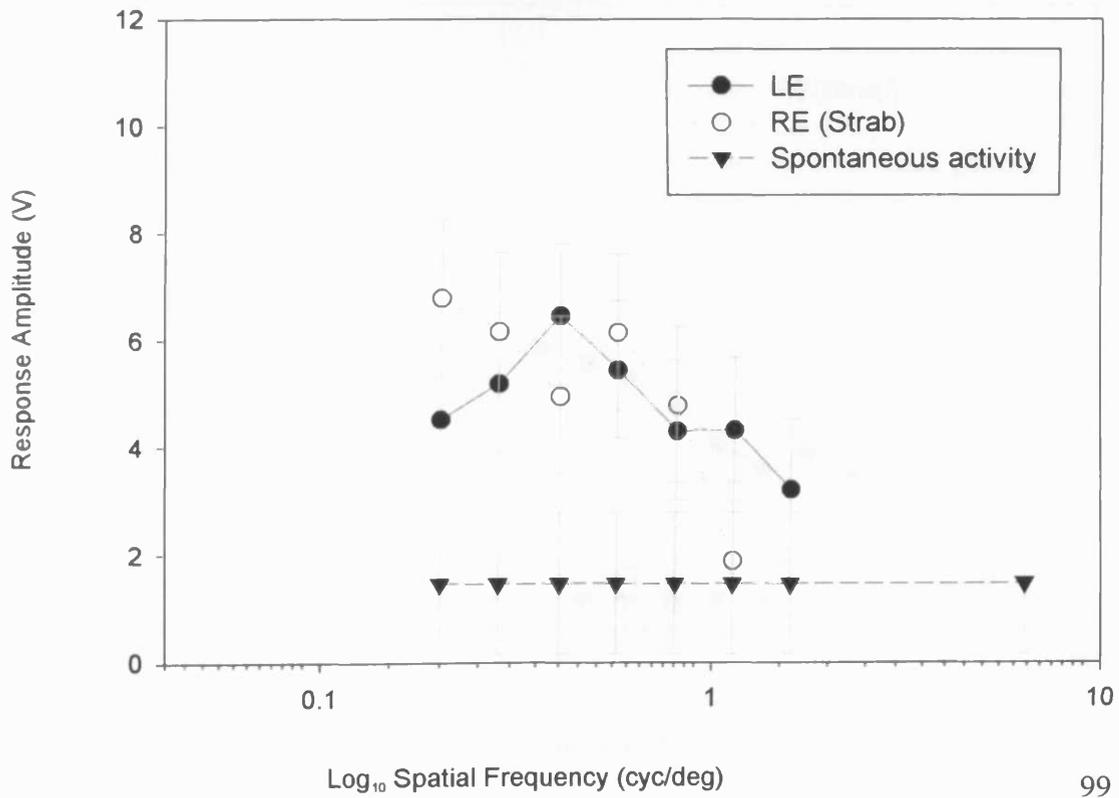
3 days of recovery - E and F.

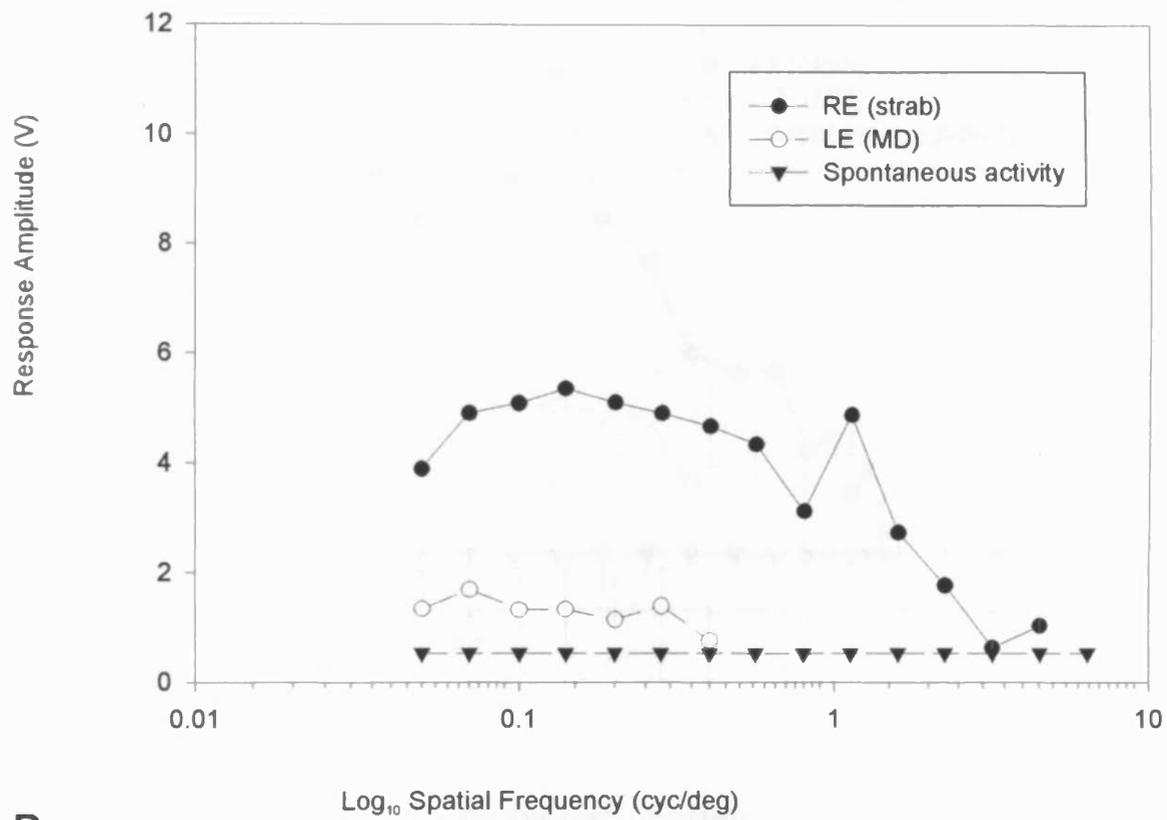
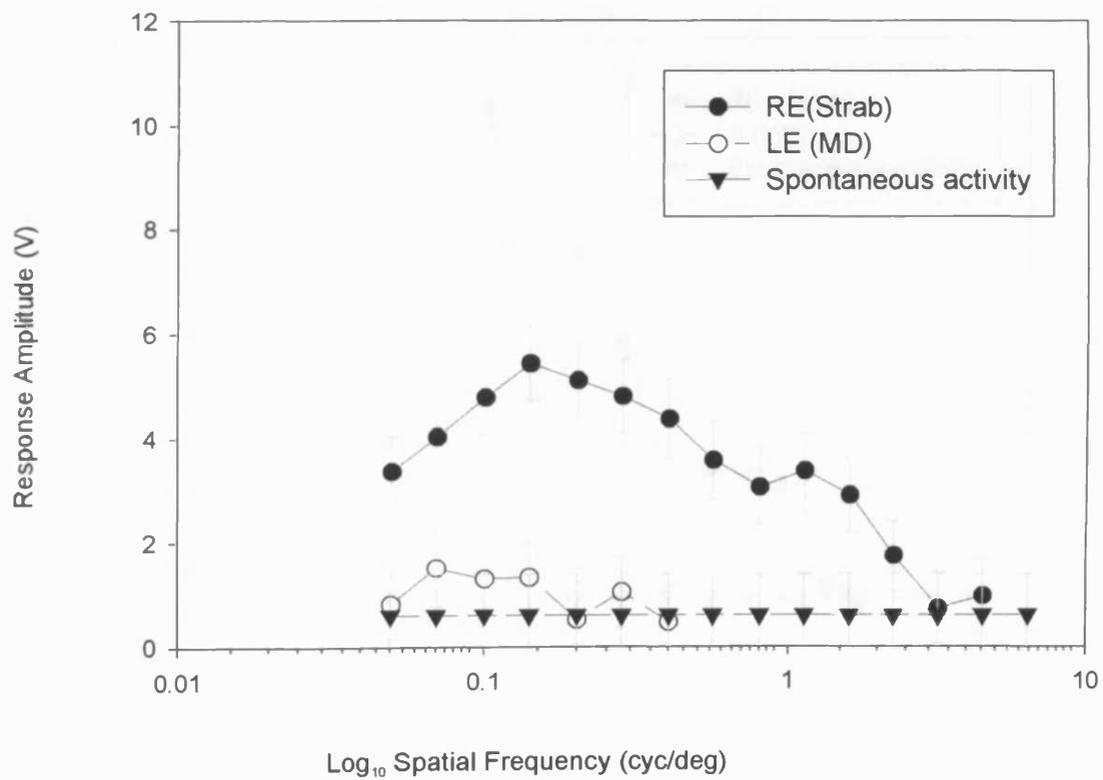
9 days of recovery - G and H.

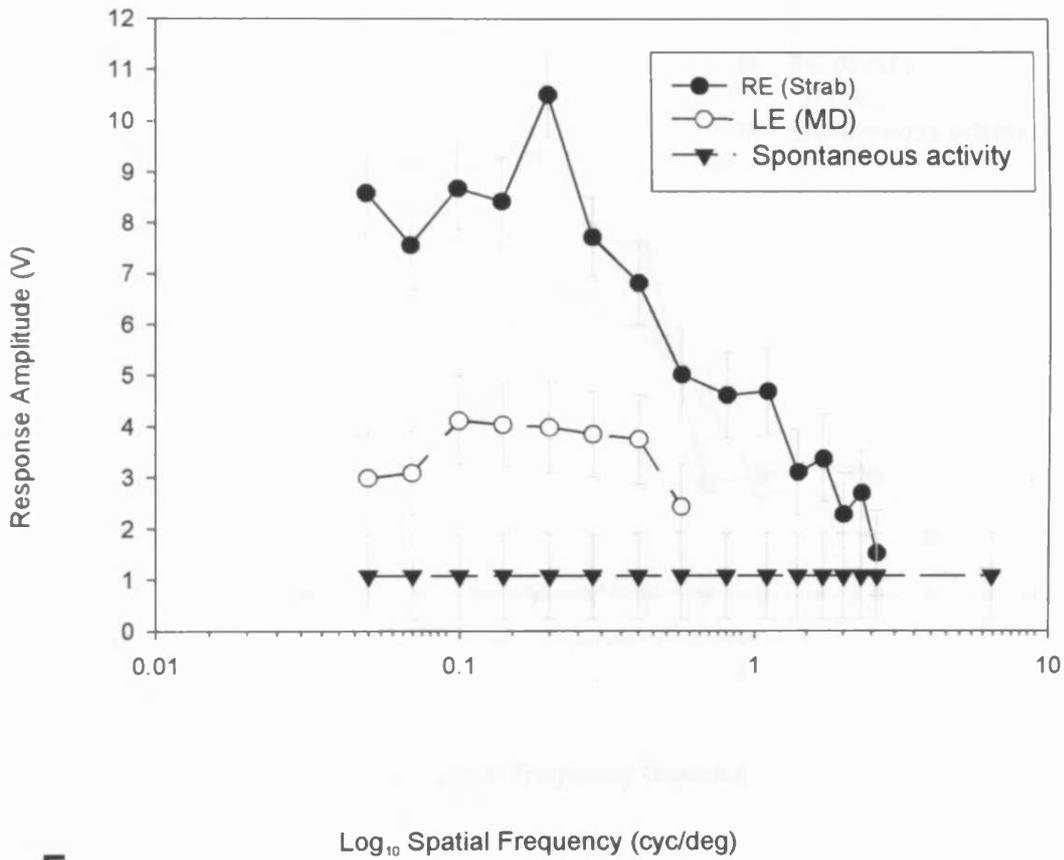
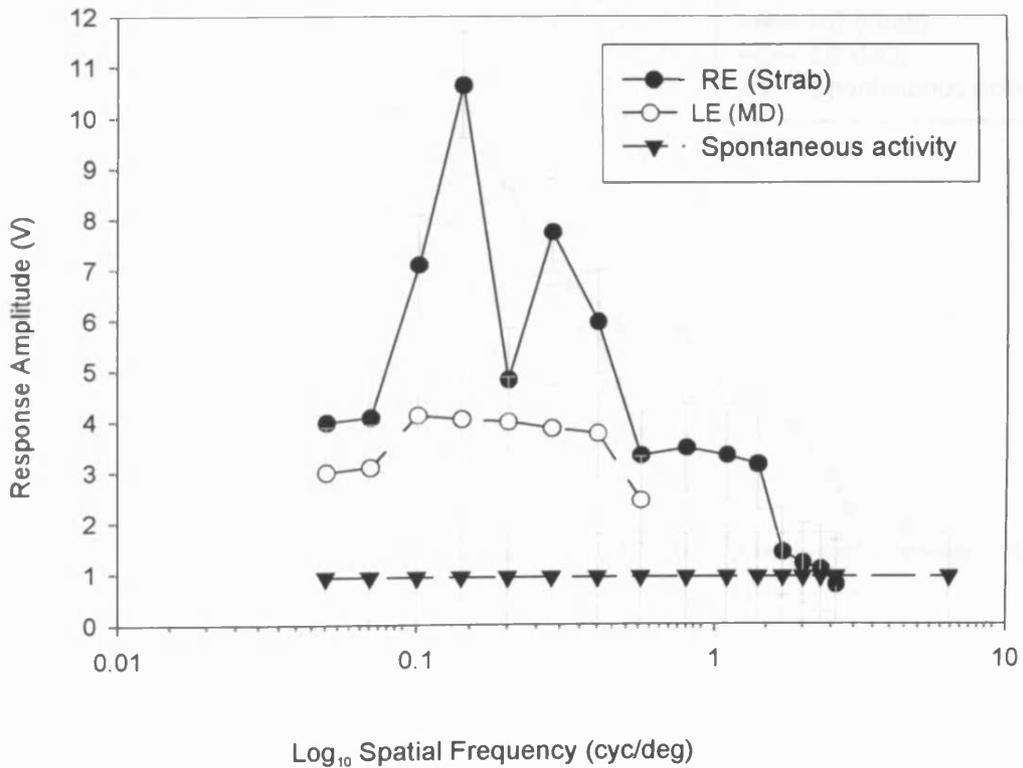
Extended recovery - I and J.

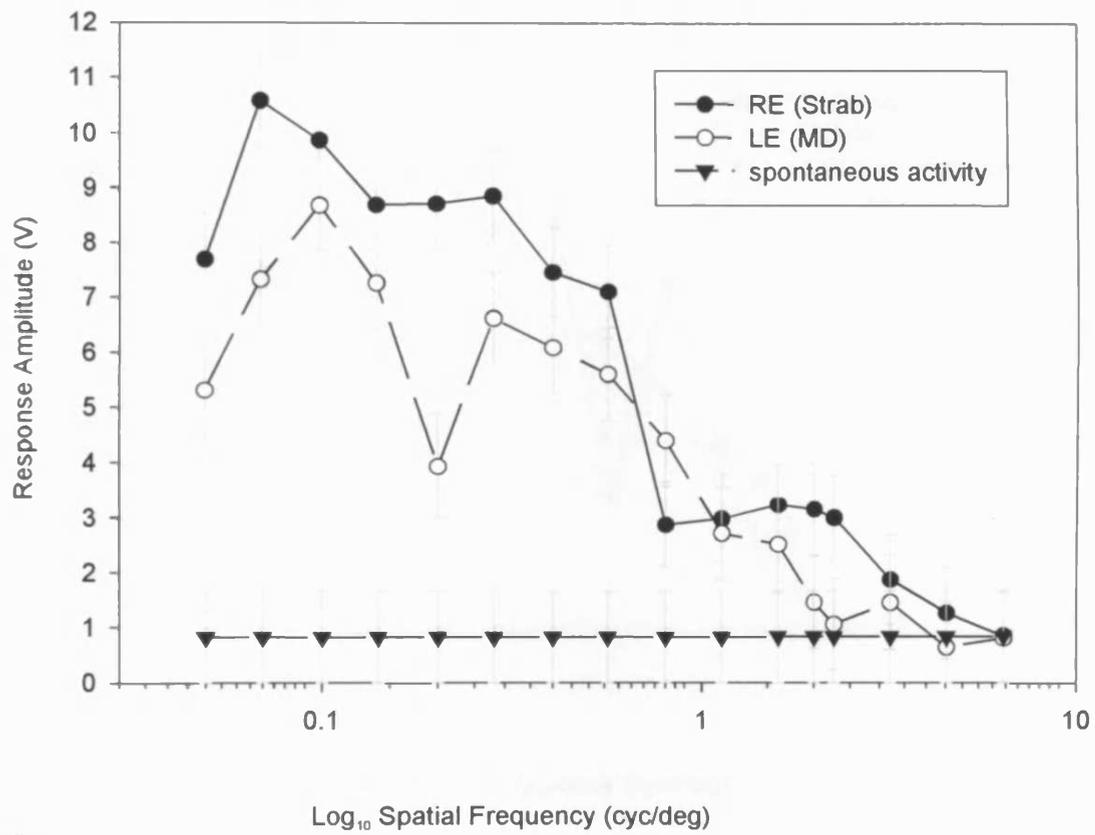
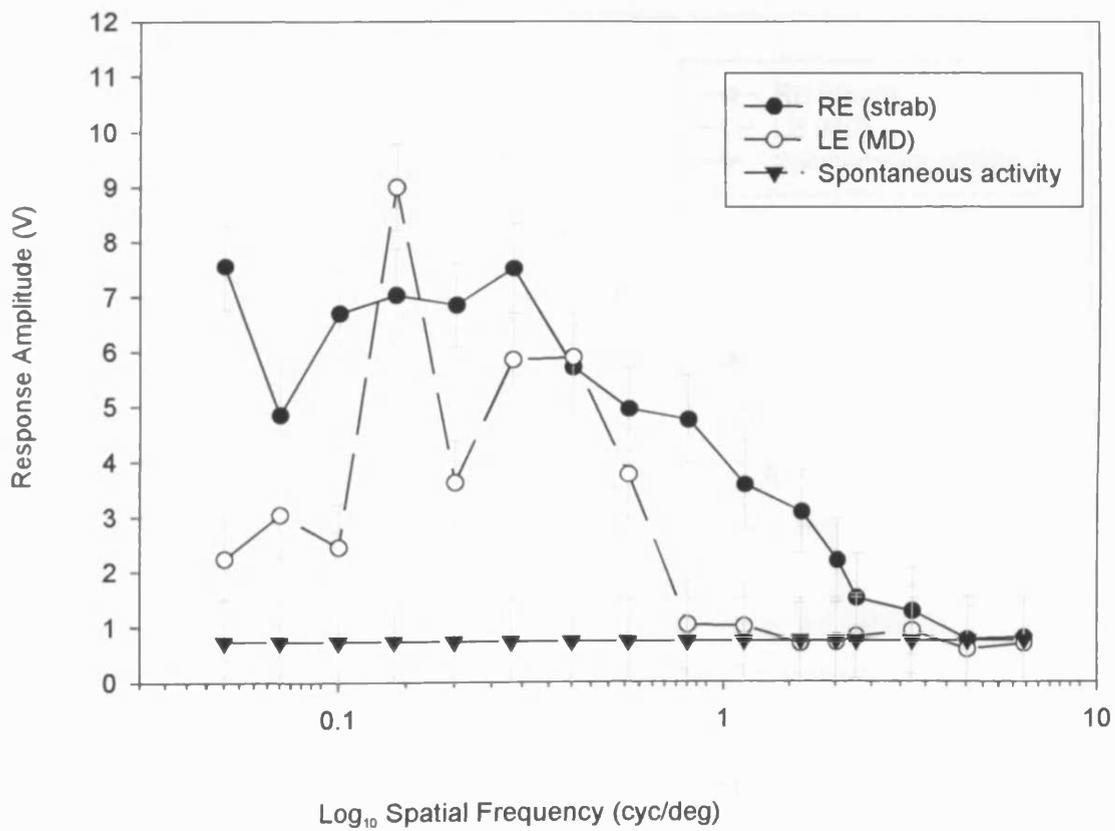
.

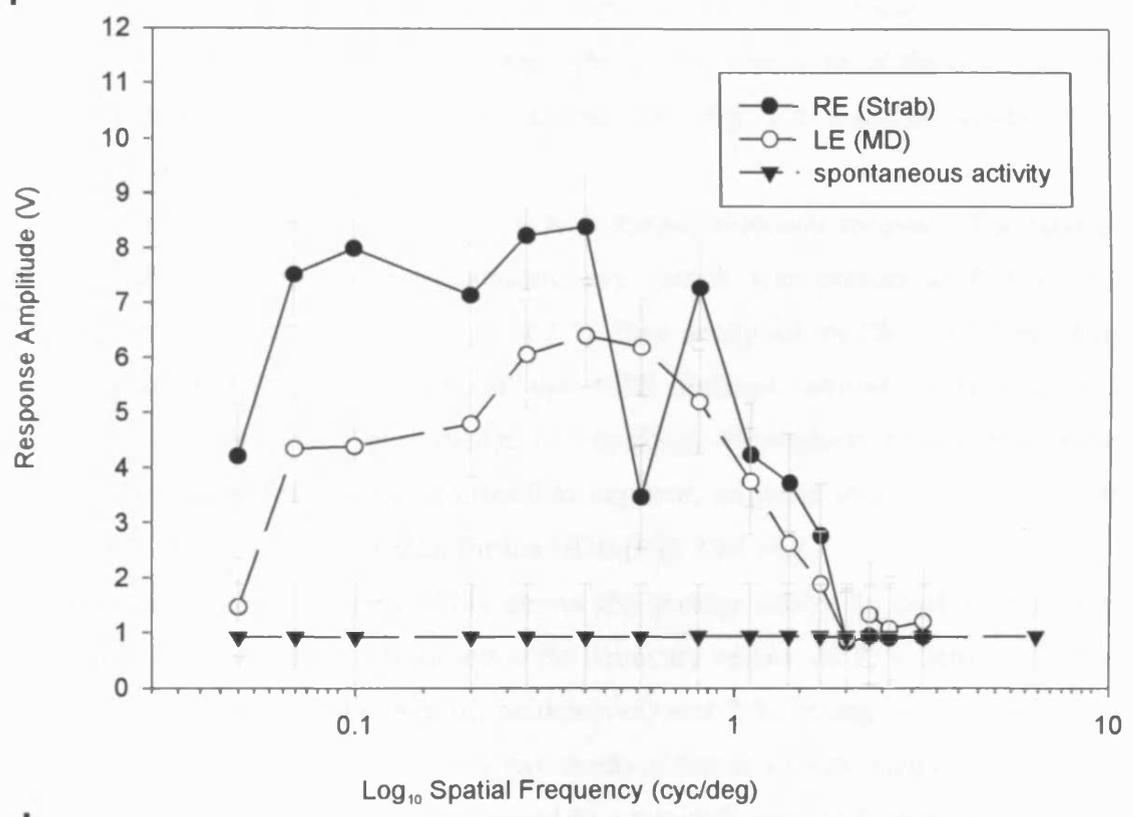
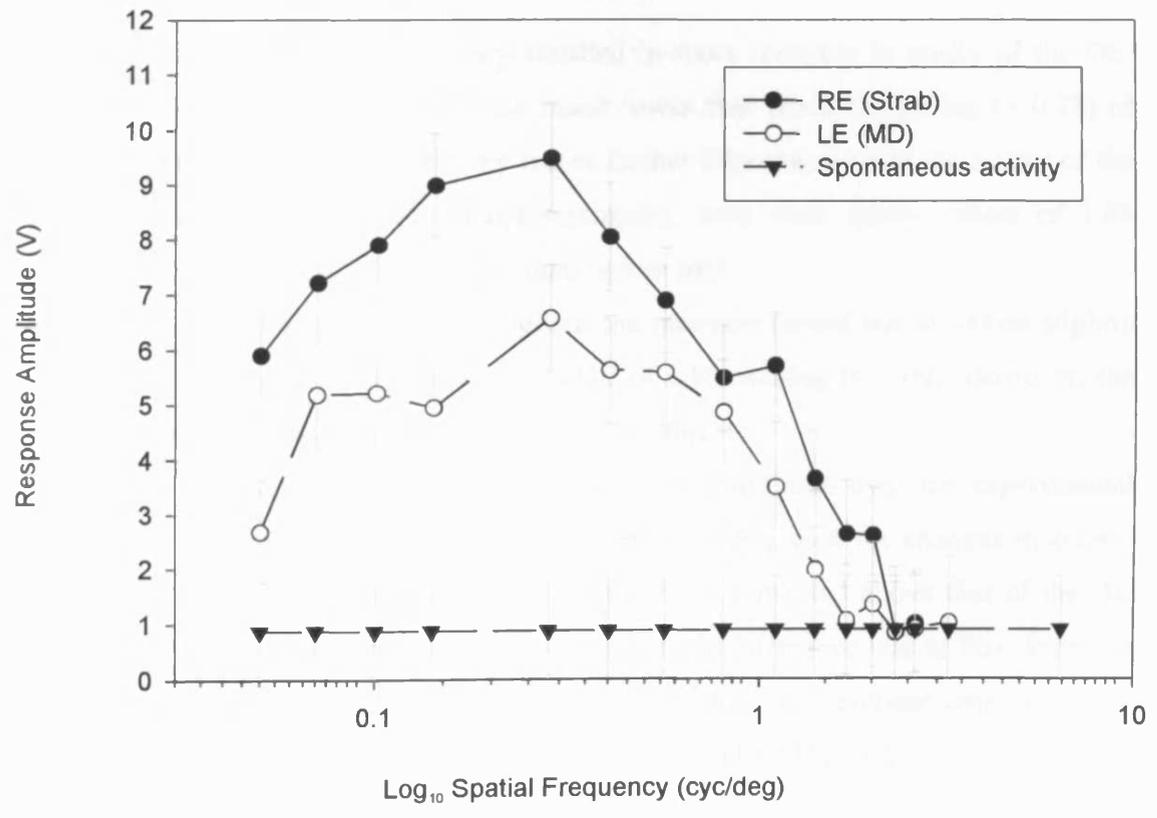
Grey bars are the standard error of the response.

A**B**

C**D**

E**F**

G**H**

I**J**

After a brief period of recovery, some improvement of DE acuity had occurred. Acuity for the DE reached 0.98 cyc/deg although the amplitude of the response was only approximately one third as much as the NDE (Fig. 2.20 e and f). Acuity of the NDE had decreased.

Acuity of the DE continued to improve with further binocular recovery. The ratio of acuity's of strabismic to non-strabismic eye, which was present at P35 (~2:3), subsequently was not present at P61 (~2:1.5). Final acuity for the DE was 1.5 cyc/deg, below that at P35. The acuity of the NDE finished similar to that at P35 (1.95cyc/deg), but above that of the DE (1.5 cyc/deg). Throughout the recovery period although the acuity of the DE continued to improve, response amplitudes for the DE remained 1.5 - 3 times lower than for the NDE (Fig. 2.20 e-h).

The summary graph in figure 2.21a shows the average acuity for both kittens. The trend seen in kitten 934 is confirmed in the summary values. At P35 (before MD) the acuity of the non-strabismic eye (to be deprived) was 2.9 cyc/deg (± 0.36) while the acuity of the strabismic eye was only two thirds of that at 1.97 cyc/deg (± 0.25). After lid closure the acuity of the DE decreased to a minimal value of 0.36cyc/deg (± 0.1). Acuity for the NDE increased to be ten times higher than that of the DE (3 cyc/deg ± 0.54).

A brief period of binocular recovery resulted in some recovery in acuity of the DE. This was to 0.85 cyc/deg (± 0.07) but much lower than the 2.15 cyc/deg (± 0.28) of the NDE. Further binocular recovery led to further improvements in the acuity of the DE. Values for the NDE fluctuated minimally, with final acuity values of 1.85 cyc/deg (± 0.17) being slightly higher than before MD.

The acuity of the DE improved throughout the recovery period and to values slightly below (1.4 cyc/deg ± 0.04) that of the NDE of 1.85 cyc/deg (± 0.08). However, the value of the DE was 40% lower than it's initial value.

Figure 2.21b shows the summary of the response amplitude over the experimental period. The trend for the two eyes is very similar to that seen for changes in acuity. Apart from P35, the response amplitude of the NDE remained above that of the DE throughout the experimental period. The only notable difference was at P61. Whereas the acuity of the DE finished below its starting value, the response amplitude was almost identical at P61 to that at P35 – 8.7V (± 0.8) and 8.5V (± 1.2).

Comparisons between MD and strabismus + MD acuity

The deficiency of the strabismic eye compared with the non-strabismic eye can be appreciated before MD in MD only (Fig. 2.19) and S+MD (Fig. 2.21a) animals. In both cases the acuity of the normal eye ranged from 2.55-2.9cyc/deg, while the strabismic eye is 2 cyc/deg). In MD only animals, the effect of MD on DE acuity appears to be less than that of the S+MD animals. This can be accounted for by an unexpected result in one MD only animal immediately after MD. A clear average response could be elicited through the DE. Positioning of the recording electrode was varied several times and the position of the eye shutters to ensure that the NDE responses were not being included in DE stimulation. It could be argued that the original deprivation was incomplete due to the sutured eye opening during the deprivation period. However, the eyes were checked daily for opening and none occurred. Moreover, optical imaging revealed very weak responses through the DE consistent with other data from MD animals. Recovery of the DE in MD only animals (Fig. 2.19) was incomplete after 2 days of recovery (60% of NDE). However, in strabismic animals (Fig. 2.21a) with an extra 24hours of vision (3 days in total compared to just 2 in MD only animals), recovery of the DE was just under 40%. Recovery of the DE in MD only animals continued and between 2-9 days of binocular vision resulted in complete recovery of the DE to match pre-MD values. Although some further recovery of the DE did occur in S+MD animals, the DE did not fully recover and acuity finished approximately 50% below that of pre-MD values.

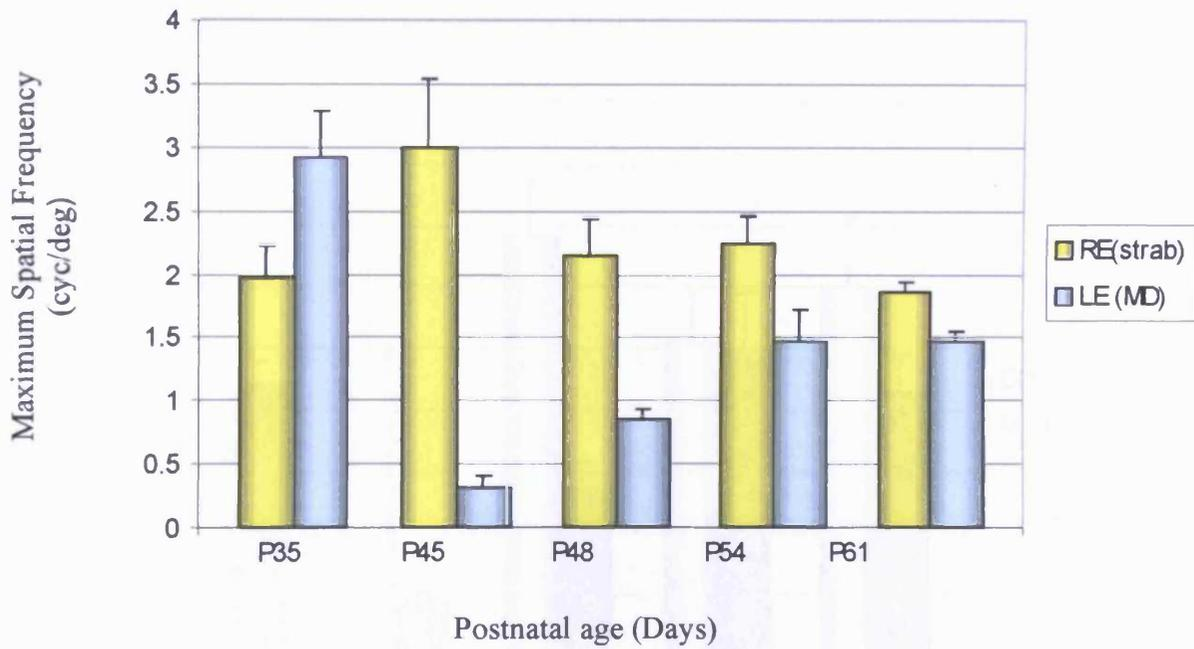


Figure 2.21a Average visual acuity based on VEP cut-offs, in both eyes for kittens made strabismic and monocularly deprived in different eyes

Kittens were made strabismic in the RE at P21/P23 followed by 9/10 day in the non-strabismic eye.

Values are the average of each hemisphere and each animal

Blue bar represents the deprived eye

Yellow bar represents the strabismic eye

Standard error bars shown

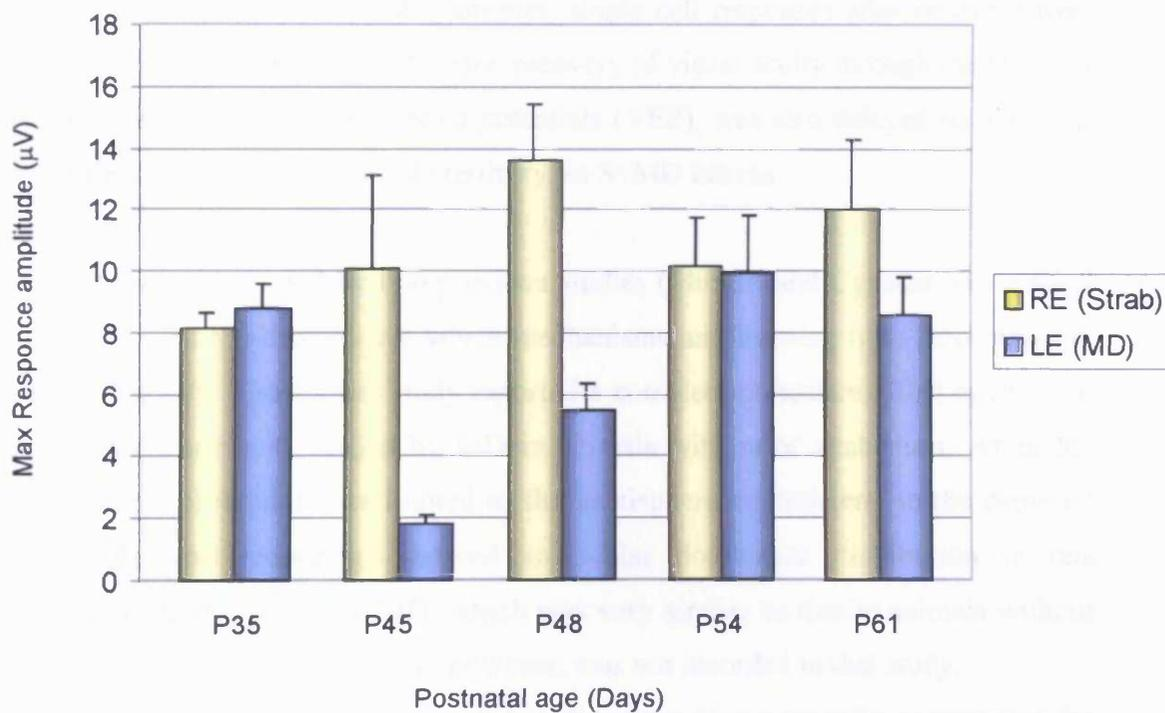


Figure 2.21b Average response amplitude of visually evoked potentials in both eyes for kittens made strabismic and monocularly deprived in different eyes

Kittens were made strabismic in the RE at P21/P23 followed by 9/10 day in the non-strabismic eye.

Values are the average of each hemisphere and each animal

Blue bar represents the deprived eye

Yellow bar represents the strabismic eye

Standard error bars shown

DISCUSSION

It has been demonstrated here that strabismus induced early in life has a considerable effect on the outcome of monocular deprivation and subsequent recovery from it. Firstly, strabismus induced before the period of MD served to significantly protect the hemisphere contralateral to the DE against the ocular dominance shift seen in kittens with just MD. Secondly, recovery of cortical territory in terms of OD was rapid in all MD only kittens. In contrast, in a number of instances with strabismus prior to MD, recovery from MD was delayed. However, single cell responses after recovery were close to normal in both groups. Thirdly, recovery of visual acuity through the DE after MD, as assessed by visually evoked potentials (VEP), was also delayed on a similar time scale to that observed for OD territory, in S+MD kittens .

This work was motivated by two previous studies (Mustari and Cynader 1981; Kind *et al* 2002), and the debate over which mechanisms and learning rules govern visual cortical plasticity. The former study reported a complete protective effect against the ocular dominance shift caused by MD in animals with prior strabismus. As in the current study, protection was limited to the hemisphere contralateral to the deprived eye. Single unit recordings showed an ocular dominance distribution in this hemisphere, after a period of MD, which was very similar to that in animals without deprivation. Orientation selectivity however, was not recorded in that study.

It was argued that, since strabismus all but eliminates binocular cells, competition for those cells would also be abolished. Hence, MD would have little or no effect on territory occupied by either eye. The latter study (Kind *et al* 2002) induced the strabismus after the period of MD. Here it was found that recovery of deprived-eye responses after re-opening was incomplete both physiologically and behaviourally, compared with a control group of kittens without strabismus. While the former study reconciled results with competitive mechanisms, the latter could only be explained with associative learning mechanisms.

Methodological considerations

Optical imaging was employed here to make chronic recordings over the time course of the experiment, from immediately before the period of MD (P35) through to an

extended period of recovery (P61-70). The technique of optical imaging provides repetitive non-invasive visualisation of the time course of development of V1 within the experimental regime. The sample size, lack of sampling bias and spatial resolution make optical imaging better suited than any other technique to assess functional plasticity of the visual cortex. Although optical imaging is becoming more widely used, longitudinal studies (repeated assessment of the same animal) are relatively rare (Chapman *et al* 1996; Godecke *et al* 1997; Sengpiel *et al* 1998) and many paradigms of cortical plasticity have yet to be fully explored in the cat.

Strabismus was induced several weeks before the period of MD, at approximately P21. This coincides roughly with the start of the critical period for ocular dominance and orientation plasticity. At the time of eye-opening (<P14) physiological OD columns are indistinguishable from background uptake of transneuronal label or activity levels in the cortex. Prior to P21 they appear to form independently of visual experience (Crair *et al* 1998; Crowley and Katz 2000; Crair *et al* 2001). Afferents serving the two eyes show a clear segregation by P21 and have an adult-like layout by approximately P39 (LeVay *et al* 1978). The layout of the orientation maps appear to change little in the first few weeks after eye opening regardless of visual experience (Chapman *et al* 1996; Godecke *et al* 1997; Crair *et al* 1998). Based on the above knowledge there would have been no benefit of inducing strabismus much earlier than P21. Despite any visible effects (physiological or anatomical) of a very early strabismus apparently elusive, changes at the molecular and anatomical level would undoubtedly occur. Such anatomical changes might be difficult to visualise due to the relatively sparse nature of afferent terminals in v1 at very early postnatal stages. The period of MD was initiated at P35, which is close to the height of the critical period. The duration of ten days of deprivation is in excess of the requirements for maximal physiological changes to occur, which are almost saturated after 2 days (Movshon and Dursteler 1977; Freeman *et al* 1981; Crair *et al* 1997). However, the anatomical changes take much longer: the shrinkage of the DE geniculocortical afferents only start after 4-7 days while the expansion of the NDE terminals takes several weeks (LeVay *et al* 1980; Antonini and Stryker 1993, 1996). Therefore, the period used here is sufficiently long to ensure that maximal physiological changes have occurred, but brief enough that irreversible degeneration is minimal and therefore recovery from MD can still occur, as MD is terminated within the critical period. This regime is also in line with that used by Kind *et al* (2002).

In the initial set of experiments, strabismus was induced in the same eye that was to be deprived in order to exclude the possibility that the strabismus might balance out the effect of MD. In short, the same eye would be disadvantaged twice. It could be argued that the strabismus itself might have a detrimental effect on vision (amblyopia or loss of motility) in that eye and could increase the likelihood that the NDE would dominate the cortex. Later, both scenarios were explored. Data presented here show that there was no significant difference in the territory occupied by the DE after MD between animals that had been subject to strabismus and deprivation in the same eye or in opposite eyes.

In control animals, the DE occupied just 16.3% of the cortex in each hemisphere, after the period of MD. This OD shift is very similar to that shown previously by optical imaging (Kind *et al*; 2002) and by electrophysiological recordings (Wiesel and Hubel 1963, 1965; Hubel and Wiesel 1970; Shatz and Stryker 1978; LeVay *et al* 1980; Mustari and Cynader 1981; Sherman and Spear 1982; Fregnac and Imbert 1984; Mitchell 1991). Recovery of DE responses to dominate 60.1% and 44.1% of the cortex (contralateral and ipsilateral hemisphere to the DE respectively) shows a stronger contralateral bias compared to that seen previously by Kind *et al* (2002). Despite this strong contralateral bias, the combined territory of the DE in both hemispheres was approximately equal for both eyes (50.9% and 49.1% for the DE and NDE respectively); overall recovery was complete. In strabismic kittens, a reduced effect of MD was seen in the hemisphere contralateral to the DE. The DE occupied 30.7 % and 28% of the cortex (strabismus and MD in the same eye and in opposite eyes, respectively). The values here are almost identical to DE values of 30% (in the contralateral hemisphere to the DE – obtained by adding OD groups 1 and 2 from their Fig.1) shown by electrophysiological recordings by Mustari and Cynader (1981). Local and long-range binocular connections and interactions are maintained and strengthened as correlated activity through both eyes activates post-synaptic cells. De-correlating the inputs to the two eyes causes a breakdown in binocularity and can be expected to cause a loss of competition between afferents representing the two eyes. If this competition is removed by strabismus, an advantage given to one eye by closing the other should have little or no effect on the overall territory occupied and the cells dominated by each eye. The values obtained here of 28-30% territory for the DE are much less than the ‘normal’ range of values (40-45%) that would be predicted by a purely competitive nature of binocular interactions, i.e. if there was no OD shift at all.

Interpretation of results in light of BCM theory

The results in this study so far cannot be fully explained by competitive mechanisms, however, they can be reconciled more easily by invoking non-competitive, associative mechanisms (BCM). Pre-synaptic activity coincides with post-synaptic activity below θ_m upon strabismus induction. The modification threshold shifts left to catch up with the falling response through the deviated eye (similar to MD). The effect of monocular deprivation on binocular and monocular cells is very different. In a predominantly binocular cortex, MD would result in loss of response through one eye. The modification threshold would left-shift, to match the falling response through the DE, while still being prevented from shifting far leftwards by the correlated activity through the open eye. The large population of cells driven exclusively by the DE caused by the prior strabismus does not have any NDE patterned input to prevent θ_m from shifting leftwards quickly. Hence for DE cells θ_m shifts leftwards very quickly and to a large extent, leaving little scope for LTD. Non deprived eye cells would remain unaffected by the deprivation. The conjecture arises as to what level θ_m has been reduced through both eyes. Through the closed eye there is only spontaneous activity to drive post-synaptic response and (theoretically) the same could be said about the deviated eye.

This above argument is based on the assumption that the strabismus has caused a complete breakdown of cortical binocularity and that the percent of cells dominated by each eye are approximately equal. Although data suggests that the absolute numbers of cells driven by the deviated eye are as numerous as those from the non-deviated eye (Chino *et al* 1983; Mower *et al* 1982; Roelfsema *et al* 1994; Singer *et al* 1980), the degree to which binocular cells have been lost imposes caveats.

Despite a breakdown of cortical binocularity as a result of strabismus, a percentage of binocular cells would remain, increasing with decreasing angle of squint.

Has the deviation had such a detrimental effect on θ_m as first thought? When the inputs through both eyes have been de-correlated, unless the size of the offset was very large (i.e. the two eyes see completely different parts of the visual field) some temporal correlation between the inputs through the two eyes will occur either by chance (random correlation of firing), or when gaze/fixation is altered and the two

eyes come to temporarily view the same part of the visual scene. With this in mind it could be predicted that intermittent temporal correlation of inputs through the deviated eye ensures that θ_m does not decrease to the large extent predicted earlier. The modification threshold does decrease to some extent but to an intermediate level, hence retaining some binocular connections.

Since the likelihood of LTD has already been reduced slightly, although synaptic weakening will occur, it will be to a lesser extent than if θ_m was higher and the likelihood for LTP and LTD were more equal. This appears to have occurred in this study. In kittens with a strabismus, the effect of MD has not been abolished. Some deprivation effect has occurred, but to a lesser extent than would be seen in kittens with just MD.

Alternative explanations

It is worth considering other homeostatic mechanisms (i.e. processes that regulate the stability and functionality of neural networks that are subject to Hebbian synaptic changes) that have been demonstrated in recent work to be active in addition to traditional Hebbian plasticity.

Mechanisms that impose competition among synapses involve a global intracellular signal that reflects the state of many synapses. Stabilization is imposed by limiting the sum of synaptic strengths received by a cell. An entirely different mechanism that does not require a global intracellular signal is Spike timing dependent plasticity (STDP); in which different synapses compete for control of the timing of post-synaptic action potentials (Song *et al* 2000). Experiments in hippocampal slice (Debanne *et al* 1998), neocortical slices (Markram *et al* 1997) and cell cultures (Bi and Poo 1998) show that LTP occurs if pre-synaptic action potentials precede post-synaptic firing by no more than 50ms; conversely pre-synaptic firing following post-synaptic firing leads to LTD. Such a mechanism is appealing in the context of this thesis since the effects of strabismus and MD could be explained by a change in timing of inputs from the affected eye. In the case of strabismus, all the inputs from the one eye would be systematically delayed or advanced, while in MD, their timing relative to those from the other eye and to post-synaptic activity would be essentially random. However, for strabismus followed by MD, a similar protective effect would

be predicted (as for traditional competitive models), since STDP replaces spatial with temporal competition.

Spike timing dependent plasticity cannot strengthen synapses without post-synaptic firing. If, for example, excitatory synapses to a neuron were too weak to make it fire, synaptic strengthening would not occur, and synaptic weakening would ensue. However, a non-Hebbian mechanism such as synaptic scaling may solve this problem. Synaptic scaling stabilises firing rates through global homeostatic regulation of synaptic strengths (see review Turigiano and Nelson 2004). The strength of a neuron's synapses can be assessed by measuring the miniature excitatory post-synaptic current (mEPSC) – the quantal amplitude. Increased activity reduces the average amplitude of mEPSC through a decrease in the number of receptors per synapse, and decreased activity has the opposite effect, while the relative strengths of left- and right-eye synapses remain the same. Experimental support for mEPSC amplitude scaling is provided by activity in rat primary visual cortex was lowered by monocular injections of tetrodotoxin. Two days of tetrodotoxin injection increased the amplitude of mEPSCs onto pyramidal cells in the deprived hemisphere, while leaving the non-deprived hemisphere unaffected (The rodent primary V1 is driven almost exclusively by one eye; monocular deprivation deprives the monocular segment of one hemisphere while leaving the other hemisphere unaffected). These effects were reversed when normal activity was allowed to resume (Desai *et al* 2002).

Synaptic scaling requires integration over long periods of time and affects all inputs to a particular neurone equally. It provides a mechanism of “metaplasticity” (the activity dependent modulation of synaptic plasticity) that is analogous to the cell-wide modification threshold of the BCM model.

Interhemispheric differences and deprivation

Why is this ‘reduced’ effect only seen in the hemisphere contralateral to the DE?

There are a number of lines of reasoning why this may be so. Firstly it could be that the reduced effect of MD in strabismic animals is due to the contralateral eye bands being larger than ipsilateral eye bands. This has been shown by radioactive label injected into the eye of normal and monocularly deprived cats (Shatz and Stryker 1978). Increased separation of these bands in strabismic kittens could mean that the distance which must be transversed by LGN afferents before they contact a cell whose

ocular dominance is to be changed is greater for contralateral than ipsilateral eye bands.

This idea can be extended with the knowledge that a significant loss of horizontal connections to opposite eye domains occurs after just 2 days of strabismus (Trachtenberg and Stryker 2001); clustered horizontal projections preferentially connect cell groups activated by the same eye (Löwel and Singer 1992). Therefore, populations of cells responding to each eye are relatively independent of each other. Cells dominated by one eye may not have connections to cells dominated by the other eye and would not be affected if the visual input to that eye were disrupted. If OD bands were further apart in strabismic animals (Löwel 1994 – however, more recent studies cast doubt over this, Rathjen *et al* 2002; Kaschube *et al* 2003) only long-range connections between cells could be effective at changing OD. Since contralateral eye bands are larger than ipsilateral eye bands, a proportion of contralateral-eye dominated cells would be out of range of long range (callosal) connections. Callosal connections share a number of features with intracortical horizontal connections (Kaschube *et al* 2003), exhibit a columnar distribution (see Innocenti 1986), and the axon arbors of callosal neurones show a patchy distribution (Houzel *et al* 1994). A percent of contralateral eye cells being ‘out of range’ of deprivation is reinforced by the finding that callosal connections are influenced by strabismus in the same way as tangential intracortical connections are (Schmidt *et al* 1997). Even if cells responded preferentially to the eye to be deprived, their OD could not be changed.

Another possible reason for the restriction of the ‘protective effect’ of strabismus lies in the disruption of connections within the corpus callosum following strabismus. The corpus callosum is a deep lying structure, which links the two cerebral hemispheres and allows the two sides of the brain to intercommunicate. Like many other experience dependent networks of connections in the brain, the corpus callosum of the cat achieves an adult connectivity pattern postnatally. The pattern can be disrupted by visual experience (Lund *et al* 1978; Lund and Mitchell 1979a, 1979b; Innocenti and Frost 1980). In normal cats, the callosal cell zone (region sending axons to the other hemisphere) and callosal terminal zone (region receiving axons from opposite zone) are located at the 17/18 border. These zones contain 4 representations, 1) a point in visual space straight ahead of the animal, 2) a representation of the visual field midline, 3) the retinal decussation line, 4) the vertical meridian of the retina. In

strabismic cats the cell and terminal zones are abnormal. Only the retinal decussation line and retinal vertical line are represented at the 17/18 border. Berman and Payne (1983) studied the connectivity of the corpus callosum in V1 in normal cats and cat reared with convergent and divergent strabismus. Abnormally wide callosal cell zones were seen in both hemispheres and abnormally wide terminal zones were seen in the hemisphere ipsilateral to the deviated eye.

Such inappropriate connections could mean that the two hemispheres no longer 'cross talk' and their behaviour could be independent of each other, therefore any changes in one hemisphere would not be reflected in the other. However, this conclusion would be logical only if strabismus abolished all callosal connections. Such links are tenuous and hence unlikely to provide a robust explanation.

A third possible explanation is related to the timing of the emergence of OD columns during development. Optical imaging and transneuronal labelling studies reveal ocular dominance and orientation patches at P14. Overall the contralateral eye dominates the cortex at this age. Responses to stimulation are markedly stronger and more selective than the responses to the ipsilateral eye (Crair *et al* 1998, 2001). The ocular dominance bias is greatest during the first 3 weeks of life (LeVay *et al* 1978; Fregnac and Imbert 1978; Albus and Wolf 1984) and even persists in kittens binocularly deprived from before eye opening until beyond 3 weeks of age (Crair *et al* 1998). Ocular dominance bands segregate from an initial 'sea' of contralateral eye input and only 'islands' of ipsilateral input. During OD column formation, ipsilateral eye responses increase and become nearly identical to those through the other eye (in normal cats) at about 3 weeks of age – the start of the critical period. However, some contralateral eye bias still remains in adult cats (Hubel and Wiesel 1962; Wiesel and Hubel 1963; Crair *et al* 1998).

The weakness of functional ipsilateral input at P14, suggests that the contralateral visual pathway develops first and is responsible for the initial scaffolding (for orientation columns) that are shared by both eyes (Crair *et al* 1998). It could be argued that since the development of ipsilateral responses are heavily reliant on contralateral eye scaffold, they would be most and firstly effected by visual deprivation. The stronger, more selective input from the contralateral eye would be less susceptible to a deprivation effect.

This hypothesis appears to be contradicted somewhat by results in this study showing that the effects of MD in normal animals are identical in each hemisphere. However, while values for the DE territory are within the range reported in the literature, some studies using optical imaging (Kind *et al* 2002) and single cell recordings (Shatz and Stryker 1978) have shown the DE to occupy slightly more territory in the contralateral hemisphere than in the ipsilateral (after a period of MD). One could speculate that an inherent contralateral bias might remain after MD, giving the false impression that a reduced OD shift occurred due to the nature of the visual manipulation (squint). However, no significant difference in area occupied by the DE between the two hemispheres has been reported in the above studies. Hence, the effects of the prior strabismus on cortical territory occupied by the DE appear to be genuinely restricted to the contralateral hemisphere to the DE.

An interesting observation in one study was that, unlike animals with normal visual experience, BD animals show no orientation selective responses in the ipsilateral eye at P26, although contralateral eye responses are still strong and selective. It is not until several weeks later that responses through the contralateral eye have deteriorated significantly (Crair *et al* 1998). This again highlights the robustness of responses through the contralateral eye and the relative susceptibility of the ipsilateral eye responses to disruptions of normal visual input.

A strabismus induced around the start of the critical period (P21), when connectivity and anatomical correlates of functional domains are not yet mature, would mean that the OD and orientation maps become functionally distinct. That is, one would predict that the OD and orientation maps for one eye develop (relatively) independently from those cortical maps from the other eye. In short, two distinct cortical maps for each eye would exist. In the present study, deprivation does not take place until P35, by which time the scaffold for ipsilateral eye responses would be expected to be sufficiently mature and past the stage at which their development is independent of visual experience (See Crair *et al* 1998). Deprivation in normal animals at this time would result in similar effects in both hemispheres. De-correlating the inputs from the two eyes at P21 could in effect 'freeze' the development of the 2 eye's maps so that the contralateral eye's underlying map structure remains robust while the ipsilateral eye's fails to mature and remains more susceptible to disruption. Such a situation could be implied from results from Crair *et al* (1998), however, the optical images from strabismic kittens (at P35) in this thesis do not suggest any difference in maturity

of orientation maps between the two eyes. Further comprehensive studies are warranted of optical maps and single unit recordings between the ages of P14-P35 to assess any differences in the relative strength of oriented responses in normal and strabismic animals.

Recovery from the effects of MD

Several strabismic kittens, most notably those with a strabismus and MD in the same eye, showed obvious delays in recovery of DE territory compared to MD only animals. After an extended period (>20 days) of binocular vision in SA kittens, the DE occupied only 35.1% of the cortex. Animals with MD and strabismus in different eyes (with the exception of kitten 280) did show recovery of the DE territory after only a few days of binocular vision. The mean final value for all strabismic kittens taken together was 37.5% for the DE. This value appears, at first sight, to be very similar to the 36.7% of cortical territory occupied by the deprived eye following recovery of strabismic kittens in the recent study by Kind *et al* (2002). A direct comparison of data between these two studies would suggest that recovery of DE territory has been disrupted by the strabismus, as was concluded by Kind *et al* (2002). However, a critical difference between the two studies is the fact that in their study, all kittens were raised normally, prior to deprivation. Here, the kittens were made strabismic before the period of MD (and strabismus remained present after MD), whereas in their study strabismus was induced only after MD.

A striking difference of results is in the greater contralateral bias in kittens (particularly with just MD) in this study compared to that by Kind *et al* (2002). The difference was much higher in this study (~61% for the hemisphere contralateral to the DE) than in theirs (~52% for the hemisphere contralateral to the DE). In the ipsilateral hemisphere to the DE, Kind *et al* (2002) saw a significant difference in the recovery of cortical territory between strabismic (~37%) and non-strabismic (~48%) animals. In the present study, the difference in recovery of DE territory in the ipsilateral hemisphere between strabismic (~37%) and non-strabismic (~40%) kittens was relatively small and not significant. It is important to note that in this study, visualisation of development of the cortex over time was carried out, with data collected before and after MD in the *same* animal. Kind *et al* (2002) used just one imaging session at the end of the experimental time period and compared these results

to *separate* control animals. The superiority of longitudinal analysis in this study is obvious. Although values for deprived eye territory at the beginning and the end of the experimental period were very similar for all animals, without knowledge of pre-MD data, one might have concluded that recovery of ocular dominance was less complete in MD-only animals, when in fact they started at a slightly lower level!

There are several possible reasons why a greater contralateral eye bias was observed than expected. First, differences in the analysis of the data. For example, differences in filtering and clipping values applied to the maps as well as slightly different criteria for the selection of the region of interest (ROI) within the maps could account for differences in values obtained for each eye's territory and orientation selectivity. However, both in this study and in that by Kind *et al.* (2002), both data acquisition and analysis were very similar, in particular the selection of the ROI to exclude any artefacts or large blood vessels. Therefore, any differences would have a relatively minor effect on the values obtained after analysis. Moreover, different criteria for analysis would have been applied to the maps as a whole and are unlikely to account for the greater contralateral bias seen here.

Another more likely explanation is genetic differences between different litters and indeed colonies. Animals with and without strabismus here were age matched from the same litter and a number of different litters used. However a recent study by Kaschube *et al* (2003) highlights that the periodicity of ocular dominance columns can be just as variable depending on genetic background as with differing visual experience. It has been well documented that the ocular dominance domains show greater segregation in strabismic animals (Shatz *et al* 1977; Löwel and Singer 1993; Löwel 1994; Löwel *et al* 1998), but it has also been claimed that the periodicity of these domains is larger in strabismic than non-strabismic animals (Shatz *et al* 1977; LeVay *et al* 1978; Löwel and Singer 1987; Diao *et al* 1990; Löwel 1994). However, more recent studies have questioned this (Sengpiel *et al* 1998; Rathjen *et al* 2002). Several experiments have indicated that the initial development of functional maps within V1 is much less dependent on experience than previously thought (Godecke and Bonhoeffer 1996; Crair *et al* 1998; Löwel *et al* 1998; Crowley and Katz 2000). More recently it has been argued that genetic variation can account for the differences in column size and the degree of contralateral bias in different groups of animals. The sizes and shapes of visual cortical orientation columns exhibit a high degree of inter-individual variability. Also column size and shape as well as a measure of

homogeneity of column sizes are significantly clustered in genetically related animals (Kaschube *et al* 2002). Two-dimensional analysis of OD column spacing in kittens from 3 different colonies confirmed this conclusion (Kaschube *et al* 2003). It was shown that not only was there no significant difference in the spacing of adjacent ocular dominance columns in strabismic and non strabismic cats, but also that column spacing between different colonies could be significantly different from each other (Kaschube *et al* 2003). So how can it be that local column spacing can vary to a similar extent in a given brain hemisphere of an individuals in an entire colony of cats, given that the mean column spacing of a given hemisphere is relatively similar in different individuals within a colony? The substantial variability of ocular dominance spacing in cat V1 has yet to be fully characterised. However, this data is consistent with the hypothesis that ocular dominance columns are functionally less relevant than other features of the cortex (such as orientation preference); they may be a highly variable epiphenomenon. Substantial inter-individual and inter-areal variability of the spacing and size of ocular dominance columns has been reported in macaque monkey V1 (Horton and Hocking 1996). An extreme example of variability is the squirrel monkey, where ocular dominance columns range from well developed in some individuals to nearly absent in others (Adams and Horton 2003). Although this result suggests a lack of functional use of OD columns in squirrel monkeys (Livingstone 1995, 1996), it does not necessarily discount their importance in other species (e.g. cat, macaque and human). However, it does point to the secondary importance and adaptive development of ocular dominance columns over other cortical features (e.g. orientation selectivity).

An extended period of recovery, in all cases, resulted in values for DE cortical territory returning to close to pre-MD values. Two other studies of a similar nature gave contrasting results. Malach and Van Sluyters (1989) claimed that mis-aligning the two eyes did not disrupt recovery from MD while Kind *et al* (2002) showed that it did. However, the study by Malach and Van Sluyters (1989) has to be considered with caution for several reasons. Firstly the period of deprivation was only 2 days in length (albeit at the height of the critical period). Although 2 days of MD can almost saturate the OD shift as determined from extracellular recordings (Movshon and Dursteler 1977; Freeman *et al* 1981; Crair *et al* 1997), such a brief period is probably insufficient to cause persistent changes of synaptic strength, and certainly will not

affect geniculocortical afferents serving the two eyes on a morphological level. Recovery from deprivation (even though through de-correlated vision to both eyes) is therefore much more likely to occur. Secondly, the period of MD was given in 2-hour sessions over two days, and at all other times the animal kept in total darkness. The ability of visual cortical neurons to undergo LTP is greatest during the critical period and, like the critical period, can be prolonged by rearing animals in darkness (Kirkwood *et al* 1995). Cortical plasticity of the animals in the study by Malach and Van Sluyters (1989) would likely have been affected by their specific rearing paradigm. Allowing a total of 6 hours of monocular vision a day (three 2-hour periods of MD) with the rest of the time spent in the dark means that the kittens were effectively dark-reared for 18 hours a day. This might have reduced the overall responsiveness of cortical neurones. Any advantage gained by the open eye during the periods of MD may well have been lost when it was effectively closed for most of the day. Finally, the angle of squint in those kittens was small, allowing for residual temporal correlation between the two eyes. It would be expected that the recovery from MD is greater for smaller than for larger squint angles (Kind *et al* 2002).

Although strabismic recovery from MD was disrupted in the study by Kind *et al* (2002), a result that was only reproduced in some instances here, a critical difference in rearing conditions should be noted. Before the period of MD animals were raised normally by Kind *et al* (2002), whereas in this study, animals had strabismus imposed *before* monocular deprivation.

Recovery of responses according to BCM

The BCM theory predicts recovery of the DE will be disrupted if after MD the input from the two eyes is de-correlated. Pre-synaptic activity would not correlate with post-synaptic activity above the modification threshold at the same time that DE afferents are active, therefore potentiation of DE synapses would not occur and recovery would not be seen.

Some disruption in the recovery of the DE was seen in this study in a number of instances. However, the above explanation is based on animals receiving normal visual experience before the period of MD. In this study they received abnormal (de-correlated) vision before the period of MD. Therefore, the effects of a strabismus alone, as well as the effects of MD, and the effects of de-correlated recovery from MD

need to be addressed. The reduced OD shift seen in strabismic animals after MD can be explained by the BCM theory. Can it account for the delayed recovery seen in some instances here, and moreover, why does the DE recover to normal levels of cortical territory after an extended period? Strabismus should result in two separate populations of cells developing (one for each eye). After the period of MD, since these populations of cells are now segregated (and have very little or no interactions) recovery would be predicted by the BCM theory. Since the populations of cells subserving each eye do not interact, pre- and post-synaptic responses from one eye have no bearing on the coincidence of pre and post-synaptic activity from the other eye. Each eye's pre- and post-synaptic response would coincide above the modification threshold for *that* eye, and recovery would occur.

So why was recovery delayed in some strabismic animals? One explanation could be the retention of some binocular cells after strabismus. If segregation were incomplete, DE recovery in those remaining binocular cells would be affected by the presence of the strabismus. Although complete recovery of purely monocular cells would be predicted by BCM, even a relatively small percentage of residual binocular cells could account for the disrupted yet complete recovery seen in a number of S+MD animals.

Another possible explanation for delayed recovery in the strabismic animals is that the strabismic eye may, in some instances, have become amblyopic. Here, in most instances delayed (but complete) recovery of the deprived (and deviated) eye was seen. In support of this argument, in some of the other animals, the strabismic but non-deprived eye became the fixating eye and the other (DE) the deviating eye. A likely consequence of this is amblyopia.

A strong negative correlation was shown between the amount of recovery of the DE and the angle of squint, after a brief period of recovery. However, the negative correlation between the angle of squint and the final territory dominated by the DE, was weak and not significant, in contrast to the study by Kind *et al* (2002). Visually evoked potentials recorded in two animals show a similar time course of delayed, but eventually complete recovery of acuity of the DE, despite the continued presence of a squint. Again, the most plausible explanation is that the early squint resulted in two distinct maps for OD and orientation preference forming for the two eyes with little interconnection between them. In contrast to normal animals with correlated binocular vision, where during development the maps for the two eyes become more similar and binocularity of neurons in V1 increases, in strabismic cats the maps become less

similar, and the proportion of binocular cells remains low. The maps for the two eyes mature separately but it appears that there is no difference in the degree of maturation of maps in strabismic and normal animals (Sengpiel *et al* 1998).

Orientation selectivity: MD effects and recovery

Although some DE territory was preserved in animals with strabismus prior to MD, orientation selectivity was not. Orientation selective responses through the DE were severely reduced to similar levels in all kittens, with and without strabismus. Strabismus causes massive rearrangement of geniculocortical afferents serving the two eyes. However, strabismus has relatively little effect on the gross layout of orientation preference maps. Unlike normal animals, there is little correlation between left- and right-eye maps for the same orientation in strabismic animals (Sengpiel *et al* 1998). However, iso-orientation maps appear to be continuous across the borders of adjacent ocular dominance columns and intersect at right angles, as in normal animals (Löwel *et al* 1998; Engelmann *et al* 2002). Neurones driven by the deviated and non-deviated eye in strabismic cats have similar orientation tuning properties (Hubel and Wiesel 1965; Freeman and Tsumoto 1983; Sengpiel *et al* 1994).

In the present study, prior to MD there was little qualitative difference in orientation maps obtained from normal and strabismic animals, although a decrease in the overall strength of responses to oriented stimuli through the strabismic eye could be seen in both imaging and VEP recordings. After MD, the ratios of DE: NDE orientation selectivity was, although slightly lower in strabismic animals, not significantly different from normal animals. Since strabismus has little or no effect on the layout of orientation maps prior to MD, it could be argued that it should have no subsequent effect on orientation selectivity after MD. This result is confirmed here. In isolated cases a trace of orientation selective responses was preserved, visible in 'angle' and 'polar' maps, after the period of MD. However, there was no 'protective' effect like that seen for ocular dominance, and remaining orientation selective responses to DE stimulation did not seem closely correlated with DE patches.

As OD is preserved to some extent in strabismic animals, it would also be predicted that orientation selectivity would be preserved to some extent in strabismic animals. However, this isn't the case and could not be accounted for by the BCM theory.

The lack of orientation preservation in strabismic animals confirms the hypothesis that the 'scaffold' for orientation preference is already formed when experience dependent modification occurs at 3 weeks of age (Crair *et al* 1998). While this underlying scaffold is relatively unchanged throughout the critical period, orientation selectivity increases with experience (Crair *et al* 1998). Intrinsic horizontal and callosal pattern of connections are also 'roughly' set-up early (Katz and Callaway 1992) before experience dependent modification occurs (Chalupa and Dreher 1991).

Several studies highlight the presence of orientation selective cells before eye opening in ferrets (Krug *et al* 2001) and in kittens at the time of eye-opening (Blakemore and VanSluyters 1975; Fregnac and Imbert 1978).

Orientation selectivity (in kittens) increases to some extent before the onset of the critical period, even in the absence of patterned visual stimulation (Crair *et al* 1998). However, despite geniculocortical axons reaching layer IV of V1 shortly before birth (Shatz and Luskin 1986; Ghosh and Shatz 1992) it is not until P14 that anatomical and functional OD columns are present (Crair *et al* 2001). It could be argued that the developing layout of OD columns adapts to the constraints set by the orientation map (see Hoffsummer *et al* 1996). In support of this argument, each OD column contains a full complement of all orientations (Löwel *et al* 1998). The orientation map remains stable despite the breakdown of intracortical tangential connections and the rearrangement of thalamic afferents (Löwel *et al* 1998), that occur with strabismus (affecting ocular dominance column development). Only by drastically reducing the visual input into one eye (monocular deprivation) does the orientation map become disrupted.

The preservation of some residual orientation selectivity after MD cannot be excluded. Optical imaging is less sensitive than single cell recordings. It cannot resolve the responses and measure the tuning of individual cells. Here, the measure of orientation selectivity is the length of the vector resulting from the summed responses to the four principal orientations for each pixel. Although the median vector length for the whole region of interest was close to zero, in some animals small 'islands' were weakly orientation selective, with vector lengths greater than zero. Using the mean vector length instead would be similarly unrepresentative, as a few patches with good orientation selectivity would bring up the mean value. Median and mean values can

only describe a unimodal distribution of data, while orientation selectivity across V1 might follow a bimodal distribution.

Ideally, NDE and DE patches identified via optical imaging would be used to target electrodes. Single cell measurements of populations of neurones in NDE and DE patches would give a more accurate representation of the distribution of orientation selectivity across the cortex. However, within the experimental paradigm employed here, this was not possible due to time constraints imposed on each but the final imaging session, which was followed by single-cell recording in some animals.

All of the above taken into consideration, it appears that orientation selectivity initially develops independently of visual experience but is not resistant against degeneration following monocular deprivation, even if this was preceded by strabismus. The subsequent recovery of orientation selectivity in these animals may, like the recovery of OD territory, be best described by associative mechanisms.

The partial protective effect of a prior strabismus on OD and lack of apparent protection of any other functional parameters (orientation selectivity and visual acuity) again raises the question of the functional relevance of ocular dominance columns. A lack of functional relevance of OD columns may yet prove controversial considering the apparent topographical (Löwel *et al* 1988) and functional relationship (Löwel *et al* 1998) between OD columns and orientation patches.

Despite of what is known about the development of orientation selectivity in V1, precisely how experience-dependent changes and refinement occur in detail has yet to be addressed.

CHAPTER 3

INTRODUCTION

Reverse occlusion and other paradigms

Severe behavioural, (Giffin and Mitchell 1978; Mitchell *et al* 1977; Wiesel and Hubel 1963, 1965) and physiological (Wiesel and Hubel 1963, 1965; Hubel and Wiesel 1970; Shatz and Stryker 1978; LeVay *et al* 1980; Sherman and Spear 1982; Fregnac and Imbert 1984; Mitchell 1991) effects have been seen in monocular deprivation studies. However these effects are not irreversible. Indeed, in kittens, substantial and complete behavioural recovery of the deprived eye can be achieved if vision is restored sufficiently early to that eye, i.e. during the critical period (Dews and Wiesel 1970; Movshon 1976; Mitchell *et al* 1977; Giffin and Mitchell 1978; Mitchell 1988; Mitchell and Gingras 1988). The physiological effects of MD can be reversed if, when the deprived eye is reopened, and the non-deprived eye is closed at the same time (Blakemore and Van Sluyters b 1974; Movshon and Blakemore 1974; Movshon 1976; Giffin and Mitchell 1978; Van Sluyters 1978; Blakemore and Hawken 1982; Malach *et al* 1984). This regimen is known as reverse lid-suture or reverse occlusion (RO). Reverse occlusion of only a few days (performed near the height of the critical period) results in most cells being dominated by the initially deprived eye (Blakemore and Van Sluyters 1974; Movshon 1976; Van Sluyters 1978). The susceptibility of the cortex to monocular deprivation and reverse occlusion is shown in figure 3.1 (from Olson and Freeman 1980). The deprivation effect (shown as an index of proportion of cells dominated by the non-deprived eye or the originally deprived eye in the case of RO) is at its greatest at 4-6 weeks of age. Thereafter the effect of deprivation decreases. This decrease is particularly drastic with reverse occlusion. At 5 weeks, maximal effects of reverse occlusion are seen. However, by 8 weeks this effect has dropped by approximately 80%, meaning that there is little reconnection of afferents from the originally deprived eye. Behavioural and physiological recovery has also been reported in reverse occluded monkeys (Blakemore *et al* 1978, 1981; LeVay *et al* 1980), while binocular recovery (re-opening the deprived eye, without closing the open eye) resulted in little anatomical or physiological recovery.

Disappointingly, the improvement in visual acuity seen for the initially deprived eye during RO is not maintained when normal binocular vision is restored after RO, and vision in the recently deprived (originally open) eye remains poor. An early study by

Mitchell *et al* (1984) deprived kittens in one eye from natural eye opening for varying periods, then reverse occluded for equal periods of time. Although vision through the originally deprived eye (ODE) improved to close-to-normal acuity levels, this was largely lost when binocular vision was restored. Vision through the originally non-deprived eye (ONDE) did improve but was also below normal levels, i.e. the animals ended up with bilateral amblyopia.

A much shorter period of RO (18 days), introduced at 5 weeks of age, was employed by Murphy and Mitchell (1986). This shorter period ensured that all of the behavioural and physiological changes would be occurring during the height of the critical period (which was not always the case in Mitchell *et al* 1984). After an extended period of binocular vision, both eyes attained acuity measurements of approximately 1/3 of normal acuity (Fig. 3.2a). Despite this impairment of behavioural acuity following binocular recovery, cortical ocular dominance and binocularity appeared normal. It appeared that simply increasing the efficacy of cortical responses to visual stimulation did not lead to recovery of visual acuity. This led to the hypothesis that the spatial resolution of the most sensitive neurones, not the total number of units responsive to each eye may be a better predictor of behavioural acuity. Moreover, the LGN cells receiving input from the originally non-deprived eye have been shown to remain hypertrophied during reverse occlusion (Sloper *et al* 1984). This could lead to larger receptive fields and overlapping ocular dominance columns resulting in a binocular cortex, but poor visual acuity.

A later, more extensive study by Murphy and Mitchell (1987) included reverse occlusion imposed at 4, 5, or 6 weeks of age, with either brief (9-18 days) or extended (9-12 weeks) of RO (Fig. 3.2b). The outcome of all these regimens was bilateral amblyopia.

The timing and length of the RO, as well as the recovery were studied in greater depth by Mitchell (1991). Again, in all but a few individual cases, the final outcome was bilateral amblyopia. Mitchell took the paradigm one step further by introducing various lengths of part time reverse occlusion in the initially non-deprived. It was shown that intermediate occlusion times of 3.5 hrs or 5hrs per day, resulted in recovery of normal acuity, contrast sensitivity and vernier acuity in both eyes.

In further experiments with this paradigm, the visual axes of the two eyes were misaligned by prisms during the daily period of binocular exposure. Recovery was found to be just as good in these animals as those with concordant visual input. This

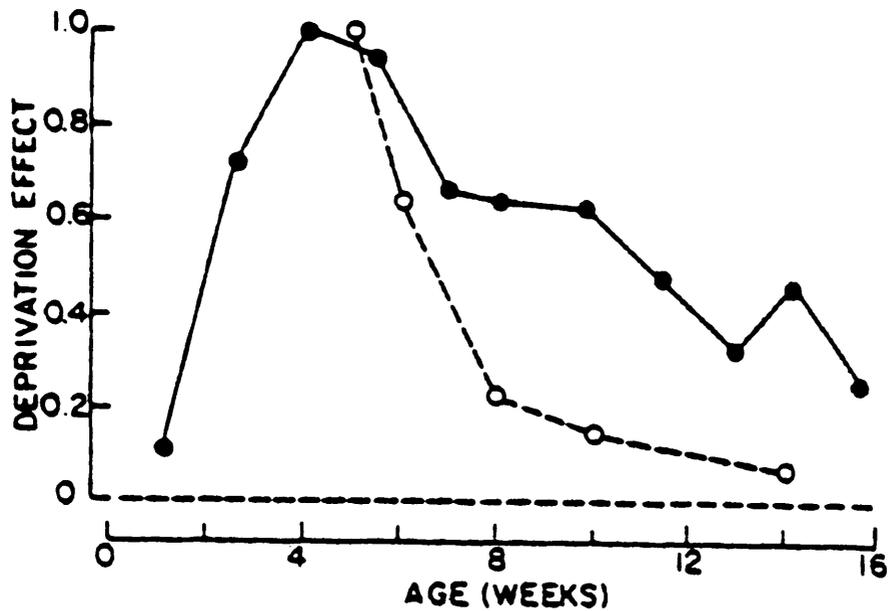


Figure 3.1 Profile of the sensitive period for monocular deprivation (and reverse occlusion) in kittens (from Mitchell and Timney 1987)

Filled circles - Degree of functional disconnection resulting from 10-12 days of monocular deprivation imposed at various ages in kittens.

Open circles - Data obtained from kittens reverse sutured for 9 weeks at various ages.

Deprivation effect - Proportion of cells dominated by the non deprived eye - MD and originally deprived eye - RO.

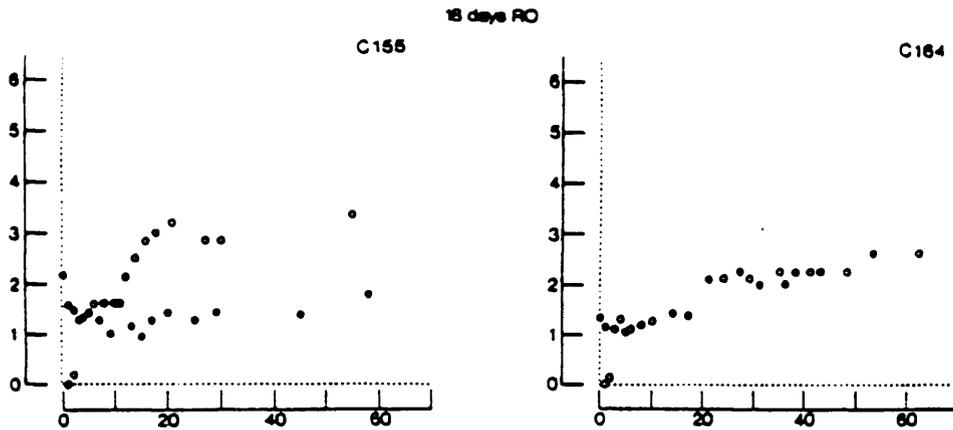


Figure 3.2 a Changes in visual acuity in 2 kittens after 18 days reverse occlusion, which had previously received monocular deprivation (from natural eye opening) imposed at 5 weeks of age (From Murphy and Mitchell 1987)

Open symbols represent the non-deprived eye and closed symbols the initially deprived eye. Axis x and y represent spatial frequency (cyc/deg) and days since termination of reverse occlusion respectively.

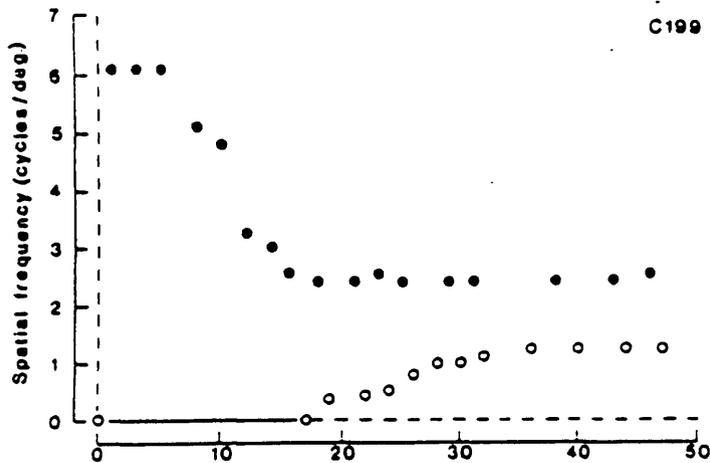


Figure 3.2 b Changes in visual acuity of a monocularly deprived kitten following termination of 12 weeks reverse occlusion, which was imposed at 4 weeks of age (From Murphy and Mitchell 1987)

Open symbols represent the non-deprived eye closed symbols, the initially deprived eye. Axis x and y represent spatial frequency (cyc/deg) and days since termination of reverse occlusion respectively.

suggested that the two eyes needed simultaneous visual exposure to recover but not necessarily concordant. This notion was later rejected, since strabismus causes recovery from monocular deprivation to be delayed and incomplete (Kind *et al* 2002). More recently interest has focused on the importance of correlated (simultaneous) activity in the two eyes for the eventual outcome.

Murphy *et al* (2002) introduced a 4-day period of binocular vision (4DBV) after the initial period of deprivation and before RO. They found that the acuity in the ODE reached levels very similar to that of a normal cat (~7.5 cyc/deg), in contrast to animals without the intermediate period of 4DBV. Acuity in the originally non-deprived eye (ONDE) also improved to a moderately high level (~3 cyc/deg). In contrast, misalignment of the eyes (strabismus) during this intermediate period was detrimental to the acuity in both eyes when binocular vision was restored.

The anatomical and physiological changes that occur after MD are well documented. The physiological changes due to MD are almost saturated after only 2 days (Movshon and Dursteler 1977; Freeman *et al* 1981; Crair *et al* 1997). The anatomical changes that occur after MD include the loss of geniculocortical terminals serving the DE in layer IV (Hubel *et al* 1977; Shatz and Stryker 1978; LeVay *et al* 1980; Antonini and Stryker 1993, 1996). However, this process takes at least one week to occur. Expansion of the NDE terminals takes many weeks (LeVay *et al* 1980; Antonini and Stryker 1993, 1996). Although ONDE arbours shrink rapidly after RO, ODE arbours do not expand greatly (Antonini *et al* 1998).

Reverse occlusion of only a few days results in most cells becoming dominated by the ODE. It has also been shown that orientation maps are restored (Kim and Bonhoeffer 1994). In animals monocularly deprived during the 5th or 6th postnatal week, orientation maps all but disappeared through the ODE, but a subsequent 7-11-day period of RO restored orientation maps that were very similar to the original maps. In a later study, kittens were raised with exclusively monocular vision from birth. At 5 weeks of age, animals were reverse occluded for 13 days. Optical imaging after the initial MD and again after RO shows a remarkable similarity between orientation maps through the two eyes even though they had never shared common visual experience (Godecke and Bonhoeffer 1996).

Several more detailed physiological studies have provided insight into the nature of the initial stages of RO. Crewther *et al* (1981, 1983) studied the physiological effects of brief periods of RO in kittens. Kittens were monocularly deprived from the time of natural eye opening until 5 weeks of age. Thereafter they received several hours of RO a day over 20 days, with the remaining hours of the day spent in total darkness. The changes in LGN cell morphology and cortical OD were more effective in promoting recovery originally DE, when RO was induced for brief periods per day, than for the same period of RO accumulated in just two sessions. The first effect of MD was the loss of binocular summation followed by a shift in OD after 6 hours. A gradual decrease in DE responses and an additional moderate increase in responses to the normal eye occurred. During RO the reduction of the response to the newly deprived eye was seen first and to a similar level to that during MD. Recovery of the responses to the previously deprived eye followed, however, was slower (Mioche and Singer 1989). Therefore, one might expect a number of neurones to become unresponsive before becoming dominated by the non-deprived eye during RO.

These earlier experiments indicated that binocular exposure after MD might lead to a faster restoration of responses to the DE than RO. This was later found to be the case with behavioural recovery after MD. Kittens with BR after MD began to recover vision in the deprived eye 12-30 hours before the subjects that were reverse occluded. Vision in the deprived eye remained superior to that of RO kittens for 4-8 days (Mitchell *et al* 2001), a result that a competitive model of binocular interaction cannot explain. As with MD, during RO one eye is placed at a competitive advantage. Synaptic weakening of the DE occurs, accompanied by strengthening of the NDE. During RO, the ONDE is now closed and placed at a competitive disadvantage, hence the originally deprived - now open eye, should quickly come to dominate the cortex, without delay.

The above findings point to a period of concordant binocular vision (even if brief) being paramount to lasting behavioural and physiological recovery of the ODE during RO. In fact, Murphy *et al* (2002) found that final acuity for *both* eyes was much better in animals, which had received a brief period of binocular vision after the initial MD and before RO. In contrast, those animals that had received binocular, but de-correlated vision in the same period ended up with poor acuity in both eyes similar to animals in which RO followed straight after MD.

Here, optical imaging, visually evoked potentials and single cell recordings are used to study the effects of RO and subsequent recovery. I also examine the effect of a brief period of binocular vision (correlated and de-correlated) intercalated between the two periods of deprivation. It is predicted that an intermediate period of correlated binocular vision will result in a physiologically relatively normal visual cortex following recovery from RO, while de-correlating the inputs from the two eyes will eliminate this beneficial effect with an outcome similar to that of ordinary RO.

METHODS

From 2 weeks of age (P14), 10 kittens were monocularly deprived in one eye (as described in Methods (Chapter 2) for 3 weeks. At P35, 3 of these kittens were reverse occluded for 18 days before allowing binocular recovery for a period of 3-4 weeks. In another 3 of these kittens a period of 4 days of binocular vision was introduced at the end of the first period of MD, before RO. In the remaining 4 kittens a period of 4 days of binocular vision was also given. However, vision was discordant through the use of goggles containing prisms each with a 4° convergent offset for each eye (equivalent to a total convergence of the visual axes by 8°).

Kittens were trained to wear the goggles without prisms for brief daily periods, several days before the end of the first period of MD. Upon opening of the deprived eye, the animals were kept in the dark while they recovered, then the goggles were fixed on the head (with the prisms in place).

Generally the animals were comfortable wearing the goggles after the initial training and behaved normally. During the day, kittens were checked hourly to ensure the goggles remained in place. Every morning the goggles were removed for a period of 5 minutes. The lenses were cleaned and each eye was checked for any signs of irritation and rinsed with sterile eye drops. On rare occasions, when checked the following morning the goggles had been removed or were in an incorrect position. Troublesome kittens were fitted with an additional collar to help prevent removal of the goggles. Even though this problem was largely unavoidable, since the kittens were kept on a 12-hour light/dark cycle, any periods without goggles would have been of minimal effect, as they would have occurred in the dark.

At the end of the RO period a chamber was implanted and optical imaging was carried out on the same time scale as in Chapter 2. In one animal imaging was carried out at the termination of the first period of MD, after 4DBV, on the day of termination of RO and two further times during binocular recovery. In the remaining animals, imaging was carried out on the days of termination of RO, 3 days and generally every 7 days thereafter. In 3 kittens, all with 4 days of de-correlated vision, VEPs were recorded following each optical imaging session.

In all cases, after the final imaging session, single cell recordings were carried out.

Electrophysiology and visually evoked potentials

Visually evoked potentials were carried out in tandem with optical imaging sessions, as in Chapter 2, in 3 of those animals. Electrophysiological recordings were carried out in the exposed part of V1 after the last imaging session, as described in Chapter 2, in 11 kittens.

RESULTS

Ocular dominance

Immediate reverse occlusion

Reverse occlusion has a profound effect on the cortical territory occupied by the two eyes. Images from one kitten are shown in figure 3.3. Both hemispheres (Fig. 3.3 a and b; row A column A) are dominated almost exclusively by the originally deprived eye (ODE). Originally non-deprived eye (ONDE) responses were sparse and weak, occupying only 14.8% and 17.5% of the cortex, respectively, for hemispheres contralateral and ipsilateral to that eye (Fig. 3.3 a and b; row A, Column A and B). After a brief period of binocular recovery, the ONDE had regained some territory (Fig. 3.3 a and b; row B column A and B), although the cortex was still activated predominantly by the ODE (Fig. 3.4), the ONDE occupies 25.8% and 26.5% of the hemispheres contralateral and ipsilateral to that eye. A further period of 3 weeks of binocular vision resulted in little further loss of territory of the ODE to the recovering ONDE as seen in figure 3.3 and 3.4 row C and D column A and B). Twenty-six days after the ONDE has been reopened, a progressive increase in strength of the response of the ONDE can be seen (Fig. 3.3 column B), although gains in cortical territory are relatively small. Final values of cortical territory still clearly favour the ODE, with the ONDE occupying just 31% and 30.5% of the cortex for hemispheres contralateral and ipsilateral to that eye (Fig. 3.3 column D, Fig. 3.4 a and b).

Four days binocular vision between the first period of MD and before RO

The ODE dominates the cortex after the period of RO as shown in figure 3.5a (Row A column A and B) to a level comparable to that seen in other deprived animals (Fig. 3.6, ONDE occupies 26.6%, 20.1% for hemispheres contralateral and ipsilateral to the ODE). Cortical gain by the ONDE is obvious in figure 3.5a; rows B-D columns A and B and in figure 3.6. Initial gains of cortical territory by the DE after 3 days of recovery appear slow and certainly is not complete. The ONDE occupies just 35.5% and 29.1% of the cortex (in the contralateral and ipsilateral hemisphere to the ONDE).

Figure 3.3 a Effects of reverse occlusion on ocular dominance and orientation selectivity in the originally non-deprived (LE)

Kitten BW - Monocular deprivation was imposed at P14-P34 (RE). Reverse occlusion P34-P50 (LE).

Columns A-D represent: Ocular dominance (right eye/left eye), single condition (0 deg/blank) angle, and polar maps obtained from V1.

Column A - Patches of black represents high neuronal activity, and white, low neuronal activity. With respects to the left vs right eye map here, dark areas represent neurons responding preferentially to the left eye and light areas responding preferentially to the right eye.

Column B -The relative strength of the response is represented on the level of darkness. The darker the patch the greater the response.

Column C -The resulting vector of responses to all orientations tested is allocated a colour to represent preferred orientation.

Column D - The relative strength of the oriented response is represented on a scale of brightness.

Rows A-D represent time course: Immediately upon reopening of recently deprived eye (P50), then P54, P62, P76.

Colour key represents preferred orientation in angle maps. Line arrows represent relative orientation of the head.

Map size differs marginally between imaging sessions.

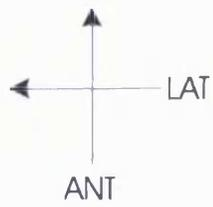
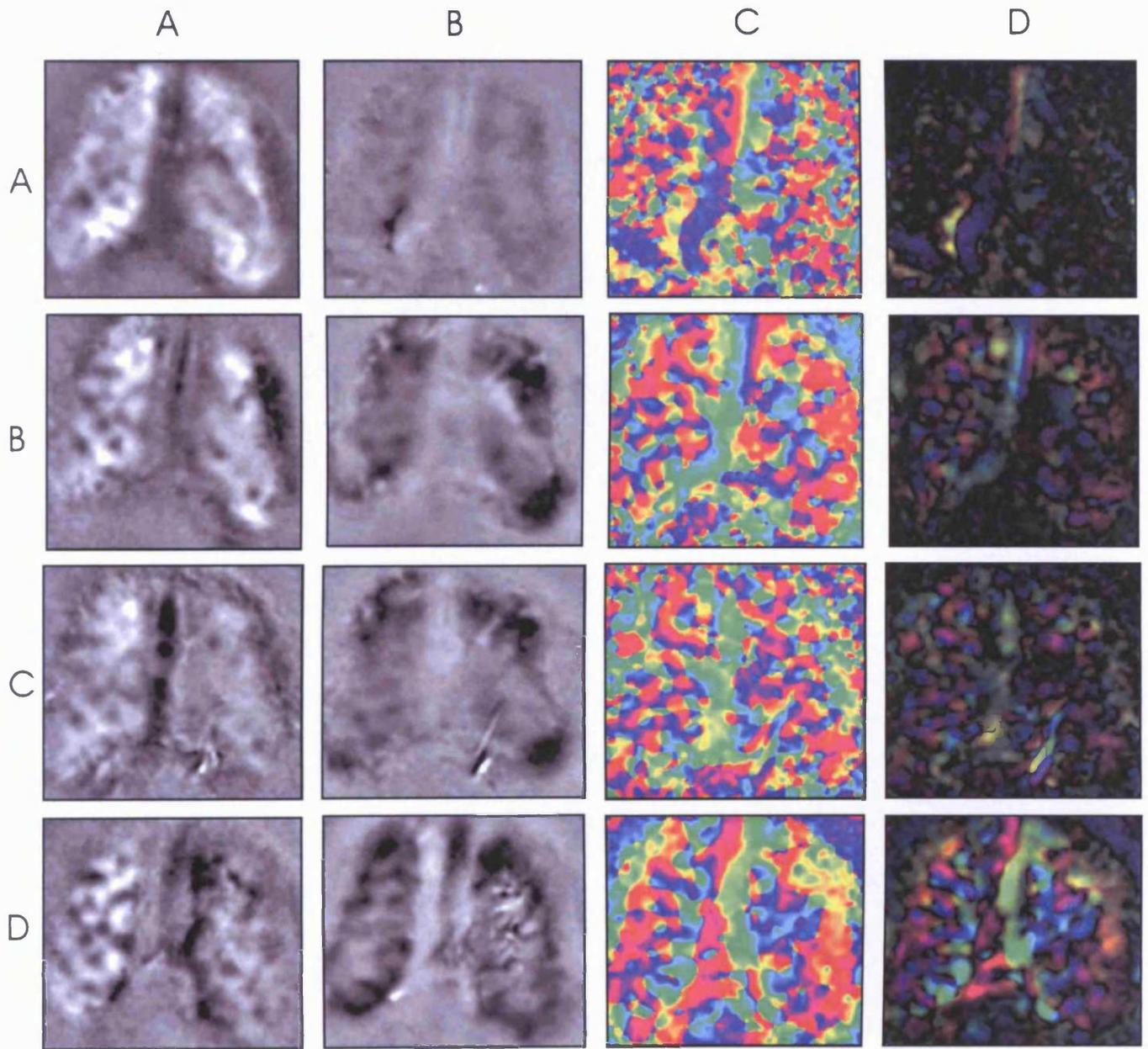


Figure 3.3b Effects of reverse occlusion on ocular dominance and orientation selectivity in the originally deprived (RE)

Kitten BW - Monocular deprivation was imposed at P14-P34 (RE). Reverse occlusion P34-P50 (LE).

Columns A-D represent: Ocular dominance (right eye/left eye), single condition (0 deg/blank) angle, and polar maps obtained from V1.

Column A - Patches of black represents high neuronal activity, and white, low neuronal activity. With respects to the right vs left eye map here, dark areas represent neurons responding preferentially to the right eye and light areas responding preferentially to the left eye.

Column B -The relative strength of the response is represented on the level of darkness. The darker the patch the greater the response.

Column C -The resulting vector of responses to all orientations tested is allocated a colour to represent preferred orientation.

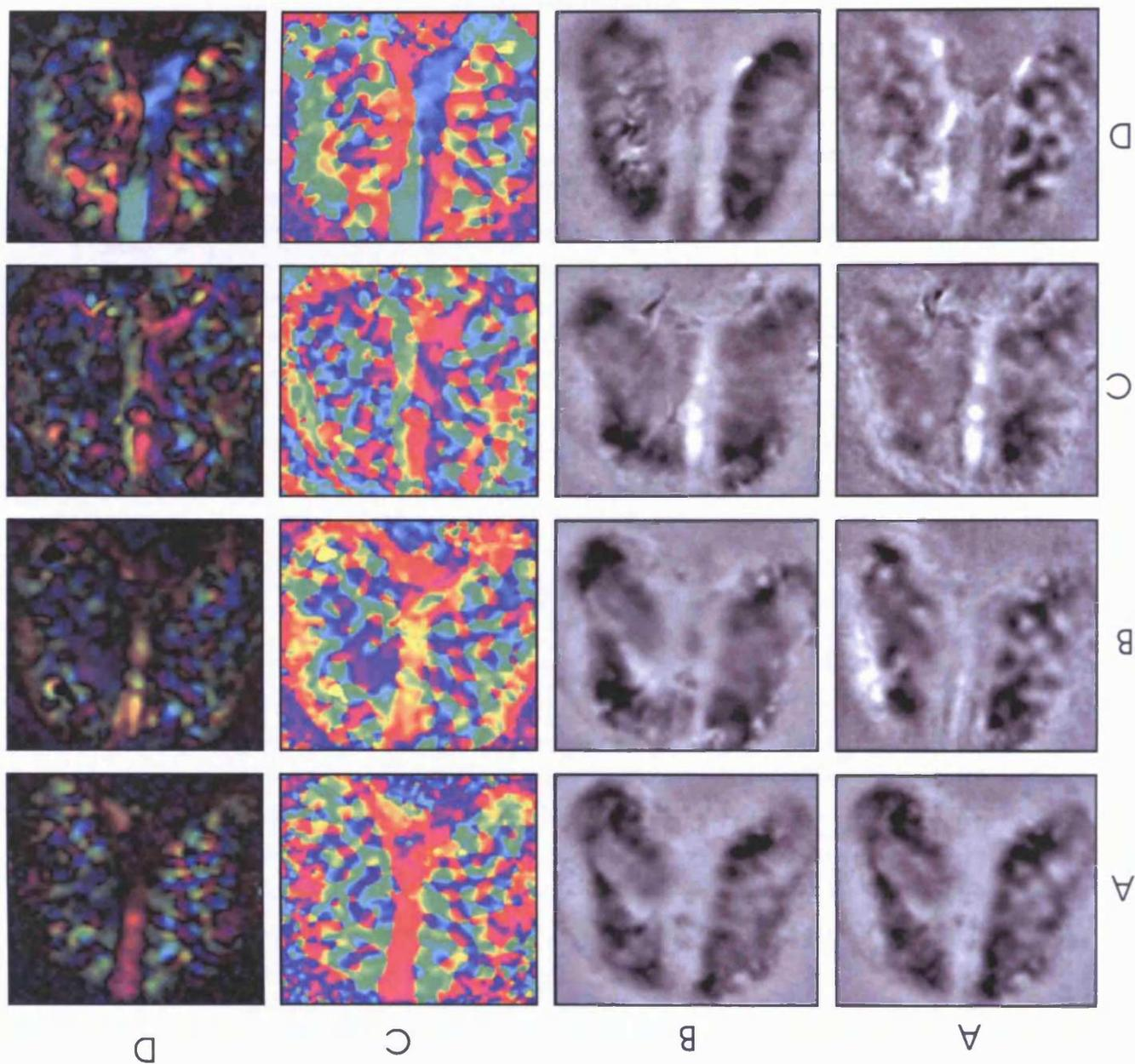
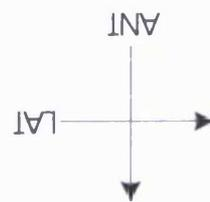
Column D - The relative strength of the oriented response is represented on a scale of brightness.

Rows A-D represent time course: Immediately upon reopening of recently deprived eye (P50), then P54, P62, P76.

Colour key represents preferred orientation in angle maps. Line arrows represent relative orientation of the head.

Map size differs marginally between imaging sessions.

1mm



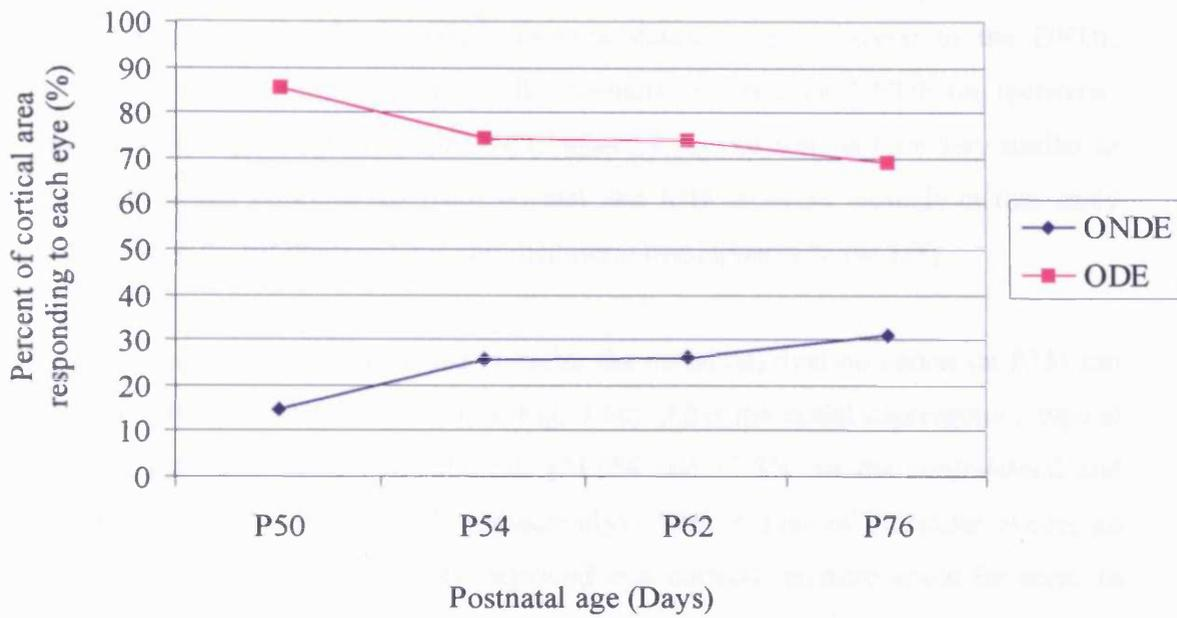
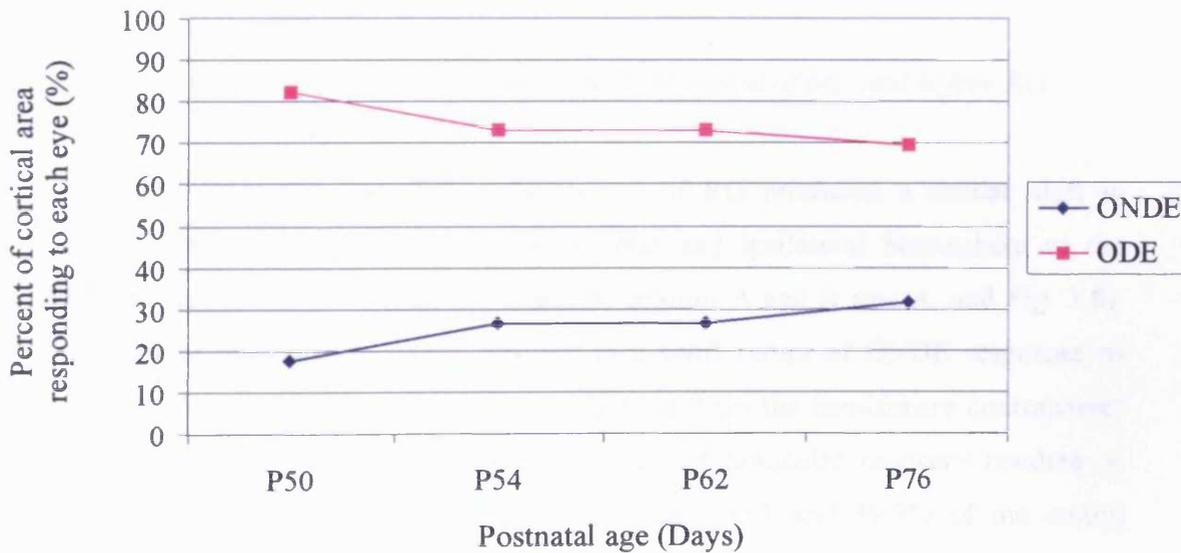
A**B**

Figure 3.4 a and b Cortical ocular dominance in a kitten after reverse occlusion

Data is from kitten BW1 which was monocularly deprived in the RE (P14) then reverse occluded in the LE for 18 days (P35-53).

Originally non-deprived eye(ONDE) is represented by the blue line.

Originally deprived eye (ODE) is represented by the pink line.

A) Data for the hemisphere contralateral to the DE.

B) Data for the hemisphere ipsilateral to the DE.

However, after 24 days of binocular recovery the ONDE now occupies 63.2% and 49.2% of the cortex (for hemispheres contralateral and ipsilateral to the ONDE respectively), much more than that in RO animals. In effect the ONDE has recovered fully and territory occupied by the ONDE after 24 days of recovery are very similar to those that would be expected from normal and MD recovery animals in this study (61.7% and 40% for contralateral and ipsilateral hemispheres to the DE).

In one animal, imaging was carried out after the initial deprivation period (at P35) and again after 4 days of binocular vision (Fig. 3.5c). After the initial deprivation a typical OD shift was seen away from the DE (21.6% and 11.8% for the contralateral and ipsilateral hemisphere to the DE respectively). After 4 days of binocular vision, an obvious increase in the originally deprived eye cortical territory could be seen. In short, good, but not complete recovery (Fig. 3.5c, row C and D) of DE territory was seen (52.4% and 31.2% for hemisphere contralateral and ipsilateral to the DE respectively).

Four days of de-correlated vision between the first period of MD and before RO

As with the other two paradigms, the period of RO produced a similar shift in dominance of 19.2% and 12.9% (contralateral and ipsilateral hemisphere to the ONDE) to favour the ODE (Fig. 3.7 a and b; column A and B row A, and Fig. 3.8). Three days of binocular recovery resulted in a swift return of ONDE responses to occupy 42.1% and 37.8% of the cortex – figure 3.8 (in the hemisphere contralateral and ipsilateral to the ONDE). A further period of binocular recovery resulted in additional territory gain by the ONDE, to occupy 60.5 and 49.9% of the cortex (hemisphere contralateral and ipsilateral to the ONDE). This result is very similar to that of 4DBV animals but greater than that of RO animals.

It should be noted that the continued recovery of the ONDE (with a further period of binocular recovery) seen in this animal is not a typical example of what happened overall in this group (ref Fig. 3.9).

Figure 3.9 shows summary data of cortical territory occupied by the ONDE of all animals in this study. Time periods are from the day of termination of RO, after 3 days of binocular recovery, and after an extended period of recovery (>21 days). It is

Figure 3.5 a Effects of a brief period of binocular vision between a period of monocular deprivation and RO on ocular dominance and orientation selectivity in the originally non-deprived (LE)

Kitten 030 - Monocular deprivation was imposed at P13-P36 (RE). Binocular vision P36-P40. Reverse occlusion P40-P56 (LE).

Columns A-D represent: Ocular dominance (right eye/left eye), single condition (0 deg/blank) angle, and polar maps obtained from V1.

Column A - Patches of black represents high neuronal activity, and white, low neuronal activity. With respects to the left vs right eye map here, dark areas represent neurons responding preferentially to the left eye and light areas responding preferentially to the right eye.

Column B -The relative strength of the response is represented on the level of darkness. The darker the patch the greater the response.

Column C -The resulting vector of responses to all orientations tested is allocated a colour to represent preferred orientation.

Column D - The relative strength of the oriented response is represented on a scale of brightness.

Rows A-D represent time course: Immediately upon reopening of the recently deprived eye (P56), then P59, P66, P80.

Colour key represents preferred orientation in angle maps. Line arrows represent relative orientation of the head.

1mm

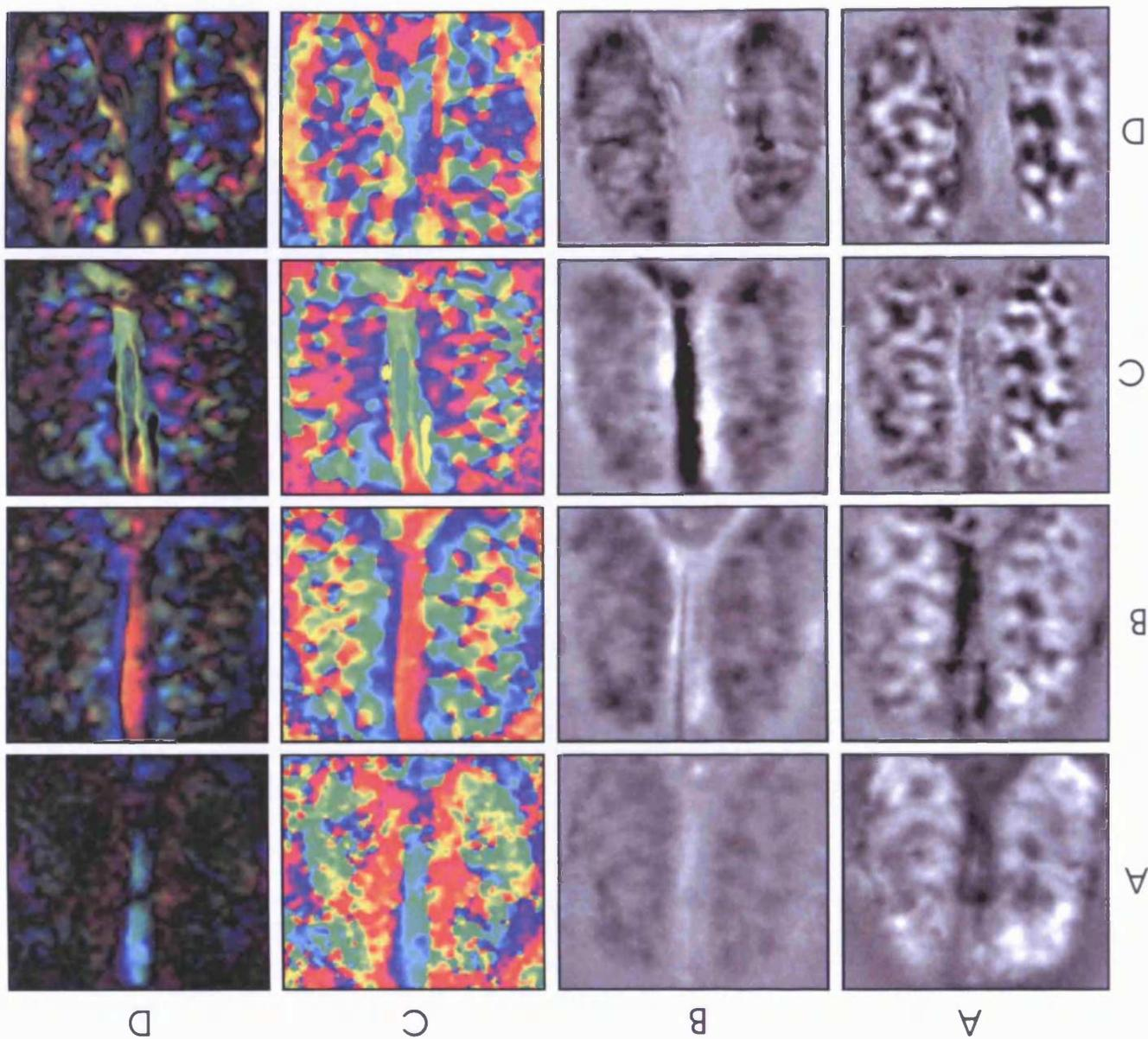
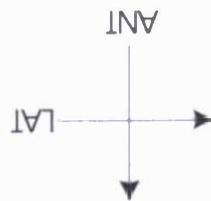


Figure 3.5 b. Effects of a brief period of vision between a period of monocular deprivation and RO on ocular dominance and orientation selectivity in the originally deprived (RE)

Kitten 030 - Monocular deprivation was imposed at P13-P36 (RE). Binocular vision P36-P40. Reverse occlusion P40-P56 (LE).

Columns A-D represent: Ocular dominance (left eye/right eye), single condition (0 deg/blank) angle, and polar maps obtained from V1.

Column A - Patches of black represents high neuronal activity, and white, low neuronal activity. With respects to the right vs left eye map here, dark areas represent neurons responding preferentially to the right eye and light areas responding preferentially to the left eye.

Column B -The relative strength of the response is represented on the level of darkness. The darker the patch the greater the response.

Column C -The resulting vector of responses to all orientations tested is allocated a colour to represent preferred orientation.

Column D - The relative strength of the oriented response is represented on a scale of brightness.

Rows A-D represent time course: Immediately upon reopening of the recently deprived eye (P56), then P59, P66, P80.

Colour key represents preferred orientation in angle maps. Line arrows represent relative orientation of the head.

1mm

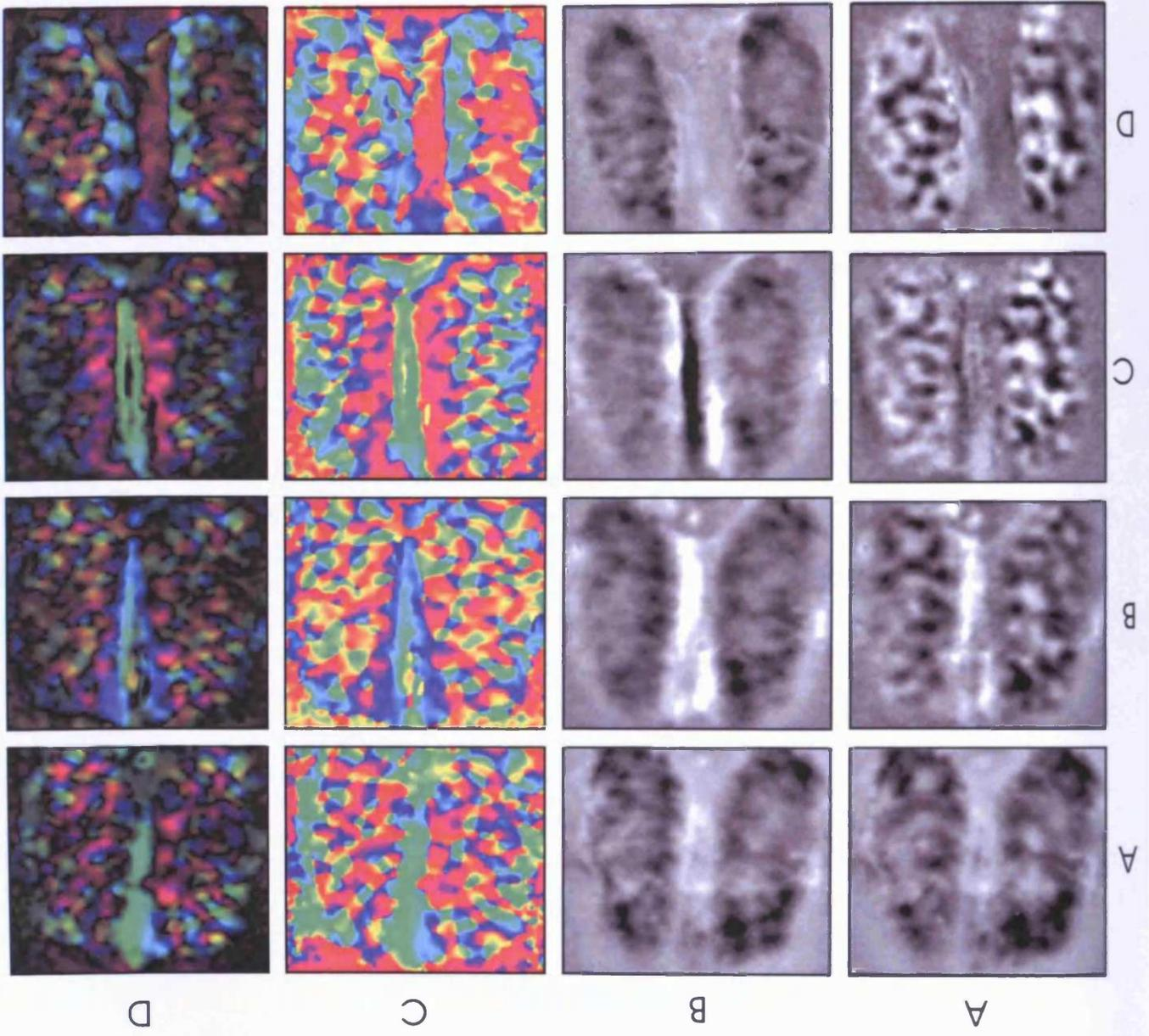
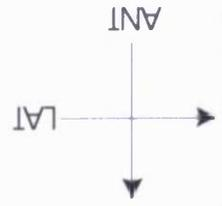


Figure 3.5 c Effects of early MD followed by 4DBV on ocular dominance and orientation selectivity in the non-deprived (top) and deprived (bottom) eye

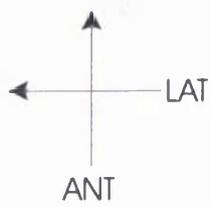
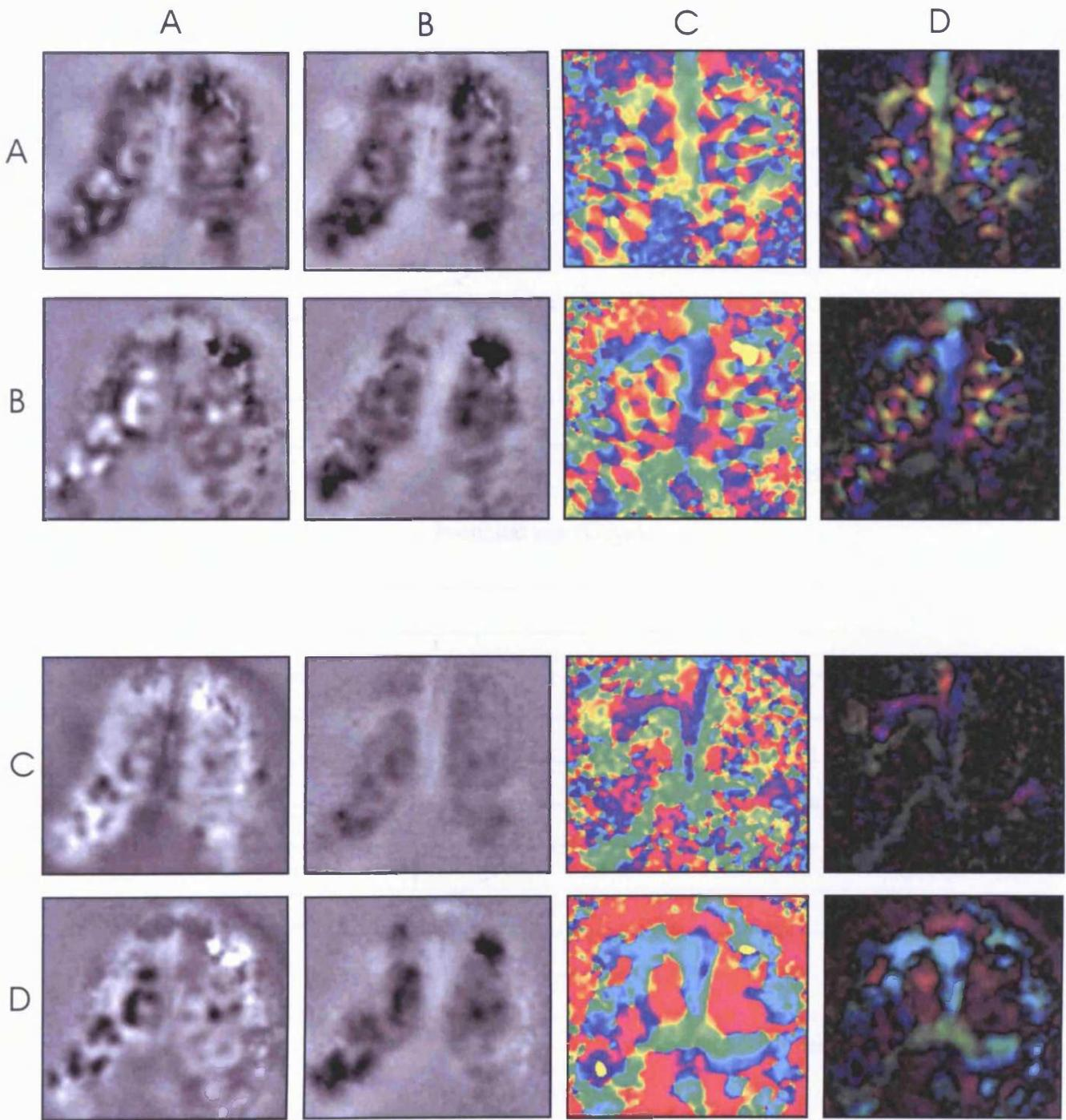
KittenB - Deprivation was initiated in the RE on P14 until P35, followed by 4DBV.

Columns A-D represent: Ocular dominance (left eye/right eye), single condition (0deg/blank) angle, and polar maps obtained from V1.

Rows A and B represent time course in non-deprived eye: Immediately upon reopening of deprived eye (P35), then at P39.

Rows C and D represent time course in non-deprived eye: Immediately upon reopening of deprived eye (P35), then at P39.

Colour key represents preferred orientation in angle maps. Line arrows represent relative orientation of the head.



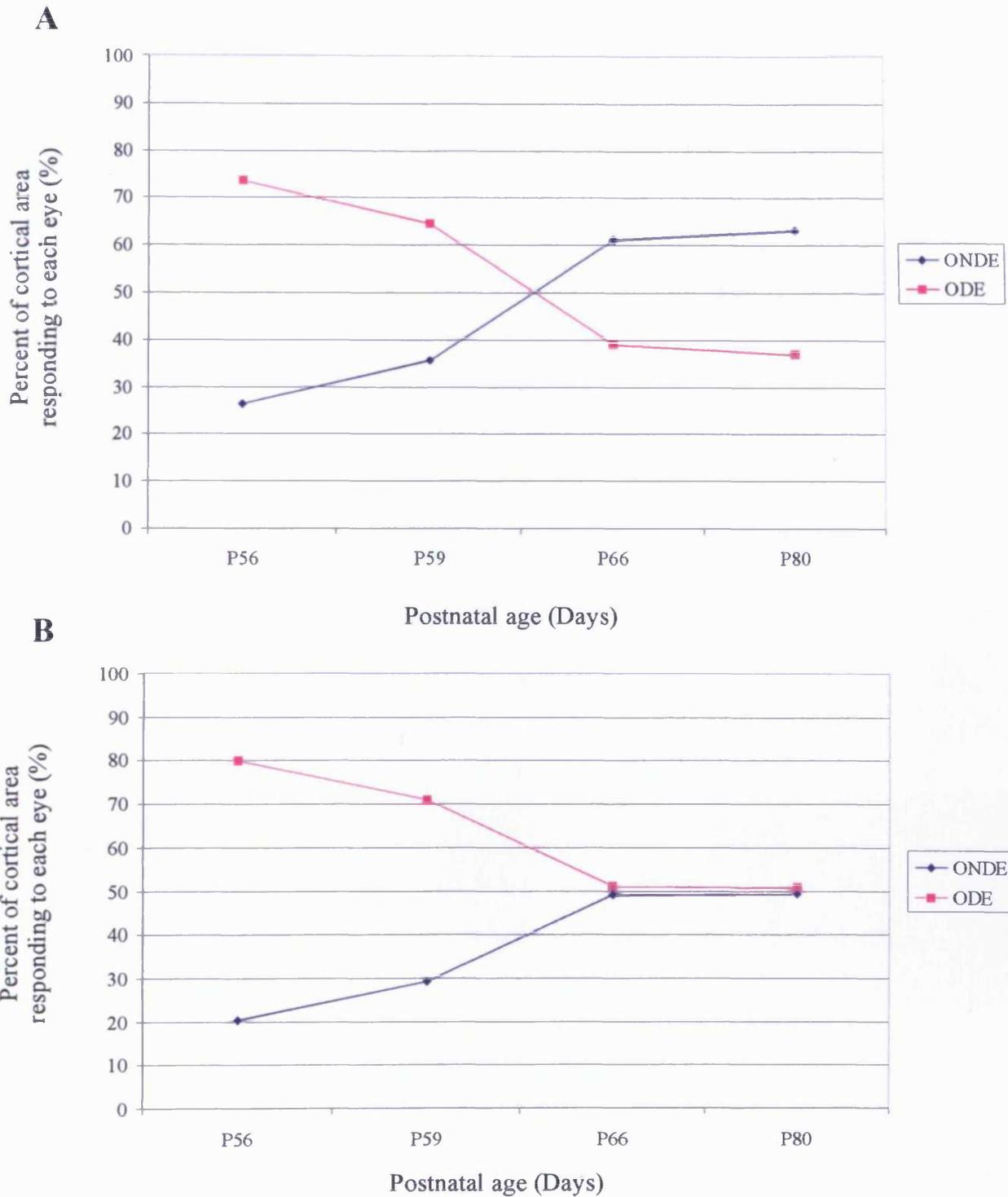


Figure 3.6 a and b Cortical ocular dominance in a kitten with an intermediate period of binocular vision between the first period of monocular deprivation and before reverse occlusion

Data is from kitten 030 which was monocularly deprived in the RE (P13). This was followed by 4 days of binocular vision (P36-40), then reverse occluded in the LE for 16 days (P40-56)

Originally non-deprived eye(ONDE) is represented by the blue line.

Originally deprived eye (ODE) is represented by the pink line.

A) Data for the hemisphere contralateral to the DE.

B) Data for the hemisphere ipsilateral to the DE.

Figure 3.7 a Effects of a brief period of de-correlated vision between a period of monocular deprivation and RO on ocular dominance and orientation selectivity in the originally deprived (RE)

Kitten 102 - Monocular deprivation was imposed at P13-P36 (RE). De-correlated binocular vision (using prism goggles) P36-P40. Reverse occlusion P40-P56 (LE).

Columns A-D represent: Ocular dominance (left eye/right eye), single condition (0 deg/blank) angle, and polar maps obtained from V1.

Column A - Patches of black represents high neuronal activity, and white, low neuronal activity. With respects to the right vs left eye map here, dark areas represent neurons responding preferentially to the right eye and light areas responding preferentially to the left eye.

Column B -The relative strength of the response is represented on the level of darkness. The darker the patch the greater the response.

Column C -The resulting vector of responses to all orientations tested is allocated a colour to represent preferred orientation.

Column D - The relative strength of the oriented response is represented on a scale of brightness.

Rows A-C represent time course: Immediately upon reopening of the recently deprived eye (P53), then P56, P63.

Colour key represents preferred orientation in angle maps. Line arrows represent relative orientation of the head.

Maps differed slightly in size between imaging sessions.

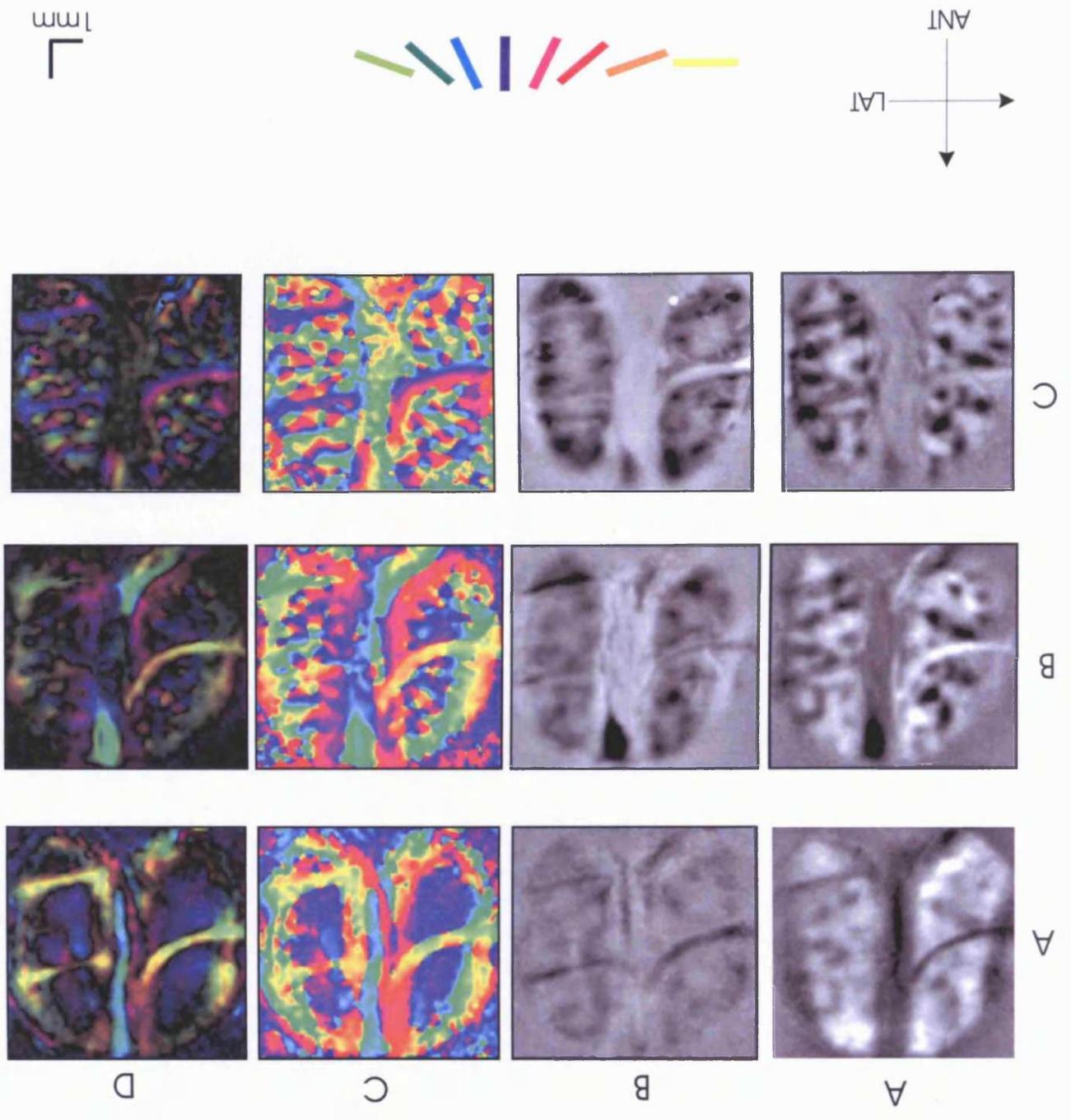


Figure 3.7 b Effects of a brief period of de-correlated vision between a period of monocular deprivation and RO on ocular dominance and orientation selectivity in the originally non-deprived (LE)

Kitten 102 - Monocular deprivation was imposed at P13-P36 (RE). De-correlated binocular vision (using prism goggles) P36-P40. Reverse occlusion P40-P56 (LE).

Columns A-D represent: Ocular dominance (left eye/right eye), single condition (0 deg/blank) angle, and polar maps obtained from V1

Column A - Patches of black represents high neuronal activity, and white, low neuronal activity. With respects to the left vs right eye map here, dark areas represent neurons responding preferentially to the left eye and light areas responding preferentially to the right eye.

Column B -The relative strength of the response is represented on the level of darkness. The darker the patch the greater the response.

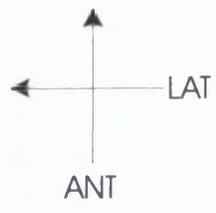
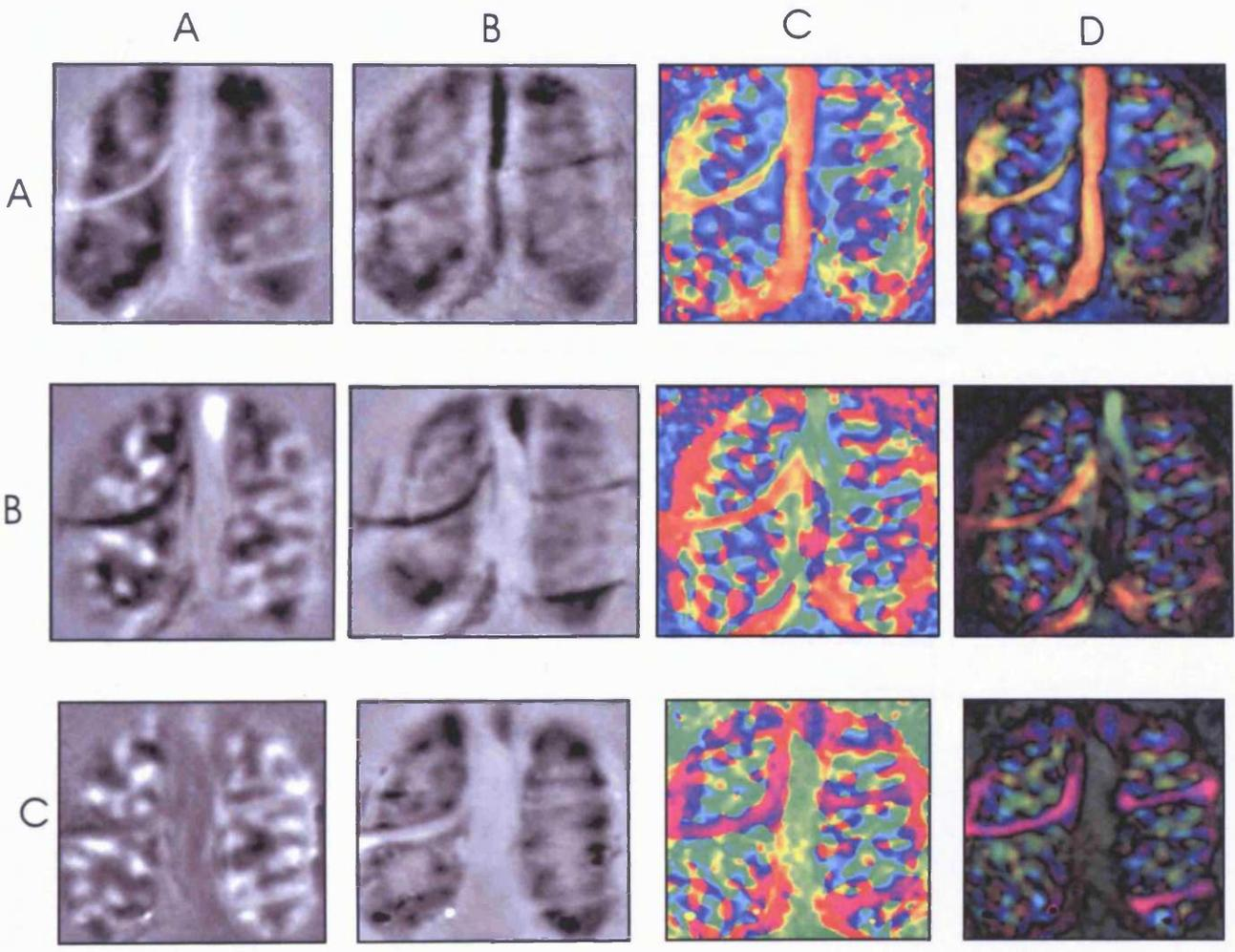
Column C -The resulting vector of responses to all orientations tested is allocated a colour to represent preferred orientation.

Column D - The relative strength of the oriented response is represented on a scale of brightness.

Rows A-C represent time course: Immediately upon reopening of the recently deprived eye (P53), then P56, P63.

Colour key represents preferred orientation in angle maps. Line arrows represent relative orientation of the head.

Maps differed slightly in size between imaging sessions.



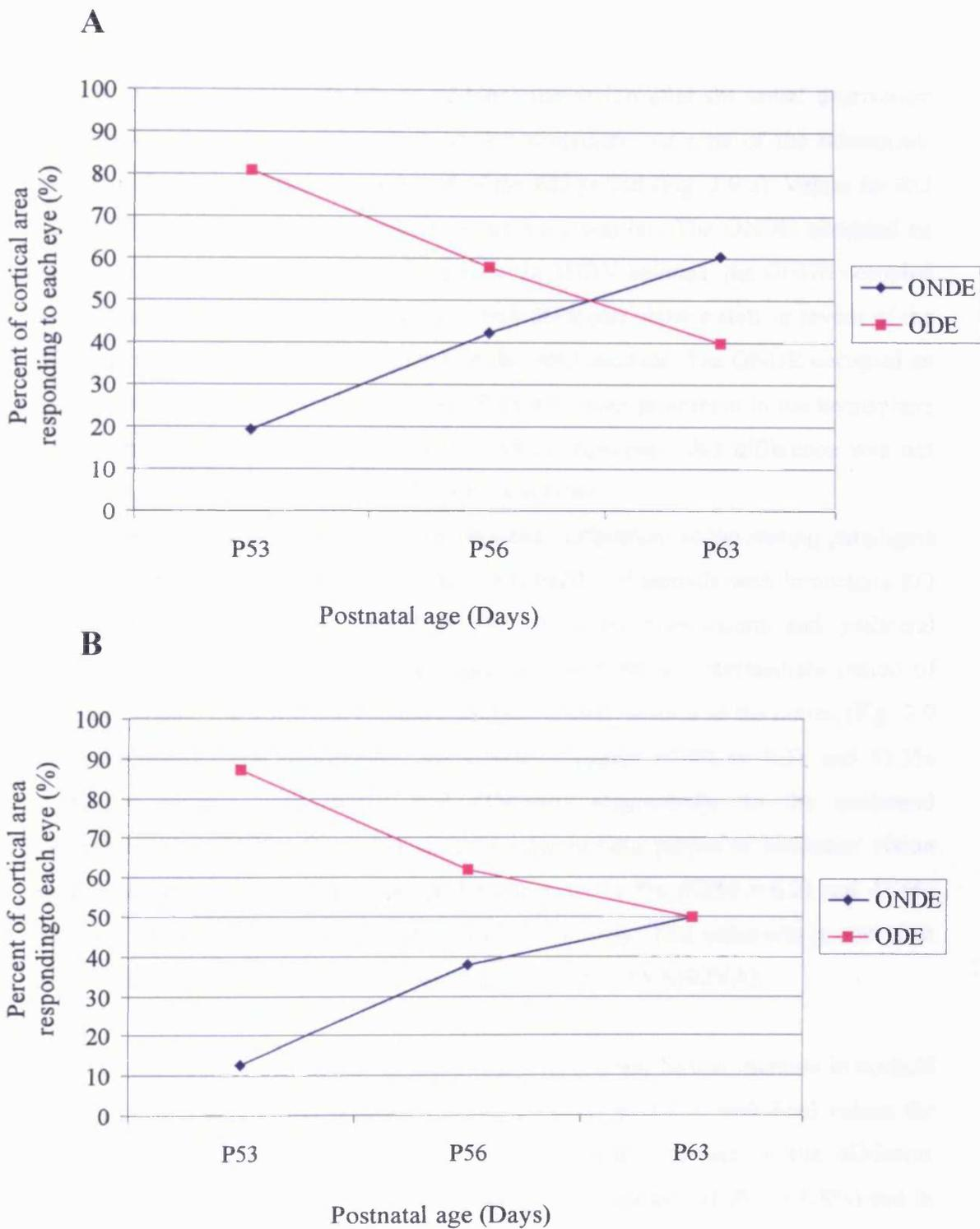


Figure 3.8 a and b Cortical ocular dominance in a kitten with an intermediate period of de-correlated vision between the first period of monocular deprivation and before reverse occlusion

Data is from kitten 102 which was monocularly deprived in the RE (P14). This was followed by 4 days of de-correlated vision (P33-37), then reverse occluded in the LE for 16 days (P37-53).

Originally non-deprived eye(ONDE) is represented by the blue line.

Originally deprived eye (ODE) is represented by the pink line.

A) Data for the hemisphere contralateral to the DE.

B) Data for the hemisphere ipsilateral to the DE.

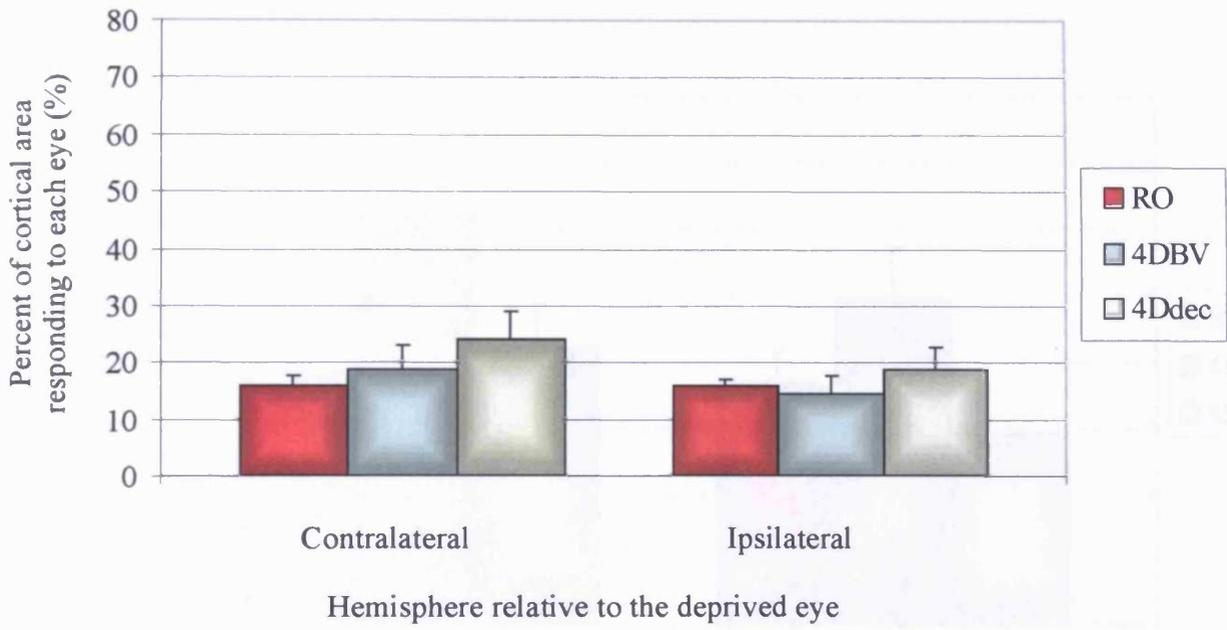
obvious that the intermediate period of binocular vision after the initial deprivation period has had no discernible effect on the immediate outcome of the subsequent reverse occlusion, as assessed at the end of the RO period (Fig. 3.9 a). Values for RO and 4DBV animals in both hemispheres are very similar, The ONDE occupied an average of 15.8% ($\pm 0.90\%$) for RO animals. In 4DBV animals, the ONDE occupied an average of 16.6% ($\pm 2.56\%$). Animals with 4Ddecorr show a shift in favour of the ODE that is slightly less prominent than in the other animals. The ONDE occupied an average of 21.2% ($\pm 3.1\%$) of the cortex. This was most prominent in the hemisphere contralateral to the ONDE at 23.8% ($\pm 5.14\%$). However, this difference was not significant from the other 2 groups ($P=0.49$ ANOVA).

It is not until after a brief period of recovery that differences in the rearing paradigms become apparent. The recently deprived eye (ONDE) of animals with immediate RO occupies just 39.7% (± 7.9) and 27.3% (± 3.2) in the contralateral and ipsilateral hemispheres. In contrast, in those animals that received an intermediate period of binocular vision, the same eye occupied a much greater portion of the cortex (Fig. 3.9 b). In the contralateral hemisphere, the ONDE occupied 50.4% (± 9.3), and 53.3% (± 3.8) for animals with 4DBV and 4Ddecorr respectively. In the ipsilateral hemisphere, the ONDE of animals with an intermediate period of binocular vision again occupied a similar proportion of the cortex at 41.5% (SEM ± 6.2) and 42.5% (SEM ± 5.6) for groups 4DBV and 4Ddecorr respectively. This value was greater than for animals with immediate RO but not significant ($P=0.16$ ANOVA).

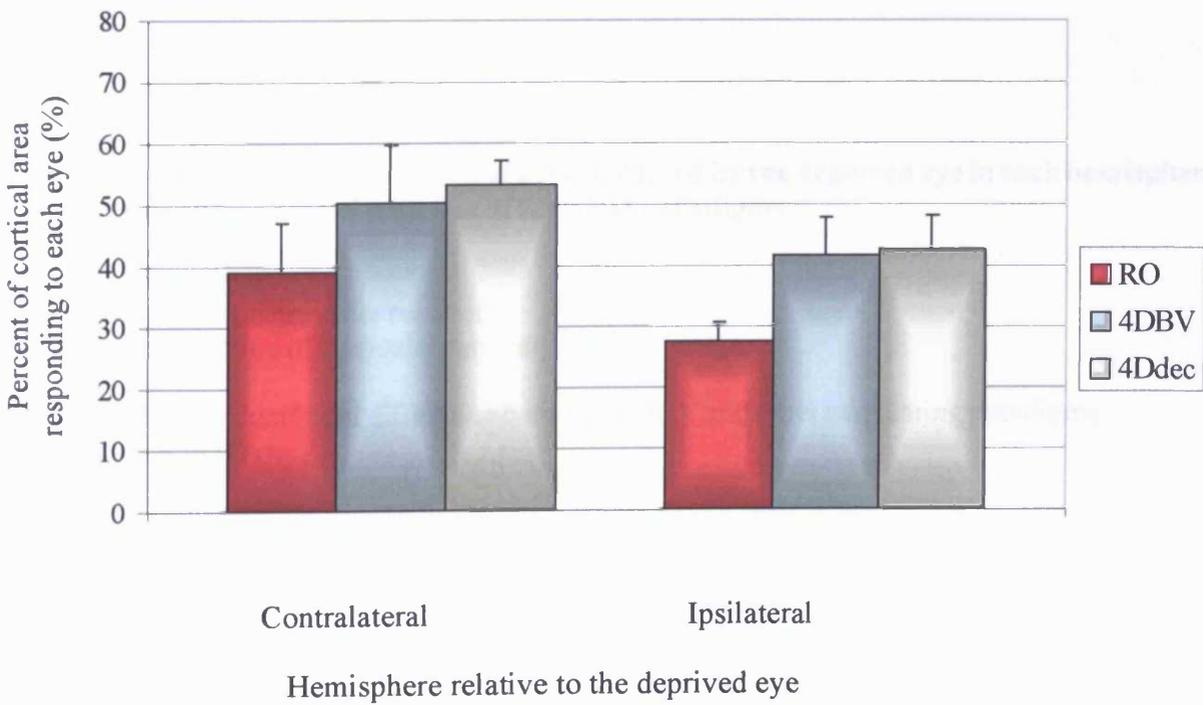
After extended recovery (>24 days) there was only a small further increase in cortical territory occupied by the ONDE for the RO group (Fig. 3.9c), with final values for combined hemispheres being 37.55 ($\pm 3.4\%$). In stark contrast, in the 4Ddecorr kittens, the ONDE actually lost cortical territory to occupy just 41.8% ($\pm 6.8\%$) and to 28.9 ($\pm 0.8\%$) for contralateral and ipsilateral hemispheres to the ONDE respectively. In comparison to RO and 4Ddecorr groups, in the 4DBV group, extended binocular recovery lead to further increase in ONDE territory. Final values for the ONDE in the contralateral hemisphere to the ONDE are 62.2% ($\pm 1.7\%$) and 49.3% ($\pm 7.8\%$) in the ipsilateral hemisphere.

Taken together, the ONDE of animals with a period of correlated vision (4DBV) occupied a significantly greater portion of the cortex than those animals that received immediate RO or an intermediate period of 4 days de-correlated vision, in the

A



B



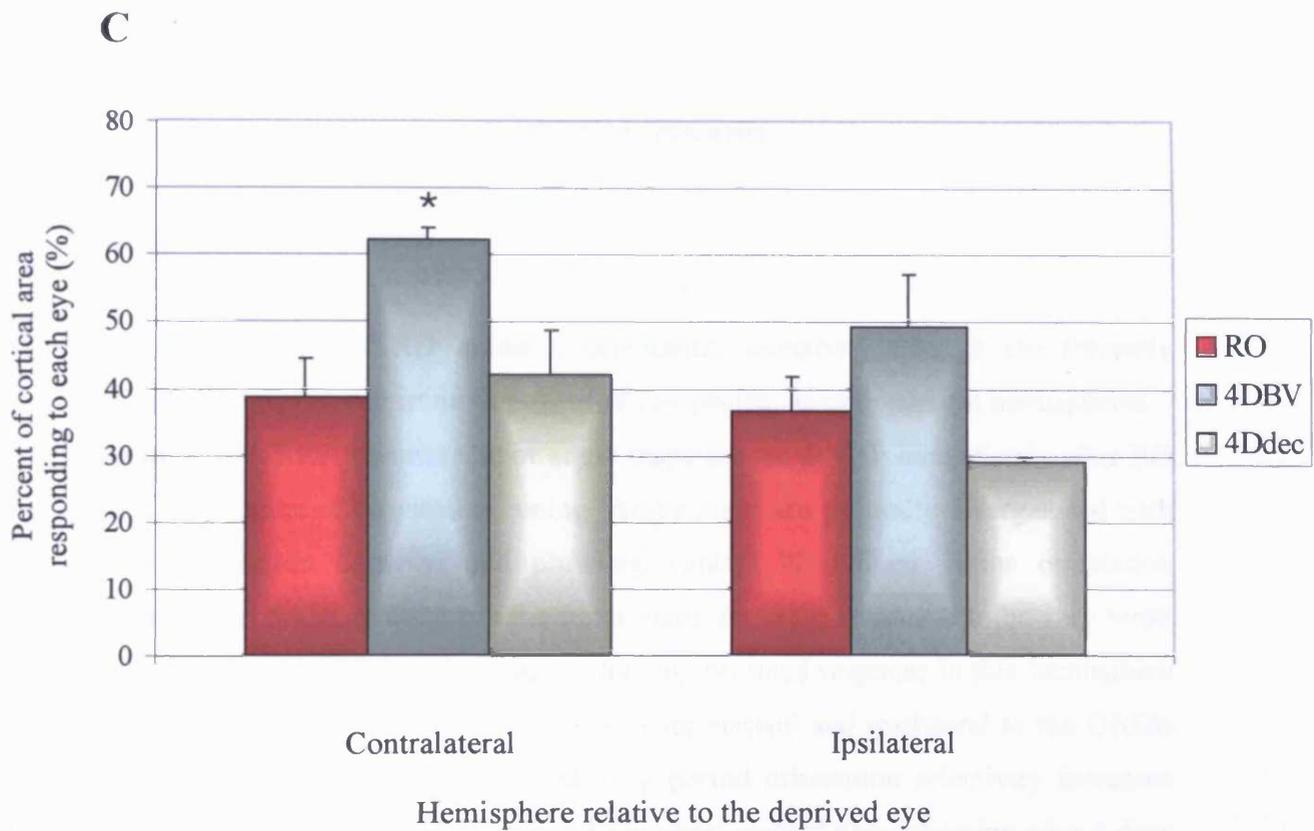


Figure 3.9 a-c Summary of cortical area occupied by the deprived eye in each hemisphere imaged in kittens reared with one of the 3 RO paradigms

- A) Immediately after MD.
- B) Brief period of binocular recovery.
- C) Extended period of binocular recovery.

Star (*) depicts significant difference between 4DBV and other two rearing paradigms (P=0.03, ANOVA).

contralateral hemisphere ($P=0.03$ ANOVA). The ONDE of the 4DBV group also occupied a much greater portion of the cortex, though not quite significantly so, of the ipsilateral hemisphere ($P=0.1$ ANOVA).

Orientation selectivity

Immediate reverse occlusion

In all three groups of RO animals, orientation selectivity through the (recently deprived) ONDE is weak immediately after re-opening, in both cortical hemispheres. In figure 3.3a (row A column C) for angle maps for the ONDE immediately after RO show a low degree of orientation tuning. Angle maps are generally disorganised with any iso-orientation domains and pinwheel centres ill defined. Some orientation patches appear medially although the polar maps show this response to be very weak (Row A column D) for this eye suggest that any oriented response in this hemisphere is very weak (Fig. 3.3c; OSI 0.45 and 0.37 contralateral and ipsilateral to the ONDE respectively). Over the subsequent recovery period orientation selectivity increases rapidly, with iso-orientation domains and pinwheel centres first appearing after 4 days (Fig. 3.3a column C and D row B-D) and becoming more distinct over subsequent weeks (Fig. 3.3c; OSI 0.77, 0.82) and continues to improve with further recovery. Angle and polar maps through the ODE remain strong and robust from the termination of RO through the recovery period.

Four days binocular vision between the first period of MD and before RO

Reverse occlusion had a similarly devastating effect on orientation selectivity of ONDE responses in animals with an intermediate period of binocular vision, as in those without. ONDE angle and polar maps show no responses selective for orientation immediately after re-opening (Fig. 3.5a, row A column C and D) while ODE responses are robust and selective for orientation (Fig. 3.5b row A column C and D). This is reflected in a low OSI for contralateral and ipsilateral hemisphere (to the ONDE) of 0.29 and 0.32. Some oriented responses return through the ONDE after a brief (3-day) period of recovery (Fig. 3.5a, row B column C and D). Oriented

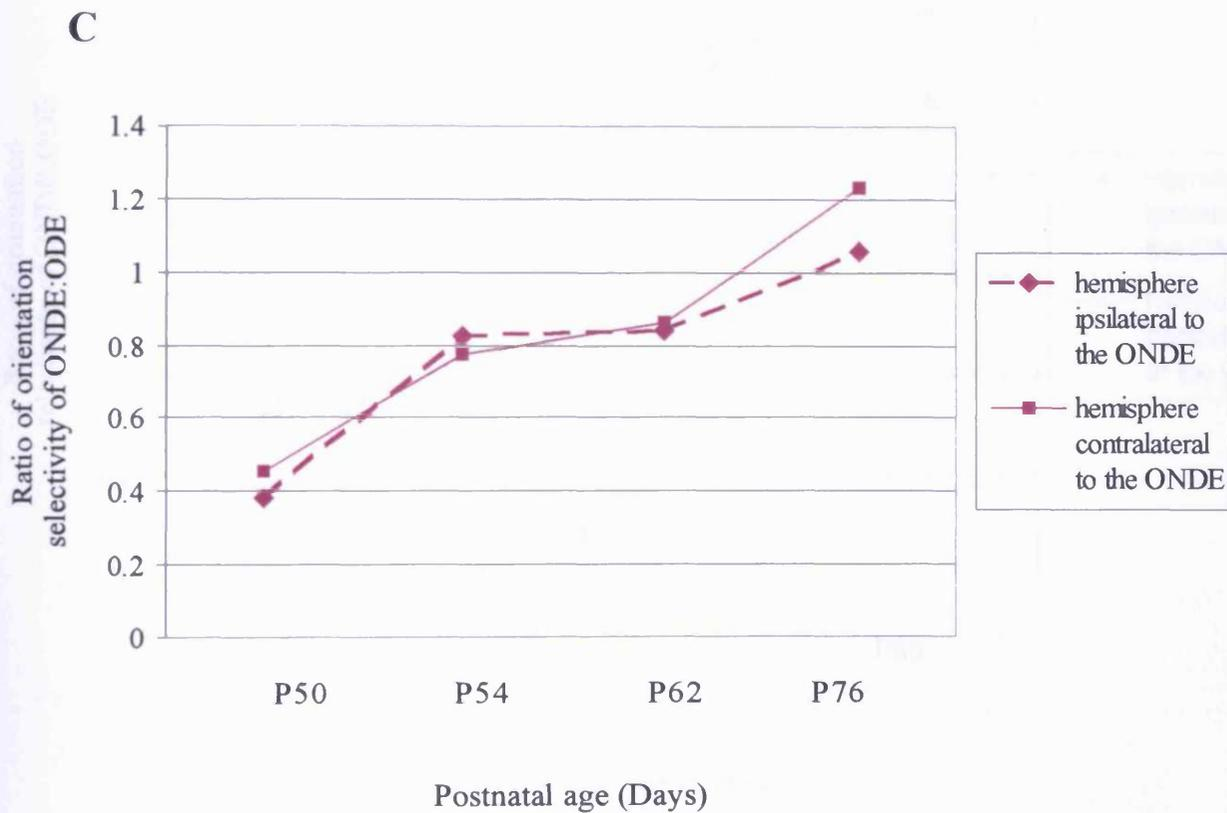


Figure 3.4 c Ratio of ONDE:ODE of cortical orientation selectivity in a kitten after reverse occlusion

Data is from BW1 kitten - Monocular deprivation in the RE at P14 followed by a 18-day period of reverse occlusion in LE (P35-53).

Contralateral hemisphere to the ONDE is represented by the continuous line
 Ipsilateral hemisphere to the ONDE is represented by the dotted line.

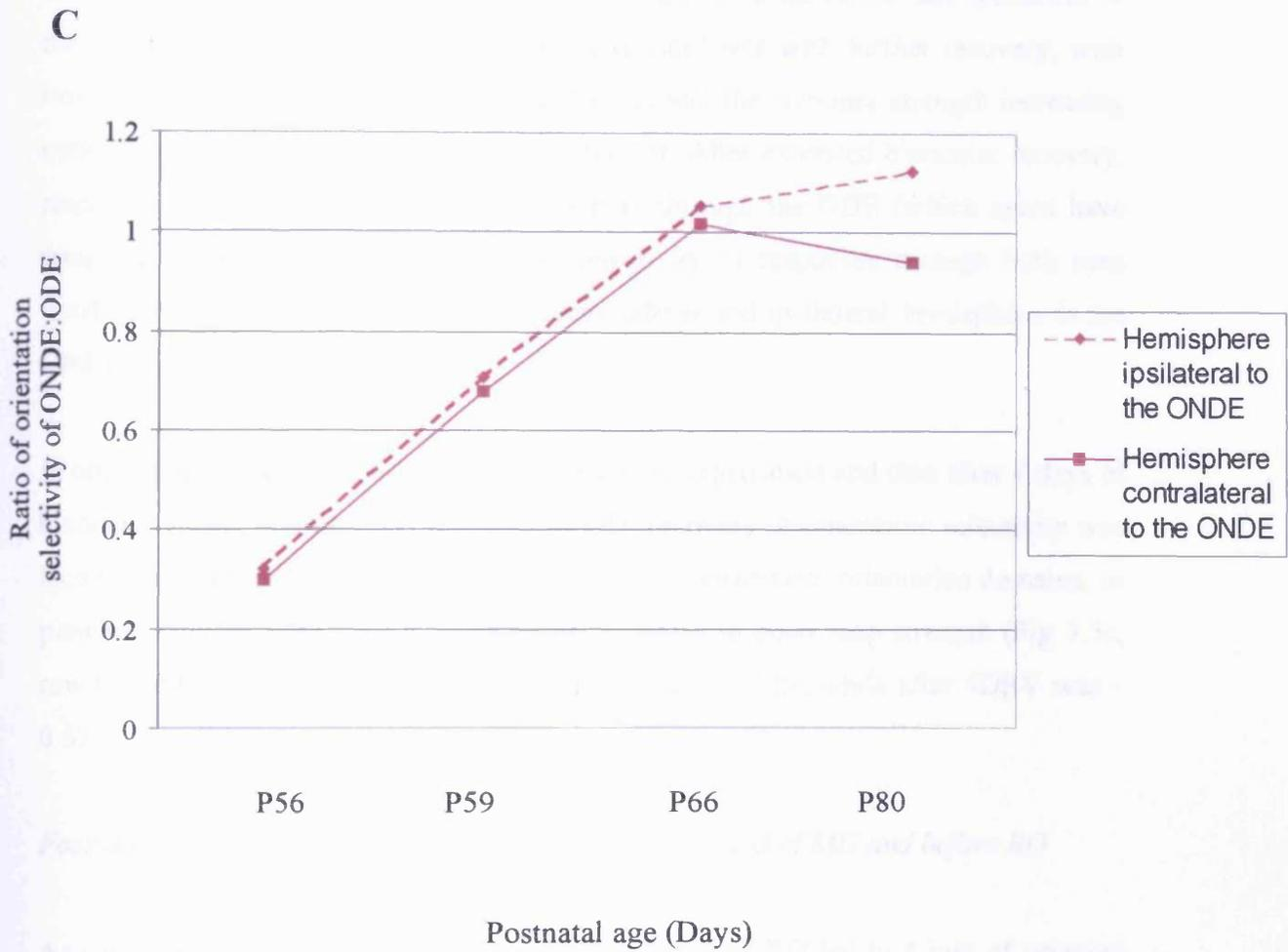


Figure 3.6 c Ratio of ONDE:ODE of cortical orientation selectivity in a kitten with an intermediate period of binocular vision after the first period of monocular deprivation and reverse occlusion

Data is from kitten 030 - Monocular deprivation was imposed in the RE at P13. This was followed by 4 days of binocular vision (P36-40) then 16 days of reverse occlusion in LE (P40-56).

Contralateral hemisphere to the ONDE is represented by the continuous line.
 Ipsilateral hemisphere to the ODE is represented by the dotted line.

patches are beginning to appear, with pinwheel centres just discernible. The relative OSI has increased to 0.67 and 0.7 for the hemispheres contralateral and ipsilateral to the ONDE (Fig. 3.6c). Orientation selectivity improves with further recovery, with iso-orientation domains becoming more distinct and the response strength increasing noticeably (Fig. 3.5a row B-D column C and D). After extended binocular recovery, responses through the ONDE are as strong as through the ODE (which again have remained fairly stable throughout). The selectivity of responses through both eyes finished similar, 1.19 and 0.87 for the contralateral and ipsilateral hemisphere to the ONDE (Fig. 3.6c).

In one animal imaged immediately after the initial deprivation and then after 4 days of binocular vision, despite good recovery of OD, recovery of orientation selectivity was incomplete. Responses through the DE showed no defined iso-orientation domains, or pinwheel centres, with only a small global increase in polar map strength (Fig 3.5c, row C and D). The OSI after the initial MD averaged ~ 0.23 , while after 4DBV was ~ 0.67 .

Four days of de-correlated vision between the first period of MD and before RO

As with the other two rearing paradigms, the period of RO led to a loss of oriented responses through the ONDE (Fig. 3.7a, row A column C and D), while responses through the ODE remain strong and oriented (Fig. 3.7b row A column C and D). The OSI at this time is unusually high, 0.51 and 0.47 (Fig. 3.8c) for hemispheres contralateral and ipsilateral to the ONDE. This can in part be explained by the weaker than normal responses through the ODE (Fig. 3.7b row A column C and D) which appear to be dominated by responses around 90° .

Faint iso-orientation domains and pinwheels begin to appear in the ONDE responses after three days of binocular recovery. The response strength through the ONDE increases slightly (Fig. 3.7a column D row B), and the relative OSI of ONDE: ODE responses increases in both hemispheres (Fig. 3.8c). With further binocular recovery, the orientation selectivity improved through the ONDE, with the responses strength in the polar maps increasing and angle maps becoming better defined (Fig. 3.7b row C Column C and D) Final OSI values are 0.94 and 0.75 (Fig. 3.8c).

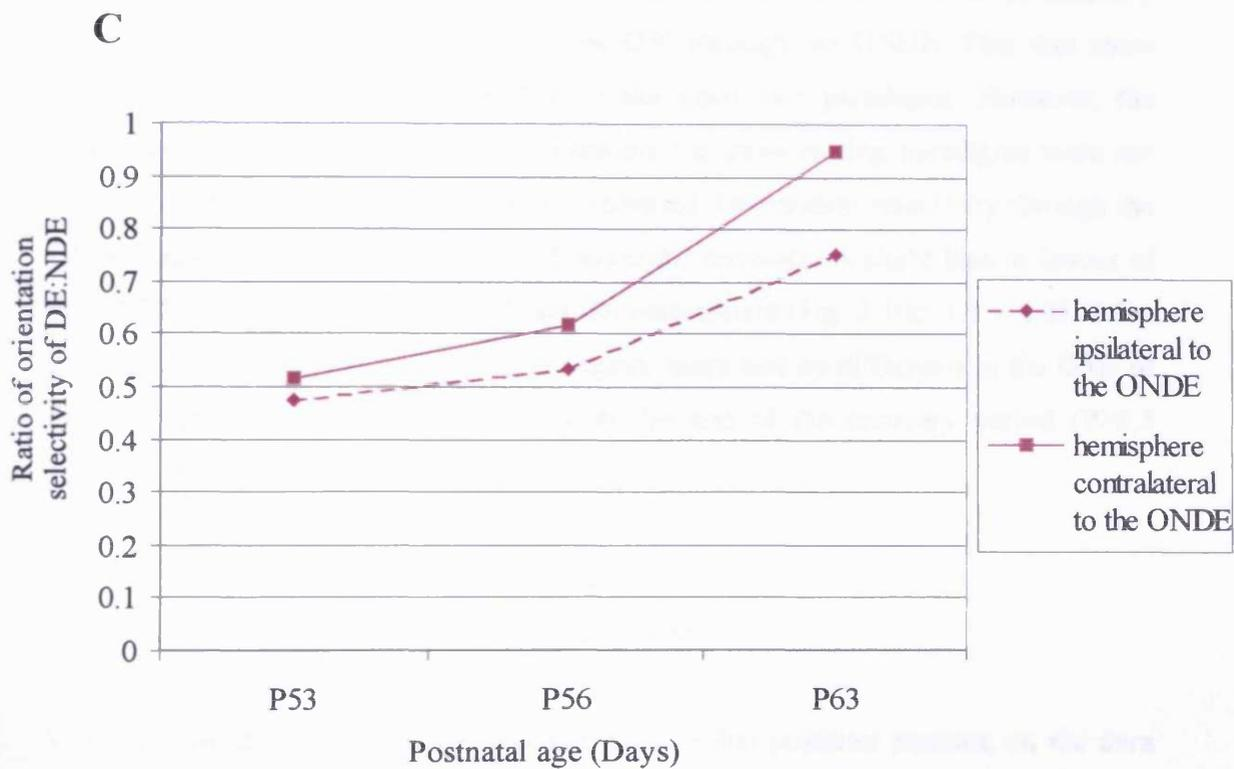


Figure 3.8 c Ratio of ONDE:ODE of cortical orientation selectivity in a kitten with an intermediate period of de-correlated vision after the first period of monocular deprivation and before reverse occlusion

Data is from 102 kitten - Monocular deprivation was imposed in the RE at P14. This was followed by 4 days of de-correlated vision (P33-37) then 16 days of reverse occlusion in LE (P37-53).

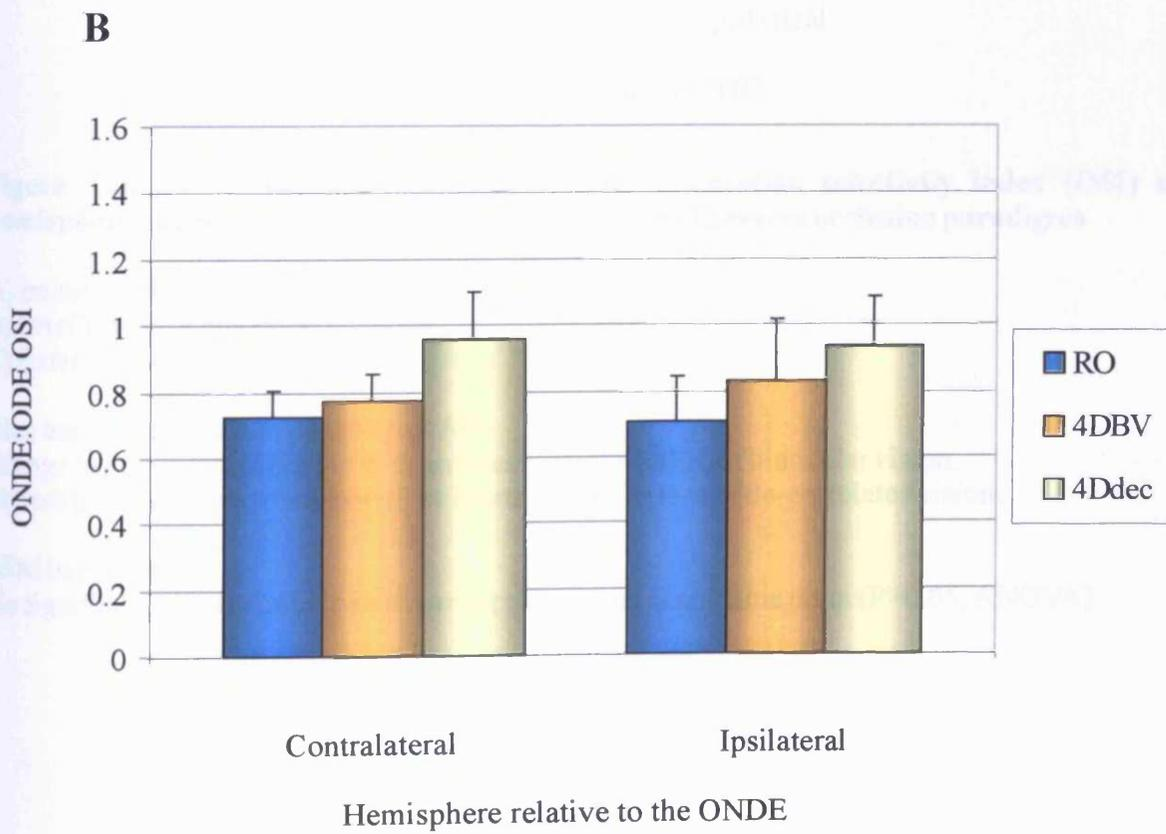
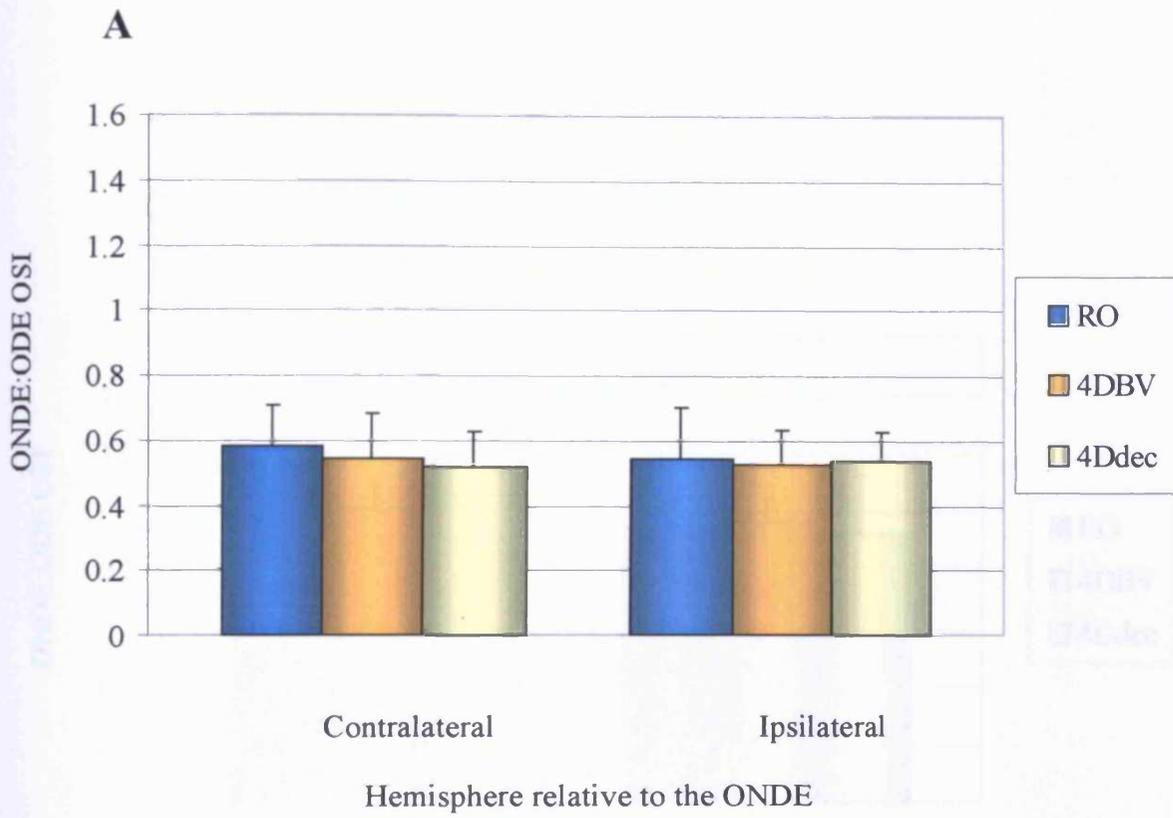
Contralateral hemisphere to the ONDE is represented by the continuous line.
Ipsilateral hemisphere to the ODE is represented by the dotted line.

Figure 3.10 summarises the OSI data from all animals in this experiment. The period of RO itself had an almost identical effect on orientation selectivity in all three rearing paradigms (Fig. 3.10.a: OSIs ranged from 0.52-0.58 and from 0.52-0.54 for the hemispheres contralateral and ipsilateral to the ONDE). A brief period of recovery (Fig. 3.10b) resulted in an increase in the OSI through the ONDE. This was more pronounced in 4Ddecorr animals than in the other two paradigms. However, the differences in the ONDE: ODE OSIs between the three rearing paradigms were not significant ($P > 0.3$ ANOVA, in both hemispheres). Orientation selectivity through the ONDE increased further with extended binocular recovery. A slight bias in favour of the ONDE was observed in the contralateral hemisphere (Fig. 3.10c: 1.1 ± 0.03 , 1.0 ± 0.07 and 1.2 ± 0.2 in the three groups). Again, there was no difference in the OSIs of the three groups for either hemisphere at the end of the recovery period ($P > 0.5$ ANOVA, in both hemispheres).

Visual acuity

Visually evoked potentials were recorded on a medial posterior position on the dura above V1, in animals with an intermediate period of 4 days of de-correlated vision. This was done on the day of termination of the period RO and in parallel with every other optical imaging session thereafter.

Figure 3.11 shows the combined data of animals with 4 days of de-correlated vision. On the day of termination of RO the acuity of the ODE was 2.7cyc/deg (± 0.45 cyc/deg). The ONDE was effectively blind. It achieved acuity of only 0.48cyc/deg (± 0.03 cyc/deg). Some improvement in the acuity of the ONDE occurred with 3 days of binocular recovery. However, this improvement was quite small with acuity reaching only 0.7cyc/deg (± 0.5 cyc/deg). The most noticeable change was in the dramatic decrease in acuity of the ODE. This fell by nearly 40% to just 1.7cyc/deg (± 1.8 cyc/deg). With further binocular recovery, acuity of the ONDE increased steadily to finish at 1.85cyc/deg (± 0.15 cyc/deg). Acuity of the ODE did not improve, finishing similar to that of the ONDE (1.6cyc/deg (± 0.1 cyc/deg)). The acuity of both eyes at the end of the experiment was below that of the ODE (on the day of termination of



C

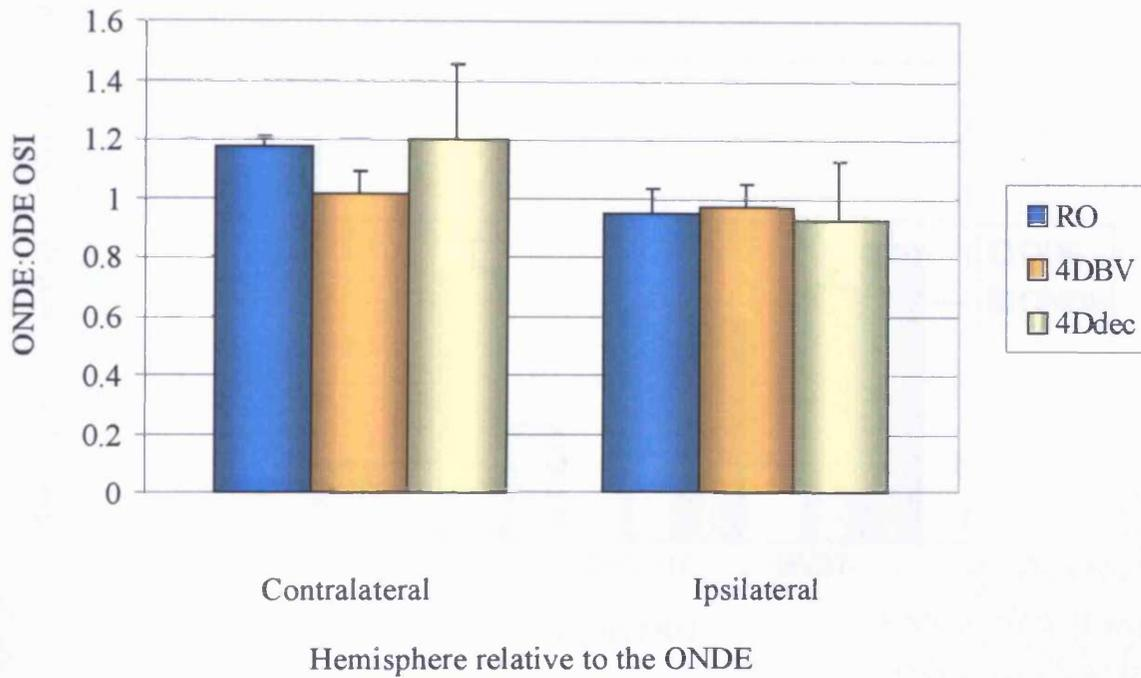


Figure 3.10 a-c Summary of ONDE:ODE orientation selectivity index (OSI) in each hemisphere imaged for kittens reared with one of the 3 reverse occlusion paradigms

- A) Immediately after MD.
- B) Brief period of binocular recovery.
- C) Extended period of binocular recovery.

Blue bar represents animals with just RO.
Orange bar represents animals with an intermediate period of binocular vision.
Yellow bar represents animals with an intermediate period of de-correlated vision.

SEM bars shown.
No significant difference between rearing paradigms at any time point ($P > 0.05$, ANOVA).

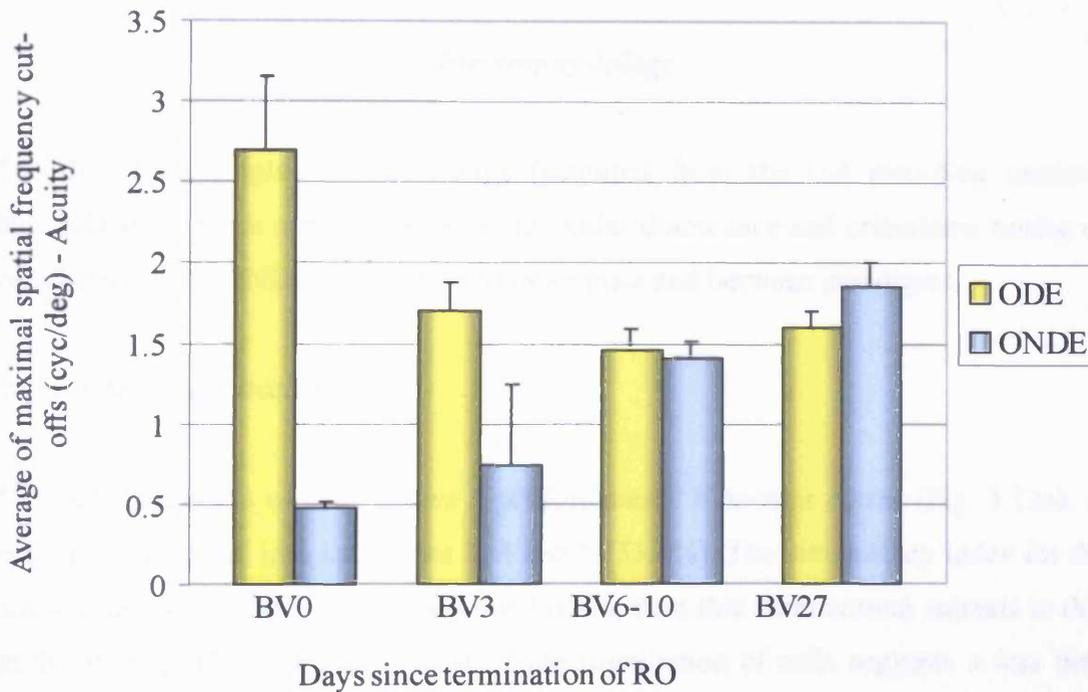


Figure 3.11 Summary data of recovery of visual acuity in animals with 4 days of de-correlated vision

Kittens received an intermediate period of decorrelated vision before RO. Visual acuity was assessed by VEPs on the day that binocular vision was finally introduced -BV0 and at 3, 6-10, and 27 days, in line with optical imaging sessions.

RO) and below that seen in either eye in animals with MD (at the start and finish of the experimental period). There, acuity in both eyes was just above 2.5 cyc/deg at the start of the experiment and just below 2.5 cyc/deg at the end of the experiment. This is much higher than compared to 1.6-1.85 cyc/deg for each eye in (4Ddecorr) animals at the end of the experimental period.

Electrophysiology

The data from single cell recordings (acquired from the last recording session) highlight some more subtle differences in ocular dominance and orientation tuning of cells between the ONDE and ODE within animals and between paradigms.

Immediate reverse occlusion

The OD distribution of cells shows a predominantly binocular cortex (Fig. 3.12a). A majority of cells fall into categories 3, 4 and 5 (53.4%). The binocularity index for the population is 47.8 (Fig. 3.13), a value that is less than that from normal animals in this study (BI 60). This more subtle test of the distribution of cells suggests a less than normal degree of binocularity. The half width half height (hwhh) of cells dominated by the ONDE is $30^{\circ} \pm 1.7^{\circ}$, while that of the ODE is significantly broader ($P=0.002$, t-test) at $38.7^{\circ} \pm 2.1^{\circ}$.

Four days of binocular vision between the first period of MD and before RO

Like RO animals, 4DBV animals shows a very similar distribution of OD (Fig.3.12b), with a binocular cortex predominating (57.6% cells in category 3, 4, and 5). The binocular index confirms this, again being very similar (BI 50) to that of RO animals (Fig. 3.13). The hwhh of cells responding to the ONDE $31.5^{\circ} \pm 1.7^{\circ}$, while that of the ODE was broader, but not significantly ($P=0.1$, t-test) at $35.2^{\circ} \pm 1.4^{\circ}$.

Four days of de-correlated vision between the first period of MD and before RO

Again, a distribution of OD is very similar for animals that received intermediate de-correlated vision (Fig. 3.12c). The average number of cells in categories 3, 4, and 5 is 56.6%, which is reflected in a BI of 49.8 (Fig. 3.12), again very similar between the 3 rearing paradigms. Tuning width for the ONDE $29.6^\circ \pm 1.77^\circ$, while that for the ODE was again significantly broader ($P=0.038$, t-test) at $34.5^\circ \pm 1.3^\circ$.

Figure 3.12 a-c Ocular dominance distribution of single cells recorded from kitten V1 after extended recovery in RO, 4DBV and 4Ddecorr animals

A - Immediate RO.

B - Intermediate period of 4 days of binocular vision before RO.

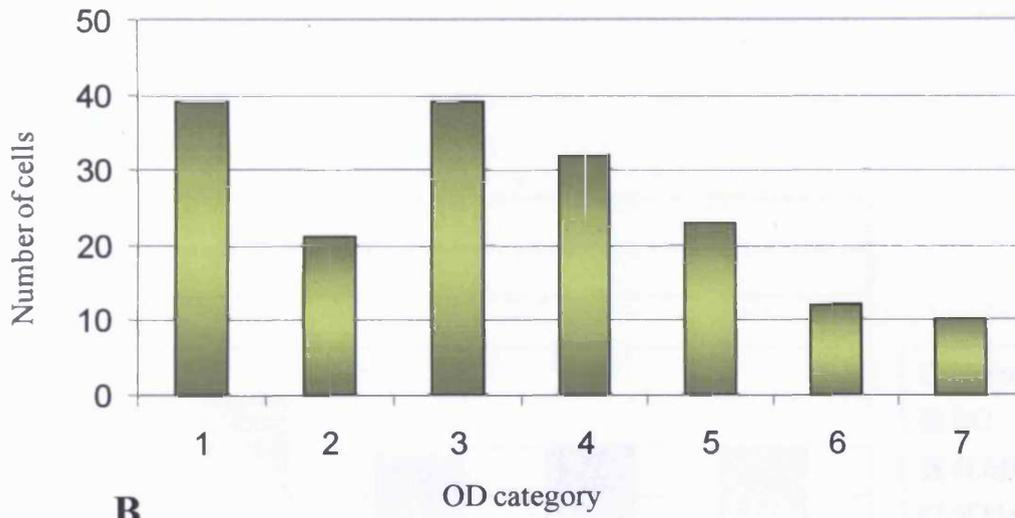
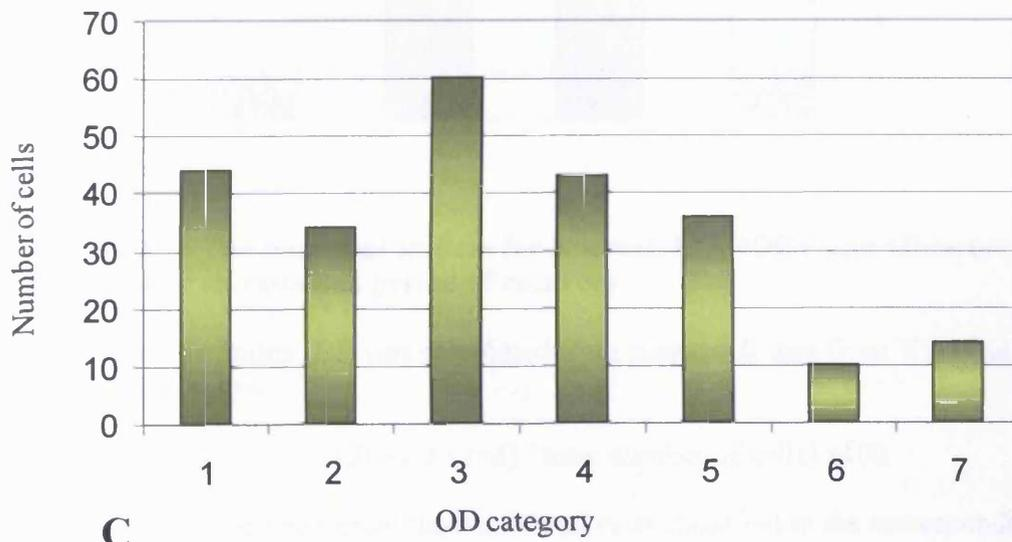
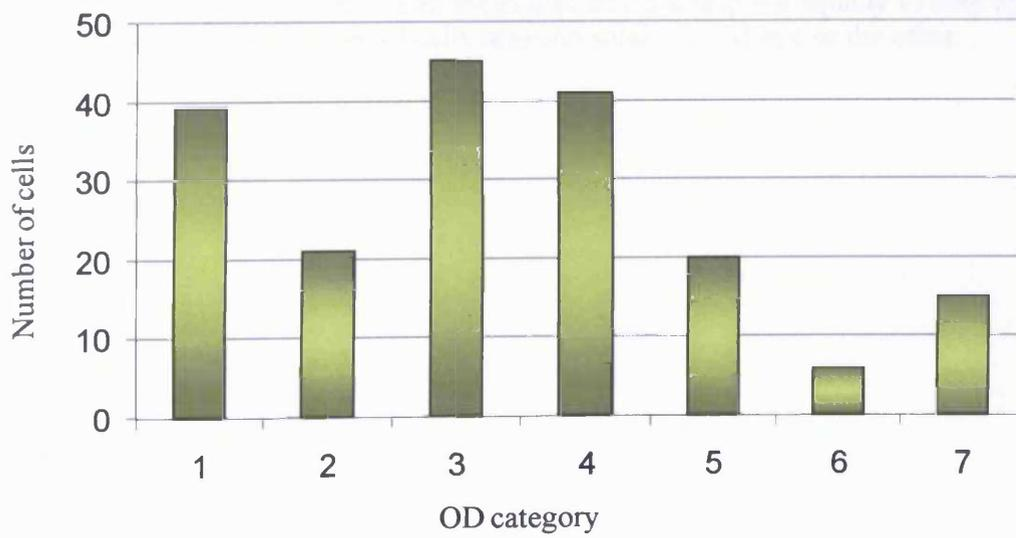
C - Intermediate period of de-correlated vision before RO.

Cells were allocated a category 1-7:

Category 1 responding solely to the left eye.

Category 7 responding solely to the right eye.

Category 4 responding equally to both eyes.

A**B****C**

DISCUSSION

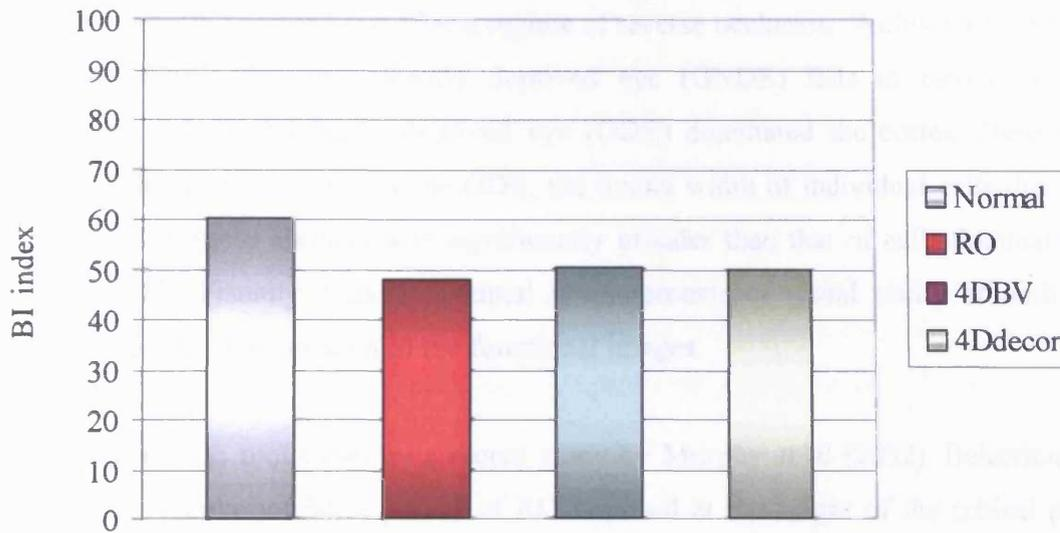


Figure 3.13 The binocular indices for Normal, RO, 4DBV and 4Ddecor kitten after an extended period of recovery

The binocular index (BI) was calculated from single cell data from V1 using the calculation below:

$$[(4 + 2/3 (3+5) + 1/3 (2+6) / \text{total number of cells}] \times 100$$

Italicized numbers represent the number of cells classified in the corresponding ocular dominance category (from Murphy and Mitchell; 1986).

A binocular index of 100 would mean that all cells respond equally to both eyes.

A value of 0 would mean all cells respond solely to one eye or the other.

DISCUSSION

The results presented here demonstrate the importance of concordant and correlated input to the two eyes (even for as brief a period as 4 days) for physiological recovery of the recently deprived eye after a regime of reverse occlusion. Without it (in RO and 4Ddecorr animals), the recently deprived eye (ONDE) fails to recover cortical territory and the originally deprived eye (ODE) dominated the cortex. Despite the overall domination of V1 by the ODE, the tuning width of individual cells driven by the ODE in these animals was significantly broader than that of cells dominated by the ONDE. Visually evoked potential measurements of visual acuity of both eyes paralleled the changes seen in the functional images.

Work here was motivated by a recent study by Murphy *et al* (2002). Behaviourally, binocular recovery after a period of RO imposed at the height of the critical period resulted in poor acuity in both eyes. However, a 4 day period of binocular vision immediately after MD and before RO led to normal acuity in the ODE (~ 7.5 cyc/deg) and moderately good acuity in the ONDE (~ 3 cyc/deg). A further set of animals that also received an intermediate period of binocular yet de-correlated vision (by means of prisms) did not exhibit recovery of acuity in both eyes when binocular vision was restored.

Imaging studies have shown that restoration of orientation selectivity and orientation maps occurs after RO (Kim and Bonhoeffer; 1994) even in animals with no common visual experience between the two eyes (Godecke and Bonhoeffer; 1996). However, in these studies, there was no follow-up of the consequences of RO during a subsequent recovery period. The depth of investigation into the behavioural responses to the timing of the initial MD, RO, and recovery has yet to be matched physiologically. In light of the above results by Murphy *et al* (2002), combined with the discrepancies between physiological and acuity measurements from the two eyes shown in this thesis for other rearing paradigms (Chapter 2), further study was warranted here.

In the paradigms used here, monocular deprivation was imposed at P14. This timing matched that employed by Murphy *et al* (2002). Postnatal day 14 is several days after

eye opening (P7-10) and is later than that used in most other RO studies, which deprived one eye from natural eye opening (Mitchell *et al* 1984; Murphy and Mitchell; 1986, 1987; Mitchell 1991; Godecke and Bonhoeffer; 1996).

When eyelid suture is carried out at the time of natural eye opening, this ensures that the (to be) DE has received no visual input. However, such early visual experience has proved to have little effect on the initial development of cortical maps. Around the time of eye-opening (<P14), OD columns cannot be demonstrated either physiologically or anatomically. Prior to P21 they appear to form independently of visual experience (Crair *et al* 1998; Crowley and Katz 2000; Crair *et al* 2001). The same applies to the development of early orientation maps. The layout of the orientation maps appears to change little in the first few weeks after eye opening regardless of visual experience (Chapman *et al* 1996; Godecke *et al* 1997; Crair *et al* 1998). Therefore, the few days visual experience allowed here (P10-P14) should be of little consequence to the early cortical map development.

Reverse occlusion was imposed at P35, near the height of the critical period, to ensure maximal effects of this reversal (and an interim period of binocular vision) could be seen and recovery after RO would still be possible. The deprivation effect for MD is highest at 5 weeks of age. It decreases slightly but still remains quite high until 10 weeks of age (Olson and Freeman 1980). However, the 'reversal index' (the proportion of recorded cortical cells dominated by the initially deprived eye) for RO decreases dramatically after 6 weeks and by 8 weeks few recorded cells reverse their ocular dominance to favour the recently opened eye (Blakemore and Van Sluyters 1974). Hence, the time period of deprivation and recovery used here allows for maximal effects of reversal of ocular dominance seen. Moreover, the period of binocular recovery after the period of reverse occlusion (starting from approximately P54), is still well within the critical period.

The effects of RO paradigms on the cortex and recovery from them

After the period of RO a complete reversal of ocular dominance to favour the originally deprived eye, was seen in all 3 rearing paradigms (values for both hemispheres - 15.8%, 16.6%, and 21.2% for RO, 4DBV and 4Ddecorr animals respectively). This reversal is in agreement with previous single-cell recordings and acuity data (Blakemore and Van Sluyters 1974; Movshon 1976; Van Sluyters 1978;

Murphy and Mitchell 1986). Animals with 4 days de-correlated vision showed a lesser reverse shift than the other animals, with their OD shift being least in the contralateral hemisphere to the recently deprived eye (ONDE). It is tempting to speculate that, as seen in Chapter 2 of this thesis, de-correlating the vision between the two eyes served to protect the cortex to some extent against the effect of deprivation. The cortical representation of the DE (23.8% in the hemisphere contralateral to the ONDE) is slightly below that seen in strabismic + MD animals (29.5% in the hemisphere contralateral to the DE). However, the protective effect of the strabismus described in chapter 1 related to a 'normal' cortex. Here, the cortex is already dominated by one eye, although the prevalence of monocular cells (regardless of which eye is dominant) in MD and strabismic animals would be similar. Secondly, as shown by Kind *et al* (2002), recovery after MD is disrupted by strabismus. In the paradigm used here, artificially de-correlating the inputs would be expected to disrupt recovery also. However, any initial delay in recovery of the ODE should be insignificant given the long period that the other eye is closed for during RO. Most importantly, statistically there is no difference in eye territories between any of the 3 paradigms ($P=0.49$ ANOVA) immediately after the termination of the period of RO. Despite this, in the light of results in Chapter 2 in this thesis, a reduced cortical shift as a direct result of de-correlated vision (in 4Ddecorr animals) should not be totally discounted. From the limited number of animals used in the 4Ddecorr group, such a conclusion could only be substantiated with a much larger group of animals.

Animals that received an intermediate 4-day period of correlated vision showed a slightly delayed (in the contralateral hemisphere to the ONDE) but complete recovery of ONDE territory (after extended recovery). Final values of 62% ($\pm 1.7\%$) and 49% ($\pm 7.8\%$) for 4DBV animals) were very similar to recovery seen in normal animals after deprivation. After extended recovery, the ONDE of 4DBV animals occupied significantly greater ($P=0.03$, ANOVA) cortical territory in the contralateral hemisphere to the ONDE, compared to the other 2 groups.

Relative orientation selectivity after the period of RO in all 3 paradigms was 0.52-0.58 (ONDE:ODE). This range appears to be higher than that of MD animals in this thesis of 0.38-0.4 (see Chapter 2). However, this ratio does not relate the ONDE to a 'normal eye' (that would be the case in MD only animals) but a previously deprived

eye; so it cannot necessarily be assumed that the ODE has achieved 'normal' selectivity. If the OSI of the ODE is lower than normal anyway, one would expect the ratio of ONDE:ODE to be higher than MD: normal selectivity. Despite this, Antonini *et al* (1998) showed that orientation specificity of the ODE, after RO, was consistent with the functional recovery seen by Kim and Bonhoeffer (1994) suggesting that functional recovery of oriented responses through the ODE was substantial immediately after RO. This finding can not be quantified here since the selectivity of individual cells after the initial MD and immediately after RO were not recorded at this point in time. Moreover such subtleties from OI maps are difficult to pinpoint. However, qualitative assessment of ODE orientation maps immediately after RO, in many animals, suggest substantial recovery of orientation selectivity (see Fig 2.3B). It is potentially problematic to speculate that RO had a less detrimental effect on orientation selectivity than MD (although morphologically this appears to be the case), a result suggested by Antonini *et al* (1998). Orientation selectivity of cortical maps (in this study) for the ONDE generally showed a delayed recovery after RO and it was not until after an extended period of binocular vision that complete recovery was seen. It could be possible that the OND eye's pathway may not be as impoverished by competition from a strong pathway serving the other eye, because the other (OD) eye's pathway is itself largely impoverished at the outset of the reverse suture (Antonini *et al* 1998).

So why does the ONDE fail to regain cortical territory in some of the paradigms after binocular recovery?

One obvious explanation would be the development of a strabismus during deprivation. A strabismus following monocular or binocular deprivation in kittens has been reported in some cases before (Sherman 1972; Blake *et al* 1974; Olson and Freeman 1978; Cynader 1979; Kaye *et al* 1982; Mitchell 1988). An early strabismus may have resulted from the initial deprivation and gone unnoticed since upon the opening of the DE, the open eye was sutured shut, and hence comparisons between both eyes were not possible. Alternatively, late strabismus onset in the ONDE upon termination of reverse occlusion would result in de-correlated vision through both eyes, and therefore disrupted recovery (Kind *et al* 2002). However, this is unlikely to provide the answer here, since the likelihood of a spontaneous strabismus to occur should have been identical in the three groups of animals in this study (see also

Chapter 2). All animals in this study were deprived for the same length of time and therefore a similar lack of recovery of the ONDE in all 3 paradigms would have been expected; this was not observed. A second point that makes strabismus an unlikely explanation lies in electrophysiological recordings from kittens in all three paradigms, after extended recovery. Murphy and Mitchell (1986) found a binocularity index (BI) of approximately 65 in animals after recovery from RO - comparable to a normal adult cortex (BI of 100 means all cells being equally activated through both eyes). A BI of approximately 50 was obtained here for all three paradigms. This is below the value of Murphy and Mitchell (1986), suggesting a more monocular cortex than normal, however there was no difference ($P > 0.05$ 2-tailed t-test) in the binocularity index between the three paradigms. A strabismus would result in a predominantly monocular cortex, hence a much lower BI, in the affected group (see also Chapter 2). The relatively low BI in all three groups likely reflects the way recording sites were chosen based on optical imaging maps of OD (patches of strong eye dominance from optical maps were chosen to target electrode penetrations as opposed to a random selection of electrode positioning). Therefore, a strabismus cannot account for the lack of recovery of the ONDE seen in two of the 3 RO paradigms.

Anatomical considerations

The anatomical effects of monocular deprivation (lasting at least 7 days) include the substantial loss of geniculocortical terminals serving the deprived eye in layer IV (Hubel *et al* 1977; Shatz and Stryker 1978; LeVay *et al* 1980; Antonini and Stryker 1993, 1996). Expansion of NDE terminals is seen only if deprivation is of several weeks duration (LeVay *et al* 1980; Antonini and Stryker 1993, 1996). Therefore, not only do anatomical changes to MD take longer than physiological responses (loss of responses saturate within 2-4 days of MD – Movshon and Durstler 1977; Freeman *et al* 1981; Crair *et al* 1997), but the loss of DE arbours occurs before the expansion of the NDE. Hence, after the extended period of MD used here (P14-P35), loss of DE terminals and expansion of NDE terminals should be extensive. The cortex, by this time should be almost completely dominated (physiologically and anatomically) by the NDE.

However, the anatomical restructuring after RO does not appear to have the same detrimental effect on arbour morphology as MD. After RO of 10 days, ONDE arbours

are larger and more complex than DE arbours after a similar period of MD. Some re-growth of ODE arbours occurs during the RO period, but this is not widespread (Antonini *et al* 1998). Physiological recordings in the same study confirmed that largely, reversal of ocular dominance had occurred after RO yet responses through the ONDE remained much more selective to orientation than the ODE after the initial period of monocular deprivation (Antonini *et al* 1998, also Crair *et al* 1997). This could be due to different functional connections forming during the initial monocular deprivation and the reverse occlusion. It has been suggested that terminals from the initially non-deprived eye do not retract during the period of reverse occlusion (as shown by Antonini *et al* (1998), but instead are rendered ineffective by synaptic suppression or interocular inhibition (Blakemore *et al* 1982; Kratz *et al* 1976 - in Mitchell *et al* 1984). However, evidence for this, as yet, is limited (see Sillito *et al* 1981).

Antonini *et al* (1998) showed only localised re-growth of ODE axonal arbours, after a period of RO of 10-11 days. The RO period used in the present study was approximately 18 days. It is likely that this extended period allowed ODE arbours to re-grow more completely. This could account for the physiological bias towards that eye seen in this study. The ONDE has been shown to retain some responses despite deprivation after RO, in contrast to ordinary MD. Also its arbours are larger after RO than DE arbours are after MD (Antonini *et al* 1998). This is likely to explain the responses through the ONDE upon reopening as well as the improvement seen over time in terms of both OD and OSI. Nevertheless, the cortex would remain dominated anatomically (and hence physiologically) by the ODE. Movshon (1976) who found differences in the relative sizes of OD columns between the two eyes of reverse sutured kittens backs up this idea. While the columns devoted to the ODE were small in animals reverse sutured for short periods (3 days) in those that underwent longer periods of reverse occlusion (63 days), the columns of the ODE were larger and the ONDE columns were smaller.

One would expect that an interim period of binocular vision could allow some (in 4Ddecor) or substantial (in 4DBV) physiological recovery of the DE. However, 4 days is insufficient time for any significant morphological changes to occur, reducing any advantage that correlated vision would afford over animals that had no such experience. Second to this, if any morphological changes did occur during the 4 day

period (i.e. decrease of NDE arbours and increase in DE arbours), one would expect that their effect would only be accentuated when RO was initiated. Therefore, after 18 days of RO, animals in all 3 paradigms should be in a similar morphological state, hence recovery from RO should be similar. However, this argument ignores the possibility that the physiological changes during the 4-day period set in motion events that result in later morphological changes. For example, during the binocular phase of rearing, some common binocular connections could begin to form during the 4DBV and continue to do so even during the first few days of RO, where normally the only changes that would occur would be the weakening of ONDE responses. Conversely, it could be that the intermediate binocular period reduced the anatomical re-arrangement during the RO period so that the arbours for two eyes ended up with more overlap and would be more balanced in their numbers after RO, than that seen with immediate RO.

In short, the lack of complete physiological recovery of cortical territory by the ONDE seen in RO animals could in part be explained by the extensive re-innervation of V1 by the ODE during the relatively long period of RO, resulting in larger OD columns compared to the ONDE. However, the differences between the three groups are difficult to account for on those grounds.

One postulation here is that the substrate for re-acquisition of normal responses through the ODE may not be just the re-establishment of connectivity that was present before deprivation. Intracortical circuitry may be more stable than the thalamocortical input and may be able to organise and maintain strong and selective responses even when the input becomes impoverished (Antonini *et al* 1998). Strong responses to weak input could be generated by an imbalance of reciprocal inhibitory input among cortical neurones located on different OD columns (Sengpiel *et al* 1994). A small advantage of the (anatomical) ODE pathway might be enhanced and increase its cortical representation. As yet this remains conjecture in the scenario presented here.

Gross anatomical correlates cannot easily explain differences in recovery between animals that did and those that did not receive an intermediate period of binocular vision, since after 18 days of RO all animals would be expected to be similar in that respect. However more subtle features like differences in spine shape between rearing paradigms cannot be ruled out. So the question remains why lack of common or

correlated vision between the two eyes before the end of RO leads to lack of recovery of the ONDE. An exploration of physiological parameters might provide the answer.

Physiological considerations

The importance of binocular visual experience in recovery of the DE (after MD) has been highlighted in a number of studies (Mitchell and Gingras 1998; Mitchell *et al* 2003; Kind *et al* 2002; Mitchell *et al* 2001; Murphy *et al* 2002; Liao *et al* 2004).

The extent and rate of recovery of the DE appears to be highly dependent on the duration of the deprivation. Recovery of the DE can occur only if vision is restored early enough. After short-term MD (of a few days), recovery of DE responses is swift, binocularity returns and receptive field properties are very similar through both eyes (Movshon 1976). However, after long-term MD (a number of weeks), although some recovery of DE responses is observed, these are abnormal, and binocular receptive fields are mismatched (Movshon 1976). Extended binocular vision, after early and long-term MD, does not completely abolish the cortical bias towards the DE (Olson and Freeman 1978; Van Sluyters 1978). With long-term MD from near eye opening the DE is visually naïve – that is, the DE ‘signature’ is not normal, hence may not be able to acquire normal visual properties later on in development. This last point is quite important; particularly in light of the lack of substantial recovery of cortical binocularity and orientation selectivity of cells, in ferrets that never received normal vision from birth (Liao *et al* 2004). Even binocular visual experience lasting 24 days did not allow complete recovery from early MD. This finding can in part be confirmed here with the one animal that was imaged after 4DBV with a preceding early onset MD. Recovery of ODE ocular dominance was substantial after 4DBV, yet not as complete as in late onset MD that was complete after 3 days (Chapter 2 figure 2.5 and 2.6). More noticeable was the minimal recovery of orientation selectivity in the animal with early MD (Fig. 3.5c).

The effects of RO and recovery from it, on a predominantly binocular cortex (i.e. after an intermediate period of binocular vision) would be different from that on a predominantly monocular cortex (i.e. with immediate RO). With RO and 4Ddecor animals, at no point have both eyes received correlated (common) input hence, few binocular connections could have been made and a cortex with two distinct cell populations (one for each eye) would have developed. When both eyes are open after

RO, one would predict that the cortex will remain predominantly monocular (i.e. cell populations for both eyes will remain separate). Little ocular dominance change would be expected, as each cell population would remain independent hence recovery of the DE would be minimal. Physiological recovery after an intermediate period of 4 days of binocular vision would be substantial if not complete through the ODE. As shown in Chapter 2, 3-5 days of binocular vision lead to a complete recovery of DE responses in animals deprived from P35. But what about animals deprived much earlier than that? Substantial recovery of OD from early MD was also verified in one animal in which optical imaging was carried out at the end of the first period of MD and again after 4 days of binocular vision (Fig. 3.5c). After 4 days of binocular vision, good but not complete recovery by the DE is seen. Despite this, orientation selectivity of the ODE showed minimal recovery during this time (Fig. 3.5c). The lack of substantial recovery of orientation selectivity presents a possible dichotomy in the plasticity of OD and orientation selectivity in recovery. Undoubtedly the effects of a further period of MD on a cortex with a comparatively normal physiological OD distribution (after 4 days BV) would be far different than that on an almost entirely monocular cortex (in the case of immediate RO). However, it is clear from this one animal and data from Liao *et al* 2004 that the cortex is far from 'normal' after binocular recovery from early MD.

During recovery from RO, one would expect that binocularity could return more readily (in 4DBV animals) since a large number of binocular connections would have been present previously during the 4DBV period. As shown here, recovery of the recently deprived eye (ONDE) in 4DBV animals takes a little longer than in MD only animals, possibly due to RO animals being slightly older, but is complete no less (slight bias towards the ONDE in ipsilateral hemisphere to the DE), supporting this hypothesis.

If the above argument was to stand, one would expect a relatively high binocularity index (BI) for 4DBV animals, as reported in the literature for animals with a similar rearing paradigm (BI ~ 65 in Murphy and Mitchell; 1986). Conversely, the BI for the other 2 rearing paradigms (RO and 4Ddecor) should be much lower (i.e. 30-35 as seen in Chapter 2 for strabismic animals). However, the BI for all 3 RO paradigms was very similar (~ 50). Although this is lower than in normal animals in this thesis (~ 60), V1 was not as predominantly monocular in RO and 4Ddecor animals as predicted. Invariably some sampling bias might have occurred. Equal numbers of ocular

dominance patches for each eye were targeted for electrode penetrations during single cell recording. On the one hand this ensured that roughly equal numbers of cells responding to ODE and ONDE were explored. In particular this allowed for an accurate measure of half height at half width tuning for both eyes that could only be achieved with sufficient numbers of cells. This method of targeting penetrations could introduce a bias that would not have been present had the penetrations been placed randomly in V1. Most importantly however, the darkest and lightest regions from functional images were targeted for single unit recording. Therefore, binocular cells (most frequent in the grey regions of the images) would probably have been under-sampled. This is likely to explain to a large extent at least, why the BI results were more or less the same for all 3 groups.

Another interesting point to come out of the single cell data is that tuning widths of cells between the two eyes show some subtle differences between paradigms. While the half width half height (hw_{hh}) of cells in each eye were similar in animals with 4DBV (recorded after binocular recovery), in those from animals with no intermediate binocular vision (RO, 4Ddecorr): the ODE tuning was significantly broader than that of the ONDE. Such a result correlates well with decrease in visual acuity in the ODE, over the experimental period, in animals with 4 days of de-correlated vision. This may initially seem like a contradiction since in these two cases, the ODE dominated the cortex. However, such a result does again highlight the importance of binocular vision; without it, an incorrect or abnormal pattern of connectivity may form, leading to abnormal cortical responses.

Work by Kim and Bonhoeffer (1994) and Godecke and Bonhoeffer (1996) suggests that orientation selectivity and the organisation of orientation preferences into a cortical map is to some extent predetermined rather than acquired. This suggestion is enhanced by the knowledge that despite the innervation of layer IV by LGN axons around the time of birth, it is not until P14 that functional and anatomical OD columns emerge (Crair *et al* 2001). However, earlier than that, orientation selective cells can be detected (Hubel and Wiesel 1962; Blakemore and Van Sluyters 1975; Fregnac and Imbert 1978; Albus and Wolf 1984). By the time OD columns become functionally visible (via optical imaging), orientation maps that match between both eyes are present (Crair *et al* 1998). Also apparent is that the effect of visual experience on cortical orientation maps is weaker than previously thought (see Godecke and

Bonhoeffer 1996; Antonini *et al* 1998). However, somewhat in contrast, it appears that OD plasticity is more pronounced than orientation map plasticity. This makes logical sense since orientation preference is far more important to the perception of the visual environment than which eye sees it. Moreover, orientation selectivity once established does not necessarily need to be plastic, since the orientation content of the 'natural' environment would not normally change. However, binocular integration does need to be plastic due to the developmental changes in eye alignment (kittens eyes are initially divergent) and development of stereopsis.

Behavioural considerations

The differences in physiological results from the three RO paradigms (i.e. the lack of recovery of the ONDE in RO and 4Ddecorr animals) could be related to different outcomes in terms of visual acuity. A link between the change in ocular dominance during RO and the speed of recovery of DE acuity has been made (Giffin and Mitchell 1978), such that the rate of reversal of the physiological effects of monocular deprivation were comparable with the behavioural recovery in animals reversed under similar circumstances. However, since visual acuity involves the measurement of a psychophysical spatial frequency threshold, it may depend more on the spatial resolution of (a subset of) V1 neurones than their total number (Mitchell *et al* 1977; Murphy and Mitchell 1986).

Changes in visual acuity during binocular recovery, in animals with 4 days of de-correlated vision, does in part match changes in functional maps shown here and changes in behavioural acuity described in the literature (Murphy *et al* 2002). Here, despite the acuity in the ODE being good (2.7 ± 0.1 cyc/deg) upon termination of RO, it decreased quickly upon restoration of vision to both eyes. Some recovery of ONDE acuity upon restoration of binocular vision occurred, yet it was not to a level seen in the ODE upon termination of RO, or to a level seen in either eye in MD recovery animals, which could be considered close to 'normal' for this type of acuity measurement (also see Chapter 2). Acuity in both eyes finished at an intermediate level (1.6-1.85 cyc/deg). The lack of a full recovery of the ONDE and loss of acuity in the ODE is similar to that shown by Murphy *et al* (2002) in animals tested behaviourally with the same rearing paradigm. That study showed a similar detrimental effect on acuity in both eyes in RO and animals with an intermediate

period of de-correlated vision. Conversely, those having received an intermediate period of BV regained good acuity in the recently deprived eye (ONDE), relative to those animals without intermediate vision, while maintaining high acuity in the ODE. Given the similarity in the trend of results between VEP recordings presented here and the behavioural acuity measurements by Murphy *et al* (2002), one would expect that RO animals with no intermediate period of binocular vision would show similarly poor acuity in both eyes. Those that received 4DBV would have better acuity in both eyes. Unfortunately, the VEP recording software was not yet available at the time when those animals were tested.

Many attempts have been made to explain the outcome of behavioural acuity tests after RO. Strabismus has been suggested as a possible explanation for the bilateral amblyopia after RO (Mitchell *et al* 1984; Murphy and Mitchell 1986, 1987; Mitchell 1991), but this has been discounted due to comparatively normal OD distribution of single cells (Murphy and Mitchell 1986). The mechanisms that underlie the formation of functional intracortical neural connections could be fundamentally different from those that permit the ocular dominance changes during early deprivation, i.e. afferents from the two eyes.

Expansion of the projections from the ODE (LeVay *et al* 1980; Swindale *et al* 1981) and LGN cells receiving input from the initially non-deprived eye remain hypertrophied, in monkeys during RO (Sloper *et al* 1984). This led Murphy *et al* (1986, 1987) to speculate that overly exuberant projections to the visual cortex from both eyes could lead to larger receptive fields and overlapping OD columns (hence the apparently binocular cortex after recovery from RO) resulting in a smearing of cortical retinotopic map. Despite this the anatomical state of the cortex and LGN with respect to *both* eyes after such an extended period of RO (as used here), has yet to be studied in any detail. Therefore Murphy's hypothesis remains to be tested.

An important link between cortical physiology and visual acuity is suggested by the results in this chapter, concerning the tuning width of ODE-dominated cells compared to ONDE-dominated cells after recovery from immediate RO. As mentioned above, in those animals that did not receive an intermediate period of binocular vision, the acuity of the ODE decrease dramatically after binocular vision was introduced (coupled with only a moderate increase in OND acuity). Moreover, the tuning width

of the ODE after recovery was significantly broader than that of the ONDE. A broad tuning of cells could in part underlie the poor acuity seen in the ODE, especially considering that the behavioural test of visual acuity entails an orientation discrimination task.

NMDA receptors and LTP

Considerable speculation has focused on the role of synaptic mechanisms in the cortex that are similar to LTP and LTD in the hippocampus. N-methyl D-aspartate (NMDA) receptor activation has been suggested as a prerequisite for the induction of experience dependent modification of neuronal responses in V1 during the critical period (Fox *et al* 1989).

For example, blockage of NMDA receptors during the critical period disrupts the normal cortical changes during monocular deprivation (Bear *et al* 1987, 1990; Kleinschmidt *et al* 1987; Daw 1994), reverse suturing (Gu *et al* 1989), recovery after dark rearing (Bear *et al* 1990), and disruption of orientation selectivity development (Kleinschmidt *et al* 1987). One of the two main subunits of NMDA receptors, NR2, has one of two forms, NR2A or NR2B. At birth, the subunit NR2B is highly expressed. Over the next few weeks a rise in NR2A is seen. The change in ratios between NR2A and NR2B is delayed during dark rearing NR2A is rapidly upregulated when the animals are then exposed to light. These sub-unit changes correlate well with the critical period, with dark rearing prolonging the closure of the critical period and the NR2B to NR2A switch (Nase *et al* 1999; Quinlan *et al* 1999; Quinlan *et al* 1999b). These findings, coupled with NMDA receptor density being high in V1 at the peak of the critical period (Bode-Greuel and Singer 1989; Reynolds and Bear 1991), have led to the postulation that one possible mechanism underlying activity dependent plasticity is NMDA-dependent LTP (Komatsu *et al* 1981; Artola and Singer 1987; Bear *et al* 1992; Kirkwood *et al* 1995, 1996), or 'metaplasticity'.

In kitten visual cortex, a number of features are arranged in a patchy manner, including horizontal connections (Callaway and Katz 1990), synaptic zinc and neurotransmitter-related molecules like serotonin (Dyck and Cynader 1993). Trepel and colleagues (1998) found a transiently patchy distribution of NMDA receptor 1(NMDAR1) sub-unit in kitten V1. Monocular deprivation prevented the expression of NMDAR1 patches, but just 4 days of subsequent binocular vision was sufficient to

express NMDAR1 patches. In addition the patches had spacing comparable to the width of one eye's OD columns and were located on the border of the OD columns.

Could NMDA receptors play a role in ocular dominance plasticity?

The laminae that NMDAR1 patches appear in (lamina II-III) at 2 weeks of age, are ones that never receives direct thalamic input (Shatz and Luskin 1986, see also Murphy *et al* 1996). This suggests that these patches may not be directly driven by geniculocortical inputs but are part of an intrinsic organisation within the cortex and their arrangement may act as a blueprint for developing synapses (Durand *et al* 1996). The idea that changes in NMDA receptors govern changes during experience dependent plasticity is furthered by a delicate experiment by Czepita and Daw (1996). Kittens were monocularly deprived for brief periods (1-5.5 days) to give a partial shift in ocular dominance. Cell responses were measured through each eye when the NMDA antagonist APV was applied by iontophoresis to the cortex. APV reduced background activity to a greater extent in the normal eye compared to the deprived eye. In other words, the contribution of NMDA receptors in the deprived eye was reduced compared to the normal eye. This could represent a reduction of NMDA receptors in the deprived eye pathway. Since the deprivation period was shorter than could be expected for gross anatomical changes to occur, it is more likely that the change in NMDA receptor expression leads to changes in afferent morphology rather than gross anatomical changes.

Cline and Constantine-Paton (1990) conducted a detailed study of NMDA receptor antagonists and agonists on retinal ganglion cell morphology in frog retinotectal projection. NMDA treatment of the optic tectum resulted in increased eye specific segregation, reduced arbour branch points or branch tips and reduced arbour density. In mammals, segregation of terminal arbours into eye specific zones requires retinal cell activity (see Shatz and Stryker 1988). Retinal activity is also required for the establishment and maintenance of topographic projections in the retinotectal system of frogs (Reh and Constantine-Paton 1985). Implanting an additional eye primordium into the forebrain region can induce a striped pattern of eye specific afferent segregation. Afferent segregation occurs whenever retinal ganglion cells from the normal and 'extra' eye attempt to establish synapses in the same region of the optic tectum. This manipulation in the frog makes for a valuable and robust model under a variety of experimental manipulations (see Reh and Constantine-Paton 1985). Based on their findings Cline and Constantine-Paton (1990) proposed a model to explain

NMDA receptor involvement in activity-dependent refinement of developing connections. Activation of NMDA receptors occurs when pre and post-synaptic activity occurs simultaneously (see Bliss and Collingridge 1993), which leads to synaptic stabilisation, survival of co-active axon arbours and restriction of new arbours. Regions that have more NMDA receptors would have a greater probability of initiating synapse stabilisation and axon restriction. The regions of binocular overlap in cat V1 are primarily near OD column borders (Hata and Stryker 1994) where NMDAR1 patches are generally found (Trepel *et al* 1998).

From the model of Cline and Constatine-Paton (1990) one could speculate that; in those animals that had received no binocular vision prior to RO (i.e. RO and 4Ddecorr), since the two eyes had never received correlated vision throughout the critical period, binocularity should be low and NMDA activation should also be low from the outset (as opposed to normal expression levels present under binocular rearing). Lower NMDA receptor activation means a lower probability of initiating synapse stabilisation and axon restriction. In this case, for the ONDE, increased branch initiation, but not stabilisation would occur. In short, many new branches would form, but they would remain weak. An immature and weak network of connections would develop for the initially open eye (ONDE), which would collapse completely when it is closed during RO. In contrast, connections through the initially closed eye (ODE) would form an sparse yet robust set of connections based on an intrinsic set of signals present before experience dependent plasticity starts. Although a similar scenario of increased branch initiation is predicted to occur for the initially closed eye during RO, due to low NMDA activation the new pattern of connections will not stabilise and the basic set of connections would remain. When binocular vision is eventually introduced, NMDA activation remains below normal, so little or no stabilisation or LTP occurs. Therefore the sparse, yet robust set of connections of the ODE will win over weak connections through the ONDE.

In contrast, in 4DBV animals, the period of binocular vision would increase NMDA activation through both eyes. This would lead to selective stabilisation of synapses, but only at the sites where correlated activity is present. A common set of connections for both eyes would begin to form, which would not be completely lost during the period of RO. During recovery from RO, the ONDE can use the pattern of connectivity established during the 4DBV to re-establish functional connections and

subsequently cortical territory. Such a postulation is easier to reconcile in this instance since there is more experimental evidence for the above hypothetical sequence of events (during 4DBV) than that proposed for recovery from immediate RO.

Although no *direct* link between NMDA activation and NMDA receptor expression can be assumed, the above postulations do have some anatomical basis with the levels of NMDA receptor expression and experience dependent activity levels through both eyes.

Expression of NMDAR1 is prevented by early MD, but just 4 days of binocular vision results in receptor expression similar to normal reared kittens (Trepel *et al* 1998; Murphy *et al* 2002). Such a result could also account for the underlying recovery of the ODE and stabilisation of ONDE afferents during the intermediate period of vision in 4DBV animals. Moreover, NMDAR1 expression could help set-up a normal 'binocular' distribution of OD columns during this period, with a segregation pattern comparable to normal animals of the same age. When RO is introduced, sufficient levels of NMDA receptors are retained (compared to straight RO). When binocular recovery vision is finally introduced, cortical (and LGN – see Fava *et al* 1999) NMDA receptor expression (and possibly NMDA activation) increases. Since LTP appears to be dependent on NMDA receptor activation (Kirkwood and Bear 1994, Kato *et al* 1991), the ONDE would recover fully.

Different mechanisms for loss and recovery of cortical binocularity

One final point remains to be explored. That is, the mechanisms for the loss and recovery of binocularity in the visual cortex appear to be fundamentally different. This fact is particularly poignant with respect to the RO period, where a binocular state is never achieved, unlike in recovery from MD, where binocularity returns as NDE responses decrease slightly, followed by a relatively large increase in DE responses. The only time where responses through both eyes are similar for a brief period (during RO) is when the responses through the ONDE have decreased to a low level, similar to that of the ODE, and before the ODE responses start to increase (see Clothiaux *et al* 1991).

Although NMDA receptors are thought to be involved in both loss and recovery of responsiveness (Gu *et al* 1989; Bear *et al* 1990), neurotrophins also have a major role. Calcium influx through NMDA receptor associated channels, activates protein kinases

such as; calcium calmodium kinase type II (see Taha *et al* 2002). A common mechanism through which such a kinase might be involved in ocular dominance plasticity is through the phosphorylation of the Ca²⁺ response binding element protein (CREB), which in turn regulates the transcription of plasticity-related genes (Deisseroth *et al* 1996; Finkbeiner *et al* 1997). A recent study by Liao *et al* (2002) demonstrated that CREB activity *is* required for the loss of deprived eye responses in MD and RO (see also Mower *et al* 2002) but *is not* required for the recovery of DE responses. In contrast, the proteolytic cascade controlled by tissue plasminogen activator (tPA) appears to be involved in reverse-occlusion-induced cortical plasticity, but not monocular deprivation-induced plasticity (Müller & Griesinger 1998). Mice lacking tPA show normal induction of LTP but show some deficits in LTP maintenance – so called late-phase LTP (Huang *et al* 1996). Late phase LTP requires protein synthesis, and possibly involves structural changes such as addition of synapses (see Geinisman *et al* 1996; Bolshakov *et al* 1997). Therefore, tPA could be involved in later synaptic changes that occur downstream from the induction step (Muller and Griesinger 1998). Evidence from sensitisation in *Aplysia* (Bailey *et al* 1992), LTP in hippocampus (Engert and Bonhoeffer 1999), and memory function in chicks (Rose and Stewart 1999), suggest that protein synthesis is required for structural changes that underlie ‘late’ stages of plasticity. However, suppression of cortical but not geniculate protein synthesis impaired ‘rapid’- electrophysiological OD plasticity, while leaving neuronal responses intact (Taha and Stryker 2002). Further to this, rapid anatomical changes in corticocortical connections in the cat are apparent in only 2 days of strabismus (Trachenberg and Stryker 2001). Very recently Krahe *et al* (neuro abst 2004) have suggested that recovery from the effects of brief MD does not require new protein synthesis.

This final discussion highlights the dichotomy of mechanisms for loss and binocular recovery of deprived eye responses during deprivation and potentially differing mechanisms governing change during MD and RO. Despite some overlap in data from different parameters: anatomical, physiological, behavioural, VEP, electrophysiological and molecular, no one theory or model can unite them or even explain the differences between the three paradigms tested here. It is perhaps too simplistic to try to link one neuronal mechanism to the effects of MD or RO. For the

moment however, NMDA function and distribution, including a whole downstream cascade of transcription events that lead to protein synthesis, are at the forefront of understanding plasticity in the visual cortex.

CHAPTER 4

INTRODUCTION

From the literature already cited in this study, it is generally accepted that the visual environment drastically influences orientation selectivity and ocular dominance of receptive fields in the visual cortex (of cats). Many theories have attempted to explain how receptive fields evolve (von der Malsburg 1973; Nass and Cooper 1975; Perez *et al* 1975; Sejnowski 1977; Bienenstock *et al* 1982; Linsker 1986; Miller 1994) and to account for the experience dependent modifications seen. Modification in this instance relates to the change in efficacy of a synapse at an individual neurone. Such changes (modifications) have been described in detail and two main sets of theories have arisen. The first entails competition between inputs (heterosynaptic) for a limiting factor (i.e. neurotrophin) in the spatial domain. Alternatively, associative mechanisms have been invoked, such as those represented by the BCM theory (homosynaptic), where patterns of input activity compete in the temporal domain. These two main learning rules are characterised by their method of stabilisation, which are discussed below (weight decay for the heterosynaptic class and a sliding threshold for the homosynaptic class).

Model neurone

A model neurone integrates electrical activity (the variables) on a spatial scale i.e. the output of the cell is a function (average) of the geniculocortical inputs and the synaptic weights (efficacy/threshold of the neurone) at time t .

In other words, the model neurone can be described by a vector of inputs, \mathbf{d} , a vector of synaptic efficacies or weights, \mathbf{m} , and a scalar output (post-synaptic activity), c which is a function (f) of the product of inputs and synaptic weights (Equ. 1). The values of the inputs represent (an averaged) pre-synaptic activity originating from either geniculate neurones or other cortical cells.

The output is given by:

$$c = f(\mathbf{d} \cdot \mathbf{m}) \quad (1)$$

(adapted From Blais 1998).

It can be assumed that the output, c , has a region of linear dependence due to the simple nature of the inputs. However, there must be maximum and minimum constraints on the output. When there is no input to a cell, neurones do not have zero output. The residual output at zero input is spontaneous activity. Therefore, for the variables, c (output), and \mathbf{d} (input) any positive value for either can be assumed to be above spontaneous activity. Inversely, it can be assumed that there can be (negative) activity below the level of spontaneous activity, although this needs to be restricted, as a cell's activity can not be as far below spontaneous activity as to be negative (Fig. 4.1). Therefore the output, c , is a non-linear sigmoid of $\mathbf{d}\cdot\mathbf{m}$ ($\sigma\mathbf{d}\cdot\mathbf{m}$).

Learning rules

All learning rules are based on Hebb's rule:

'When an axon in cell A excites cell B and repeatedly or persistently takes part in firing it, some growth processes or metabolic changes take place between one or both cells, so that A's efficiency as one of the cells firing B is increased' (Hebb 1949).

Mathematically, **heterosynaptic** synaptic modification can be expressed in the form:

$$\mathbf{dm}/dt = f(c)\mathbf{d} - g(c)\mathbf{m} \quad (2)$$

(Blais *et al* 1999)

Where \mathbf{m} is the vector of synaptic weights, \mathbf{d} is the pre-synaptic activity and c is the post-synaptic activity of the cell, and $f(c)$ and $g(c)$ are functions of the post-synaptic activity. This basic form of the equation (2) includes most Hebb-like rules.

Synaptic strengthening and weakening must be constrained to some extent. If synaptic strengthening went unchecked, all synapses would eventually saturate and no selectivity would develop. Or worse still, excitation would cause positive feedback leading to epilepsy and excitotoxicity. Within Hebb's rule, synaptic weights can be normalised to stabilise the weight growth. One way this problem was solved

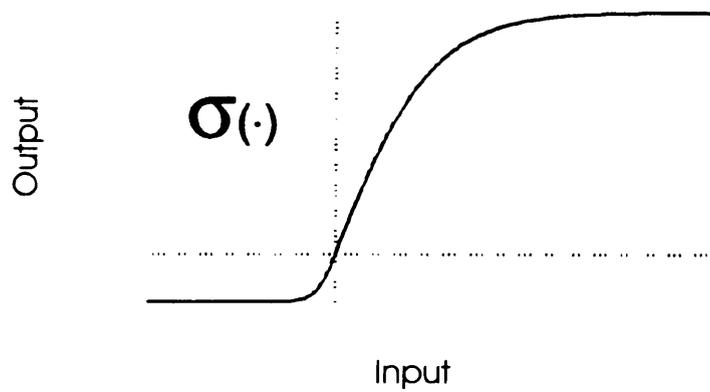


Figure 4.1 The sigmoid function of a model neurons (Blais 1998)

A neurons consists of a vector of inputs, \mathbf{x} , vector of synaptic weights, \mathbf{w} , and a scalar output, y . With no input, neurons still have spontaneous activity. By making y a non-linear sigmoid of $\mathbf{w}\cdot\mathbf{x}$, realistic values of cell activity can be achieved for above zero and just below zero. Output values above zero are easily achieved when the cell is active (linear part of curve). The lowest negative value of the sigmoid is smaller than the highest positive value as a cell cannot have activity as far below spontaneous as it can above.

(discussed later) was by allowing the weights to decay over time (Oja 1982), with the decay being stronger the stronger synaptic weights are:

$$dm/dt = cd - c^2m \quad (3)$$

(adapted from Blais 1999)

This above equation (3), is a general form of a stabilised Hebb rule (Oja 1982) which is very similar to the multivariate statistical technique PCA (principle component analysis). Principal component analysis (PCA) involves a statistical procedure that transforms a number of correlated variables into a number of un-correlated variables called *principal components*. The first principal component accounts for a majority of the variability (of the data) with each successive component accounting for as much as possible of the remaining variability. The close similarity of the heterosynaptic rule to PCA means that the heterosynaptic model of synaptic modification described hereafter will be referred to as the PCA model. The subtractive term in this equation (3) allows the increase in strength of some synapses to be accompanied by a decrease in strength in other synapses onto the same neurone. This type of synaptic stabilisation is in contrast to the **homosynaptic** modification (BCM rule) proposed by Bienenstock *et al* (1982) where synaptic stabilisation is obtained by a sliding modification threshold, which is a function of the time-averaged post-synaptic responses (4).

$$dm/dt = \phi(c, \theta_M)d \quad (4)$$

Where, ϕ is a scalar function of the post-synaptic output c , with θ_M representing the so-called modification threshold.

Originally, Nass and Cooper (1975) explored a theory where the modification of synapses was governed by purely Hebbian mechanisms - such that a change to a synapse was based upon the product of the levels of pre- and post-synaptic activity.

Stabilisation of the synaptic weights was produced by limiting modification to keep responses below a maximum. (Without this stabilisation, purely Hebbian learning continually strengthens synaptic weights without limit).

This theory was taken one step further by allowing the sign of the modification (positive or negative) to be based on whether the post-synaptic response occurred above or below a threshold θ (Cooper *et al* 1979). To stabilise the synapses the threshold was allowed to slide as a non-linear function of the recent time-averaged post-synaptic response of the cell (Bienenstock *et al* 1982). This (BCM) ‘single-cell’ theory was extended to a network of interconnected neurones which was later simplified by Cooper and Scofield (1988). They introduced a set of ‘effective synapses’, which replaced the individual connections to a neurone from all other cortical neurones with the average activity of all of the other cells in the network. From this it was shown that the evolution of geniculo- cortical synapses was similar for an individual neurone or one incorporated in a mean field network. In a mean field network the intracortical connections to the ‘*i*th’ cell in a network are replaced by a set of synaptic weights that convey to the cell the average activity of other cells in the network (Clothiaux *et al* 1991).

As mentioned already, in the BCM rule, the modification of the synapse depends on the post-synaptic response occurring above or below a sliding threshold. The threshold acts as a negative feedback. Kept stationary and the neurone would respond to all inputs that cause firing above the threshold and weights would increase indefinitely, leading to ever increasing activity. Allowing the threshold to slide allows the modification threshold to ‘catch’ up with the increase in activity. In other words, the BCM model has two stable points ($\phi = 0$) in the equation (4), when $c = 0$ and when $c = \theta_M$. These points allows the synaptic weights to become stable.

Presented above are the two main learning rules of which there are a number of variations. A brief summary of the implementation of these rules in simple systems is explored later. While detailed explanation of the rules within a system and their comparisons are beyond the scope of this thesis, some basic properties and parameters are explored below.

Other learning rules

There have been various attempts at simulating the cellular mechanisms for plasticity, with some producing ocular dominance patches (Willshaw and Malsburg 1976; Miller *et al* 1989). While some have focused on solutions to limiting synaptic strengths (Bienenstock *et al* 1982; Bear *et al*; 1987), many have focused more on the pattern of initial connectivity, activity of afferents, and lateral connectivity using correlation based models. Correlation-based models (Linsker 1986; MacKay and Miller 1994; Miller 1992; Miller *et al* 1989) follow a common set of rules based on such correlations for example; between initial input activity or correlations between left eye and right eye inputs. Correlation-based models have 4 main assumptions:

a) The environment (which governs the pattern of activity in afferents) is determined by a correlation function, C (e.g. left and right eye correlation functions). One needs to distinguish between correlation in activity between afferents serving the same eye, left or right (C^{LL} and C^{RR}), or serving different eyes (C^{LR} and C^{RL} ; Miller *et al* 1989).

b) Strict limits are placed on synaptic weights (efficacy) i.e. w_{max} (MacKay and Miller 1994; Miller 1994). If weights grow past a limit they will be kept at that maximum value.

c) The weights change in a Hebb-like fashion

d) A competition mechanism is added to match that observed in such processes as monocular deprivation (one set of synapses decrease their efficacy as another increases). Most simple Hebb-like learning rules lack a competition mechanism to control synaptic efficacies, and lack stability. This has been widely debated (MacKay and Miller 1994; Miller 1996; Abbott and Nelson 2000; Song *et al* 2000; van Rossum *et al* 2000; Rao and Sejnowski 2001; van Ooyen 2001). More recently correlation-based (Hebb) models have been refined further to show that activity-induced synaptic changes can be temporally asymmetric with respect to the timing of pre-synaptic and post-synaptic action potentials with a precision of down to tens of milliseconds (Gutig *et al* 2003).

However, despite these improvements correlation-based models still have some fundamental problems:

a) These models use second order statistics to represent the environment. In other models very basic retinal stimulation is used, such as Clothiaux *et al* (1991), producing realistic comparisons with experimental results. The two-point correlation used in correlation-based models have been shown not to be a sufficient representation of visual space (Olshausen and Field 1996).

b) Orientation selectivity in the models is not very robust.

Strictly correlation based models (like PCA rules) show inconsistencies with experimental results under binocular deprivation (neuronal selectivity is not lost: see Blais 1998) and reverse suture paradigms (deprived-eye responses start to recover long before the responses through the originally experienced, now deprived eye have decreased appreciably: see Mioche and Singer 1989).

For some of the above reasons, only the two main rules of synaptic learning, PCA and BCM are explored briefly below. In particular, how parameters such as weight decay, learning rate and the threshold averaging constant affect the behaviour of the neurone. Also how the range of each of these parameters is set based on the experimental evidence (deprivation studies) that is already known. These two main models and their variants have been incorporated into a computer model called '*Plasticity*' written by Brian Blais. This program (discussed later) was used for running simulations of the paradigms used in the core of this thesis to compare and contrast to what was observed experimentally.

Parameters of learning rules

BCM neurone

The behaviour of a BCM model neurone depends on three parameters. One, is the input value, x . Second, is the learning rate, η . Third, is the memory constant (threshold averaging constant), τ (Fig. 4.2).

PCA neurone

The behaviour of the PCA neurone is easier to analyse than the BCM neurone. This is due in part to the PCA rule depending on just a two-point correlation. Therefore, it can be described by the correlation function of the inputs and the initial conditions. Further details of parameter dependence refer to Blais (1998) and Clothiaux *et al* (1991).

I will focus on the particulars of the 'Plasticity' (Blais 1998) program that was used here.

The inputs to the cortex are patches taken from natural images that are spatially filtered, as they would be by retinal ganglion cells. In this case the LGN acts only as a relay for the signals and the receptive field properties are assumed not to change here. The images are processed with a difference of gaussians (DOG) to model the receptive fields of retinal ganglion cells (Fig. 4.3). This type of transformation is commonly used to model retinal processing of images (Law and Cooper 1994). Examples of retinal receptive fields produced by PCA and BCM learning rules are shown in figures 4.4 and 4.5.

While assumptions about the parameters used to represent the visual environment can vary, those for deprivation are quite similar between different models. While it is assumed that patterned correlated input through the two retinas will result in activity that is correlated between LGN cells dominated by the two eyes, without patterned input into the retina of one eye, activity of LGN cells dominated by the two eyes becomes independent or uncorrelated. This raises the obvious issue of what is a realistic deprived eye input. It is incorrect to assume that no patterned input from one eye would lead to absolutely no signals reaching the LGN cells. (If that were true, no synaptic input would result in no modification (in BCM model only) and no decrease in the response from the closed eye, which is clearly not the case (see Figs. 4.4, and 4.5)). Retinal and LGN cells have a level of spontaneous activity, which persists with monocular deprivation; this can be considered as (intrinsic) 'noise'. Note that abolishing *all* (including spontaneous) retinal activity by intraocular injection of tetrodotoxin, results in a lesser depression of deprived eye responses than merely closing the eye and leaving spontaneous activity intact (Rittenhouse *et al* 1999).

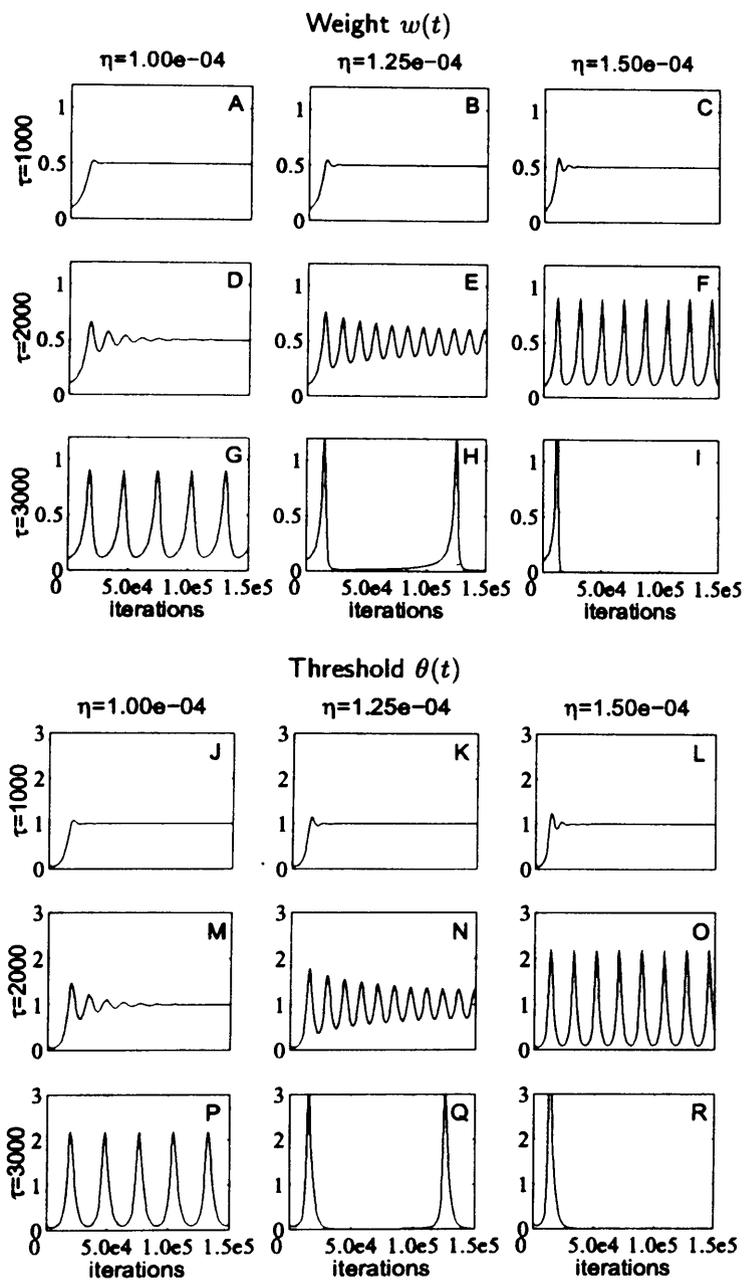


Figure 4.2 Effects of parameters on the development of the one-dimensional neurons (Blais 1998)

The value of the synaptic weight, w , and the threshold, θ , are shown as functions of time for different values of the learning rate, η , and the memory constant, τ . If the memory constant is too large relative to the learning rate, the learning rate moves too slowly relative to the change in synaptic weight. This results in the synaptic weight overshooting the fixed point until the threshold catches up again. In turn, the value of the threshold becomes larger than the output and the weights decrease. These small oscillations eventually damp out (D, E, M, N). If the memory constant is larger still, no dampening occurs and large oscillations occur (F, G, O, P).

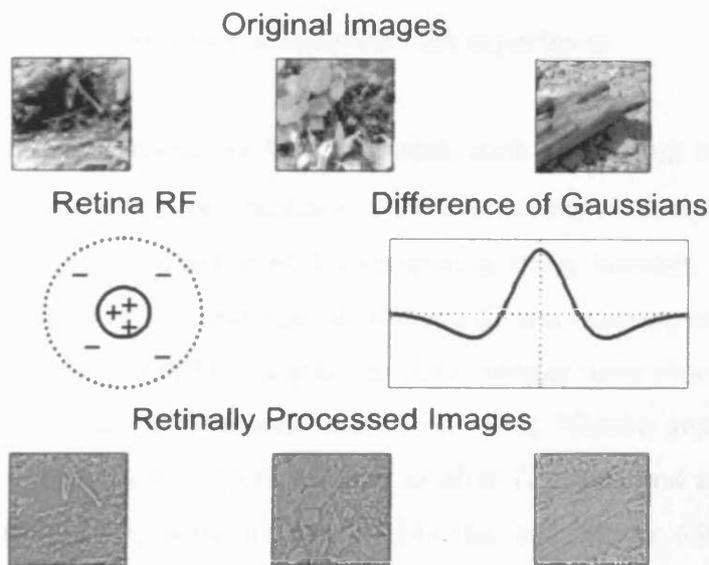


Figure 4.3 Input environment to retinally processed images (Blais 1988)

The original 'natural environment' images are processed with a difference of gaussians (DOG) filter, which is used as a model of receptive field (RF) properties of the retinal cells.

Noise affects the behaviour of a cell in the two models in different ways. In the BCM model, the more noise is present in the input from the closed eye the faster the loss of response, whereas with the PCA model the opposite occurs, the less noise in the closed-eye input the faster the loss of response (Fig. 4.6). Taking into account the above experimental data, the BCM model provides a more realistic representation of the loss of deprived eye responses than the PCA model.

Comparing simulation with experiment

In order to set realistic parameters for the models such as learning rate, η , memory constant, τ , and closed eye noise variance, σ^2 , model results must realistically match experimental results. This is achieved by comparing times between simulation and experiment, i.e. for loss of eye responses to DE in MD and recovery of newly opened eye in RO. For example, with MD, significant OD changes were observed in the DE after approximately 6 hours (Freeman and Olson 1982; Mioche and Singer 1989), substantial loss of response to the DE as early as after 12 hours, and almost complete loss occurring after 24 to 48hours hours (Mioche and Singer 1989). However, comparisons between simulations and experiment can be difficult, since the duration of an iteration in real time is not known. For example, a direct comparison, between simulation time for the loss of response to the DE and MD and the loss of response in binocular deprivation, to real experimental data (MD loss 12-24 hours: Mioche and Singer 1989; BD loss within 72 hours: Freeman *et al* 1981) would be questionable. However, indirect comparisons between ratios of change in simulation and ratios in experiment are possible, as used by Blais (1998). For example, we can compare the half rise/half fall time for the growth/decay of neuronal responses, T . In the case of MD, T^{MD} fall is ~ 6 -12hours, similar to that of T^{RS} fall (reverse suture paradigm). Simulations can then be run over a range of parameters to best match the ratios of neuronal responses (half times) in all three deprivation experiments – MD, BD and RO. Detailed discussion of such parameter dependence is not required here.

As mentioned earlier, the learning rate and memory constant are inherently inter-linked. If τ is very large, oscillations of the modification threshold will occur and synaptic weights will not converge. In turn these weight changes are governed by the

Figure 4.4 Examples of PCA simulation of various simulation paradigms
(Blais 1998)

Two left columns are the final weight configurations for each eye. Right column (graph) is the maximum response to oriented stimuli over time.

NR = normal rearing.

MD = Monocular deprivation following normal rearing.

RS = Reverse suture following MD.

BD = Binocular deprivation following normal rearing.

It should be noted that during RS, originally deprived eye responses start to increase at the same time or before those from the newly deprived eye begin to decrease. During BD selectivity **is not lost**.

Figure 4.5 Examples of BCM simulation of various simulation paradigms
(Blais 1998)

Two left columns are the final weight configurations for each eye. Right column (graph) is the maximum response to oriented stimuli over time.

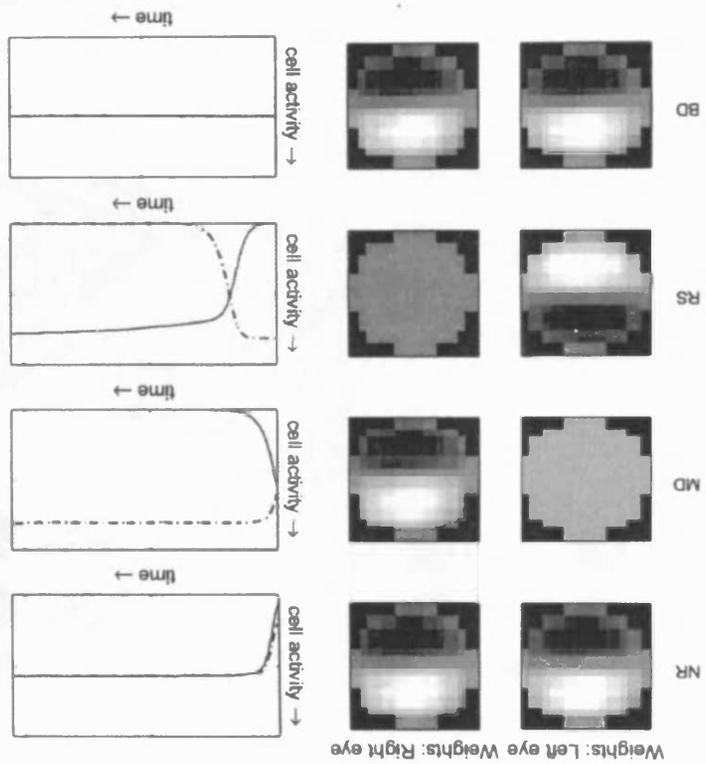
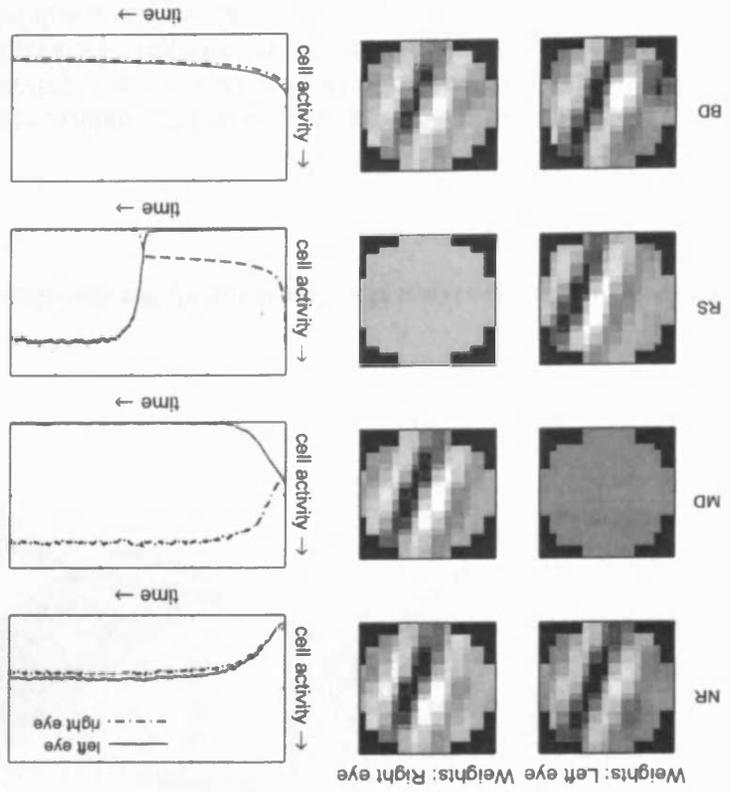
NR = normal rearing.

MD = Monocular deprivation following normal rearing.

RS = Reverse suture following MD.

BD = Binocular deprivation following normal rearing.

It should be noted that during RS the newly deprived eye responses decrease substantially before originally deprived eye responses begin to increase. During BD selectivity **is eventually lost if the simulation is run for longer**.



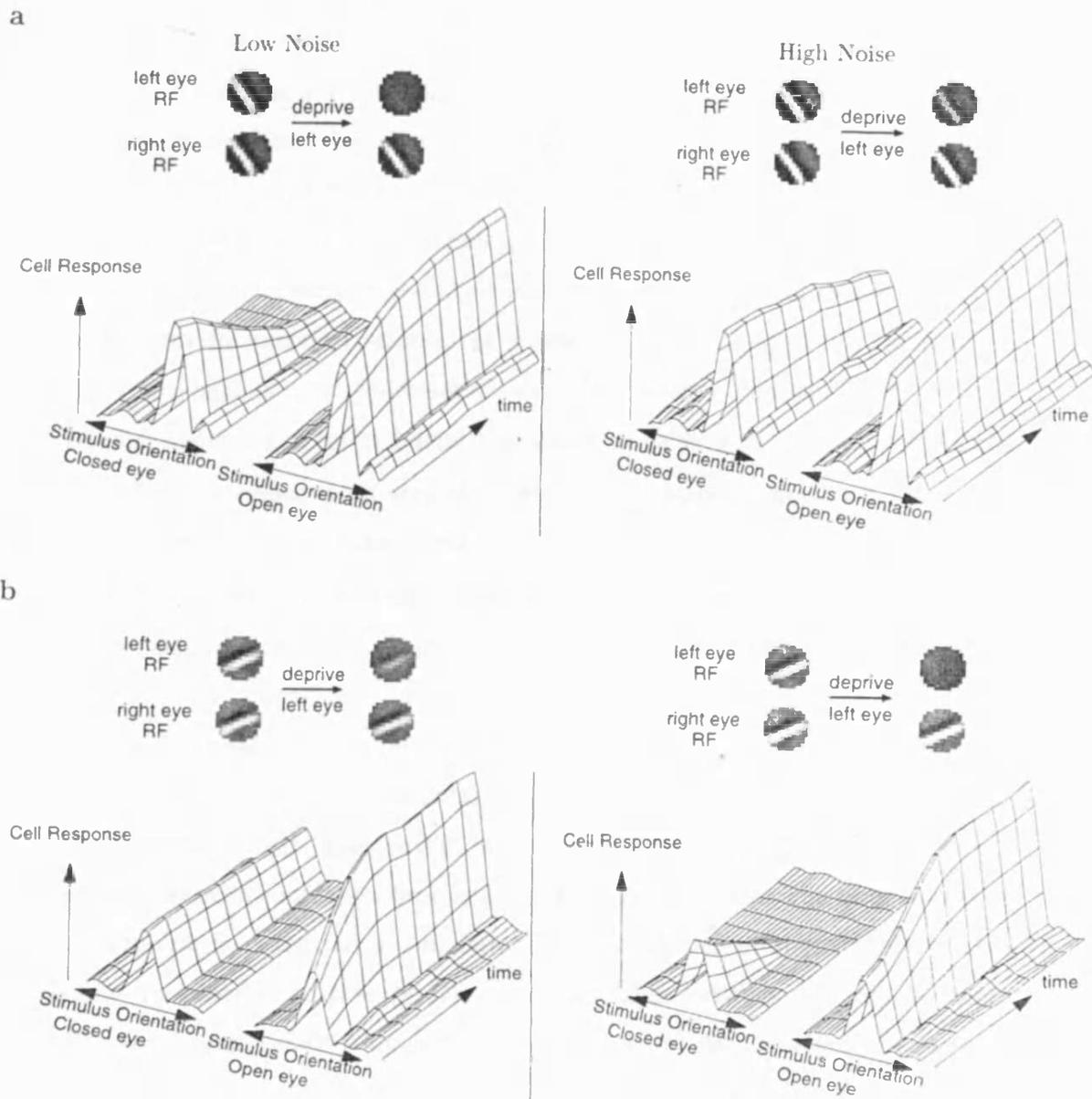


Figure 4.6 The effects of noise from the closed eye on the disconnection of the closed eye in MD (Blais *et al* 1999)

A) Heterosynaptic rule.

B) Homosynaptic rule.

Starting from a binocular state, a neurons was trained in a natural scene environment to obtain oriented receptive fields. This was followed my monocular deprivation in which the level of noise was varied in the DE. Left side is low noise and right side is high noise. Left and right eye receptive fields are shown before and after deprivation. The graph below each set of receptive fields is the responses of the cell to oriented sine gratings over time.

Noise effected the disconnection of the DE in the two rules in opposing fashions.

learning rate, η . Lower the learning rate and the magnitude of the fluctuations will decrease (see Fig. 4.2). If τ is too small ($\ll 1$) then rapid oscillation occurs, which is not realistic. Therefore a lower bound for τ would be '1' although no tight lower bounds can be set. Since the memory constant in the models used by Blais (1998, 1999) affected the half times of the three deprivation paradigms minimally, upper bounds for this parameter remain unknown.

The learning rate, inherently inter-linked with the memory constant (see Fig. 4.2), is not set too low for practical reasons, as it would take too long to run simulations. Setting it too high can, in combination with the memory constant, lead to large oscillations. Therefore, a lower bound was found to be $\eta=5 \cdot 10^{-7}$ with upper bounds $\eta=5 \cdot 10^{-5}$. Noise variance is set around 1, which is the standard deviation found in a natural scene environment (Blais 1998).

All of the above taken into account, Blais found $\eta = 5 \cdot 10^{-6}$ and $\sigma = 0.9$ to be suitable parameter values (τ is not critical since it has no appreciable effect on the half times).

The last major problem to be addressed is a comparison between simulation time units (iterations) and real time units (seconds). Given a parameter range that yields realistic results in terms of half times in the various experimental conditions, an indirect comparison between simulation time and real time can be made. The time course of loss of response from the DE in simulation gives a halftime of approximately $2 \cdot 10^5$ iterations. In experiment, loss of DE responses takes between 12 and 24 hours (Mioche and Singer 1989). Although the time course for the reduction of responses through the newly open eye in RO was slightly longer: 24-48hrs, it was well within an order of magnitude of the loss of DE responses. Also the time course for the reduction of responses through the newly deprived eye in reverse occlusion was on a similar time scale (Mioche and Singer 1989). If one considers 12 hours as the halftime of MD effects, then one iteration of the programme using Blais's parameters equals approximately 0.2 sec. For the parameters used in the present study, halftime loss of responses through the DE during MD took approximately half the time ($1 \cdot 10^5$) than that suggested by Blais (1998). This makes one iteration approximately 0.4 seconds in real time. This value is less than that found by Clothiaux *et al* (1991) who estimated 1.3 seconds. It should be noted however that Clothiaux *et al* (1991) did not define the

term 'disconnection' (of the deprived eye) when making direct comparisons between simulation time and real time. Their real-time value is therefore open to interpretation.

It is important to note that LTP and LTD (which are thought to underlie at least some of the processes involved in OD plasticity) occur on a time scale of minutes rather than hours (Kirkwood and Bear, 1995). Different parameter choices for the model would lead to different half times, hence make one iteration correspond to a longer or shorter real-time period. However, the three estimates of one iteration in 'real time' described above are all in the same order of magnitude on the time scale, consistent with the time-course of the manipulations of visual experience explored here.

METHODS

'Plasticity' program

(Written by Brain Blais 1998)

Many different models to explaining synaptic plasticity have been put forward; including Hebbian learning (Linsker 1986; MacKay and Miller 1994; Erwin and Miller 1998), Bienenstock Cooper Munro - BCM (Bienenstock *et al* 1982; Intrator and Cooper 1992; Blais *et al* 1999) and independent component analysis-ICA (Hyvarinen and Oja 1997; Bell and Sejnowski 1997; Blais *et al* 1998). The '*Plasticity*' program written in MATLAB by Blais (1998) incorporates all of these learning rules and stabilisation methods. It allows the experimenter to test all of the above learning rules separately on single neurons and networks of cells, and to vary the input environment.

Stabilisation of BCM and PCA models

Simulations were run for BCM and PCA models in their simplest forms. In the BCM model, a sigmoid function was taken to describe the neurone's input-output dependence (see Fig. 4.1). No extra stabilisation of synaptic weights was required. The PCA model does require further stabilisation of synaptic weights. As mentioned earlier, Hebbian learning is unstable. Some form of weight decay is required to prevent synaptic strengthening from increasing weights to infinity. It is possible to implement a maximum weight, although often the synapses will just go to this maximum very quickly and little change will be seen after. Subtracting the mean weight every iteration can solve this. It makes it impossible for the weights to reach their maximum. Another solution is to normalise the weight. All the weights are divided by the square root of the sum of the squares of the weights. Then, one can make the sum of the squares of the weights equal to '1' all of the time. The problem with these two solutions is their biological relevance. Each synapse must "know" the values of the other synapses within the time scale of one iteration (milliseconds). A plausible mechanism of how this may take place has yet to be put forward. The Oja normalisation approach uses a subtractive term for the equation: $\frac{d\mathbf{m}}{dt} = c\mathbf{d} - c^2\mathbf{m}$, where \mathbf{m} is the vector of synaptic weights, and c is the post-synaptic activity of the cell. This form of stabilisation uses only local information at that synapse to normalise

weights, and is therefore a more realistic approximation of stabilisation within the time frame of one iteration. This form of stabilisation of Hebb's rule is used here in these simulations.

Input patterns were of 12 natural grey-scale images that were difference-of-gaussian filtered. Monocular deprivation was simulated by replacing the patterned image with a uniform noise of mean = 0.0 and standard deviation of 1.0. Uniform noise of mean = 0.0 allows noise to be included without actually adding or subtracting any data from the image. Strabismus was stimulated horizontally by shifting the input to one eye by 16 pixels. Initial synaptic weights were random. A learning rate of $\eta = 5 \cdot 10^{-6}$ and a memory constant of $\tau = 1000$ were applied.

Qualitative parameters

Figure 4.7a and b shows a screen shot of the main program (for BCM and PCA learning). A network of 3x3 neurones is shown. It consists (clockwise from top left) of a window of synaptic weights (left and right eye), synaptic threshold, inputs from the environment (left and right eye), orientation and ocular dominance map (ORI/OD), magnitude of response through both eyes and orientation tuning curves. It should be noted that this screenshot is at a time where simulation has run for a few iterations. This allows the synaptic threshold (top middle) and responses to each eye (bottom middle) to be visualised without any gross changes in other parameters occurring. The ORI/OD map window consists of the ocular dominance of the cell represented on a greyscale; white represents left eye dominance and black represents right eye dominance. The angle of the yellow bars represents the orientation preference of the cell and the length of the bar represents the relative strength of that response. In the response window, the blue line represents the left eye and green, the right eye. Tuning curves are represented by blue, left eye, and yellow, right eye.

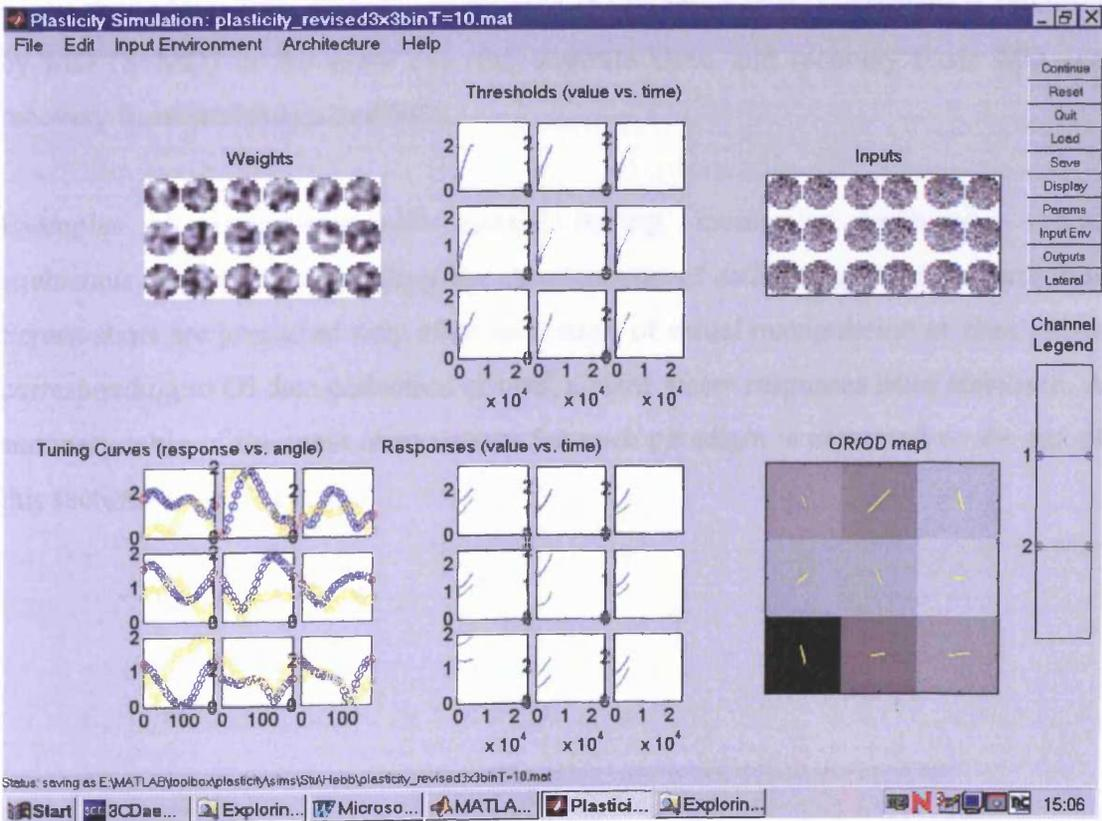
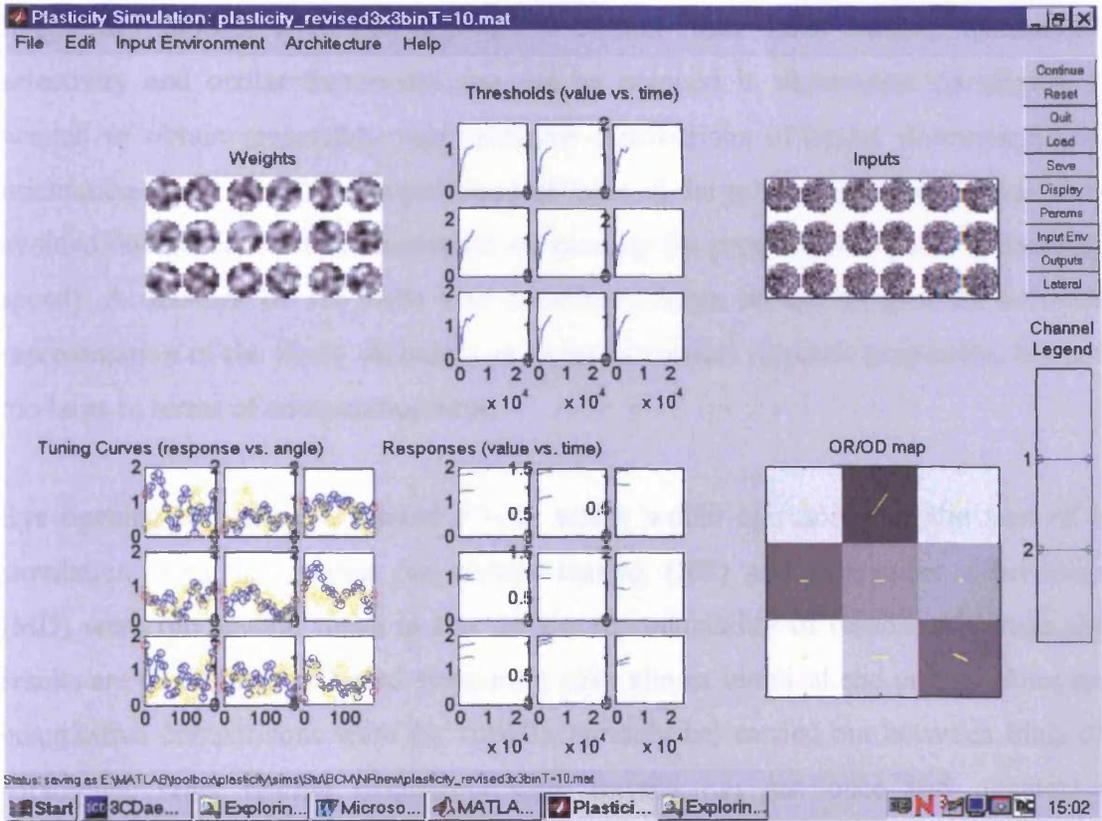
It is immediately noticeable that at the start of the simulation (Fig. 4.7a and b) visually naïve cells have a degree of orientation preference and tuning. How accurate this representation is continues to be contested. However, several studies highlight the presence of orientation selective cells before eye opening in ferrets (Krug 2001) and in kittens (Blakemore and Van Sluylers 1975; Fregnac and Imbert 1978).

Figure 4.7 a and b 'Plasticity' programme -example of main screenshot of BCM (top) and PCA (bottom) learning at time (t) = few seconds

A network of 3x3 neurons is used. Clockwise from top left window of synaptic weights (left and right eye), synaptic threshold, inputs from the environment (left and right eye), orientation and ocular dominance map, magnitude of response through both eyes and orientation tuning curves. The ORI/OD map window consists of the OD of the cell represented on a greyscale - white represents left eye dominance and black represents right eye dominance. The angle of the yellow bars represents the orientation preference of the cell and the length of the bar represents the relative strength of that response. In the response window the blue line represents the left eye and green, the right eye. Tuning curves are represented by blue, left eye and yellow, right eye.

BCM learning - Note: Responses to both eyes can be quite different through each eye. Oriented responses vary in magnitude and preference in all cells.

PCA learning - Note: Responses to both eyes are generally similar through each eye. Oriented responses are quite broad and of similar magnitude in cells.



Single cell models were not appropriate in this study since realistic orientation selectivity and ocular dominance can not be mapped in deprivation paradigms. I wanted to obtain reasonably representative distributions of ocular dominance and orientation selectivity from populations of cells. A large network of cells was also avoided due purely to time constraints on running the program (computer processing speed). A network of 3x3 cells was considered large enough to give an accurate representation of the likely outcomes in terms of cortical response properties, but not too large in terms of computation time.

Eye opening in kittens is around P7-10, which would correspond to the start of a simulation. Test simulations for normal rearing (NR) and monocular deprivation (MD) were run several times to test for the reproducibility of results. Although the results are qualitative, repeated simulation gave almost identical end points. Since no quantitative comparisons were (or could accurately be) carried out between trials or paradigms, other rearing paradigms were usually run just once and qualitative comparisons are described. Simulations were run for all the paradigms covered in this thesis for both BCM and PCA models. These were normal rearing, monocular deprivation (MD) from P35-45, strabismus (S) imposed at P21, strabismus followed by MD (S+MD) in the same eye and separate eyes, and recovery from MD and recovery from strabismus and MD.

Examples of simulations with normal rearing, monocular deprivation and/or strabismus are shown chronicling the development of cells at regular time intervals. Screen shots are presented only after each stage of visual manipulation at time points corresponding to OI data collection or until a point where responses have stabilised. A summary table of the main observations for each paradigm is presented at the end of this section (Table 1 and 2).

RESULTS

As mentioned earlier, simulations were run several times for normal rearing and monocular deprivation to ensure reproducibility. Here, examples of simulations with an image offset and deprivation were run several times from new starting points for each learning rule. It was concluded that the predictions of both learning rules were largely reproducible.

BCM model

Normal Rearing

At $t = \text{few seconds}$ (10 epochs), synaptic weights were random and receptive fields not well organised (Fig. 4.7a). Of the 9 cells, two were strongly monocular; one left eye (cell 2) and one right eye (cell 7), with the others (except cell 5, which was binocular) responding preferentially to one eye or the other. Some orientation preference was present also. Most noticeable was cell 2, preferentially responding to the LE. This cell was strongly orientation selective, shown by the long yellow line in cell 2 in 'ORI/OD' window and confirmed by the sharp tuning curve (yellow) seen in the 'tuning curves' window (It is interesting to note that one of the 2 monocular cells shows the best orientation tuning. This is in agreement with data from Fregnac and Imbert (1984) who showed that not only that most cells in early visual cortex were monocular, but also those cells that were monocular had stronger orientation selective responses than those that were more binocular). In contrast, cells 1 and 6 lack any tuning for either eye, as seen in the 'tuning curves' window.

At this time it is easy to appreciate the two eyes' responses in the two 'graph windows'. The first is the 'threshold' window (top middle). This increased very quickly from t_0 as input from the two eyes resulted in synaptic strengthening. The relative strength of responses through the two eyes (blue line left eye, and green line right eye) is seen in the 'responses' window (bottom middle). Most cells began responding preferentially to one eye, reflected in their relative ocular dominance. As time progresses, each cell's response started to converge to equal response strength.

At $t = \sim 6$ hrs (approximately 108 epochs), most of the parameters were heading towards a stable state (Fig. 4.8a). The modification threshold for each cell continued to increase, while most had reached a peak and began to fluctuate around that peak. Synaptic weights for most of the cells had stabilised to give distinct receptive fields. Responses through both eyes continued to increase in strength generally. Ocular dominance of cells was much more evenly matched between the eyes, with most cells gaining strong binocular responses and only minor eye preference still visible. Orientation preference had all but stabilised with a selection of different preferred orientations forming within the network of cells.

At $t = 24-36$ hours (432-648 epochs), the network of cells had reached a mature and stable state (fig 4.8b). Synaptic weights had converged to give crisp ON/OFF regions. The modification threshold continued to fluctuate around its maximum value. Absolute responses through both eyes in all cells had converged and again fluctuated around their equilibrium point. The cells were now completely binocular, with generally a sharply tuned response through both eyes. All parameters were stable thereafter. Figure 4.8b shows a screen shot at the equivalent of P21.

At this point a caveat presents itself. After a period of normal simulation - >24hrs, the network appeared to consist only of group 4 cells. After this time the network remains stable. An unvaried OD distribution such as this does not present an entirely realistic nature of ocular dominance responses under normal rearing conditions. One would expect predominantly group 4 cells, but at the very least a notable percent of group 3 and 5 cells similar to that seen in figure 4.8a. A very small divergent offset in both eyes would have allowed a more realistic OD distribution to form prior to any visual manipulation. Unfortunately, the relevant software to create bilateral divergence was unavailable at the time.

Therefore, it should be noted that the results from the model simulations presented here only applies to one class of cells – group 4, hence does present some caveats when interpreting the eventual outcome and timing of simulations under visual manipulation.

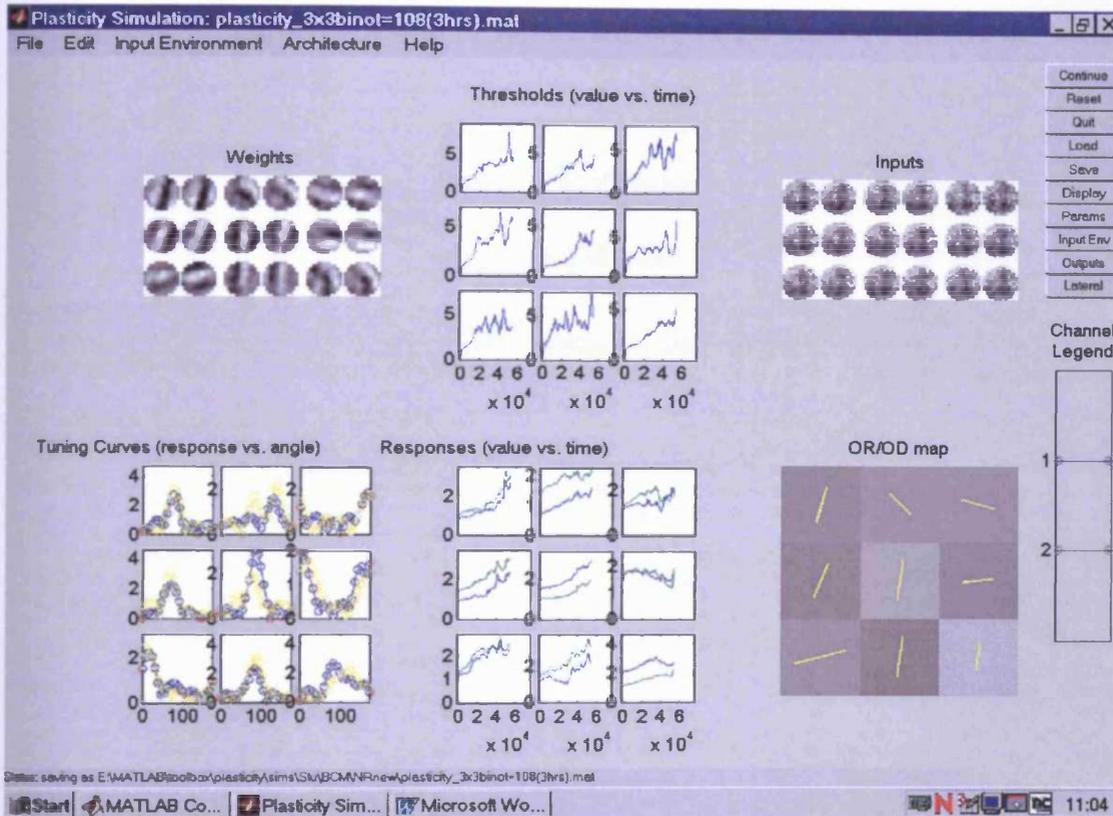


Figure 4.8 a Example of screenshot from BCM learning at time (t)= 6hrs

Clockwise from top left: window of synaptic weights (left and right eye), synaptic threshold, inputs from the environment (left and right eye), orientation and ocular dominance map, magnitude of response through both eyes and orientation tuning curves. Even at this early stage most parameters have converged and began to stabilize. Weights are distinct through both eyes. Threshold rises quite quickly to its maximum value and has begun to fluctuate around its maximum. Responses through both eyes have converged in some cells while in other cells both eye's responses are still increasing, but have yet to converge. Tuning of cells has yet to reach a mature state through both eyes, however OD is predominantly binocular.

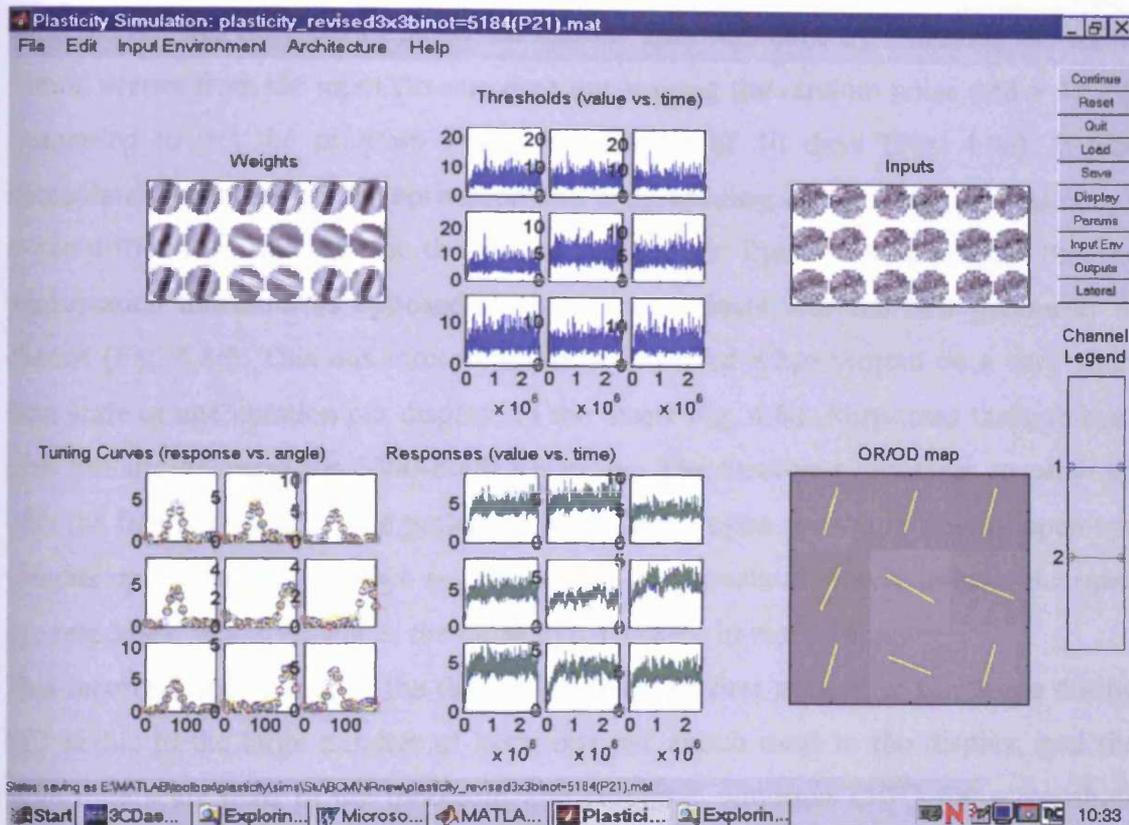


Figure 4.8 b Example of screenshot from BCM learning at time (t)= P21

This screenshot is from a new simulation run under normal rearing conditions to equivalent of P21. Clockwise from top left, window of synaptic weights (left and right eye), synaptic threshold, inputs from the environment (left and right eye), orientation and ocular dominance map, magnitude of response through both eyes and orientation tuning curves. All parameters have stabilized. This screenshot was be used for comparisons in later experiments for an example of normal rearing (It should be noted that different paradigms were run with different randomly generated networks of cells at t=0. Although minor differences in such parameters as the orientation preference of the cell develop from different start points of the networks, the overall outcome of all parameters in was always highly comparable).

Monocular Deprivation

The simulation was run to the equivalent of P35 (refer to Fig. 4.8b at P21). At this point the RE was deprived of patterned vision. This was done by removing the set of natural scenes from the input (to one eye) but leaving the random noise ($\text{std} = 1$) and continuing to run the program for an equivalent of 10 days (Fig. 4.9a). It was immediately visible that the deprivation had a devastating effect on the DE. Although it was difficult to appreciate on the time scales used in figure 4.9a, it appears that the modification threshold as opposed to the response level was the first parameter to change (Fig. 4.8c). This mis-interpretation is corrected when viewed on a very short time scale of one iteration per display, in the insert Fig. 4.8d. Responses through both eyes initially decrease for 1000-2000 iterations. The threshold decreases to catch up with the falling response. The patterned input to the open eye starts driving open eye weights up and hence open eye responses up. The threshold slowly follows the open eye responses, which enhances the close eye decrease in response.

This incorrect appearance of the threshold being the first parameter to change during MD is due to the large number of iterations per epoch used in the display, and the large time scale used in the threshold and response windows (10^{-5}) for screenshots with simulations run for long periods, that may give a misleading representation of the time scale of changes of parameters.

It was also noticeable that due to there being input through only one eye that the fluctuations of the threshold were much less compared to when both eyes were open.

Appreciable changes in the responses through the deprived eye began in less than 3hrs. While the DE response continued to decrease towards zero, the NDE reached its maximum response, above the pre-MD response level of each eye, then stabilises. Approximately 24hrs of deprivation and responses have diverged and the DE response reached a value just above zero and also stabilises. Synaptic weights through the NDE remain strong, while those through the DE have decreased to such an extent that no ON/OFF regions were visible (Fig 4.9a). This is reflected in the ORI/OD map, which was now completely dominated by the open eye. Orientation preference did not change. The tuning curves of responses through the DE are flat (yellow line) while those through the NDE remained sharp and with a marginal increase in their response amplitude. Some residual activity remained through the DE in OD maps after 24hrs despite all other parameters showing minimal responses through the DE.

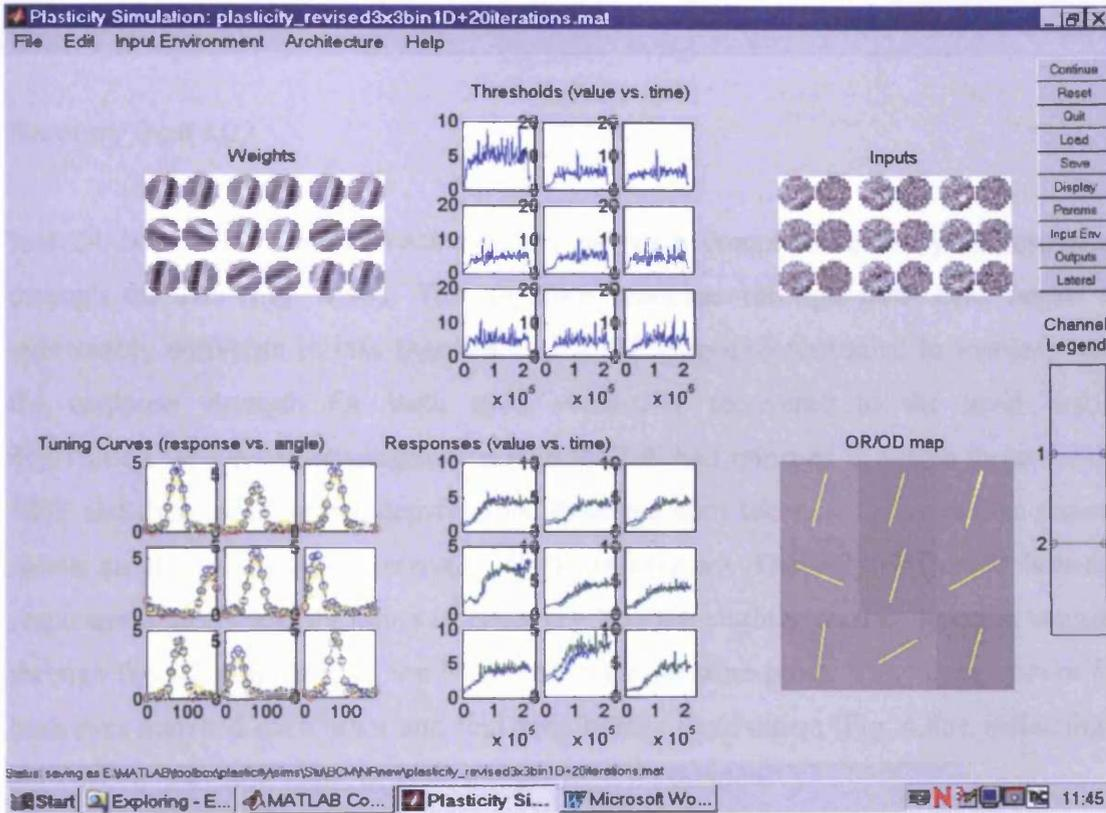
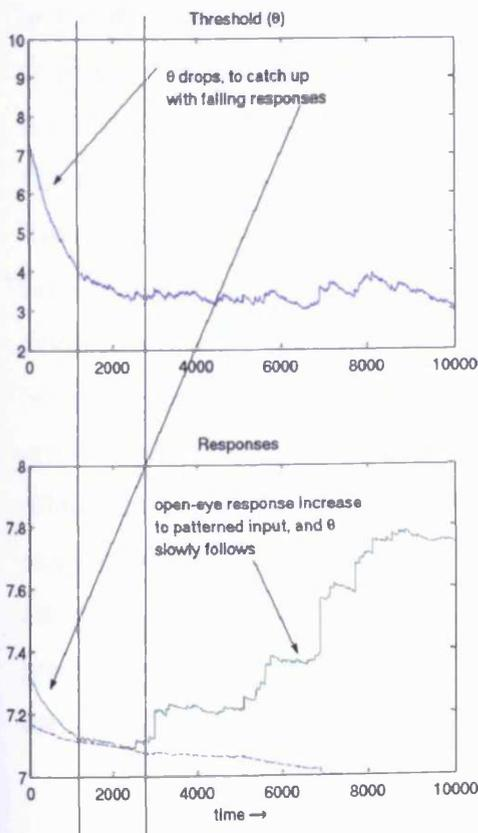


Figure 4.8 c Example of screenshot from BCM learning at time (t)= P10+MD for 20 iterations

A few iterations after the induction of MD in the RE, the threshold could be seen to drop before any discernible change in the responses through both eyes. This is in contrast to what the BCM theory would predict. The response through the DE should change first, before the threshold of the 'time averaged' post-synaptic activity level changes. This peculiarity may be due to time scales used for the graphs, leading to an inaccurate assessment of the time scale of changes.



Insert Figure 4.8d - Simulation of MD run with 1 iteration per display epoch

Responses through both eyes initially decrease for 1000-2000 iterations. The threshold decreases to catch up with the falling response. The patterned input to the open eye starts driving open eye weights up and hence open eye responses up. The closed eye is driven down as the closed up is driven up.

The threshold slowly follows the open eye responses, which enhances the close eye decrease in response.

Diagram and information courtesy of Blais 2004 - pers. com.

Recovery from MD

Just 24 hours of binocular recovery has led to a complete recovery of responses through the DE (Fig. 4.9b). The absolute response through both eyes began to appreciably converge in less than 3hrs. The DE response continued to increase with the response strength for both eyes eventually recovered to the level before deprivation. The synaptic weights through the DE had returned to match those for the NDE and those seen before deprivation. A screen shot taken at 12 hours (not shown) shows an almost complete recovery of all parameters. The only difference between responses after 12 and 24 hours of recovery was the slightly weaker synaptic weights through the DE compared to the NDE at the earlier time-point. The tuning curves for both eyes matched each other and that seen before deprivation (Fig. 4.8b), reflecting a network of binocular cells, as seen in the ORI/OD window.

Rearing with an image offset (“strabismus”) in one eye

Simulations were run to the equivalent to P21. It should be noted that a new naïve network state (t_0) was used for each different rearing paradigm. A screenshot is included for the comparison between states before and after the introduction of visual manipulation (refer to Fig. 4.10a, and b). At P21, to simulate an imposed strabismus in the RE, the input environment was offset by 16 pixels in the right eye. This is approximately equivalent to 8 degrees in real terms. (One-pixel offset = ~ 0.5 degrees, Blais 2004 pers.com).

Figure 4.10a shows the effects of an offset imposed in the right eye between P21-P35. Twenty four hours after offset introduction, the effects are complete. Binocularity has been lost and all cells are monocular. Orientation selective responses through the deviated eye have been lost and deviated eye weights have disappeared. Responses have diverged. The non-deviated eye dominates 6 of the 9 cells the network, with the remaining 3 cells being dominated by the deviated eye.* The effect of this large image offset had a very similar effect on parameters as MD did. All cells were monocular and the extent to which the threshold was reduced were similar between image offset and MD. In those cells dominated by the non-deviated eye, with an image offset present; responses through the non-dominant eye after image offset were reduced to the similar extent compared to responses through the DE in MD. However, those cells

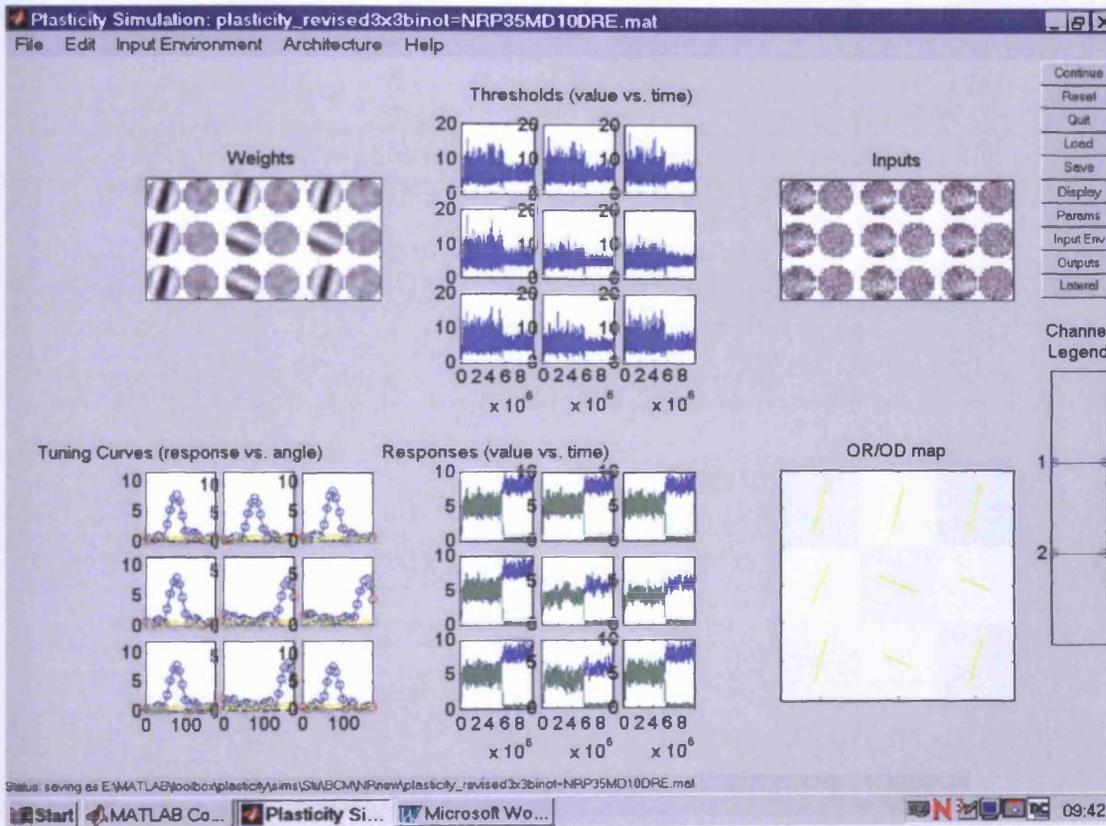


Figure 4.9 a Example of screenshot from BCM learning at time (t)= P45. Normal rearing up to P35 then MD in RE for 10 days

Just 24hrs of deprivation led to a complete loss of DE responses and a small enhancement of NDE responses. Orientation selectivity through the DE was lost. Nothing else changed over the rest of the deprivation period.

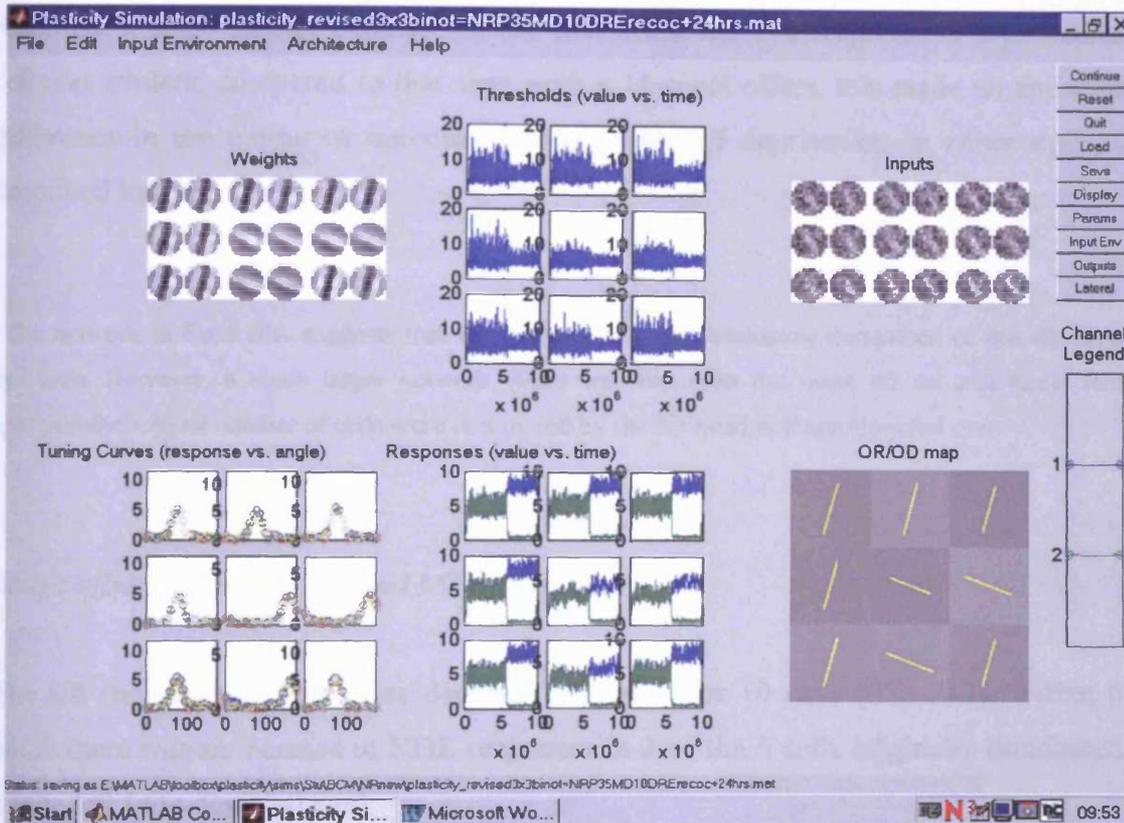


Figure 4.9 b Example of screenshot from BCM learning (at time (t)= P46) showing 24 hours recovery from MD (RE)

Normal rearing up to P35, MD in RE for 10 days followed by 24hrs of binocular vision

Twenty-four hours of binocular vision resulted in complete recovery of DE parameters. The absolute response through both eye began to converge in less than 3hrs. The DE response continued to increase with the response strength for both eyes eventually recovered back to the level before deprivation. The synaptic weights through the DE have returned to match those for the NDE and those seen before deprivation. The tuning curves for both eyes match each other and that seen before deprivation mimicking a binocular network of cells seen in the OR/OD window.

dominated by the deviated eye (after image offset) retained some input through the non-deviated eye, unlike that seen in MD where complete disconnection from the disadvantaged eye (deprived eye) occurred.

A much larger offset (30-pixels) was tested for comparison (data not shown). Although a small further decrease in the non-dominant eye response in a particular cell was evident, compared to that seen with a 16-pixel offset, this made no apparent difference in the timing or outcome of the period of deprivation in either eye, as described below.

*The network in Fig.4.10A suggests that the network was predominately comprised of non-deviated eye cells. However, a much larger network (6x6) was run with the same off set and found that approximately equal number of cells were dominated by the deviated and non-deviated eye.

Image offset (“strabismus”) and MD in different eyes

The left (non-deviated) eye was deprived of vision for 10 days (P35-P45). Within 6 hours there was an increase in NDE responses in 3 of the 6 cells originally dominated by the left (non-deviated eye).

Twenty-four hours of MD resulted in 3 of the 6 originally LE dominated cells changing OD to be dominated by the NDE. The other 3 remaining LE dominated cells’ OD remain unchanged after 24hrs of MD, although responses through the DE had decreased. Between 3 and 4 days after deprivation induction, all cells were dominated by the NDE, however, responses in some cells had not fully diverged, yet it took 4 to 5 days for all cells in the network to fully. The network was now dominated by the NDE in every respect (Fig. 4.10b). Nothing changed thereafter during the period of MD.

Recovery from MD with a preceding image offset (“strabismus”) in the different eyes

After the period of deprivation (Fig. 4.10b), the natural scene was re-introduced to the DE and the simulation continued to run as before MD (retaining the same offset in the RE).

Within 6hrs there was a small increase in the tuned responses through the deprived eye in 2 cells. Twenty-four hours on and no further change had occurred. Within 3-4 days of binocular recovery little had changed. Of note, in the 3 cells that were dominated by the deviated eye prior to MD, the response through the deprived eye started to increase. This can be appreciated from figure 4.10c (after 14 days of recovery). Sixteen to eighteen days of recovery, and in those cells that were showing some recovery, the response of the DE has stopped increasing and has stabilised, and the NDE response has now started to decrease. Parameters in all other cells had not changed at this time. The decrease in NDE responses was however, brief and did not continue to decrease further. The simulation was stopped after 29 days of recovery when responses had stabilised (Fig. 4.10d). At this time, despite some response returning to the DE in those 3 cells that were dominated by the right (deviated and deprived) eye prior to MD, recovery was incomplete. The other cells within the network remained completely dominated by the NDE. In short the network did not recover to the pre-MD state despite some DE input being re-established in 3 of the 9 cells.

Image offset ("Strabismus") and MD in the same eye

Within 12 hours of deprivation onset, the tuning within the NDE in the 3 cells that were previously dominated by the now DE, have increased. Within 24hrs, 2 of the 3 previously RE dominant cells have changed OD and become binocular or slightly dominated by the NDE. In those cells already dominated by the NDE no change occurred during the period of deprivation. Three to four days of deprivation lead to all of the 3 DE dominated cells changing OD to be dominated by the NDE, however, responses in these cells were far from stable at this point. It took 5-6 days for responses through the two eyes in all cells to diverge completely and become stable. At this point the network was dominated by the NDE in all parameters and did not change further during deprivation (Fig. 4.11a)

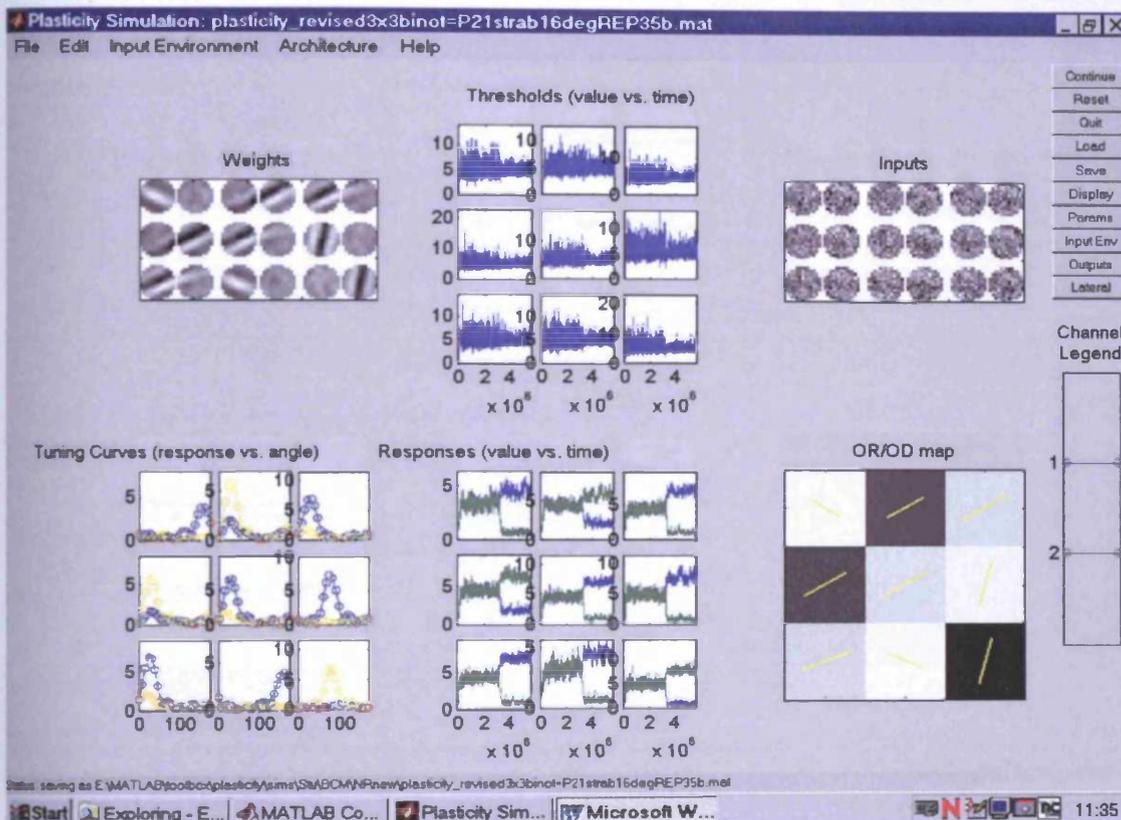


Figure 4.10 a Example of screenshot from BCM learning (at time (t)= P35) with a 16 pixel offset in RE up to P35

At P21, to simulate an imposed strabismus in the RE, the input environment was offset by 16 pixels in the right eye and run up to P35.

After 24hrs of offset introduction, the effects are complete. Binocularity has been lost and all cells are monocular. Orientation selectivity through the deviated eye has been lost and deviated eye weights have disappeared. Responses have diverged. The non-deviated (left) eye dominates the network - 6 cells. The remaining 3 cells were dominated by the deviated (right) eye.*

*The network in Fig. 4.10 a suggests that the network was predominately comprised of non-deviated eye cells. A much larger network (6x6) was run with the same off set and found that approximately equal number of cells were dominated by the deviated and non-deviated eye

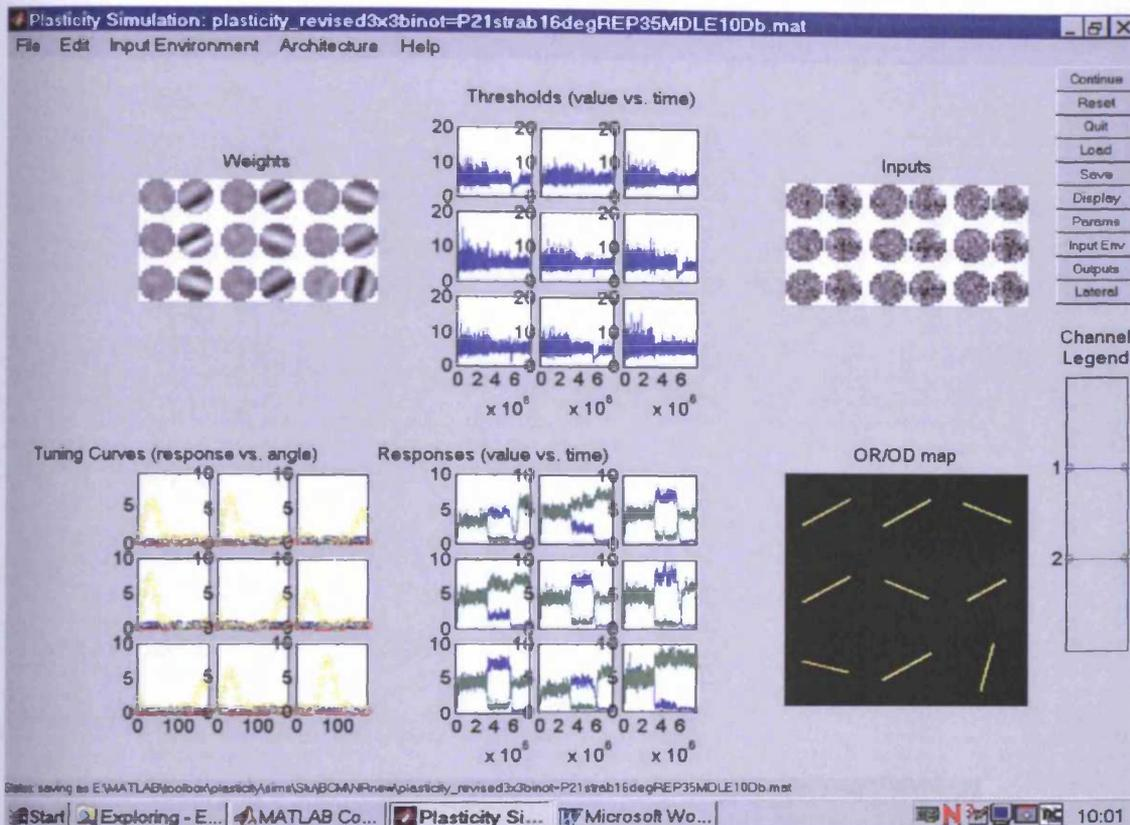


Figure 4.10 b Example of screenshot from BCM learning (at time (t)= P45) with a 16 pixel offset in RE followed by MD in LE

At P21, to simulate an imposed strabismus in the RE, the input environment was offset by 16 pixels in the right eye and run up to P35. Vision was then deprived in the LE for a further 10 days (P35-P45).

Twenty-four hours of MD resulted in 3 of the 6 originally LE dominated cells changing OD to be dominated by the NDE. The other 3 remaining LE dominated cells' OD remain unchanged after 24hrs of MD, although responses through the DE were decreasing. Between 3 and 4 days after deprivation induction and all cells were dominated by the NDE, however responses through some cells had not fully diverged and become stable. It took 4 to 5 days for all cells in the network to fully stabilize, responses to diverge and the NDE to dominate the cortex in all parameters.

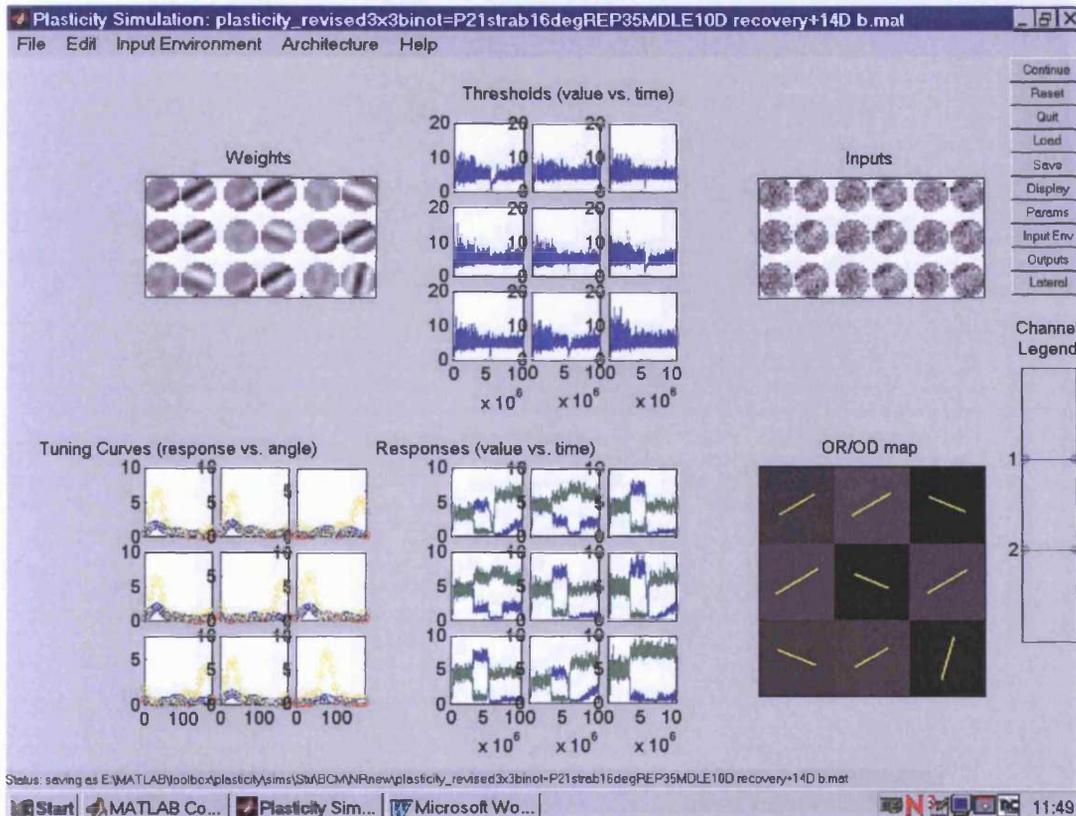


Figure 4.10 c Example of screenshot from BCM learning (at time (t)= P59) with 14 days of binocular recovery, after an offset in RE and monocular deprivation in LE

At P21, to simulate an imposed strabismus in the RE, the input environment was offset by 16 pixels in the right eye and run up to P35. Vision was then deprived in the LE for a further 10 days. At P45 patterned vision was restored in the LE and run for 14 days. Within 3-4 days of binocular recovery little had changed. Of note, in the 3 cells that were dominated by the deviated eye prior to MD, the response through the deprived eye started to increase.

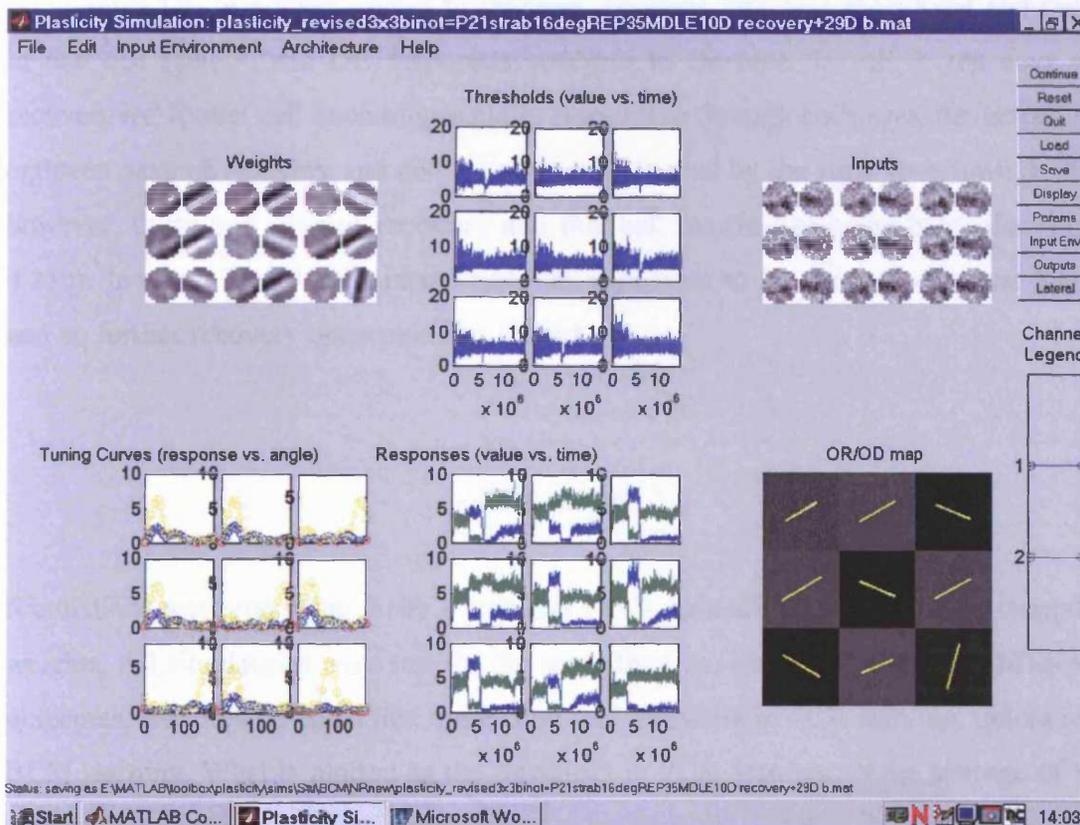


Figure 4.10 d Example of screenshot from BCM learning (at time $(t) = P74$) with 29 days of binocular recovery, after an offset in RE and monocular deprivation in LE

At P21, to simulate an imposed strabismus in the RE, the input environment was offset by 16 pixels in the right eye and run up to P35. Vision was then deprived in the LE for a further 10 days. At P45 patterned vision was restored in the LE and run for 14 days. With sixteen to eighteen days of recovery, those cells that were showing some recovery, the response of the DE has stopped increasing and has stabilized, and the NDE response has now started to decrease. The simulation was stopped after 29 days of recovery when responses had stabilized. In short, the network did not recover to the pre-MD state. Despite some DE input being re-established in 3 of the 9 cells, all other cells within the network remained completely dominated by the NDE.

Recovery from Image offset (“Strabismus”) and MD in the same eye

After 48hrs DE responses started to increase, however, this was short lived and only in one cell (cell 9) did DE responses continue to increase. In cell 9, ten days of recovery led to that cell becoming equally responsive through both eyes. Seventeen to eighteen days of recovery and cell 9 became dominated by the right (previously) DE, however, thirty-one days of recovery and that cell returned to being binocular (Fig. 4.11b). In short, 8 of 9 cells in the network continued to be dominated by the NDE and no further recovery occurred (Fig. 4.11b).

PCA model

Simulations were run using Hebb’s rule and Oja’s normalisation to stabilise synaptic weights. All simulations were run for the same time as with BCM with very different outcomes. It should be noted that there is no real threshold in PCA learning, unlike in BCM learning. What is plotted as the threshold in PCA learning, is the average of y^2 (output²).

Normal rearing

At $t = \text{few seconds}$ (10 iterations), it was immediately noticeable that several differences appear between PCA and BCM models, even at this early stage (ref Fig. 4.7b). Orientation tuning of responses through both eyes was broad (Fig 4.7b). Although generally the degree of orientation tuning prior to visual experience was similar to that in the BCM simulation, it is worth noting that the broader tuning allowed for a small response at almost all orientations. The synaptic modification threshold increased at a similar rate to BCM, however responses through both eyes increased quickly, in contrast to the very gradual increase in responses seen in BCM. In less than 3 hours of normal rearing, the threshold had reached its maximum and stabilised. The network exhibited a binocular OD distribution. In less than 6 hours, responses through both eyes had converged. Tuning through both eyes was equal and broad. After approximately 12 hours both eyes’ responses reached their maximum. There were only small fluctuations in the threshold and responses through both eyes.

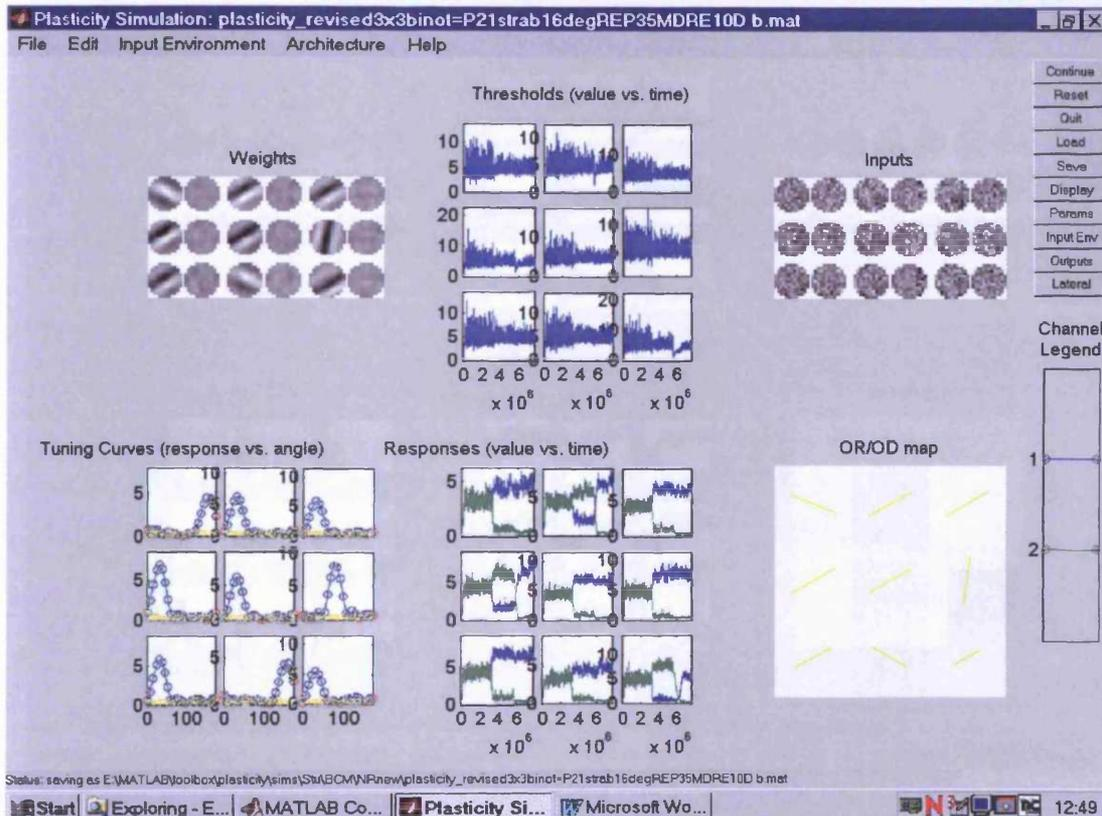


Figure 4.11 a Example of screenshot from BCM learning (at time (t)= P45) with a 16 pixel offset in RE followed by MD in LE

At P21, to simulate an imposed strabismus in the RE, the input environment was offset by 16 pixels in the right eye and run up to P35. Vision was then deprived in the RE for a further 10 days.

Within 24hrs, 2 of the 3 previously RE dominant cells have changed OD and become binocular or slightly dominated by the NDE. In those cells already dominated the NDE no change occurs during the period of deprivation. Three to four days of deprivation lead to all of the 3 DE dominated cells changing OD to be dominated by the NDE. It took 5-6 days for responses in all cells to diverge completely and become stable. At this point the network was dominated by the NDE in all parameters and did not change further during deprivation.

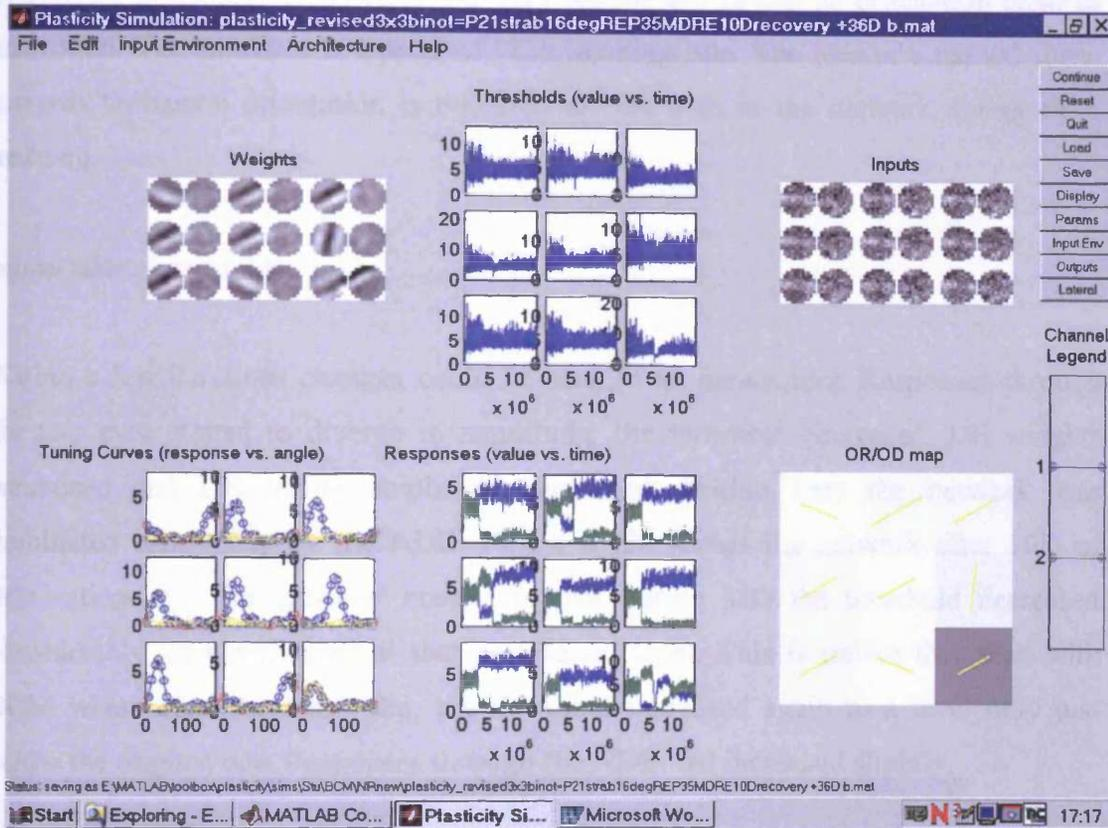


Figure 4.11 b Example of screenshot from BCM learning (at time (t)= P81) with a 16 pixel offset in RE followed by MD in RE

At P21, to simulate an imposed strabismus in the RE, the input environment was offset by 16 pixels in the right eye and run up to P35. Vision was then deprived in the RE for a further 10 days, then binocular recovery for 36 days.

There was an increase in all cells oriented response through the DE. After 48hrs DE responses started to increase, however this was short lived and only in one cell (cell 9) did DE responses continue to increase. In cell 9, ten days of recovery led to that cell becoming equally responsive through both eyes. Seventeen to eighteen days of recovery and cell 9 became dominated by the right (previously) DE, however thirty-one days of recovery and that cell returned to being binocular. The simulation was stopped after 36 days of recovery when no further change occurred and all other cells in the network (8 of 9) continued to be dominated by the NDE.

The network remained stable thereafter. In figure 4.12a (P21), one can appreciate that orientation preference of all cells was very similar and favour an orientation close to horizontal. This outcome is typical of PCA learning rule. The bias of a natural scene towards horizontal orientation is reflected in that seen in the network during PCA learning.

Monocular deprivation

Within a few iterations changes could be seen in all parameters. Responses through the two eyes started to diverge in amplitude, the threshold decreased, DE weights weakened and DE tuning amplitude decreased. Within 3hrs the network was dominated completely by the NDE. Figure 4.12b shows the network after 10D of deprivation. It is immediately noticeable that during MD the threshold decreased considerably, then stabilized at that new lower level. This is unlike that seen with BCM where after the initial dip, the threshold increased again to a level only just below the original one. Responses through the NDE had increased slightly.

Recovery from MD

Responses through the deprived eye started to recover within a few iterations after re-introduction of patterned vision. In less than 6hrs responses through the two eyes had converged and complete recovery of response amplitude and orientation selectivity through the DE had occurred. This state (Fig. 4.12 c) was qualitatively identical to that seen before MD.

Rearing with an image offset (“strabismus”) in one eye

A large 16-pixel offset was introduced into the RE at P21 and simulations run to P35 (Fig. 4.13a). There was a 3-4 day cycle of a small degree of divergence and re-convergence of responses through the two eyes, but strikingly, binocularity was maintained. The threshold did not change, neither did synaptic weights or orientation tuning through either eye. In two cells (5 and 6), a slight decrease in tuning through the deviated eye occurred, reflected in a marginal shift of ocular dominance and

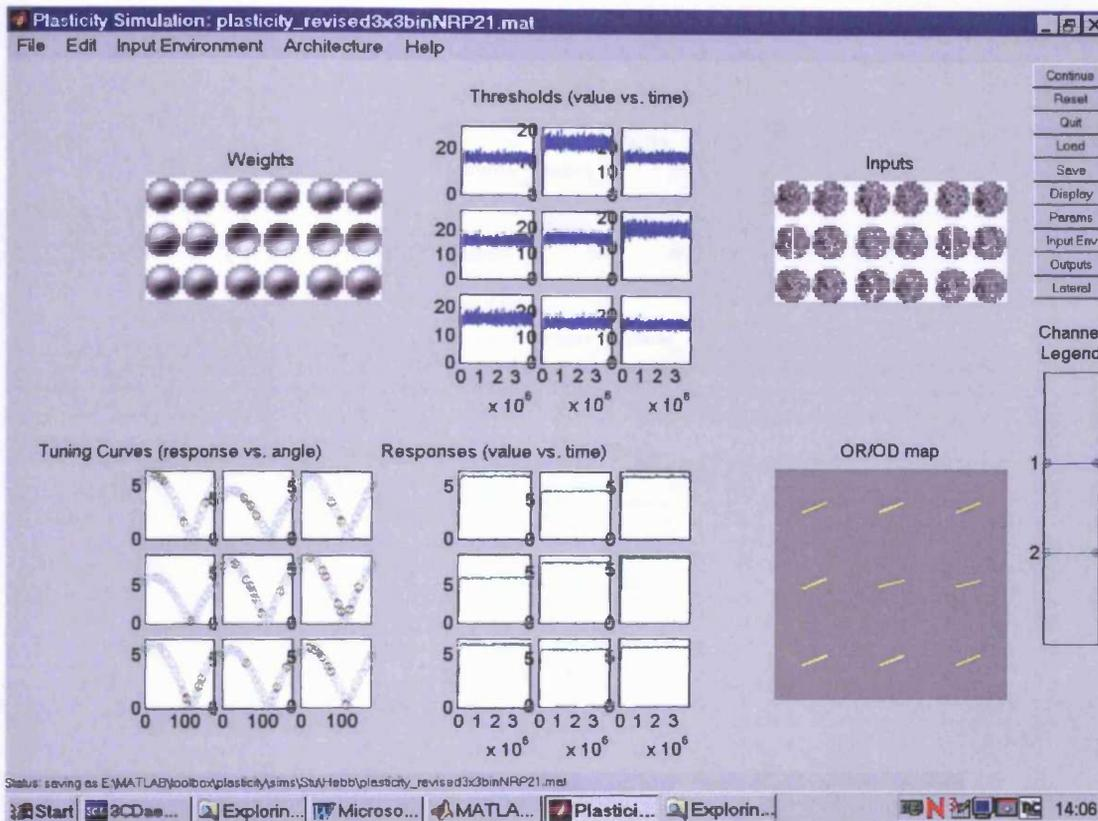


Figure 4.12 a Example of screenshot from PCA learning at $t=P21$

Normal rearing was run up to equivalent of P21

Convergence of responses is very quick. In less than 3 hours the network expresses a binocular OD distribution. In less than 6 hours, responses through both eyes have converged. Orientation preference of all cells are very similar and favour an orientation close to horizontal. This is reflected in the tuning curves and weights. However, oriented responses are broad over the network. Fluctuations in the threshold and responses of both eyes are minimal.

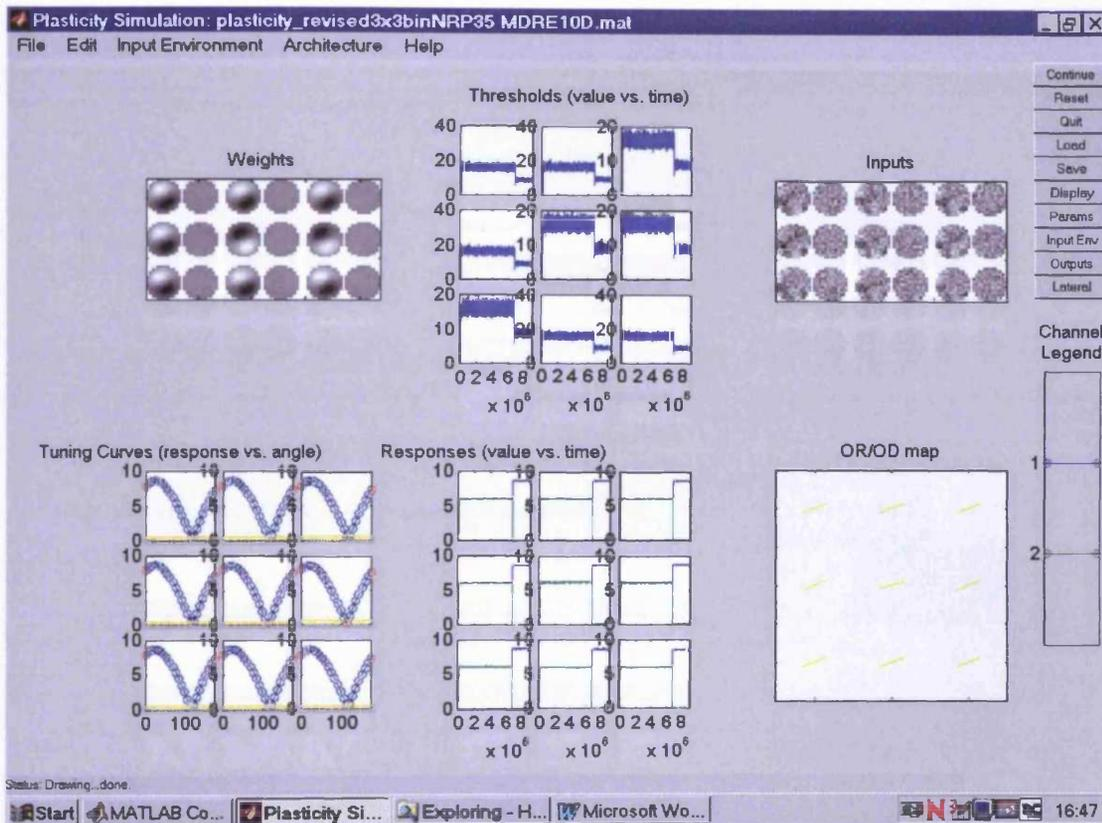


Figure 4.12 b Example of screenshot from PCA learning (at time (t)= P45) with MD in the RE

Normal rearing up to P21 where a 16-pixel off set was introduced in the RE up to P35, then MD in the RE P35-P45.

Within 3hrs responses have completely diverged and the network is dominated by the NDE. The threshold decreases considerably, then stabilizes at that new lower level. This is unlike that seen with BCM where after the initial dip, the threshold increases again to a level only just below the original one.

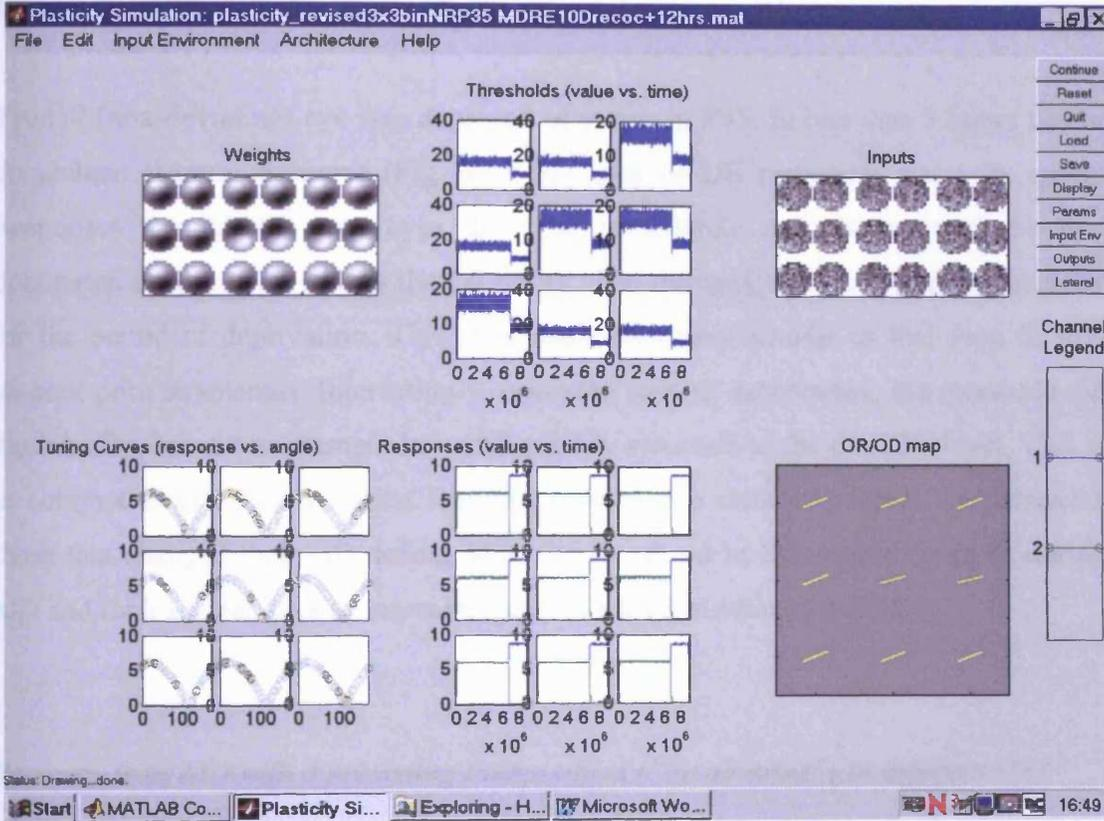


Figure 4.12 c Example of screenshot from PCA learning (at time $(t) = P45 + 12\text{hrs}$) with MD in the RE P35-P45 then binocular recovery for 12 hrs

Normal rearing up to P21 where a 16-pixel off set was introduced in the RE up to P35, then MD in the RE P35-P45, then re-introduction of vision into the RE and run for 12hrs.

Responses converge very quickly. Within 6hrs the DE has recovered fully and mimics that seen before MD.

synaptic weights in favour of the non-deviated eye in those cells. After 14 days of image offset in the RE, the network remained largely unchanged and binocular.

Image offset (“Strabismus”) and MD in different eyes

The left (non-deviating) eye was deprived of vision at P35. In less than 3 hours ocular dominance changes occurred (Fig. 4.13 b). Loss of DE responses was very quick. Responses through the two eyes diverged completely and the network became dominated by the NDE in less than 6 hours. The network remained stable thereafter for the period of deprivation. This time scale was very similar to that seen in MD without prior strabismus. Interestingly, upon the start of deprivation, the threshold did dip initially, but did not remain low and quickly returned to the pre-MD level. This is in contrast to that seen in BCM learning, where in a number of cells, in particular those that changed their OD during MD, the threshold in those cells dropped during MD and took several days to increase again to a level similar to pre-MD.

Recovery from MD with a preceding image offset (“Strabismus”) in different eyes

After 3 days of recovery, responses are converging, but have yet to match between the two eyes (Fig. 4.13 c). The amplitude of deprived eye responses increased, with orientation tuning widths through both eyes identical. Deprived eye weights were increasing steadily. The cortex is predominantly binocular with a slight bias towards the NDE. It took 6-7 days of recovery until binocular responses completely converged and the DE responses matched those through the NDE in every respect.

Image offset (“Strabismus”) and MD in the same eye

The right (deviating) eye was deprived of vision. Within 3hrs, DE responses had decreased and in less than 6hrs, the cortex was dominated entirely by the NDE (fig. 4.14a). The time-course and outcome here were identical to those seen with the offset and MD in different eyes. Again of note, apart from an initial dip immediately after deprivation, there was no change in the level of the threshold (see above).

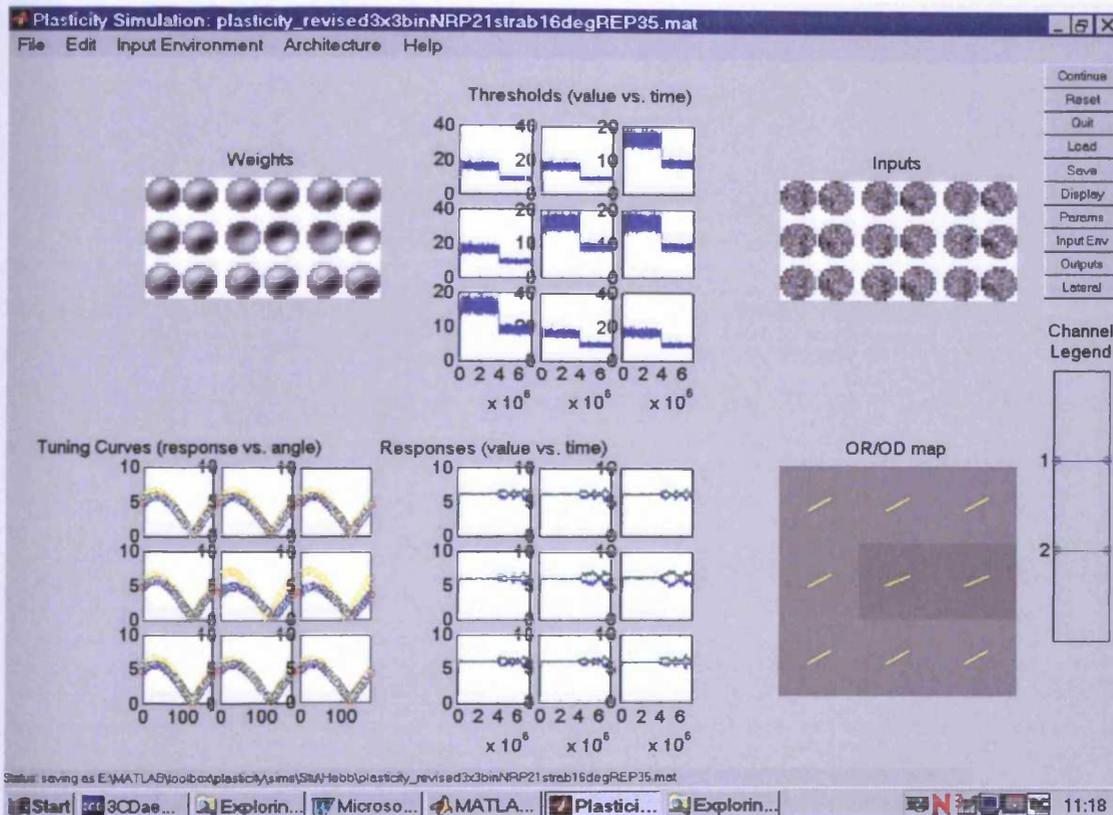


Figure 4.13 a Example of screenshot from PCA learning (at time (t)= P35 with large offset in the RE

Normal rearing up to P21 where a 16-pixel off set was introduced in the RE up to P35

There is a cycle of a small degree of divergence and re-convergence of responses. The threshold does not change, neither do weights or tuning through either eye. In two cells (5 and 6) with the greatest degree of divergence, a slight decrease in tuning through the deviated eye occurs, reflected in a marginal shift of ocular dominance and weights to favour the non-deviated eye in those cells. However, the network remains predominantly binocular.

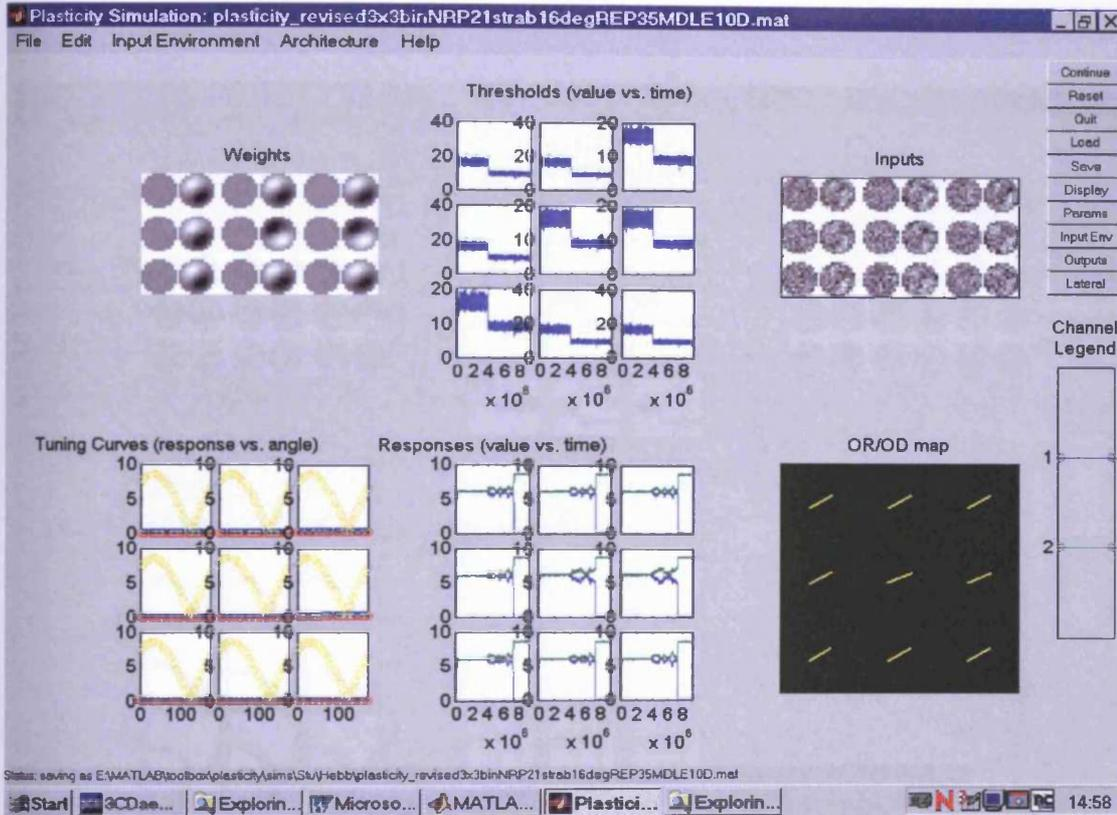


Figure 4.13 b Example of screenshot from PCA learning (at time (t)= P45 with large offset in the RE up to P35 then 10 days of deprivation)

Normal rearing up to P21 where a 16-pixel off set was introduced in the RE up to P35 then deprivation in the LE for 10 days.

Responses had diverged completely and the network dominated by the NDE in less than 6 hours. This is on a very similar time scale to that seen in MD. Interestingly upon the start of deprivation, the threshold did dip initially, but did not remain low and quickly returned to the level it was at with an offset present.

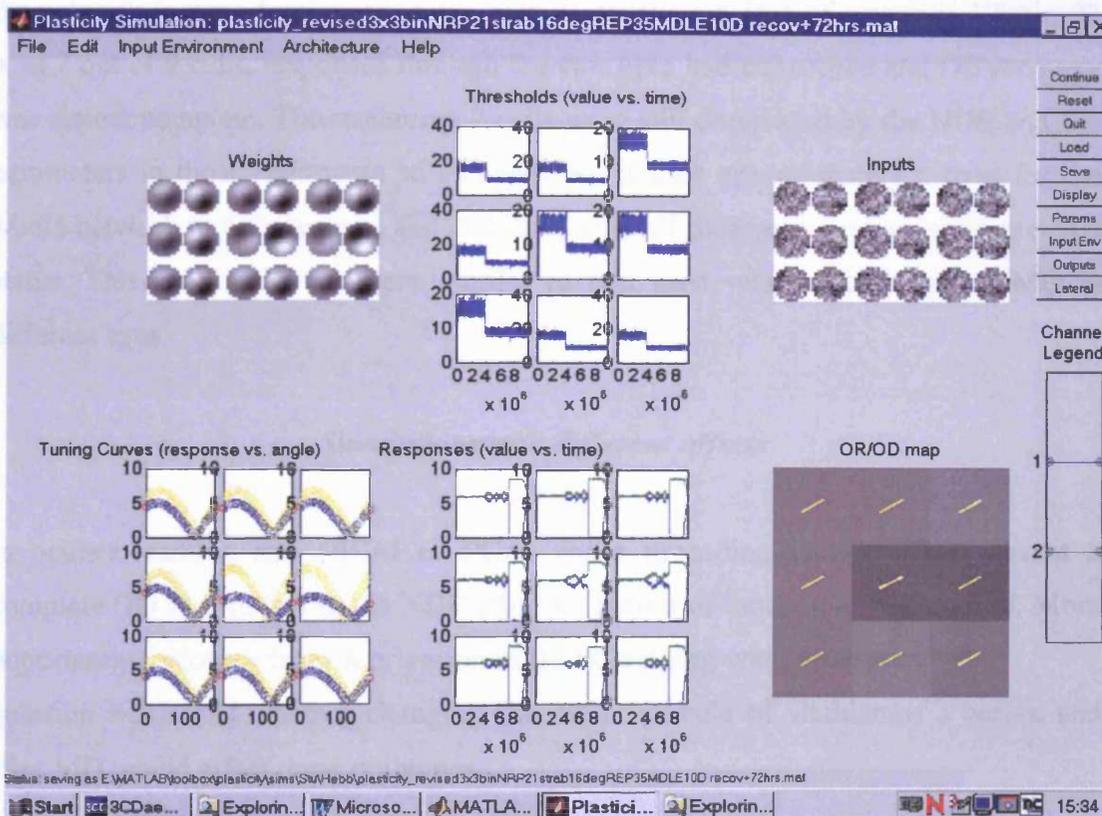


Figure 4.13 c Example of screenshot from PCA learning (at time (t)= P48 with large offset in the RE up to P35, 10 days of deprivation in the LE then 3 days of binocular recovery

Normal rearing up to P21 where a 16-pixel off set was introduced in the RE up to P35 then deprivation in the LE for 10 days, then reintroduction of vision in the LE and run for 3 days.

After 3 days of recovery, responses are converging, but have yet to match between the two eyes. Tuning widths through both eyes identical but DE amplitude is lower than NDE. The cortex is predominantly binocular with a slight bias towards the NDE. It took 7 days of recovery until responses completely converged and the DE recovered fully.

Recovery from MD with a preceding image offset (“Strabismus”) and MD in the same eye

Fig. 4.14b shows the network after 3 days of binocular recovery from MD. Changes in the network (ocular dominance) were seen as early as at 3hrs of recovery. Within 72 h, in 7 out of 9 cells, responses through the two eyes had converged and DE recovery was almost complete. The remaining 2 cells were still dominated by the NDE and DE parameters in those cells were still improving. It took approximately 6 days for the whole network to fully recover and stabilize, with all parameters returning to pre-MD status. This time scale was very similar to that seen with strabismus and MD in different eyes.

Simulations with different offsets

In neither learning rule (BCM or PCA) did a preceding image offset prevent a complete OD shift to favour the NDE after the period of monocular deprivation. More importantly, recovery from deprivation in BCM learning was incomplete. The question was asked whether changing the offset (“angle of strabismus”) before and after MD would affect these outcomes.

Within each learning rule:

- a) The degree of offset was varied (16, 10 and 5 pixel offset) but remained the same before and after MD.
- b) Simulations were run again as in *a*, but the offset was altered after deprivation (e.g. 16 pixels before MD and 10 pixels after MD). This was done to simulate the possibility that during biological experiments, the angle of the squint decreased over time. Squints were always clearly visible for 2 weeks after their induction. However, after the period of MD (in either eye), they were sometimes less obvious. Results are summarised in Tables 1 and 2.

It is predicted for *a*, that reducing the offset (“strabismus”) prior to MD would increase the percentage of cells remaining binocular. In turn the deprivation effect would be quicker, since there would be fewer cells dominated by the DE that would need to undergo a complete shift in ocular dominance. Subsequent recovery would therefore also be quicker and more complete. Conversely, increasing the offset prior

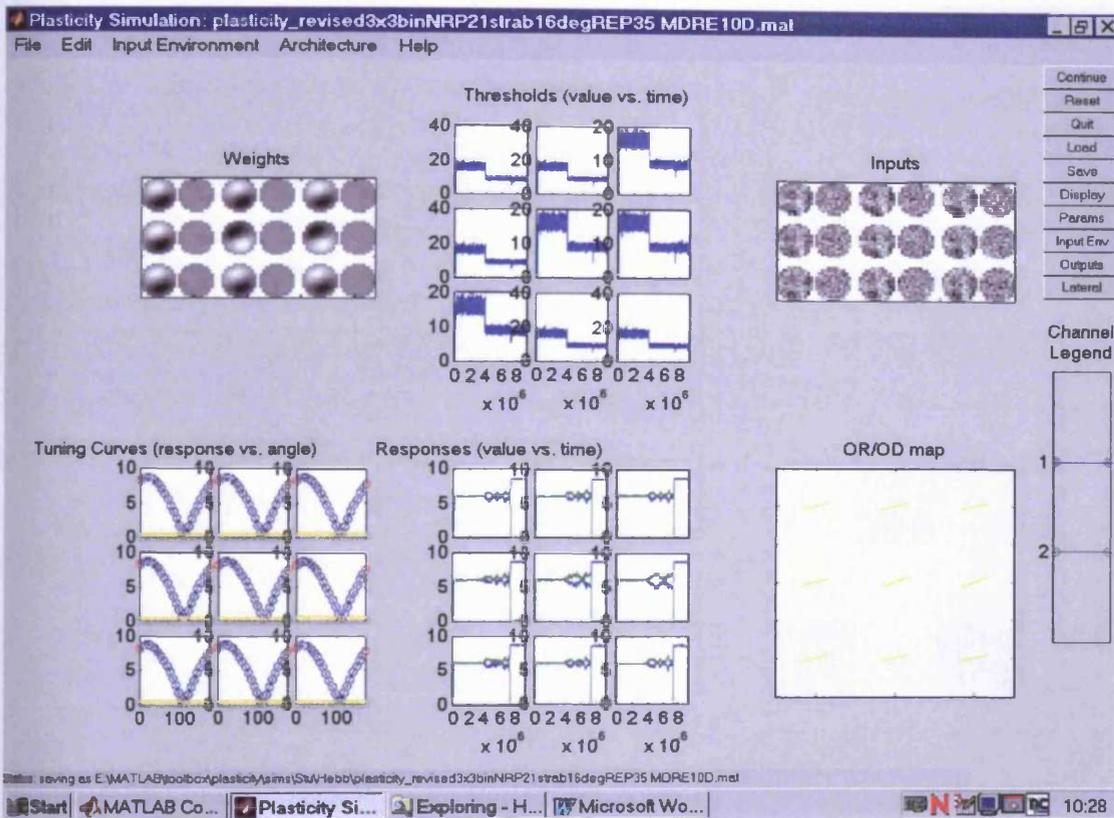


Figure 4.14 a Example of screenshot from PCA learning (at time (t)= P45 with large offset in the RE up to P35, 10 days of deprivation in the RE

Normal rearing up to P21 where a 16-pixel off set was introduced in the RE up to P35 then deprivation in the RE for 10 days, then reintroduction of vision in the RE.

Within 3hrs responses had converged and in less than 6hrs, the cortex was dominated entirely by the NDE. The timing and outcome were identical to that seen with the offset and MD in different eyes. Again of note, apart from an initial dip immediately after deprivation, there was no change in the level of the threshold.

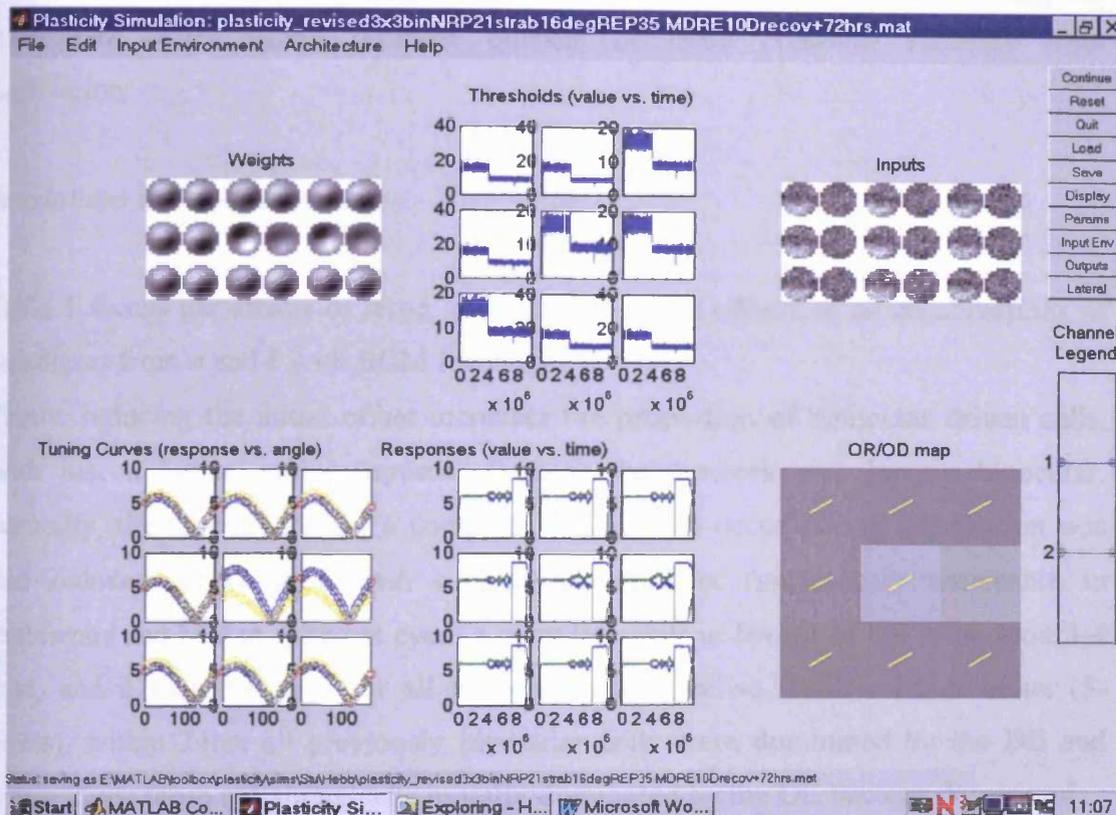


Figure 4.14 b Example of screenshot from PCA learning (at time (t)= P48 with large offset in the RE up to P35, 10 days of deprivation in the RE, then 3 days of binocular recovery

Normal rearing up to P21 where a 16-pixel off set was introduced in the RE up to P35 then deprivation in the RE for 10 days, then reintroduction of vision in the RE and run for 3 days. After 72hrs of binocular vision, DE recovery was complete in 7/9. In the remaining 2 cells, responses are still converging. It takes approximately 6 days for the whole network to fully converge and stabilize. This time scale is very similar to that seen with strabismus and MD in different eyes.

to MD may delay further (or even prevent) the OD shift seen after 10 days of deprivation.

It is predicted for b that regardless of the size of the initial offset, reducing the subsequent offset would promote quicker or more complete recovery from deprivation.

Simulations with BCM learning

Table 1 shows the effects of large, medium and small offsets in all combinations of paradigms from a and b with BCM learning.

Firstly, reducing the initial offset increases the proportion of binocular driven cells. With just a 5-pixel offset (approx. 2.5deg) the network was largely binocular. Secondly, the time it took for a complete OD shift to occur during deprivation was also reduced. In contrast, with a large pixel offset (particularly noticeable in strabismus and MD in different eyes) a complete shift in favour of the NDE took 3-4 days, and it took 5-6 days for all parameters to stabilise. With a small offset (5-pixels), within 24hrs all previously binocular cells were dominated by the DE and within 72hrs those remaining cells initially dominated by the DE became dominated by the NDE. The same was true when strabismus and MD were in the same eye. With a small image offset, a complete OD shift took just 24hrs. On the basis of these simulations, one predicted that with a larger offset (>25 pixels) an incomplete OD change would be seen within the 10-day deprivation period. This was found not to be the case. A very large image offset in one eye (30-pixels) did not change the timing or outcome of a subsequent period of MD when compared to a 16-pixel offset.

I address recovery from deprivation in two stages. Firstly, where the offset remained the same before and after deprivation, recovery of pre-MD responses in previously binocular cells was complete within 24-36hrs hrs. However, cells that had already been monocularly driven before MD remained so.

Secondly, if the offset was reduced during recovery, DE responses recovered more quickly and in some cases completely. For example, with a large initial offset remaining after deprivation, little or no recovery of the DE occurred during recovery (see Fig. 4.10a). Reducing the offset to 5 pixels led to some delayed (compared to just MD) recovery of DE responses and a number of cells became binocular (Table 1).

Squint angle (deg) in RE	Effects of squint	MD eye	Effect of Deprivation On ocular dominance (OD) and orientation tuning	Squint angle (deg) after MD	Recovery On ocular dominance (OD) and orientation tuning
16	Complete breakdown of binocular responses. 3 cells dom. by deviated eye and 6 cells by the non-deviated eye.	LE	3-4days –all cells changed OD to favour NDE. 4-5days –complete loss DE responses. Network stable.	16	Despite residual DE input returning, incomplete recovery of OD or ORI tuning through the DE.
16	Complete breakdown of binocular responses. 3 cells dom. by deviated eye, 6 cells by the non-deviated eye.	LE	3-4days –all cells changed OD to favour NDE. 4-5days –complete loss DE responses. Network stable.	10	24hrs - start OD change. 48hrs - 5/9 cells binocular and stable. In 4/9 cells some DE input but NDE still dominates. Recovery incomplete.
16	Complete breakdown of binocular responses. 3 cells dom. by deviated eye, 6 cells by the non-deviated eye.	LE	3-4days –all cells changed OD to favour NDE. 4-5days –complete loss DE responses. Network stable.	5	24hrs – 8/9cells binocular and stable. 1 cell still large NDE input/small DE input.
10	6/9 cells slight bias towards one or other eye. 3/9 cells monocular (2 LE, 1 RE).	LE	24hrs – 7/9 cells dominated by NDE. 36-48hrs – complete loss DE responses. Network stable.	10	24-36hrs – recovery of previously binocular cells (3/9) and some monocular cells now binocular. 3/9 cells remain monocular. Recovery incomplete.
10	6/9 cells slight bias towards one or other eye. 3/9 cells monocular (2 LE, 1 RE).	LE	24hrs – 7/9 cells dominated by NDE. 36-48hrs – complete loss DE responses. Network stable.	5	24hrs – cells predominantly binocular.
5	Predominantly binocular. Slight eye bias in 2 cells.	LE	24hrs – complete loss DE responses. NDE dominates and is stable.	5	3-6 hrs - First OD changes occur. Increase in DE tuning response. 12-24hrs - complete recovery.

16	Complete breakdown of binocular responses. 3 cells dom. by deviated eye, 6 cells by the non-deviated eye.	RE	24hrs – 2-3 of RE dominated cells change OD. 5-6days – complete loss DE responses. NDE dominates and is stable.	16	Little recovery. 10-days - 1 cell binocular. No change in other cells. No recovery.
16	Complete breakdown of binocular responses. 3 cells dom. by deviated eye, 6 cells by the non-deviated eye.	RE	24hrs – 2-3 of RE dominated cells change OD. 5-6days – complete loss DE responses. NDE dominates and is stable.	10	24hrs – 2 cells binocular, 6 cells some DE input, 1 cell no change. 48hrs – further increase in DE input but no further OD change. Incomplete recovery.
16	Complete breakdown of binocular responses. 3 cells dom. by deviated eye, 6 cells by the non-deviated eye.	RE	24hrs – 2-3 of RE dominated cells change OD. 5-6days – complete loss DE responses. NDE dominates and is stable.	5	<3hrs – first OD change. 36hrs –8/9 cells binocular and stable. 1 cell still NDE dominated.
10	6/9 cells slight bias towards one or other eye. 3/9 cells monocular (2 LE, 1 RE).	RE	12hrs – 8/9 cells dominated by NDE. 24-36hrs – complete loss DE responses. NDE dominates and is stable.	10	6hrs – OD change in previously binocular cells. 24hrs – recovery of previously binocular cells (6/9). Previously monocular cells remain NDE dominated.
10	6/9 cells slight bias towards one or other eye. 3/9 cells monocular (2 LE, 1 RE).	RE	12hrs – 8/9 cells dominated by NDE. 24-36hrs – complete loss DE responses. NDE dominates and is stable.	5	24hrs - cells predominantly binocular. 1 cell still NDE bias.
5	~6hrs 2 cells monocular. Decrease in tuning. Most cells predominantly binocular.	RE	24hrs – complete loss DE responses. NDE dominates and is stable.	5	24hrs – cells predominantly binocular.

Table 1 Summary of simulations with BCM learning with varying image offsets before and after deprivation in the same or opposite eye

Offset was always in the RE. Deprivation was either in the LE (first part of table) or RE (second part of table) and either remained the same before and after deprivation, or the offset was reduced after the period of deprivation.

However, it is important to distinguish between recovery of DE responses and recovery to a pre-MD state. Only with MD, and a small offset and MD did the network 'recover' to the state that was present before MD, i.e. a binocular cortex. In all other cases (even with a greatly reduced offset in the deviated eye after deprivation) the state of the network never returned to the exact state that was present before MD. Any cells binocular prior to MD recovered first and to the greatest extent. However, those cells that were monocular prior to MD remained dominated by the NDE during recovery (regardless of their pre-MD eye preference), or in the case where the offset was reduced during recovery, sometimes became binocular.

A slightly different outcome was seen with strabismus and MD in the same eye.

Reducing the offset after deprivation permitted some binocular cells to emerge (after 24hrs of recovery) from a previously monocular state, and some recovery of DE parameters in the other cells. However, the cortex remained dominated by the NDE after further recovery. This domination by the NDE was reduced with decreasing further the offset during recovery. However, even with a small offset during recovery and a predominantly binocular network, a slight bias towards the NDE remained.

Simulations with PCA learning

Table 2 shows the effects of large, medium and small offsets in all combinations of paradigms from *a* and *b* with PCA learning.

The initial image offset made little difference to the network. Different offsets did not affect ocular dominance, with all cells remaining binocular. Oriented responses were similarly unaffected, the only exception being with a medium offset (10-pixel). Here orientation selectivity through both eyes was broad, with the weight configuration of excitatory and inhibitory zones through one eye being vertically mirror-imaged in the other eye for a given cell.

The effect of deprivation was very quick to set in and was indifferent to the degree of pre-MD offset. Response through the DE was lost in 3-6hrs, and in all instances the NDE quickly came to dominate the network. The degree of initial offset did affect recovery after deprivation. With a large offset, after deprivation, complete recovery took 6-7 days. This recovery was reduced to a few hours with the smallest offset. Reducing the degree of offset after deprivation also speeded up recovery of DE responses considerably. For example, with a large offset before and after deprivation,

recovery took 6-7 days. When the offset during recovery was reduced to only 5 pixels, this recovery time was cut to just 12hrs.

Comparisons between BCM and PCA learning rules

Although it initially appears that changes took place a lot quicker in PCA learning than BCM learning, direct comparisons of *absolute* timing between the two models would be misleading. The parameter regime and hence the conversion of iterations to 'real' time used for the BCM model was optimised to give a realistic time scale for experimental MD (see Blais 1998). Only then did the model compare favourably to other experimental time scales, i.e. RO and BD. If the parameter regime was set so that the conversion of iterations to time, in the PCA model, gave a realistic time scale for MD, would the PCA stand up against other experimental time scales?

In short, a comparison of the *relative* timing between the BCM and PCA models is required before one can conclude which model most accurately predicts the timing and outcomes from experiments in Chapter 2 (and the literature). Half-rise, half-fall times for simulations were not studied in simulation here and measurements of the corresponding half-times in experiment were not carried out in the experiments in Chapter 2 or 3, hence the *total* time for loss and recovery of responses to one or either eye are compared here. A comparison of loss and recovery times (and general outcomes of the network) between BCM and PCA learning rules to those from experiment are summarised in table 3.

Taking the loss of DE responses for each learning rule: 24hrs for BCM and 6hrs for PCA, gives a ratio between the two models of 4:1. Since this ratio also stands for both models for the recovery of DE responses after MD in this instance, and MD is a less complex rearing paradigm than RO, this ratio is taken for later comparisons. The conversion of iterations to 'real' time was multiplied by 4 to make the timing of PCA learning equal to BCM, for MD, then compared to all other simulation and experimental manipulations (refer to table 3). For this relative comparison PCA rule will be referred to as PCA^f.

With this in mind, the time for the loss of DE responses was similar in both learning rules, which is comparable to experiments by Mioche and Singer (1989) and Crair *et al* (1997). Recovery of DE responses was predicted on a similar time scale although

Squint angle (deg) in RE	Effects of squint	MD eye	Effect of Deprivation On ocular dominance (OD) and orientation tuning	Squint angle (deg) after MD	Recovery On ocular dominance (OD) and orientation tuning
16	12-24hrs small divergence of responses through each eye, unstable. Remains binocular.	LE	< 6hrs - Responses diverge. Complete loss DE in all parameters.	16	24-48hrs – slight OD change. Responses start to converge. 7days –most responses converged, predominantly binocular cortex.
16	12-24hrs small divergence of responses through each eye, unstable. Remains binocular.	LE	< 6hrs - Responses diverge. Complete loss DE in all parameters.	10	6-12hrs-First OD change. Loss tuning both eyes. 12-24hrs convergence of responses.
16	12-24hrs small divergence of responses through each eye, unstable. Remains binocular.	LE	< 6hrs - Responses diverge. Complete loss DE in all parameters.	5	6-12hrs – responses converged, stable.
10	12-24hrs – Responses continue to decrease. Orientation selectivity lost. No OD change, binocular.	LE	< 3hrs – Decrease threshold and DE tuning. Complete OD shift.	10	3-6hrs – Start OD change. Decreased NDE tuning. 12hrs – complete recovery of DE.
10	12-24hrs – Responses continue to decrease. Orientation selectivity lost. No OD change, binocular.	LE	< 3hrs – Decrease threshold and DE tuning. Complete OD shift.	5	3hrs- Start OD change. 6-12hrs – responses converged, completely binocular.
5	3<6hrs – small decrease in threshold and both eyes responses. No OD change or loss of tuning.	LE	< 3hrs – Decrease threshold. Divergence responses. Loss DE tuning only.	5	3-6hrs Complete recovery of DE parameters.

16	12-24hrs small divergence of responses through each eye, unstable. Remains binocular.	RE	<3hrs OD change. Orientation preference identical for all cells 3-6hrs complete loss DE responses, stable.	16	<3hrs start OD change 24-48hrs – in 7/9 cells almost complete DE recovery. 2/9 cells little change 6days – all cells binocular. Complete recovery of all parameters.
16	12-24hrs small divergence of responses through each eye, unstable. Remains binocular.	RE	<3hrs OD change. Orientation preference identical for all cells. 3-6hrs complete loss DE responses, stable	10	<3hrs OD change. 6-12hrs – complete binocular cells. Loss of tuning in both eyes. 24hrs – Responses converged, stable parameters.
16	12-24hrs small divergence of responses through each eye, unstable. Remains binocular.	RE	<3hrs OD change. Orientation preference identical for all cells 3-6hrs complete loss DE responses, stable.	5	<3hrs OD change. 12hrs – complete recovery DE parameters.
10	12-24hrs – Responses continue to decrease. Orientation selectivity lost. No OD change, binocular.	RE	3-6hrs – responses diverged very quickly. Complete OD shift.	10	<6hrs – Increase DE tuning, very broad. Change in OD. <12hrs – complete binocular. Broad tuning through both eyes.
10	12-24hrs – Responses continue to decrease. Orientation selectivity lost. No OD change, binocular.	RE	3-6hrs – responses diverged very quickly. Complete OD shift.	5	6-12hrs – binocular responses. Tuning matches through both eyes.
5	3<6hrs – small decrease in threshold and both eyes responses. No OD change or loss of tuning.	RE	3-6hrs – responses diverged very quickly. Complete OD shift.	5	6-12hrs – complete recovery of DE parameters.

Table 2 Summary of simulations with PCA learning with varying image offsets before and after deprivation in the same or opposite eye

Offset was always in the RE. Deprivation was either in the LE (first part of table) or RE (second part of table) and either remained the same before and after deprivation, or the offset was reduced after the period of deprivation.

experiments suggest this takes slightly longer than 24hrs, namely 2-3days (Chapter 2, Liao *et al* 2004). When an image offset (“strabismus”) was introduced, binocularity broke down with the BCM rule which is comparable to experiments (Trachtenberg *et al* 2001), yet with PCA^f learning binocularity was never lost.

With an image offset and MD, the BCM model predicted up to 6 days for the NDE to dominate the cortex, while PCA^f just 24hrs. An incomplete OD shift was seen experimentally with a strabismus and MD (Chapter 2 and Table 3). Again the BCM rule most accurately predicts the timing and outcome, while the timing of the PCA^f prediction appears far too brief to account for the loss of DE responses.

Recovery of DE responses after MD (with preceding image offset) was more difficult for either model to predict compared to that shown in experiment. The PCA^f predicted recovery to be longer (~28days) than that seen in experiment (Chapter 2 and Table 3). However, this was only with the largest offset prior to MD. With smaller offsets PCA^f predicted recovery of DE responses on the scale of 1-2 days, much shorter than in experiment. The BCM rule predicted different recovery times and outcomes for different offsets prior to MD too. With the largest offset little or no recovery of DE responses occurred (even after 31 days recovery). However, with decreasing offset before and/or after MD, the percentage of binocular responses increased and the time to reach that state decreased considerably. Generally, any cells that became binocular during recovery did so in 24-48hrs and little changed thereafter. Although neither model appears to accurately predict the recovery of DE responses after image offset and MD, the lack of, or only partial, recovery of binocular responses predicted with the BCM model does match that shown in experiment. Although full recovery of OD was seen in strabismic animals, single cell data suggest the cortex was predominantly monocular (Chapter 2, Fig. 2.18c).

Also noteworthy is that orientation tuning width was not affected by offset in BCM learning, but there was a reduction in the response amplitude. In PCA learning, only with a medium offset was orientation tuning disrupted. As mentioned earlier, this result is a peculiarity of PCA learning. Looking at the equations for PCA learning (appendix 1), the two-eye correlation function is invariant to a parity transformation, i.e. simultaneous sign ‘flip’ of a set of co-ordinates or eigenvalues.

With the above *relative* comparisons between the two learning rules taken into account, the BCM rule more often accurately predicts the timing and outcome of experimental results under conditions of MD, strabismus and strabismus and MD. This also appears to stand for reverse occlusion and binocular deprivation (table 3), which will be explored in the next chapter.

Visual manipulation	BCM	PCA	Experimental results
Monocular deprivation	Loss of DE responses within 24hrs. Recovery of DE responses within 24hrs.	Loss of DE responses ~ 6hrs Recovery of DE responses ~ 6hrs.	Loss of DE responses 24-48hrs (Mioche and Singer 1989, Crair <i>et al</i> 1997). Recovery of DE responses 2-3 days (Chapter 2). As early as 3 days (Liao <i>et al</i> 2004).
Strabismus	Loss of binocularity < 24hrs.	No loss of binocularity.	Breakdown of binocular connections in 2 days (Trachtenberg <i>et al</i> 2001).
Strabismus +Monocular deprivation	Loss of DE responses with large offset – All cells dominated by the NDE takes up to 6 days. Recovery of DE responses with large offset – little or no recovery of DE responses. Small offset – varying degrees of binocular cells.	All cells dominated by the NDE takes ~ 6hrs. Recovery of DE responses with large offset took up to 7 days. Small offset – recovery took < 24hrs.	Incomplete shift to favour the NDE after 10 days (Chapter 2). Some animals took 9-19 days for complete recovery of DE territory (Chapter 2).

Table 3 Comparison of loss and recovery times of the DE in BCM and PCA learning during simulation and that seen in experiments from the literature

DISCUSSION

The general outcome of simulations with BCM learning showed a number of similarities to experimental data, while PCA simulations were less closely matched to the outcomes of experimental data. Moreover, in a number of instances, when comparisons of the *relative timing* between the two learning rules were taken into account, the BCM rule more often predicted the timing of experimental changes in responses, than the PCA rule.

Work in this chapter was motivated by the growing complexity of computer networks for synaptic plasticity. The similarities in timing and outcome of simulated results to those of real experimental data (Blais 1998; Clothiaux *et al* 1991) have added further weight, in particular, to BCM-type learning playing a role in *in vivo* plasticity. Could BCM learning mimic the experimental outcomes in Chapter 2 under identical rearing paradigms, or would PCA provide a more realistic representation of plasticity in the cortex? If simulations do not mimic the experimental results seen, under what circumstances would simulations most closely match the experimental results seen, and shed further light on to what may be *actually* happening during the experimental period?

Convergence of responses with PCA and BCM learning during normal rearing

Generally, the relative speed of changes to response parameters was similar in both learning rules. From an initial naïve network in simulation (corresponding approximately with the day of eye opening in animals), reached a stable and mature state in a matter of hours. This is obviously a lot faster than in 'real life' (see Crair *et al* 1998, 2001).

The most notable difference between the parameters was the orientation tuning of cells; in BCM learning cells were sharply tuned and orientation preference varied across the network, while with PCA learning orientation tuning was broader and orientation preference was the same for all cells. Due to the dynamics of the equations governing the two learning rules, increasing the input to a neurone, leads to the convergence of responses being faster in PCA learning, while in BCM convergence is slower. The equation for the weight dynamics for PCA is quite basic. The input, x ,

determines the rate of an exponential convergence of values so that the synaptic weights equal '1'. In effect the PCA rule is trying to maximise the average squared activity, such that most of responses are strong.

In contrast, in the BCM learning rule, the output is merely the projection of the input, x , onto the synaptic weights. The BCM rule is trying to find structure in the inputs in the form of multi-modality, such that a small subset of responses is strong and the others are weak (Blais 1998).

PCA and BCM learning rules with input offset

The comparisons between simulation and experiment during normal rearing and MD are not required here (refer to Blais 1998 for detailed study). It is worth noting that in simulation and experiment, deprivation is caused by a loss of *patterned* vision (Blais 1998; Blais *et al* 1999) not just a reduction in retinal activity. Retinal cells are primarily 'contrast' not 'light' detectors. Using opaque contact lenses (which severely diffuses the patterned retinal input, but only reduce the total amount of light entering the eye minimally) was just as effective as lid suture at promoting an OD shift to favour the NDE (Blakemore 1976; Wiesel and Hubel 1963). The distinction between absolute and relative levels of activity between the two eyes becomes apparent when 'strabismic rearing' is introduced.

Shouval *et al* (1996) reported differences in the outcomes from BCM and PCA learning with a lateral offset of inputs ("strabismus"). While for PCA learning neurones always remained binocular, binocularity broke down to various extents with BCM learning; the larger the offset the lesser the degree of binocular responses. These different outcomes for the two learning rules are confirmed here. With a large image offset (16 (and 30)-pixel) binocularity was lost completely and all cells in the network were strongly monocular; with the smallest offset (5-pixels) binocularity was maintained with only occasional monocular dominance in 1 or 2 cells. In addition to changes in OD, shown here and by Shouval *et al* (1996), the size of the offset also affected orientation selectivity in different ways in the two learning rules. With BCM learning, orientation selectivity generally remained highly selective with image offset. However, with PCA learning, a non-progressive outcome occurred; with a medium angle offset orientation selectivity was greatly reduced, but with a large or small angle offset, orientation tuning changed minimally, remaining robust. A better

understanding of how orientation selectivity (and ocular dominance) is formed in PCA learning is required before the above result can be understood.

A simple interpretation of the Hebbian learning rule is that with appropriate stabilising constraints, PCA learning leads to the extraction or approximation of the principal components (Shouval *et al* 1996). In this case the principal component corresponds to the statistical distribution of the visual environment. With retinal pre-processing, the first principal component of the data is orientated, however it will always be found to be near horizontal (Shouval and Liu 1996). The strong preference for the horizontal orientation is due to a slight bias in the correlation function of natural images in this direction (Shouval *et al* 1996; Baddeley and Hancock 1991; Shouval and Liu 1996).

In PCA learning, the degree of overlap of the receptive fields through both eyes does not alter the optimal orientation, but does affect the shape of the receptive field and the degree of orientation selectivity. Orientation selectivity has been shown to decrease as the amount of overlap increases, while when there is no overlap at all, high selectivity is maintained (Shouval *et al* 1996). So the results obtained here regarding the degrees of orientation selectivity with varying overlap of receptive fields are in agreement with what has been shown previously (Shouval *et al* 1996).

Therefore, the robustness of PCA rule to an offset in receptive fields with respect to binocularity and orientation selectivity can be accounted for by the PCA equation being invariant to a sign change i.e. positive and negative weight vectors are eigenvectors. The slightly perplexing outcome of poor selectivity seen with a 10-pixel offset is related to the size of the receptive field being 13x13 pixels. With a 10-pixel offset a few pixels are still correlated between each eye and the neuron will form a receptive field based on those few pixels, hence selectivity in this instance will be broad.

In BCM learning binocularity is lost when the inputs are offset. This has been shown in detail by Shouval *et al* (1996). The less overlap in receptive fields between the two eyes the lesser the degree of binocularity.

At the point where the two inputs become completely de-correlated, the eye that has the dominant input to a cell, holds on to that particular cell. The weaker eye becomes “disconnected” on a time scale similar to MD (also see Clothiaux *et al* 1991). Effectively there is no stable binocular state, with the only stable selective state being

monocular. The only difference between de-correlating vision and MD is that the distribution of inputs to the DE (noise) and NDE (structured) determine a cell's eye preference, whereby with image offset (strabismus) it is the pre-existing eye preference of the cell that determines its eventual preference after "strabismus" induction.

PCA and BCM learning with offset ("strabismus") and MD

As I have demonstrated, simulations run for strabismus and MD did not prevent the OD shift towards the NDE after deprivation as such, with either PCA or BCM learning. However, the BCM rule predicted that, when a large-angle offset was imposed before MD, the complete loss of DE responses took up to 6 days to occur (slightly less with MD and offset in different eyes). The reason for the absence of persistent protection from MD in the model simulation comes from several sources. One could draw the conclusion that residual input from the NDE to any particular cell remained during deprivation, which would act as a substrate for binocular interactions, hence assisting in driving DE responses down (LTD). However, LTD is homosynaptic. It would still occur to some extent in those cells affected by deprivation (Chapter 2), but would just take longer – like binocular deprivation. The time course of results from simulation could have been observed in experiment more precisely had the length of deprivation in experimental animals been slightly different. One can hypothesize a shorter period of MD (i.e. 6-7days) in experimental animals would have resulted in little or no deprivation effect. Likewise a longer deprivation effect (14-18 days) would have resulted in a complete deprivation effect. Secondly, differences in the calculated length of one iteration in simulation would also result in a greater or lesser effect of deprivation after a 10-day period of deprivation in the computer simulation.

Since a graded increase in the time taken for complete loss of DE responses was seen with increasing image offset, one could predict that an even larger angle offset (>20 degrees), would result in complete loss of the non-dominant eye's responses for a particular cell. Therefore, an incomplete OD shift would occur within the 10 days of deprivation, or indeed within any length of time. Theoretically, with a large enough offset all cells would be completely dominated by one eye, hence should not be unable to switch OD. Despite the theoretical outcome of very large angle squints, the

size of the receptive field used for each eye (in simulation) was a radius of 13 pixels. Therefore, any offset greater than 13 pixels in one eye would mean that the receptive fields from each eye would no longer overlap and binocularity would no longer be produced. With a very large offset used (30-pixel) a small further decrease in non-dominant eye responses for a given cell was noted, but the predicted time for complete OD shift to favour the NDE during further MD was no longer than that seen with a 16-pixel offset. Therefore, the previous theoretical predication of a very large image offset (or strabismus) preventing an OD shift, was not predicted by either model.

In those cells whose OD was to be changed by deprivation, the DE response decreased to match that of the NDE eye before the latter could increase its efficacy (similar to RO); hence, the greater the input from the eye to be deprived relative to the eye to be left open, the longer the deprivation effect took.

During recovery from MD, the greater the degree of correlation between the two eyes, the extent to which the network became binocular increased in speed and magnitude. At this stage some important distinctions should be made. Only in situations of just MD, or a small offset (strabismus) prior to MD, did the network recover to the exact state that was present *before* deprivation (i.e. binocular and stable). In all other cases any cells binocular prior to MD recovered first and to the greatest extent. However, those cells that were monocular prior to MD remained dominated by the NDE during recovery from MD (regardless of their pre-MD eye preference), or in the case where the offset was reduced during recovery, sometimes became binocular.

This level of precision with regards to the exact state of ocular dominance (or orientation selectivity) of individual cells that has been analysed in the computer simulations here, was not tested in individual cells in experiments. This would be impossible, unless one recorded chronically from a single cell; even then, chronic recordings from single cells over longer periods of time (days) suffer from degeneration of response quality and responses are often lost altogether. Only OD and OS of large groups of cells before and after MD were studied in experiments, so certain caveats must be taken when comparing simulation to experiment, in particular to the extent of 'recovery' under different conditions. With this in mind, overall comparisons between BCM learning and experimental results can be made. Comparisons of the relative time between the two learning rules, for the loss of DE responses, were the same in both learning rules. When an image offset was introduced

("strabismus"), binocularity broke down with the BCM rule yet with PCA learning binocularity was never lost. With an image offset and MD, the BCM model predicted up to 6 days for NDE to dominate the cortex, while PCA just 24hrs. Recovery of DE responses after MD was more difficult for either model to predict compared to that shown in experiment.

The above trends *do* match the experimental data; namely that the larger the angle of squint during recovery from MD, the lesser the recovery of the DE (Kind *et al*, 2002), and the larger the squint angle prior to MD the longer the recovery of the DE took (see Chapter 2). Finally, a large angle of squint prior to MD prevented a complete OD shift (see Chapter 2) towards the NDE after MD, which in part was predicted also in simulation.

Taken together, the data from simulation and experiment clearly shows that the BCM model produces results that are much closer to experimental results in this thesis in *outcome* and *relative timing* than PCA learning. In general, the BCM model is in agreement with biological findings: Oriented receptive fields with various degrees of binocularity emerge (Hubel *et al* 1962; Van Sluyters and Levitt 1980). This conclusion is supported by earlier comparisons of simulations and experiments for deprivation paradigms - MD, BD, RO (Clouthiaux *et al* 1991; Blais 1998; Blais *et al* 1999; Law and Cooper 1994). With reference to classical experiments; more noise into the closed eye during deprivation, the slower the response, which is the opposite what occurred during an experiment (Rittenhouse *et al* 1999). During MD and RO, times are identical for loss and recovery of responses, yet in experiment recovery during RS took longer than in MD (Mioche and Singer 1989).

Biological basis of theoretical models

Experimental verification for synaptic plasticity has occurred mainly in the hippocampus, but also in visual cortical slices. Experimental verification of memory storage (a small, yet consistent modification of synapses' neuronal selectivity to a particular input pattern), was found by Bliss and Lomo (1973) and Bliss and Gradner-Medwin (1973). The dentate area – part of the hippocampus, was stimulated with high frequency electrical pulses, then tested with low frequency simulation. After high

frequency stimulation, the tested response was higher than before and lasted a long time. In later experiments by Kirkwood and Bear (1995), the opposite was shown using low frequency stimulation. Both results were predicted by the BCM theory. Bear *et al* (1987) had previously suggested that θ might be related to the membrane potential at which the NMDA receptor mediated Ca^{2+} influx reaches the threshold for induction of synaptic long-term potentiation. Experimental verification for the sliding modification threshold came from studies in the visual cortex of dark reared animals. Tested over a range of stimulation frequencies, in the visual cortex of animals reared in complete darkness, LTP was enhanced and LTD diminished. Moreover, even brief periods of light exposure in dark reared animals was enough to return the magnitude of LTD to nearly normal levels (Kirkwood *et al* 1996), provides further evidence that the modification threshold slides as a average cortical activity increases. Abolishing all (including spontaneous) retinal activity by intraocular injection of tetrodotoxin, results in a lesser depression of deprived eye responses than merely closing the eye and leaving spontaneous activity intact (Rittenhouse *et al* 1999). Therefore, the more noise is present in the input the faster the loss of responses as predicted by BCM simulation.

CHAPTER 5

METHODS

As in the set of reverse occlusion experiments described in Chapter 3, MD in simulations was initiated early in the RE and lasted from P14-P35. At P35, one of 3 further manipulations of visual input was carried out: Immediate reverse occlusion (RO), an intermediate period of 4 days of binocular vision (4DBV) followed by RO, or an intermediate period of 4 days of de-correlated vision (4Ddecor) followed by RO. In the present simulations, recovery from each of these regimens was studied on a time scale similar to the actual experiments. De-correlated vision in the two eyes was achieved by offsetting the image in one eye by 4 pixels and a vertical rotation of the image by 4 pixels in the other eye (i.e. vertical image offset). In experiment, de-correlation of inputs was achieved by using convergent prisms in each eye (neither eye looking straight); however, in the 'Plasticity' program, the software available at the time allowed image offset only in one direction. Therefore to achieve a scenario where neither eye would be seeing a 'normal' visual scene, one image was offset and the other rotated.

Monocular deprivation, image offset, learning rate and memory constant were applied as described in Methods (Chapter 4).

RESULTS

BCM learning

Immediate reverse occlusion

The time course and eventual outcome of the early, extended period of initial deprivation (P14-P35) were very similar to those seen with a briefer and later onset of MD (see Chapters 3 and 4). Figure 5.1a shows the network after early MD and is highly comparable to that from later MD (see fig. 4.9 from Chapter 4).

Upon restoring vision to the DE, the NDE was deprived of vision for 18 days.

After 24 hours, a small but appreciable decrease in the response of the ONDE had occurred. The threshold has risen minimally and stabilised below its previous level. A slight OD change in all cells was seen at this point. After 48 hours, the response of the ONDE had decreased to a very low level as had the tuned response. Figure 5.1b shows the network at 72hrs; the OD shift to favour the ODE at this stage was advanced. The ODE dominated a majority of the network. In several cells, responses were still weak and neither eye dominated. After 4 days of RO the transition was complete, the ONDE response had been lost completely, and the network was stable (refer to Fig. 5.1c after 18 days RO). No further changes occurred during the rest of the RO period. Of note, unlike MD, where a cell's orientation preference was restored to that observed before deprivation, after RO, orientation preference was the same for all cells.

Recovery from immediate RO

Recovery from RO started only a few hours after restoring binocular vision. Orientation tuning through the ONDE (recently deprived eye) started to reappear and OD changes were visible. Within 12 hours the ODE tuning response had decreased while that of the ONDE had increased. Within 24 hours, complete recovery of ONDE parameters had occurred (Fig. 5.1d) and the network was binocular and stable. Overall, recovery from RO was on the same time scale as recovery from MD. Of note, after the period of RO, orientation preference of all cells was the same (Fig. 5.1d)

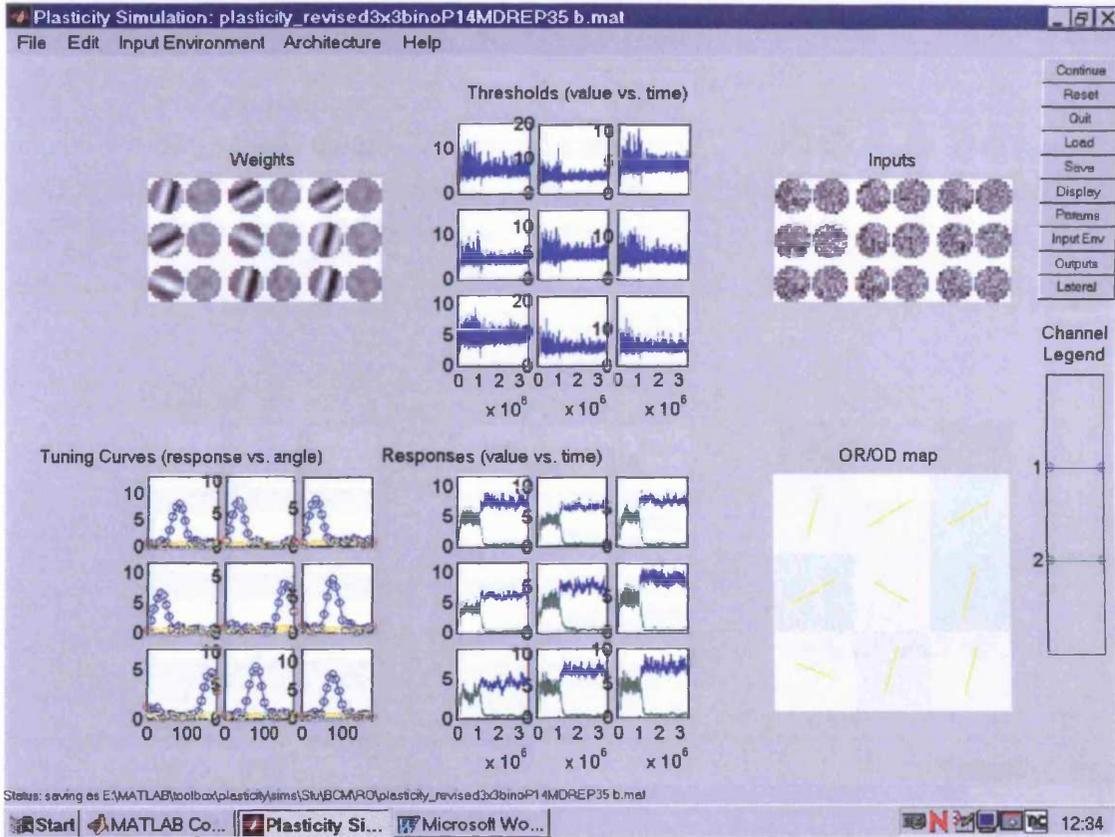


Figure 5.1 a State of BCM model simulation after MD in RE P14-P35

The time course and eventual outcome of the early, extended period of initial deprivation were very similar to those seen with a briefer and later onset of MD (in Chapter 4). Deprived eye responses have decreased dramatically, while those through the NDE have increased. The network is dominated by the NDE in all parameters.

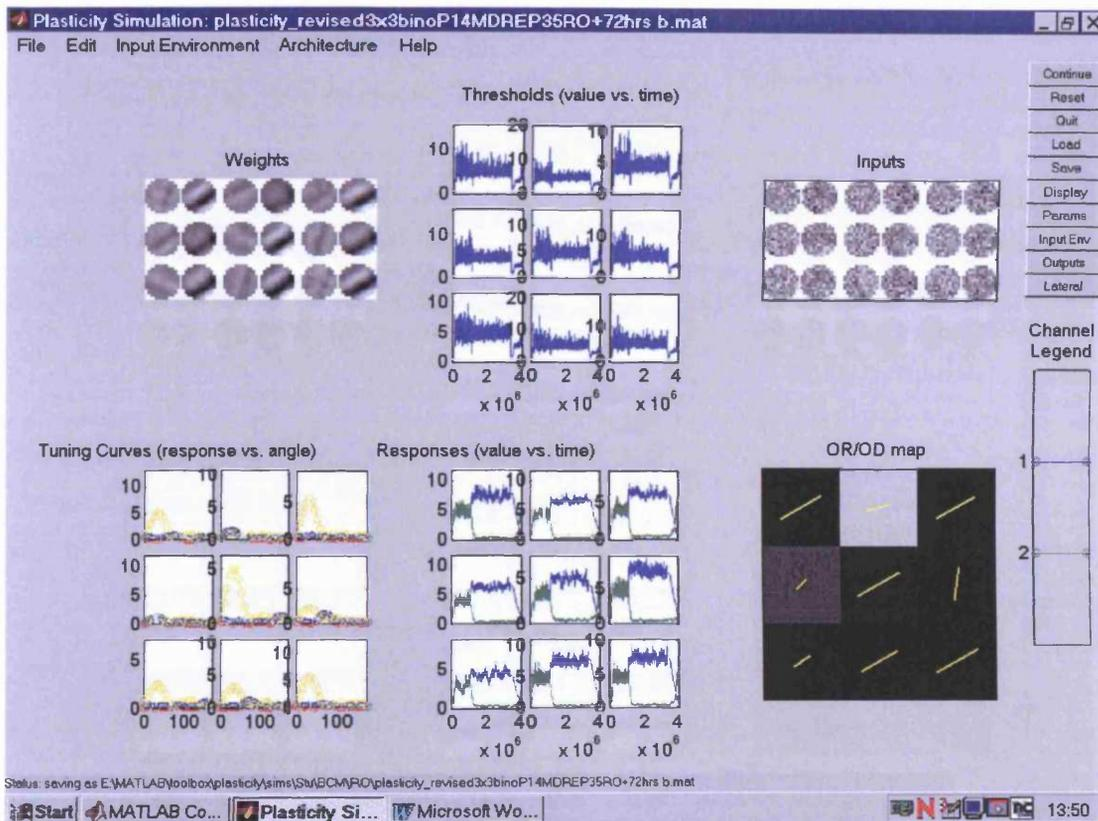


Figure 5.1 b State of BCM model simulation after 3 days of (out of 18) RO

After 24 hours, a small decrease in the response of the ONDE had occurred. After 48 hours, the response of the ONDE had decreased to a very low level as had the tuned response. At 72hrs, the OD shift to favour the ODE was advanced. The ODE dominated a majority of the network. In several cells responses were still weak. After 4 days of RO the transition was complete, the ONDE response had been lost completely, and the network stable.

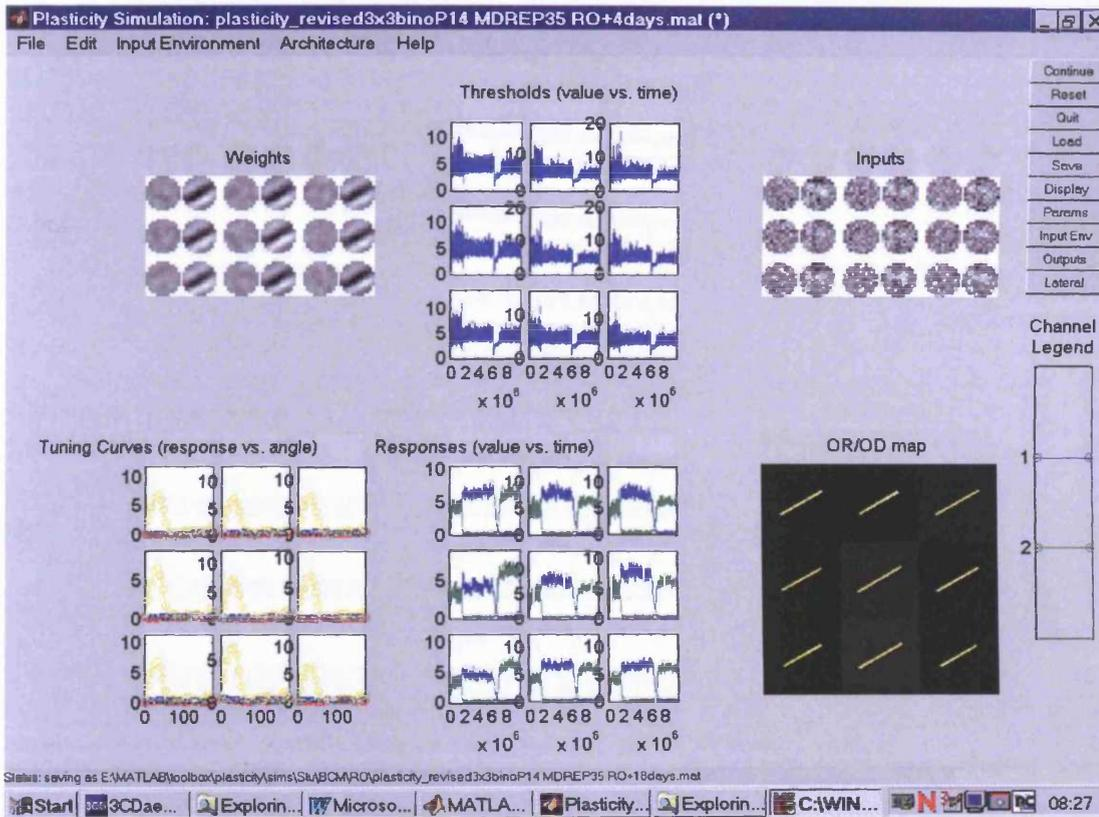


Figure 5. 1c State of BCM model simulation after 18 days RO

The network was dominated by the ODE in every parameter. Unlike MD; where a cell's orientation preference remained intact after deprivation, after RO; orientation preference was the same for all cells.

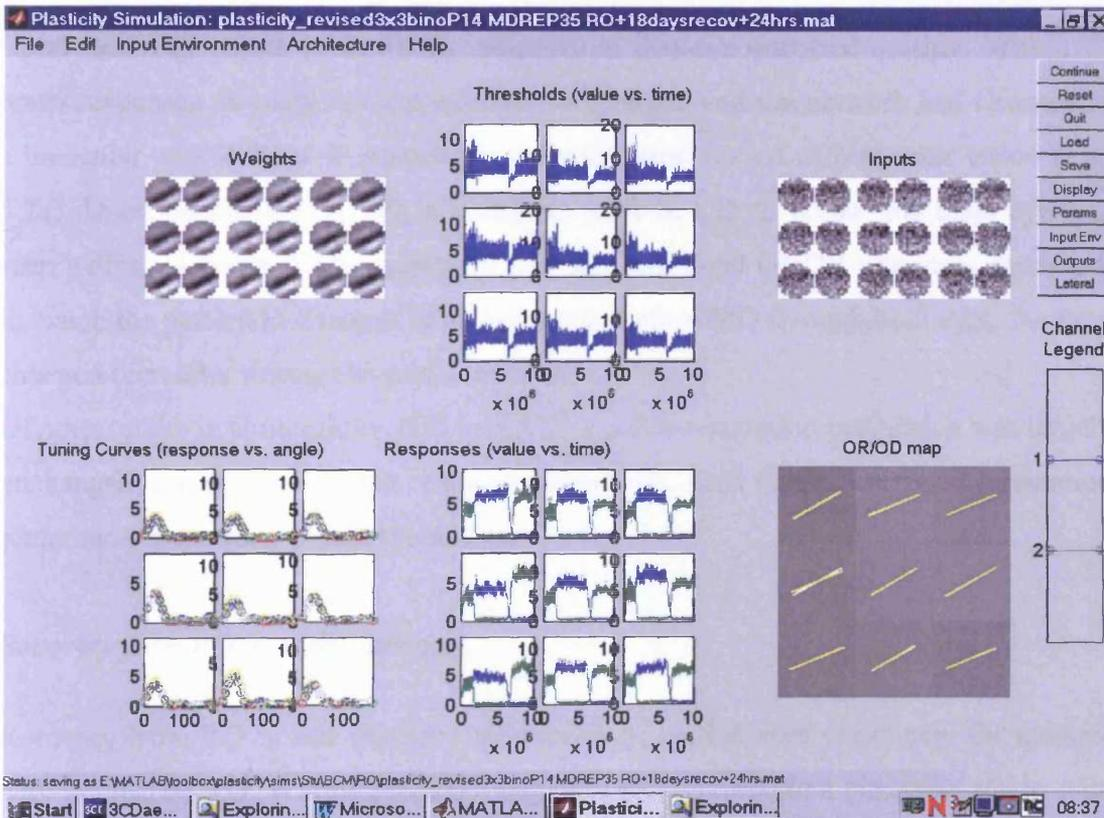


Figure 5.1 d State of BCM model simulation after; 18 days RO, then 24hrs of binocular recovery

Recovery from RO started to occur only 3hrs after restoring binocular vision. Within 12hrs the ODE tuning response had decreased while that of the ONDE had increased. Within 24hrs complete recovery of ONDE had occurred. The network was binocular and stable. However, orientation preference did not return to pre-RO state and remained the same for each cell.

unlike under normal conditions or MD where the variety of orientation preferences observed initially remained unchanged (see Fig. 5.1a after MD).

Four days of binocular vision between the first and second period of MD

Upon restoring vision to the ODE, recovery of that eye occurred quickly. Within 24 hours responses through the two eyes had converged and the network had returned to a binocular, stable state. It remained so for the brief period of binocular vision (Fig. 5.2a). Upon implementing RO, a complete shift in OD to favour the open eye was seen within 24 hours. ODE responses had increased and ONDE responses decreased to match the pattern in changes in activity seen before MD through both eyes. Nothing changed thereafter during the period of RO.

Of note, unlike in simulations with just RO, a cell's orientation preference was largely unchanged during the RO and restored afterwards, such that a variety of orientation preferences were seen within the network.

Recovery from RO in 4DBV animals

Recovery from RO in this instance was identical to that seen previously for animals with immediate RO. Within 24hrs the network had returned to a binocular stable state (Fig. 5.2b). Orientation preference of cells remained unchanged from that present before any visual manipulation.

Four days of de-correlated vision between first and second period of MD

An intermediate period of de-correlated vision resulted in no change in the state of the network from that seen right at the end of the initial period of MD. That is, no ODE recovery occurred and the network remained dominated by the ONDE in all parameters. During 18 days of RO, changes took longer than in simulations with immediate RO (Fig. 5.1 b and c). Some minor changes in parameters were seen after 24hrs, i.e. decrease in tuned response through the ONDE. Within 3 days of RO, ONDE responses had decreased to a level similar to the ODE (Fig. 5.3a). Orientation tuning through the ODE and ODE and synaptic weights were still weak in most cells. After 4 days, responses through the ODE started to increase in some cells. It took 5-6

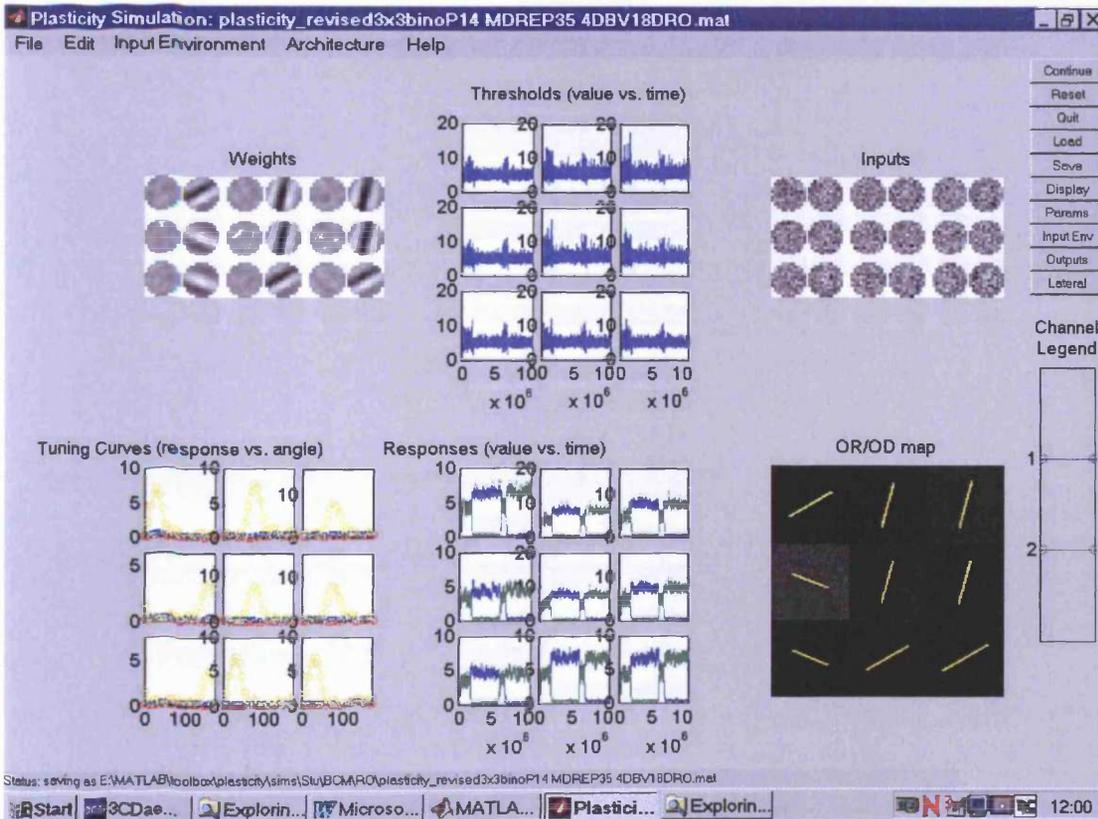


Figure 5.2 a State of BCM model simulation after; 4DBV followed by 18 days RO

Within 24 hours responses had converged and the network had returned to a binocular, stable state. Upon implementing RO, initial changes in OD and orientation tuning through both eyes occurred after 12 hours, with a complete shift of parameters to favour the open eye was seen within 24 hours.

Of note, unlike simulations with just RO, a cell's orientation preference remained intact during the RO and varied over the network.

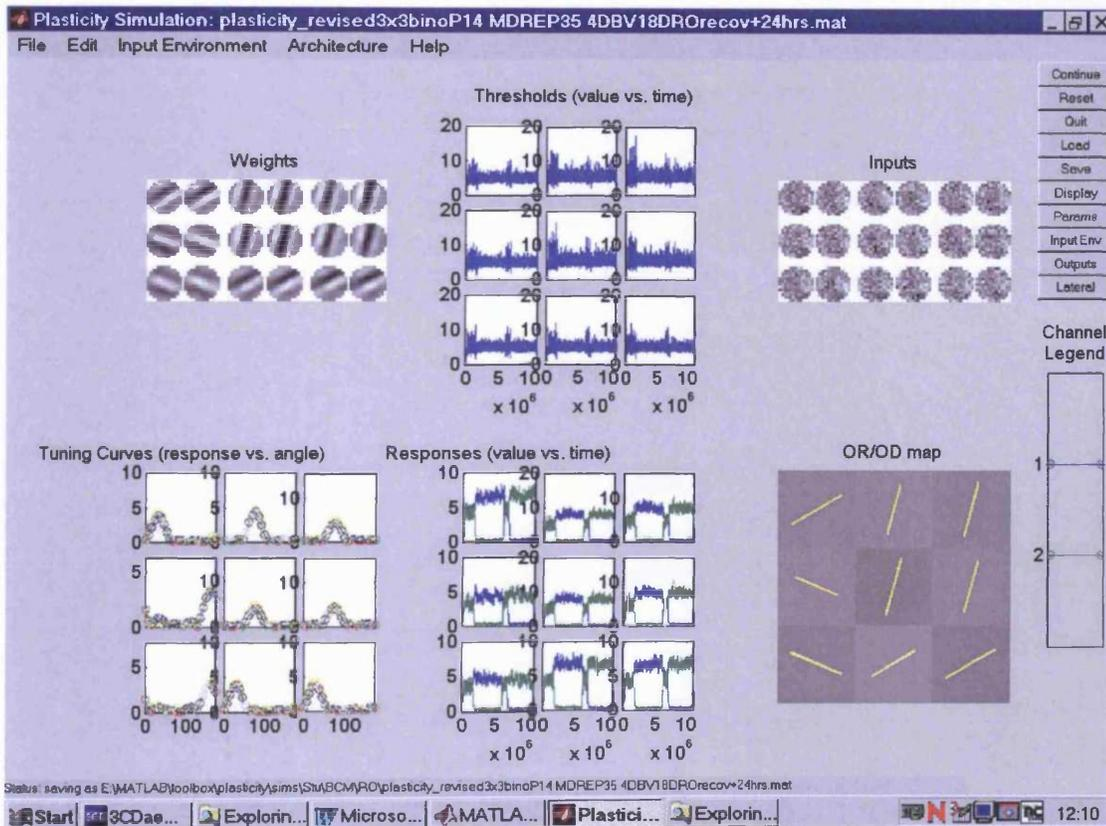


Figure 5.2 b State of BCM model simulation after; 4DBV followed by 18 days RO, then 24hrs of recovery

Recovery from RO in this instance was identical to that seen previously with immediate RO. Within 24hrs the network had returned to a binocular stable state. Orientation preference of cells remained unchanged.

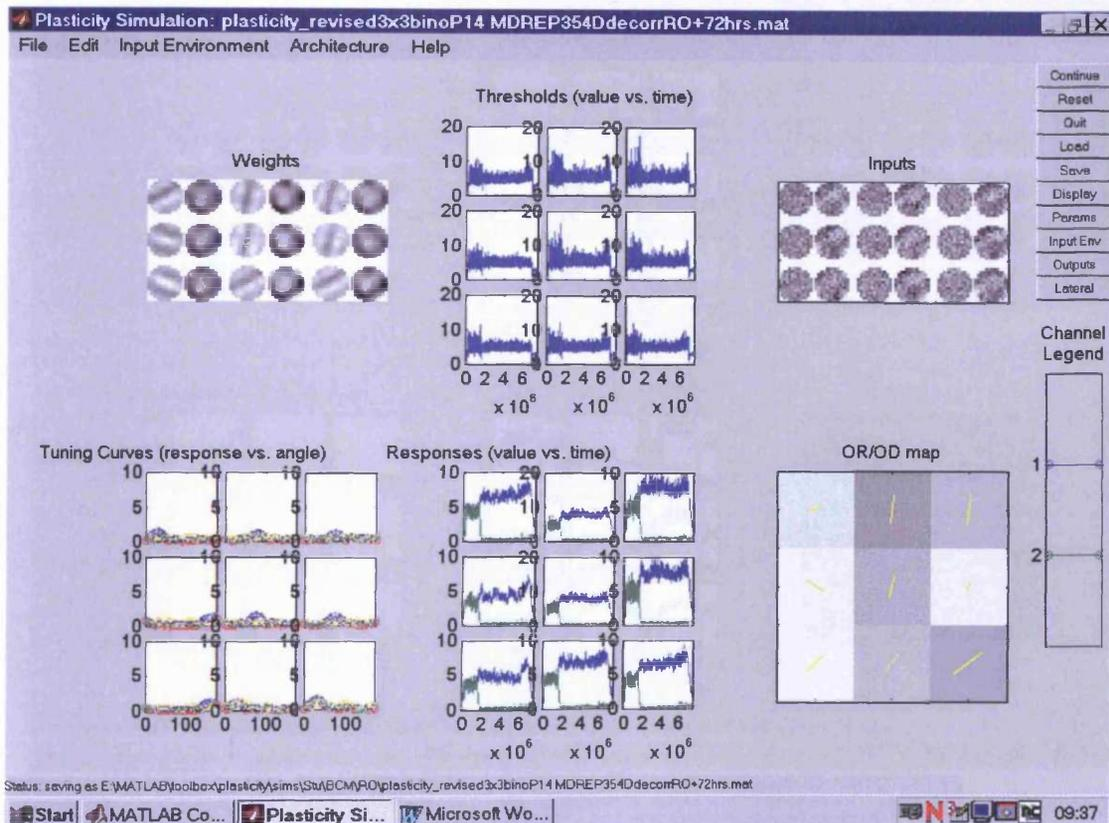


Figure 5.3 a State of BCM model simulation after; 4Ddecor followed by 3 (of 18) days RO

An intermediate period of de-correlated vision resulted in no change in the state of the network from that seen right at the end of the initial period of MD. That is, no DE recovery occurred and the remained dominated by the NDE in all parameters.

During 18 days of RO, changes took longer than in simulations with immediate RO (fig 4.1 b and c). Within 3 days of RO, ONDE responses had decreased to a level similar to the ODE. Orientation tuning through the ODE and ODE and synaptic weights were still weak in most cells. After 4 days responses through the ODE started to increase in some cells. It took 5-6 days for the network to become completely dominated by the ODE and stable.

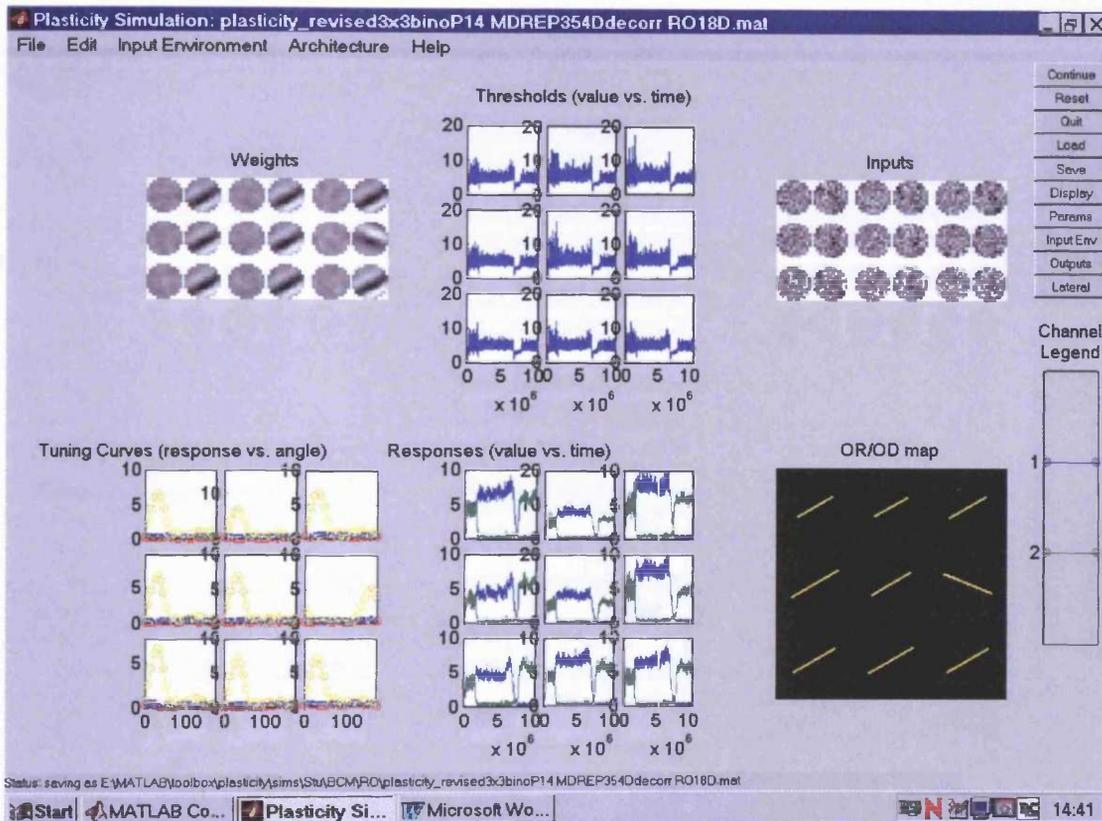


Figure 5.3 b Example of screenshot from BCM learning at time (t)= P57 after 4Ddecorr vision, the 18D RO

Normal rearing up to P14 then MD in the RE up to P35. Upon restoring vision to the RE both eyes, vision was de-correlated for 4 days then the LE was deprived of vision for 18 days.

Four days of RO and DE responses had decreased to a similar level of the ODE and that eye's response has increased, yet divergence of responses was not complete in all cells. Orientation tuning and synaptic weights were still weak in several cells. It took 7 days for responses to completely diverge and the network to become stable.

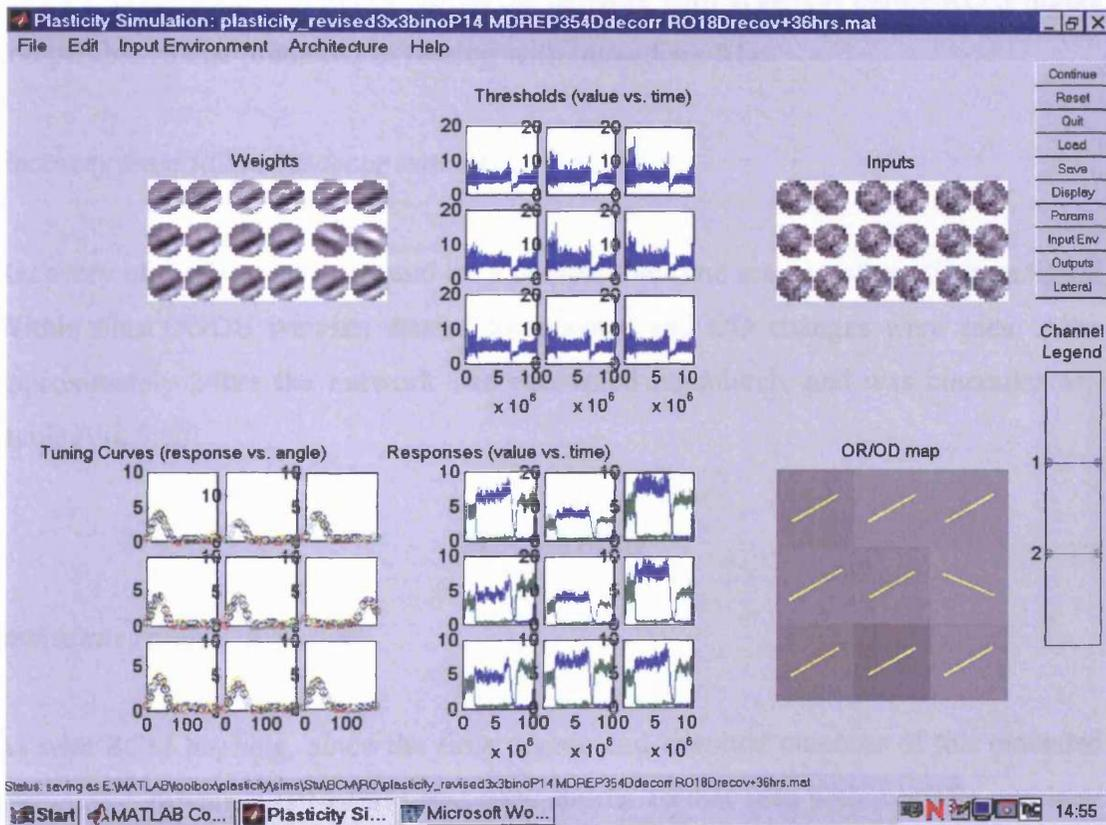


Figure 5.3 c State of BCM model simulation after; 4Ddecorr followed by 18 days RO, then 36hrs binocular recovery

Recovery of the DE was swift and on a comparable time scale to other RO paradigms. Within 6hrs ONDE weights started to increase and OD changes were seen. After 24-36hrs the network had recovered completely and was binocular and stable.

days for the network to become completely dominated by the ODE and stable (fig. 5.3 b after 18D RO). Orientation preference was very similar in 8/9 cells in the network at this stage. This contrasts to that predicted by simulations where 4DBV was followed by RO; where varied orientation preference was predicted after RO. The almost identical orientation preference across the network with 4Ddecor before RO is highly comparable to that predicted in rearing with immediate RO.

Recovery from RO in 4Ddecor animals

Recovery of the DE was swift and on a comparable time scale to other RO paradigms. Within 6hrs ONDE weights started to increase and OD changes were seen. After approximately 24hrs the network had recovered completely and was binocular and stable (Fig.5.3c).

PCA learning

Immediate reverse occlusion

As with BCM learning, since the time course and eventual outcome of this extended period of deprivation (P14-P35) was very similar to that seen with a briefer and later onset of MD, the simulation in Chapter 4 of a 10-day period of MD (P35-45, see Fig. 4.9a) was used for subsequent qualitative comparisons.

Upon implementing RO, within 6 hours changes started to occur. Responses through the ONDE decreased quickly and those through the ODE increased quickly (from the low level immediately after the initial deprivation). The modification threshold briefly dropped very low during the transition but quickly recovered to the pre-RO level. Oriented responses became broadly tuned, with some cells losing selectivity all together. At this point OD started to change (Fig. 5.4a). Within 12 hours a complete OD shift had occurred, but synaptic weights and orientation selectivity continued to change. After 36-48hours all weights reached a stable symmetrical state for each eye in all cells (Fig. 5.4b). Orientation preference through the ODE was now identical for all cells. Hereafter the network was stable.

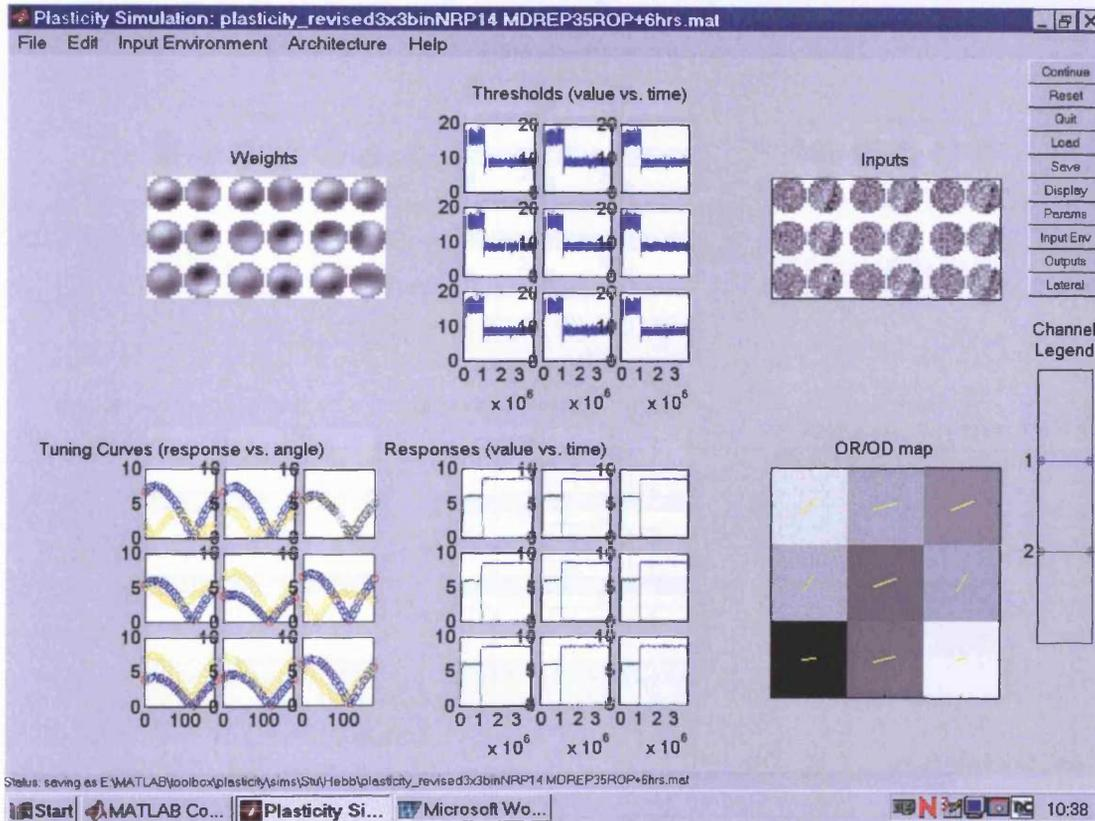


Figure 5.4 a State of PCA model simulation after 6hrs of RO

Upon implementing RO, within 6 hours changes started to occur. Responses through the ONDE decreased quickly and those through the ODE increased quickly (from the low level immediately after the initial deprivation). The modification threshold briefly dropped very low during the transition but quickly recovered to the pre-RO level. Oriented responses became broadly tuned, with some cells losing selectivity all together. At this point OD started to change.

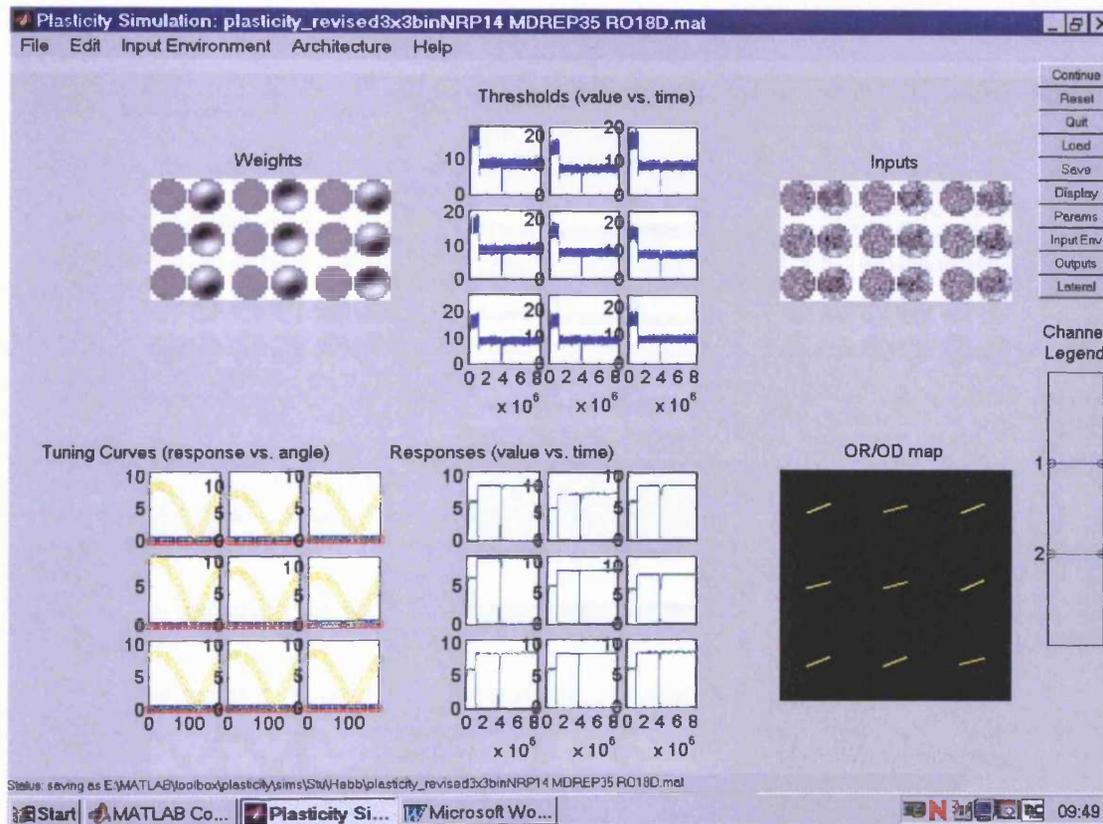


Figure 5.4 b State of PCA model simulation after 18 days of RO

Within 12 hours a complete OD shift had occurred but synaptic weights and orientation selectivity continued to change. After 36-48 hours all the weights reached a stable symmetrical state for each eye in all cells. Orientation preference through the ODE was now identical for all cells. Hereafter the network was stable.

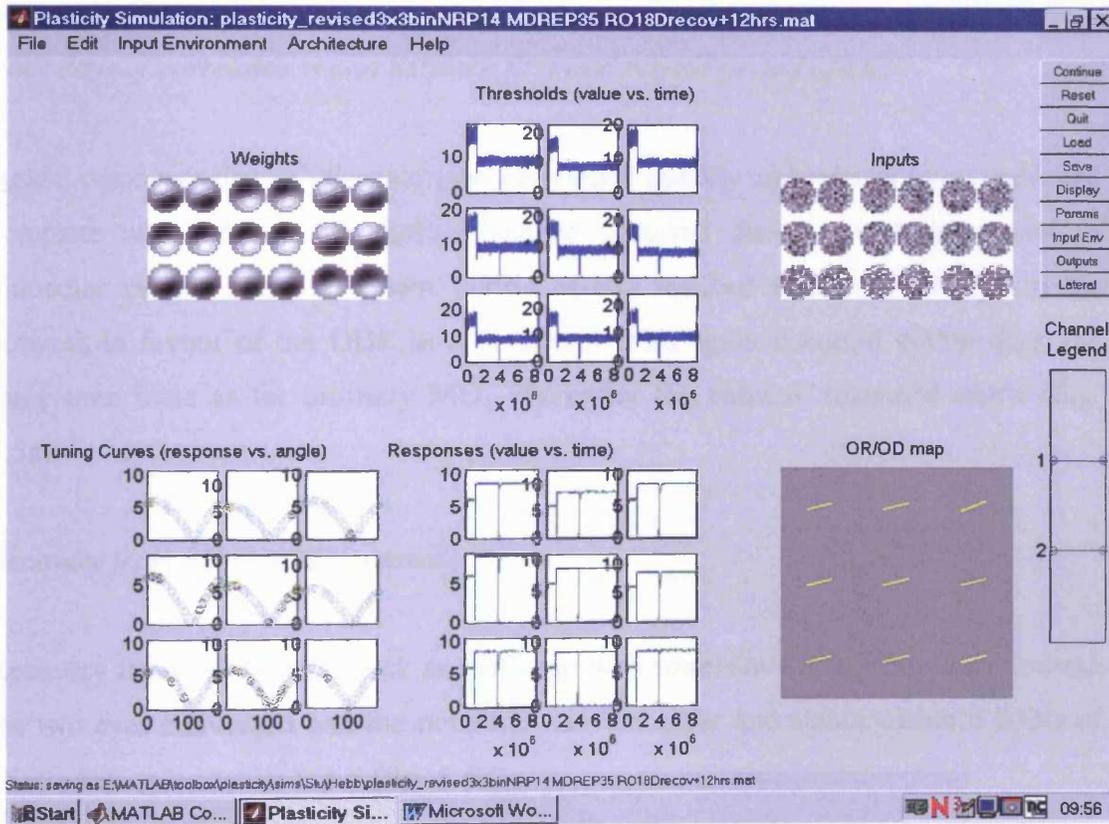


Figure 5.4 c State of PCA model simulation after; 18 days of RO, then 12hrs of binocular recovery

Recovery from RO was very quick. Responses had converged, the network was binocular and stable within 6hours of reintroducing binocular input.

Recovery from immediate RO

Recovery from RO was swift. The level of responses through the two eyes equalised, and the network was binocular and stable within 6 hours of re-introducing binocular input (Fig.5.4c).

Four days of correlated vision between first and second period of MD

Again, responses through the two eyes converged quickly and recovery was swift and complete within 6 hrs. No further change occurred during the 4-day period of binocular vision. The subsequent period of RO resulted in a swift change in the network in favour of the ODE in all respects. This again occurred within 6hrs, the same time scale as for ordinary MD. Thereafter the network remained stable (Fig. 5.5a).

Recovery from RO in 4DBV animals

Recovery from RO was as quick as that seen with immediate RO. Responses through the two eyes converged and the network was binocular and stable within 6 hours of reintroducing binocular input (fig. 5.5b).

Four days of de-correlated vision between first and second period of MD

This scenario presented a dichotomy in results from the state immediately after the early deprivation in the RE. The eye that received the rotated image for the 4 days was ultimately disadvantaged the most and the other eye came to dominate the cortex (i.e. regardless whether the ONDE or ODE was rotated). For example if the rotated image was in the LE; some ODE input (LE) returned. After 12hrs ODE weights and orientation tuning had improved noticeably. In less than 24hrs the network was binocular. Orientation tuning matched through both eyes and synaptic weights were almost equal. However, after 48hrs the ONDE responses had weakened, and the ODE responses had increased in amplitude, so the network was now dominated by the ODE (Fig. 5.6a). No further changes were seen over the subsequent 48hrs. If the rotated image was in the RE, some input returned to the ODE after 3hrs. This increased

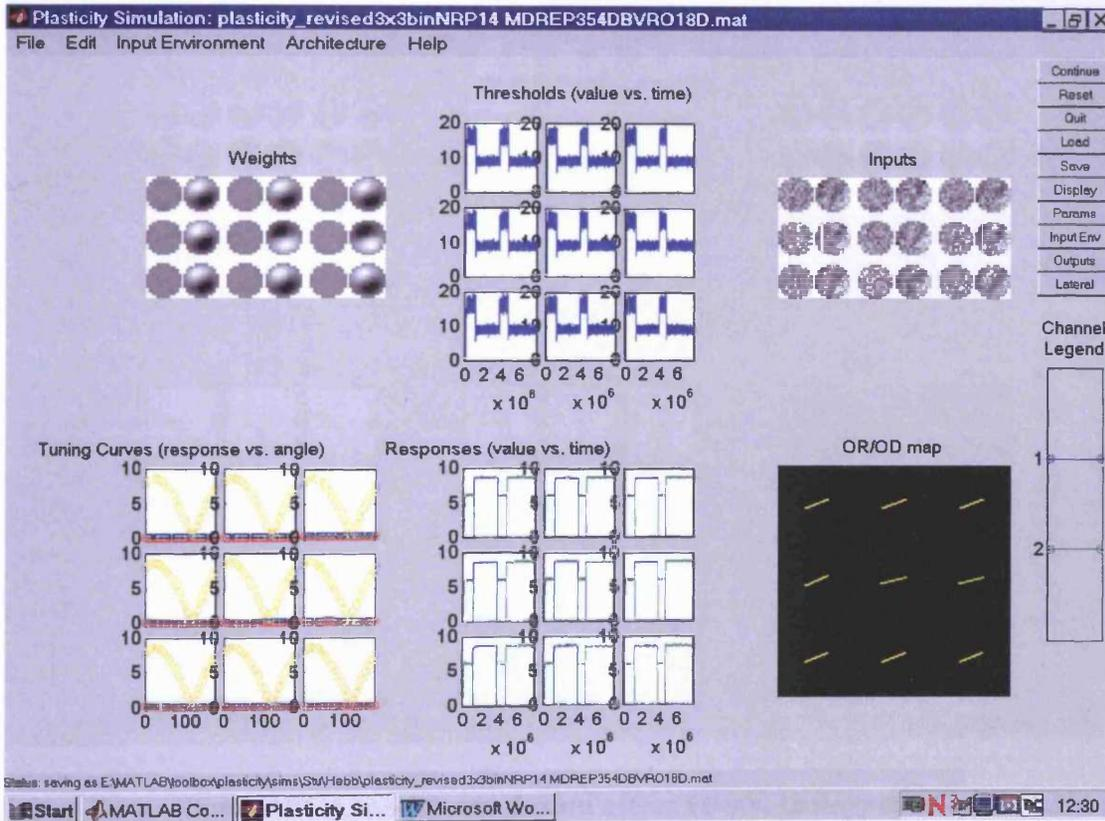


Figure 5.5 a State of PCA model simulation after; 4DBV, then 18 days of RO

With the onset of 4DBV, responses converged quickly; recovery of the ODE was swift and complete within 6hrs. RO resulted in a swift change in the network away from the ONDE. This occurred within 6hrs, the same time scale to that of a normal period of MD. Thereafter the network remained stable.

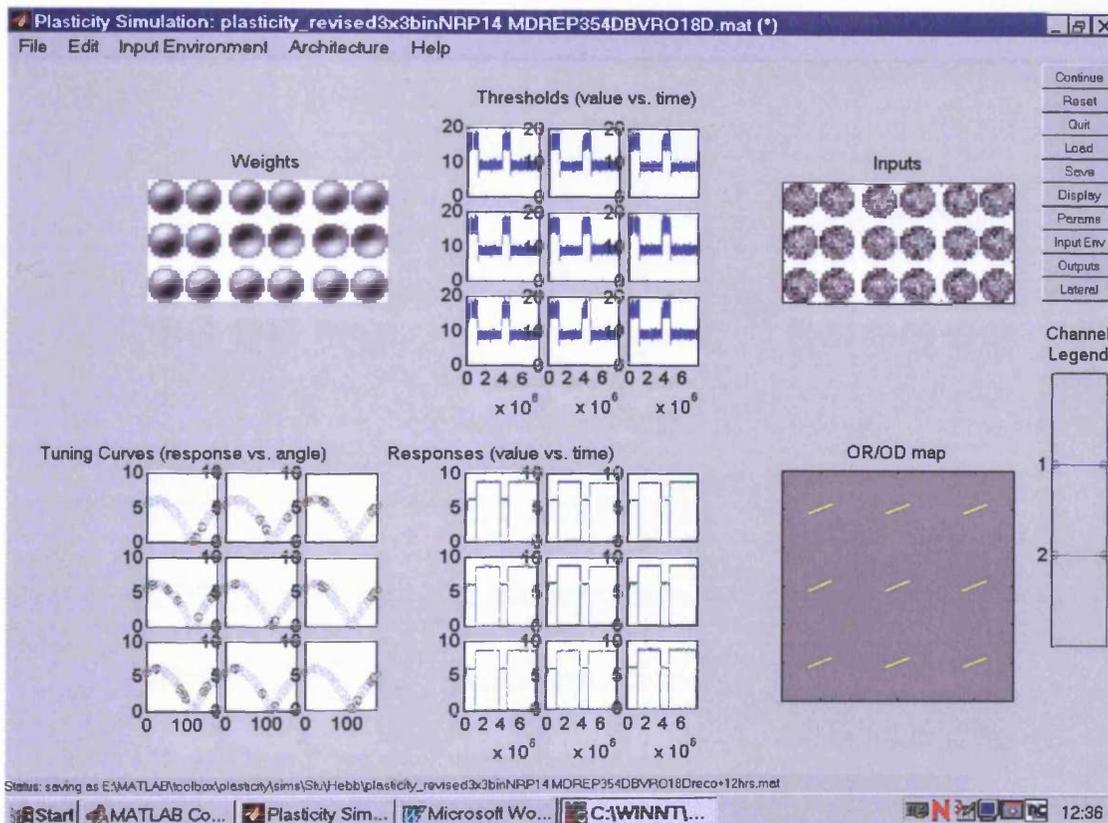


Figure 5.5 b State of PCA model simulation after; 4DBV, 18 days of RO, then 12hrs of binocular recovery

Recovery from RO was as quick as in other RO paradigms. Responses had converged, the network binocular and stable within 6hours* of reintroducing binocular input. This occurred within 6hrs, the same time scale to that of a normal period of MD. Thereafter the network remained stable.

*Network is shown at 12hrs to allow changes in parameters to be seen more clearly on such a small timescale.

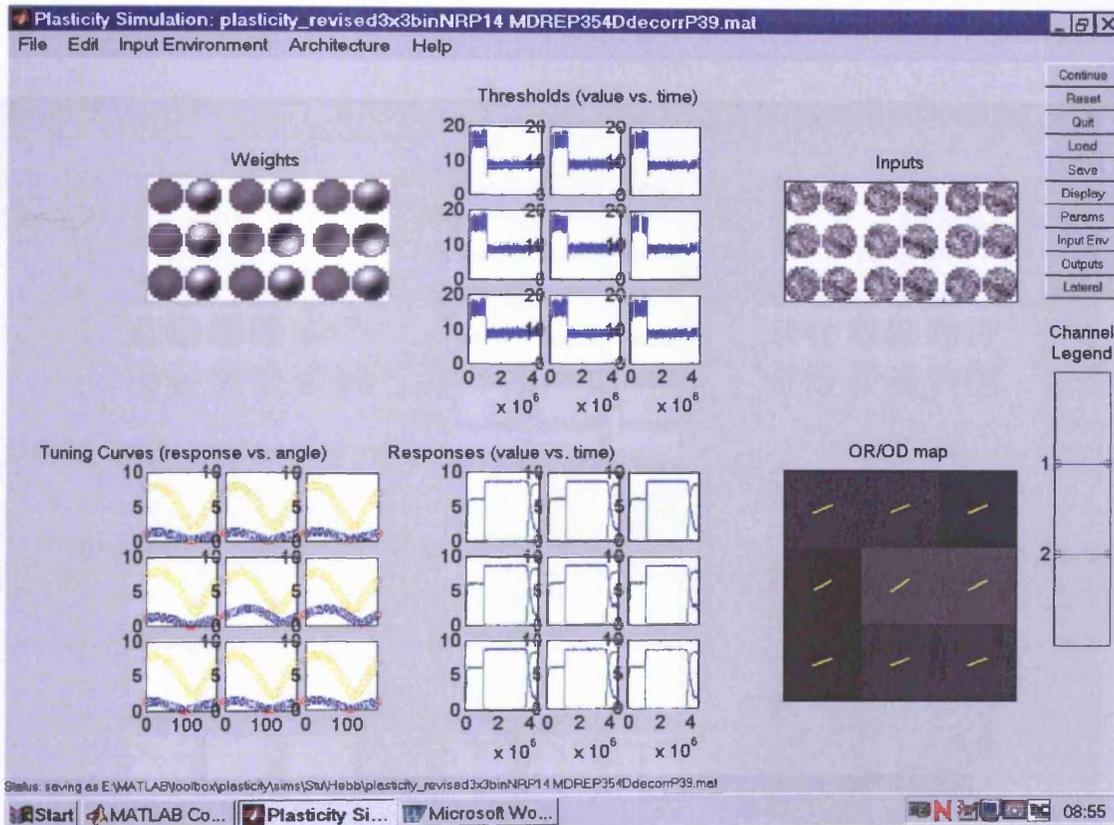


Figure 5.6 a State of PCA model simulation after 4D de-correlated vision

After 12hrs RDE weights and tuning are improving notably. In less than 24hrs the network was binocular. However, after 48hrs responses had diverged again, so the network was now dominated by the RDE. Non-deprived eye responses had weakened although still obvious. No further changes were seen over the subsequent 48hrs.

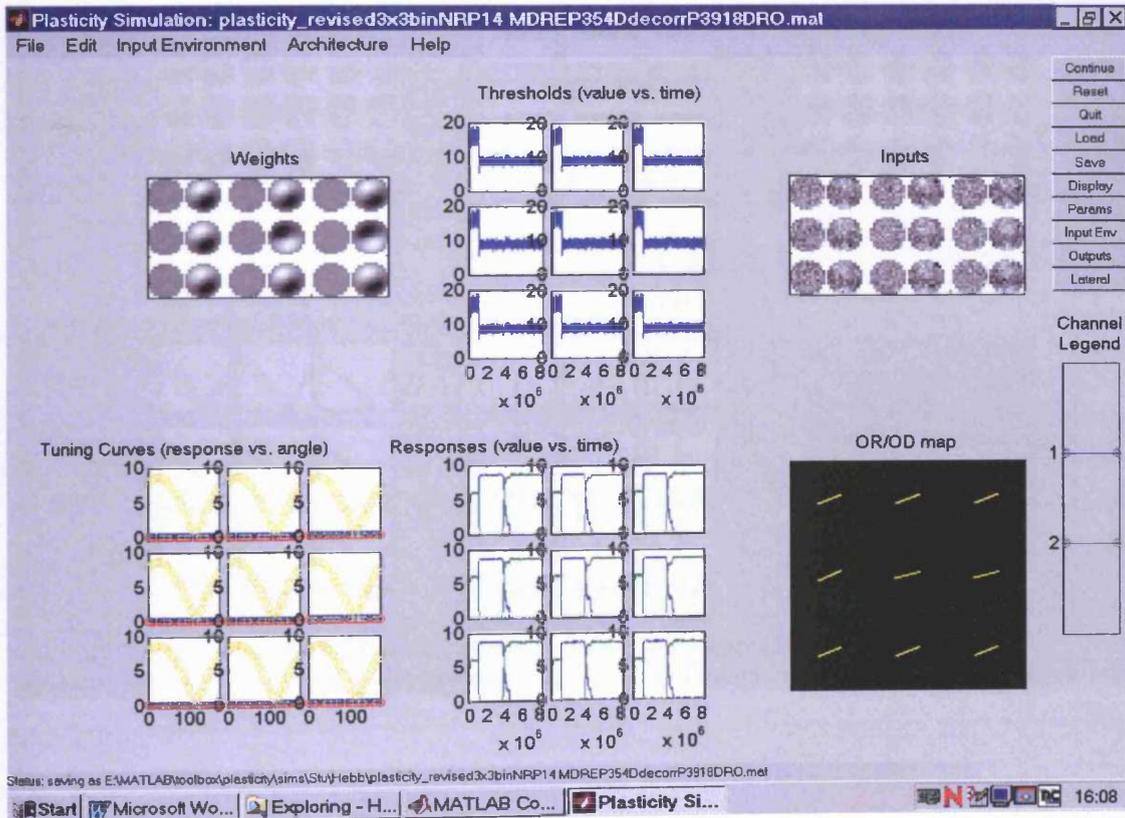


Figure 5.6 b State of PCA model simulation after; 4D de-correlated vision, then 18D RO

Upon introducing RO, the residual ONDE responses were quickly lost and the network was completely dominated by the ODE within 6hrs .

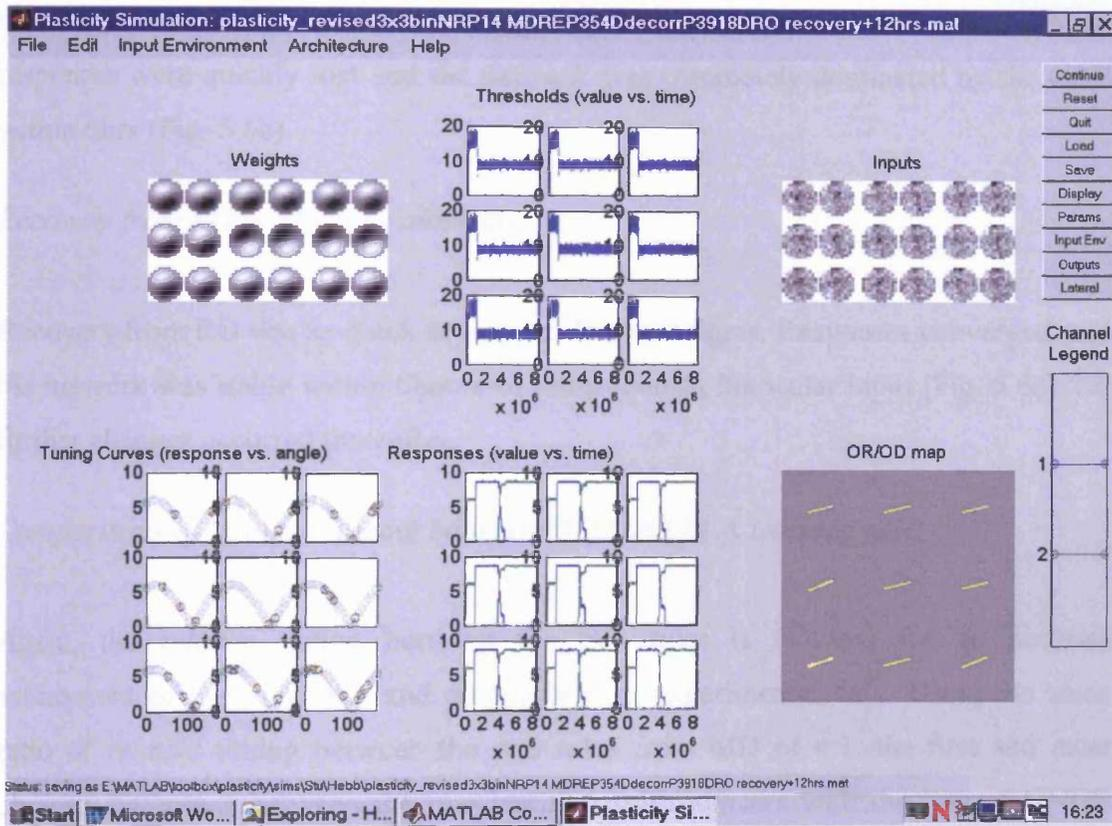


Figure 5.6 c State of PCA model simulation after; 4D de-correlated vision, then 18D RO, then 12hrs of binocular recovery

Recovery from RO was as quick as in other RO paradigms. Responses had converged, the network binocular and stable within 6hours of reintroducing binocular input.

marginally within the next 24hrs to about 1/3 of the LE. The recovery of the ODE did not progress any further and the cortex remained dominated by the ONDE.

Although the above result casts some doubt over the suitability of the rotation in this paradigm, no such problems were encountered with BCM learning. Moreover, despite the above dichotomy, upon introducing RO, in both instances the residual ONDE responses were quickly lost and the network was completely dominated by the ODE within 6hrs (Fig. 5.6b).

Recovery from RO in 4Ddecor animals

Recovery from RO was as quick as in other RO paradigms. Responses converged, and the network was stable within 6hours of reintroducing binocular input (Fig. 5.6c). No further changes occurred thereafter.

Comparisons of 'relative' timing between BCM and PCA learning rules

Again, the *relative* timing between the two rules is required for an accurate assessment of their viability and comparison to experimental data. Using the same ratio of *relative* timing between the two rules from MD of 4:1, the first and most obvious difference between the two learning rules appears with the loss of ONDE responses during RO. The BCM rules predicted 2-3 days for the loss of ONDE responses before the ODE began to recover, while PCA^r (relative timing of PCA compared to BCM) predicted the loss of ONDE responses within 24hrs. Moreover, the recovery of ODE responses began before the ONDE responses had decreased appreciably (similar to MD) and were complete within 24-48hrs. Although the overall relative time scale of changes are not vastly different between learning rules, the important difference is that the loss of ONDE responses has been shown in experiment to occur *before* any changes in ODE responses can occur. Mioche and Singer (1989) suggested that it was at least 24-48hrs of RO was required for the loss of ONDE responses, and that at least 24hrs before any ODE responses reappear (Table 4). Complete recovery of ODE responses would most likely take several days, which in this comparison is most accurately predicted by the BCM model. The PCA rule fails to predict the loss of ONDE response occurring appreciably *before* ODE response increases.

Visual manipulation	BCM	PCA	Experimental results
Reverse Occlusion	Loss of ONDE responses 2-3 days. Recovery of ODE responses 3-4 days. Recovery from RO – ONDE responses within 24hrs.	Loss of ONDE responses <6hrs. Recovery of ONDE responses begin <6hrs. Complete recovery >12hrs. Recovery from RO – ONDE responses within 6hrs.	24-48hrs before complete loss ONDE responses. At least 24hrs before ODE responses re-appear (Mioche and Singer 1989). Recovery of ONDE is disrupted and incomplete after 3 days. ODE dominates (Chapter 2). Recovery from RO generally resulted in bilateral amblyopia (Murphy <i>et al</i> 1986, 1987, Mitchell 1991).
4DBV	Recovery of ODE responses within 24hrs during BV. Loss of ONDE during RO within 24hrs. Recovery after RO of ONDE within 24hrs.	Recovery of ODE responses within 6hrs during BV. Loss of ONDE during RO within 6hrs. Recovery after RO of ONDE within 6hrs.	Recovery of ODE responses substantial yet incomplete after 4 days (Chapter 2). Incomplete recovery from early MD (Liao <i>et al</i> 2004). Recovery of ONDE responses after RO within 3 days (Chapter 2).
4Ddecorr	No recovery of ODE responses during BV. Loss of ONDE responses took 3 days during RO. Recovery of ODE responses took 5 days. Recovery of ONDE after RO took 24hrs.	ODE or ONDE dominated the cortex during 4DBV (depending on which eye had greatest disadvantage). Loss of ONDE responses <6hrs. Recovery of ONDE responses begin <6hrs. Complete recovery >12hrs Recovery from RO – ONDE responses within 6hrs.	Recovery of ONDE is disrupted and incomplete after 3 days. ODE dominates (Chapter 2).
Binocular Deprivation	Selectivity is lost and responses reduced (Blais 1998).	Weights perform a walkabout the normal stable state (Blais 1998).	Cortical responses reduced within 3 days (Freeman <i>et al</i> 1981).

Table 4 Comparison of loss and recovery times of the ODE and ONDE in BCM and PCA learning during simulation and that seen in experiments from the literature (RO)

Recovery of ONDE responses after RO, predicted by both models, was on the same time scale as MD; within 24hrs, and more importantly, was complete. The physiological recovery of ONDE OD shown in Chapter 3 (after immediate RO) was minimal (with near normal OS). Behavioural data generally showed bilateral amblyopia after recovery from RO (Murphy *et al* 1986, 1987; Mitchell 1991, see Table 4). Therefore, in this instance, neither model predicated the outcomes or timing of experimental data.

During 4DBV, both models predicted recovery of ODE responses on the same time scale as seen with recovery of DE responses in MD. With, subsequent RO, the deprivation was qualitatively the same as MD. However, in experiments (Chapter 3), although substantial recovery of ODE responses occurred during the 4DBV, it was not complete, in particular, recovery of ODE orientation tuning was minimal. Liao *et al* (2004) also showed that recovery from early MD was incomplete. Recovery from RO, in both models again was on the same time scale as recovery from MD (24hrs). In experiment, recovery of ONDE responses occurred within 3 days. In this scenario, neither model accurately predicted the timing or general outcome from 4BDV. Although recovery from RO (after 4DBV) was predicted, as seen in experiment, a caveat presents itself, as complete recovery was also predicted from immediate RO; a result not seen in experiment.

Finally, with 4 days of de-correlated vision, both models predicted disrupted recovery between the first period of MD and RO. The BCM rule predicted little or no recovery of ODE responses. A similar scenario was shown experimentally by Kind *et al* (2002). The PCA rule predicted disrupted recovery to some extent, but this was probably due to the nature of the offset in each eye (the rotated eye appeared to be disadvantaged the most during the 4 days of de-correlated vision – see above). An offset image in one eye and a rotated image in the other eye were used to ensure neither eye saw the same points in visual space compared to looking straight. Image offset has already been shown to have minimal effect on recovery from deprivation or effect on a subsequent period of deprivation in PCA learning (Chapter 3). Disruption only occurred through the eye that received the rotated image, therefore ultimately direct comparisons between BCM and PCA here are more problematic.

DISCUSSION

In general, the outcome of simulations with BCM learning again was consistent with experimental data, while PCA learning was not. Most noteworthy was the *relative* timing in changes to responses through both eyes during RO. While BCM learning predicted loss of ONDE responses before an increase in ODE responses, the PCA rule predicted response changes through both eyes simultaneously. Neither model accurately predicted the varying degrees of recovery from RO in the three experimental rearing paradigms.

Work in this chapter was motivated partly by the accuracy of the BCM rule to predict results from Chapter 2, but also to see if the apparent physiological importance of binocular vision in the development of normal responses through both eyes, with RO paradigms, would be predicted by either of the learning rules.

Early monocular deprivation

Early monocular deprivation (P14) was qualitatively similar in timing and outcome to late MD (P35) with both learning rules. This outcome in itself was not surprising, but was in contrast to experimental results. One of the main limitations of simulations to date is that the neuronal responses in networks are always maximal, i.e. there is no critical period or developmental change in a cell's ability to undergo LTP or LTD over time. Deprivation imposed at P14 is only a few days after the time of eye opening (in kittens) but, in simulations, within 24hrs of binocular input to a naïve network state, the cells' responses changed quickly, became binocular and stable - 'mature'. More importantly, parameters were susceptible to changes to visual input from t_0 , and susceptibility did not change with time. However, in experimental studies prior to P14, functional OD columns are indistinguishable and prior to P21 OD columns appear to form independently of visual experience (Crair *et al* 1998; Crowley and Katz 2000; Crair *et al* 2001). The layout of the orientation maps also appears to change little in the first few weeks after eye opening regardless of visual experience (Chapman *et al* 1996; Godecke *et al* 1997; Crair *et al* 1998). Therefore, in this instance both learning rules did not mimic the early visual cortex.

Immediate reverse occlusion with BCM and PCA learning

In simulation, with BCM learning, significant loss of ONDE responses occurred first, after 48hrs; ONDE responses were near '0'. Moreover, only after 48hrs had increases in ODE responses begun. A complete disconnection of ONDE responses took 2-3 days and complete recovery of ODE responses took 3-4 days. This is in line with reports by (Clothiaux *et al* 1991), and Blais (1998). All these simulation results are in good agreement with experimental results. Although some ODE responses are seen after 24hrs of RS, substantial recovery of ODE took 2-3 days (Mioche and Singer 1989). One could argue that this experimental result was perhaps an underestimate of the timing of recovery since Mioche and Singer (1989) recorded chronically from the same cells for several days and those cells could have deteriorated over time. However, the slight delay in recovery of the ODE responses during RO (compared to just reopening the DE) has been further verified more recently in behavioural studies in kittens (Mitchell *et al* 2001).

With PCA learning the difference in timing (decrease in ONDE responses before the increase in ODE responses) was not seen. Both eyes responses changed in a similar manner to that predicted for MD.

Intermediate period of vision between the first period of MD and RO in BCM and PCA learning

Recovery of ODE responses during 4DBV, in both learning rules, followed the same dynamics and timing as seen during recovery from MD (as seen in Chapter 4). The speed of this simulated recovery did not match the physiological responses observed experimentally in Chapter 3, where although substantial ODE recovery occurred during the 4DBV, it was not as complete as in animals deprived from a later age (P35); which showed complete recovery after 3 days (see also Liao *et al* 2004).

Nevertheless, the BCM rule did predict an outcome shown experimentally. When vision through both eyes was offset (de-correlated) after the initial MD, with BCM learning no ODE recovery was predicted during the 4-day period. Such a result was indeed observed, and has been shown earlier by Kind *et al* (2002) who found that de-correlating the inputs to the two eyes after a period of MD disrupted recovery. PCA

learning also showed some disrupted recovery during 4Ddecorr in some situations, but overall predicted experimental data less accurately.

In the instances where an intermediate period of vision was introduced before RO, the dynamics and timing of responses during RO were quantitatively similar to those with immediate RO. As yet this outcome in simulation has not been verified experimentally.

Recovery from RO with BCM and PCA learning was similar in all three paradigms, and was not qualitatively different from recovery from a single period of MD. Although the visual cortex has been shown to be predominantly binocular after recovery from RO (Murphy *et al* 1986) and no significant difference in binocularity between rearing paradigms was found in Chapter 3, differences in cortical territory from OI maps were apparent in experimental data which were not predicted by either model. Namely, with 4DBV, ONDE responses recovered fully, while recovery with immediate RO and 4D de-correlated vision resulted in minimal or no recovery of cortical territory. This part of the simulation was the least accurate in predicting the experimental data.

Comparisons of the relative timing between BCM and PCA learning

BCM learning more accurately reflected absolute and *relative* the timing of changes to ONDE and ODE responses in experiments than PCA learning. The *relative* timing and outcome during 4DBV and 4Ddecorr predicted by both learning rules were comparable, although the lack of ODE recovery with image offset (“strabismus”) was only predicted accurately by BCM learning.

Recovery from RO in all paradigms was predicted to be swift and complete by both models, on a time scale similar to MD. This is in contrast to experimental results, where significant differences were seen between the three paradigms after recovery from RO (Table 4). The reasons for this discrepancy between simulation and experiment are discussed below.

Of the 2 models, the more accurate was the BCM model, in particular at predicting the loss of ONDE responses before the recovery of ODE responses, as shown in experiment (Mioche and Singer 1989). In other respects however, both models failed

to predict real experimental outcomes from the three rearing paradigms seen in Chapter 3 (see Table 3).

Limitations of simulations

With such discrepancies between simulation and experimental data in mind, it should be remembered that, despite the usefulness of these simulations and the more recent introduction of realistic representations of the visual environment (Hancock *et al* 1992; Law and Cooper 1994; Liu and Shoual 1994; Shouval and Liu 1996), simulations still have shortcomings. The limitations of correlation-based learning rules (like PCA) have already been highlighted (Chapter 4 - Introduction). Some programs like 'Plasticity' have the option to include the influence of lateral connectivity. However, most previous model studies used just single cell for testing the different learning rules. Placing a single cell in a network, in theory, should not change the properties at equilibrium since the network in this instance is effectively just a collection of functionally independent cells placed together. However, changes the dynamics of the evolution of synapses during simulations of paradigms might be expected to occur. In single-cell simulations, the spontaneous activity increases and decreases with the cell's synaptic weights. In a network, spontaneous activity of one cell might be more governed by inhibitory and excitatory inputs from other cells than its own LGN input (see Clothiaux *et al* 1991). Despite this, further influences of lateral and long range connectivity between individual or groups of cells are not accounted for in the simulations presented in this thesis.

There is still debate over the degree of orientation selectivity of visual naïve cells in newborn kittens (Blakemore and Van Sluyters 1975; Fregnac and Imbert 1978). The most important shortcoming of simulations is the lack of developmental plasticity. The age of the animal has a crucial bearing on the developmental plasticity of OD and orientation selectivity. The relatively immutable development of functional properties during the first few weeks of visual experience (Crair *et al* 1998) in kittens is not predicted by simulation. During normal rearing in simulation, stable mature states of OD and orientation selectivity occur in a relatively short time (hours), yet *in situ*, stable OD and sharply orientated cells are not apparent until weeks after eye opening (Crair *et al* 1998, 2001; Crowley and Kratz 2000). Simulations lack the subtleties in different developmental time scales and critical periods of different functional

properties of cortical cells (Mitchell and Timney 1984; Daw *et al* 1978; Harwerth *et al* 1986; Daw 1995). The size of the network in simulation only hints at what may be happening in the real cortex. Although bigger network sizes were tested here for consistency, the relative sizes of simulation networks are infinitesimally small compared to the number of cells present even in the portion of V1 imaged by optical imaging.

CHAPTER 6

GENERAL DISCUSSION

In this thesis, the importance of correlated binocular experience during early postnatal development of the visual cortex was examined in two sets of experiments, which were each backed up by model simulations.

The cortex of S+MD animals was partially 'protected', yet only in one hemisphere and orientation selectivity was not preserved. Such an outcome cannot be accounted for by purely competitive mechanisms, since protection would be expected to encompass both hemispheres and orientation selectivity. The Bienenstock-Cooper-Munro (BCM) model (Bienenstock *et al* 1982) accurately predicted the loss and recovery of DE responses (OD and OSI) associated with MD. In animals with a strabismus prior to MD, it also predicted a slower OD shift away from the DE in cells, which this eye was dominant. Depending on the length of deprivation, this would result in an incomplete shift to favour the NDE after MD, as seen experimentally. The finding here that a greater rate of recovery of recovery in DE VEP's and physiological maps occurred in MD only animals compared to strabismic + MD animals, fits in well with that shown by Kind *et al* (2002) and is in further agreement with what the BCM model would predict. This is, that initial recovery from MD would be faster with concordant vision than without (Mitchell *et al* 2001).

Secondly, despite the obvious behavioural benefits to DE recovery during RO, anatomical (Antonini and Stryker 1993, 1996; Antonini *et al* 1998) and physiological mechanisms provided few robust clues to the underlying bilateral amblyopia often encountered upon restoring binocular vision after amblyopia (Murphy *et al* 1986, 1987; Mitchell 1991). Two important physiological links underlying the changes occurring during RO have been provided here. Recovery of ONDE OD territory was complete during recovery from RO in those animals that received an intermediate period of binocular vision, but was disrupted in those animals that did not. A further physiological link underlying the physiological (shown in Chapter 3) and behavioural amblyopia (Murphy *et al* 2002) seen in animals without an intermediate period of binocular vision, is shown here, where the orientation tuning width of single cells was significantly broader in the ODE than the ONDE. It appears that to achieve success in obtaining good acuity after RO, incorporating periods of binocular vision may be

attributed to obtaining sufficient expression and activity of NMDA receptors (Murphy *et al* 2002; Trepel *et al* 1998).

Together, the studies presented here highlight several important findings. Firstly, correlated binocular input is of critical importance for the postnatal development and maturation of normal cortical properties (i.e. ocular dominance and orientation selectivity) and behavioural acuity. Although initial formation of functional properties appears largely independent of very early visual experience, the basic 'scaffold' of functional connections must be consolidated and built upon through binocular visual input. Without concordant binocular vision during the critical period, inappropriate inter-eye and intra-eye connections evolve, as is the case with strabismus, MD and RO. Each eye's input may become functionally independent of the other eye. Functional distinct sets of geniculocortical afferents and may never develop a 'correct' network of functional connections through one or both eyes, or be able to receive 'influence' from the other eye once disconnected, even if simultaneous inputs are presented at a later stage.

Data presented here and the consensus emerging from the recent literature is that the loss and recovery of responses during and after deprivation are fundamentally different (Mower *et al* 2002; Liao *et al* 2002). Work is now focusing more on investigating the underlying molecular mechanisms of plasticity. Initial attention focused on neurotransmitters and neurotrophins (Daw 1995; Bonhoeffer 1996; Beradi and Maffei 1999), i.e their role in increasing transmitter release (Sala *et al* 1998; Jovanovic *et al* 2000), depolarising neurons (Kafitz *et al* 1999), or modulating gene expression (Poo 2001). However, it has become clear that plasticity in the brain involves a whole host of different molecules involved in a cascade of events. Most notable is the glutamatergic N-methyl, D-aspartate (NMDA) receptor which is known to be involved in synaptic plasticity and developmental plasticity in the visual cortex (Daw 1995; Bear and Rittenhouse 1999). The NMDA receptor has been suggested to act as a 'coincidence detector'; detecting pre-synaptic glutamate release and post-synaptic depolarisation and cause the influx of calcium into the cell that leads to potentiation (Schrader *et al* 2004; review; Kaczmarek *et al* 1997). It is suggested that the calcium conductance through the NMDA channel initiates the stabilisation of co-active synapses (Cline and Constantine-Paton 1989, 1990). The NMDA receptor comprises of over 75 proteins (Husi and Grant 2001). Interference with any of

these proteins may affect synaptic plasticity, which has collectively got them the title 'Hebbosome' due to their reputed role in Hebbian plasticity (Husi and Grant 2001). For example, three prominent intracellular kinases; cAMP dependent protein kinase (PKA), extracellular-signal-regulated kinase (ERK) and alpha Ca^{2+} /calmodulin-dependent protein kinase II (alphaCaMKII) activate numerous intracellular proteins such as: Protein phosphatase 1 (PP1), synaptic GTP-ase-activating protein (SynGAP), and microtubule-associated protein 2 (MAP2) - See review by Berardi *et al* 2003 and Fig. AppI (i). Long lasting changes in neuronal circuitry are likely to occur through the pattern of kinase activity being translated into a pattern of gene expression via activation of transcription factors. Activated kinases translocate to the nucleus where they begin gene expression under cAMP-responses-element (CRE) promoter through the activation of cAMP/ Ca^{2+} response element binding protein (CREB) binding protein.

Clinical implications

The present results emphasise the critical role for binocular vision in recovery from instances of early abnormal visual experience. The importance of binocular vision in the speed and degree of recovery from deprivation is highlighted here and in the recent studies by Kind *et al* (2001), Murphy *et al* (2002), and Liao *et al* (2004). This conclusion is supported further by a recent study showing that initial recovery of vision after MD is faster when both eyes are open than in reverse occluded animals (Mitchell *et al* 2001). Although clinical results indicate that patching the better eye of a child is required to improve spatial resolution of the amblyopic eye, most visual acuity improvements in the amblyopic eye occur following prescription of appropriate optical correction spectacles, but prior to unilateral occlusion (Moseley *et al* 1997). Several reports demonstrate swift and substantial recovery of vision in the affected eye in infants following corrective surgery to unilateral cataract, where no patching of the good eye was used (Jacobson *et al* 1983; Maurer *et al* 1999). This outcome has an added importance, since compliance with patch therapy is notoriously difficult to enforce and accurately quantify in human studies (Woodruff *et al* 1994).

Part time reverse occlusion in kittens in some instances lead to good acuity through both eyes (3.5-5hrs per day – see Mitchell *et al* 1991). Clinical practice is moving in

this direction for part time occlusion therapy (of the non-amblyopic eye) in infants that have undergone early corrective unilateral cataract surgery. Immediately after surgery, part time occlusion of an average of 9 hours of binocular vision per day during the first six months of age is incorporated into the waking hours. This figure rises to 12 hours per day past one year of age (see review- Mitchell and MacKinnon 2002). Not only is extensive binocular vision incorporated into contemporary patching therapy regimens permitting recovery and maintenance of acuity, but also in some cases contributing to the development of stereopsis (Birch *et al* 1993).

The site of the neural deficit in human amblyopia is still largely unresolved. In primates with visual deprivation, the primary site of cortical deficit appears in the input layers (IVc) of the striate cortex (Blakemore and Vital Durand 1986). Human fMRI maps show a striate deficit through the amblyopic eye (Barnes *et al* 2001). And more recently a possible extrastriate deficit in the form of global motion processing and detection of contrast-defined contours has been found in human amblyopes (Wong *et al* 2001; Simmers *et al* 2003).

Where next?

Animal models of amblyopia have had a remarkable effect on clinical practice in the last 20 years. The refining of the critical period and in particular pinpointing windows of maximal vulnerability in the first few months of life have reshaped treatment and hence improved outcomes. Although specific quantitative data from animals that lead to precise treatment regimes may still seem sparse, the plethora of indirect data concerning the outcomes of patching regimes, combined with an increased understanding of the early development and underlying mechanisms of the visual system and how it copes with changes in visual input, have offset this disadvantage. The molecular basis for plasticity is rapidly becoming the 'front runner' for research, with the number of *known* neurotransmitters, receptor proteins and downstream cascade of events (including protein synthesis) ever growing. Despite the shift of focus to the molecular underpinnings of synaptic plasticity, large gaps still remain in some of the most basic, 'traditional' measurements in the outcomes and timing of changes in physiological, anatomical, and morphological parameters underlying the recovery from early and late MD, and in particular the timing and extent of recovery

after RO (with and without intermediate vision). Moreover, large gaps exist in our understanding of the critical periods for cortical changes that occur in the presence of strabismus and anisometropia. This is especially important since strabismus and form deprivation have fundamentally different effects on binocular connections in the cortex. These more 'traditional' measures of development and maturation of the visual cortex can still provide much insight into the workings of the visual system by themselves and are essential as a 'vehicle' for testing molecular correlates of plasticity.

REFERENCES

- Abbott LF, Nelson SB (2002) Synaptic plasticity: taming the beast. *Nat Neurosci*; **Suppl**: 1178-83. Review
- Adams DL, Horton JC (2003) Capricious expression of cortical columns in the primate brain. *Nat Neurosci*; **6**: 113-4
- Albus K, Wolf W (1984) Early post-natal development of neuronal function in the kitten's visual cortex: a laminar analysis. *J Physiol*; **348**: 153-85
- Altar CA, Cai N, Bliven T, Juhasz M, *et al* (1997) Anterograde transport of brain-derived neurotrophic factor and its role in the brain. *Nature*; **389**: 856-60
- Aminoff MJ, Goodin DS (1994) Visual evoked potentials. *J Clin Neurophysiol*; **11**: 493-9
- Antonini A, Stryker MP (1993) Rapid remodeling of axonal arbors in the visual cortex. *Science*; **260**: 1819-1821
- Antonini A, Stryker MP (1996) Plasticity of geniculocortical afferents following brief or prolonged monocular occlusion in the cat. *J comp Neurol*; **369**: 64-82
- Antonini A, Stryker MP (1998) Effect of sensory disuse on geniculate afferents to cat visual cortex. *Vis Neurosci*; **3**: 401-9
- Arden GB, Barnard WM, Mushin AS (1974) Visually evoked responses in amblyopia. *Br J Ophthalmol*; **3**: 183-92
- Artola A, Singer W (1981) Long-term potentiation and NMDA receptors in rat visual cortex. *Nature*; **330**:649-52

Baddeley R, Hancock P (1991) A statistical analysis of natural images matches psychophysically derived orientation tuning curves. *Proc.R Soc. B*; **246**: 219-223

Bailey CH, Chen MC, Weiss KR, Kupfermann I (1992) Ultrastructure of a histaminergic synapses in *Aplysia*. *Brain Res*; **238**: 205-10

Baker FH, Grigg P, von Noorden GK (1974) Effects of visual deprivation and strabismus on the response of neurones in the visual cortex of the monkey, including studies on the striate and prestriate cortex in the normal animal. *Brain Res*; **66**: 185-208

Bandettini PA, Wong EC, Hinks RS, Tikofsky RS, Hyde JS (1992) Time course EPI of human brain function during task activation. *Magn Reson Med*; **25**: 390-7

Barnes GR, Hess RF, Dumoulin SO, Achtman RL, Pike GB (2001) The cortical deficit in humans with strabismic amblyopia. *J Physiol- London*; **533**: 281-97

Bear MF, Cooper LN, Ebner FF (1987) A physiological basis for a theory of synapse modification *Science*; **237**: 42-8

Bear MF, Kleinschmidt A, Gu QA, Singer W (1990) Disruption of experience-dependent synaptic modifications in striate cortex by infusion of an NMDA receptor antagonist, *J Neurosci* **10**:909-25

Bear MF, Press WA, Connors BW (1992) Long-term potentiation in slices of kitten visual cortex and the effects of NMDA receptor blockade. *J Neurophysiol*; **76**: 841-51

Bear MF (1996) A synaptic basis for memory storage in the cerebral cortex. *Proc Natl Acad Sci USA*; **93**: 13453-9

Bear MF, Connors BW, Paradiso MA (1996) Neuroscience: Exploring the brain. Williams and Wilkins; USA

- Bell AJ, Sejnowski TJ (1997) The independent components of natural scenes are edge filters. *Vision Research*; **37**: 3327-3338
- Berman, NEJ Daw, NW (1977) Comparison of the critical period for monocular and direction deprivation in cats *J. Physiol* **265**: 249-259
- Berardi N, Maffei L (1999) From visual experience to visual function: roles of neurotrophins. *J Neurobiol*; **41**: 119-26
- Berardi N, Pizzorusso T, Ratto GM, Maffei L (2003) Molecular basis of plasticity in the visual cortex. *TINS*; **26**: 369-78
- Berman NEJ and Payne BR (1983) Alterations in connections of the corpus callosum following convergent and divergent strabismus. *Brain Res*; **274**: 201-12
- Bi, GQ, Poo MM (1998) Activity-induced synaptic modifications in hippocampal culture: dependence on spike timing, synaptic strength and cell type. *J Neurosci*; **18**: 10464-10472
- Bienenstock EL, Cooper LN, Munro PW (1982) Theory for the development of neuron selectivity: orientation specificity and binocular interaction in visual cortex. *J Neurosci*; **2**: 32-48
- Birch EE, Swanson WH, Stager DR, Woody M, Everett M (1993) Outcome after very early treatment of dense congenital unilateral cataract. *Invest Ophthalmol Vis Sci*; **34**: 3687-99
- Blais BS (1998) The role of the environment in synaptic plasticity: Towards an understanding of learning and memory (*PhD Dissertation*) found on: <http://web.bryant.edu/~bblais/research.html>
- Blais BS, Shouval HZ, Cooper LN (1999) The role of presynaptic activity in monocular deprivation: Comparison of homosynaptic and heterosynaptic mechanisms *Proc. Natl. Acad. Sci USA*; **96**: 1083-1087

Blake R, Crawford ML, Hirsch HV (1974) Consequences of alternating monocular deprivation on eye alignment and convergence in cats. *Invest Ophthalmol*; **13**: 121-6

a Blakemore C, Van Sluyters RC (1974) Experimental analysis of amblyopia and strabismus. *British Journal of Ophthalmology*; **58**: 176-182

b Blakemore C, Van Sluyters RC (1974) Reversal of the physiological effects of monocular deprivation in kittens: Further evidence for a sensitive period. *J Physiol*; **237**: 195-216

Blakemore C, Van Sluyters RC (1975) Innate and environmental factors in the development of the kittens' visual cortex *J. Physiology*; **248**: 663-716

Blakemore C (1976) The conditions required for the maintenance of binocularity in the kitten's visual cortex. *J Physiol*; **261**: 423-44

Blakemore C (1978) Physiological correlates of human developmental disorders. *Metab. Opthal*; **2**: 123-125

Blakemore C, Eggers HM (1978) Effects of artificial anisometropia and strabismus on the kitten's visual cortex. *Arch. Ital Biol*; **116**: 385-389

Blakemore C, Hawken MJ (1982) Rapid restoration of functional input to the visual cortex of the cat after brief monocular deprivation. *J Physiol*; **327**: 463-87

Blakemore C, Vital Durand F (1986) Effects of visual deprivation on the development of the monkey's lateral geniculate nucleus. *J Physiol*; **380**: 493-511

Blakemore C, Vital-Durand F (1992) Different neural origins for 'blur' amblyopia and strabismic amblyopia. *Opthal Physiol Opt*; **12**: 83

Blamire AM, Ogawa S, Ugurbil K, Rothman D, McCarthy G, Ellermann JM, Hyder F, Rattner Z, Shulman RG (1992) Dynamic mapping of the human visual cortex by high-speed magnetic resonance imaging. *Proc Natl Acad Sci USA*; **89**: 11069-73

Blasdel GG, Salama G (1986) Voltage sensitive dyes reveal a modular organisation in monkey striate cortex, *Nature*; **321**: 579-585

Blasdel GG (1992) Differential imaging of ocular dominance and orientation selectivity in monkey striate cortex. *J Neurosci*; **12**: 3115-3138

Blasdel GG (1995) Organisation of ocular dominance columns in the striate cortex of neonatal macaque monkeys. *Vis. Neurosci*; **12**:589-603

Blasdel G, Campbell D (2001) Functional retinotopy of the monkey visual cortex. *J Neurosci*; **21**: 8286-301

Bliss TV, Lomo T (1973) Long lasting potentiation of synaptic transmission in the dentate area of the anaesthetised rabbit following stimulation of the perforant path. *J Physiol*; **232**: 331-56

Bliss TV, Gardner-Medwin AR (1973) Long lasting potentiation of synaptic transmission in the dentate area of the un-anaesthetised rabbit following stimulation of the perforant path. *J Physiol*; **232**: 357-74

Bliss TV, Collingridge GL (1993) A synaptic model of memory: long-term potentiation in the hippocampus. *Nature*; **361**: 31-9

Bode-Gruel KM, Singer W (1989) The development of N-methyl D-aspartate receptors in the cat visual cortex. *Brain Res Dev Brain Res*; **46**: 197-204

Bolshakov VY, Golan H, Kandel ER, Siegelbaum SA (1997) Recruitment of new sites of synaptic transmission during the cAMP-dependent late phase of LTP at CA3-CA1 synapses in the hippocampus. *Neuron*; **19**: 635-51

Bonhoeffer T (1995) Optical imaging of the layout of functional domains in cat area 17 and across the area 17/18 border in cat visual cortex. *Eur J Neurosci*; **7**: 1973-88

Bonhoeffer T (1996) Neurotrophins and activity-dependent development of the neocortex. *Curr Opin Neurobiol*; **6**: 119-26

Bonhoeffer T, Grinvald A (1996) *Brain mapping: The methodology*. Academic, London, pp 55-97

Bornsterin Y (1976) Visual evoked response bei der Schiel-amblyopie. *Ophthalmologica*; **172**: 188-193

Bozzi Y, Pizzorusso T, Creminisi F, Rossi FM, Barsacchi G, Maffei L (1995) Monocular deprivation decreases the expression of messenger RNA for brain-derived neurotrophic factor in the rat visual cortex. *Neuroscience*; **69**: 1133-1144

Buchweitz E, Weiss HR (1986) Alterations in perfused capillary morphometry in awake vs anaesthetised brain. *Brain Res*; **377**: 105-111

Cabelli RJ, Hohn A, Shantz CJ (1995) Inhibition of ocular dominance column formation by infusion on NT-4-5 or BDNF. *Science*; **267**: 1662-1666

Cabelli RJ, Allendorfer KL, Radeke MJ, Welcher AA, Feinstein SC, Shatz CJ (1996) Changing patterns of expression and subcellular localization of TrkB in the developing visual system. *J. Neurosci*; **16**: 7965-7980

Cabelli RJ, Shelton DL, Segal RA, Shatz CJ (1997) Blockade of endogenous ligands of trkB inhibits formation of ocular dominance columns. *Neuron*; **1** :63-76

Callaway EM, Katz LC (1990) Emergence and refinement of clustered horizontal connections in cat striate cortex. *J Neurosci*; **10**: 1134-53

Callaway EM, Katz LC (1991) Effects of binocular deprivation on the development of clustered horizontal connections in cat striate cortex. *Proc Natl Acad Sci USA*; **88**: 745-9

Castern E, Zafra, F, Thoenen H, Lindholm D (1992) Light regulates expression of brain derived neurotrophic factor mRNA in rat visual cortex. *Proc Natl Acad Sci USA*; **89**: 9444-9448

Cannestra AF, Black KL, Martin NA, Cloughesy T, Burton JS, Rubinstein E, Woods RP, Toga AW (1998) Topographical and temporal specificity of human intraoperative intrinsic signals. *Neuroreport*; **9**: 2557-63

Cannestra AF, Bookheimer SY, Pouratian N, O'Farrell A, Sicotte N, Martin NA, Becker D, Rubino G, Toga AW (2000) Temporal and topographical characterisation of language cortices using intraoperative optical intrinsic signals. *Neuroimage*; **12**: 41-54

Chalupa LM, Dreher B (1991) High precision systems require high precision "blueprints"; a new view regarding the formation of connections in the mammalian visual system. *J Cogn Neurosci*; **3**: 209-219

Chance B, Cohen P, Jobsis F, Schoener B (1962) Intracellular oxidation-reduction states *in vivo*. *Science*; **137**: 499-508

Chapman B, Stryker MP, Bonhoeffer T (1996) Development of orientation preference maps in ferret primary visual cortex *J Neurosci*; **16**:6443-53

Chapman B (2000) Necessity for afferent activity to maintain eye-specific segregation in ferret lateral geniculate nucleus *Science*; **287**: 2479-82

Chino YM, Shansky MS, Jankowski WL, Banser FA (1983) Effects of rearing kittens with convergent strabismus on development of receptive-field properties in striate cortex neurons. *J Neurophysiol*; **50**: 265-86

Chino YM, Ridder WH 3rd, Czora EP (1988) Effects of convergent strabismus on spatio-temporal response properties of neurons in cat area 18. *Exp Brain Res*; **72**: 264-78

Cleland BG, Crewther DP, Crewther SG, Mitchell DE (1982) Normality of spatial resolution of retinal ganglion cells in cats with strabismic amblyopia. *J Physiol*; **326**:235-49

Cline HT, Constantine-Paton M (1989) NMDA receptor antagonists disrupt the retinotectal topographic map. *Neuron*; **3**: 413-26

Cline HT, Constantine-Paton M (1990) The differential influence of protein kinase inhibitors on retinal arbor morphology and eye-specific stripes in the frog retinotectal system. *Neuron*; **4**: 899-908

Clothiaux EE, Bear MF, Cooper LN (1991) Synaptic plasticity in visual cortex: comparison of theory with experiment. *J Neurophysiol*; **66**: 1785-804

Cohen MS, Bookheimer SY, (1994) Localisation of brain function using magnetic resonance imaging. *TINS*; **7**: 268-77

Cook PM, Prusky G, Ramoa AS (1999) The role of spontaneous retinal activity before eye opening in the maturation of form and function in the retinogeniculate pathway of the ferret. *Vis Neurosci*; **16**: 491-501

Cooper LN, Liberman F, Oja E (1979) A theory for the acquisition and loss of neuron specificity in visual cortex. *Biol. Cybern*; **33**: 9-28

Cooper LN, Schofield CL (1988) Mean field theory of the neural network. *Proc. Natl. Acad. Sci USA*; **85**: 1973-1977

Crair MC, Gillespie DC, Stryker MP (1998) The role of visual experience in the development of columns in cat visual cortex. *Science*; **279**: 566-70

Crair MC, Horton JC, Antonini A, Stryker MP (2001) Emergence of ocular dominance columns in cat visual cortex by 2 weeks of age. *J Comp Neurol*; **430**: 235-49

Crewther DP, Crewther SG, Mitchell DE (1981) The efficacy of brief periods of reverse occlusion in promoting recovery from the physiological effects of monocular deprivation in kittens. *Invest Ophthalmol Vis Sci*; **21**: 357-62

Crewther SG, Crewther DP, Mitchell DE (1983) The effects of short-term occlusion therapy on reversal of the anatomical and physiological effects of monocular deprivation in the lateral geniculate nucleus and visual cortex of kittens. *Exp Brain Res*; **51**: 206-16

Crewther DP, Crewther SG (1990) Neural site of strabismic amblyopia in cats: spatial frequency deficit in primary cortical neurones. *Exp. Brain. Res*; **79**: 615-622

Crowley JC and Katz LC (1999) Development of ocular dominance columns in the absence of retinal input. *Nat neurosci*; **12**: 1125-30

Crowley JC, Katz LC (2000) Early development of ocular dominance columns. *Science*; **290**: 1321-4

Crowley JC, Katz LC (2002) Ocular dominance development revisited. *Current Opinion Neurbiol*; **12**: 104-9

Cynader MB, Timney B, Mitchell DE (1980) Period of susceptibility of kitten visual cortex to the effects of monocular deprivation extends beyond six months of age. *Brain Res*; **191**: 515-550

Czepita D, Daw NW (1996) The contribution of NMDA receptors to the visual response in animals that have been partially monocularly deprived. *Brain Res*; **728**: 7-12

Daniel PM, Whitteridge D (1961) The representation of the visual field on the cerebral cortex in monkeys. *J Physiol*; **159**: 203-21

Daw NW, Berman NEJ, Ariel M (1978) Interaction of critical periods in the visual cortex of kittens. *Science*; **199**: 565-567

Daw NW (1994) Mechanisms of plasticity in the visual cortex. *Inv. Opth. Vis. Sci* **35**: 4168-4179

Daw NW, Reid SN, Wang XF, Flavin HJ (1995) Factors that are critical for plasticity in the visual cortex. *Ciba Found Symp*; **193**: 258-76

Debanne D, Gahwiler GH, Thopson SM (1998) Long-term synaptic plasticity between pairs of individual CA3 pyramidal cells in rat hippocampal slice cultures. *J Physiol (Lond)*; **507**: 237-47

Deisseroth K, Bito H, Tsien RW (1996) Signalling from synapse to nucleus: postsynaptic CREB phosphorylation during multiple forms of hippocampal synaptic plasticity. *Neuron*; **16**: 89-101

Derrington AM, Fuchs AF (1979) Spatial and Temporal properties of X and Y cells in the cat lateral geniculate nucleus. *J Physiol*; **293**: 347-64

Desai NS, Cudmore RH, Nelson SB, Turrigiano GG (2002) Critical periods for experience-dependent synaptic scaling in visual cortex. *Nature Neurosci*; **5**: 783-789

Dews PB; Wiesel TN (1970) Consequences of monocular deprivation on visual behaviour in kittens. *J Physiol London*; **206**: 437-455

Diamond ME, Huang W, Ebner FF (1994) Laminar comparison of somatosensory cortical plasticity. *Science*; **265**: 1885-8

Diao YC, Jia WG, Swindale NV, Cynader MS (1990) Functional organisation of the cortical 17/18 border region in the cat. *Exp Brain Res*; **79**: 271-82

Durand GM, Kovalchuk Y, Konnerth A (1996) Long-term potentiation and functional synapse induction in developing hippocampus. *Nature*; **381**: 71-5

Dyck RH, Cynader MS (1993) An interdigitated columnar mosaic of cytochrome oxidase, zinc, and neurotransmitter-related molecules in cat and monkey visual cortex. *Proc Natl Acad Sci USA*; **90**: 9066-9069

Engert F, Bonhoeffer T (1999) Dendritic spine changes associated with hippocampal long-term synaptic plasticity. *Nature*; **399**: 66-70

Engelmann R, Crook JM, Löwel S (2002) Optical imaging of orientation and ocular dominance maps in area 17 of cats with convergent strabismus. *Vis neurosci*; **19**: 39-49

Ernfors P, Ibanez CF, Ebendal T, Olson L, Persson H (1990) Molecular cloning and neurotrophic activities of a protein with structural similarities to nerve growth factor: developmental and topographical expression in the brain. *Proc Natl Acad Sci USA*; **87**: 5454-8

Erwin E, Miller MD (1998) Correlation-based development of ocularly matched orientation and ocular dominance maps: determination of required input activities. *J Neurosci*; **18**: 9870-95

Eschweiler GW, Rauschecker JP (1993) Temporal integration in visual cortex of cats with surgically induced strabismus. *Eur J Neurosci*; **5**: 1501-9

Fagiolini A, Kupfer DJ, Houck PR, Novick DM, Frank E (2003) Separable features of visual cortical plasticity revealed by N-methyl D-aspartate receptor 2A signaling. *Proc Natl Acad Sci USA*; **100**: 2854-9

Fava MA, Duffy KR, Murphy KM (1999) Experience-dependent development of NMDAR1 subunit expression in the lateral geniculate nucleus. *Vis Neurosci*; **16**: 781-

Finkbeiner S, Tavazoie SF, Maloratsky A, Jacobs KM, Harris KM, Greenberg ME (1997) CREB: a major mediator of neuronal neurotrophins responses. *Neuron*; **19**: 1031-47

Finney EM, Shatz CJ (1998) Establishment of patterned thalamocortical connections does not require nitric oxide synthetase. *J Neurosci*; **18**: 8826-38

Fox K, Sato, Daw H (1989) The location and function of NMDA receptors in cat and kitten visual cortex. *J Neurosci*; **9**: 2443-54

Frahm J, Bruhn H, Merboldt KD, Hanicke W (1992) Dynamic MR imaging of human brain oxygenation during rest and photic stimulation. *J Magn Reson Imaging*; **2**: 501-5

Freeman RD, Mallach R, Hartley S (1981) Responsitivity of normal kitten striate cortex deteriorates after binocular deprivation. *J Neurophysiol*; **45**: 1074-84

Freeman RD, Tsumoto T (1983) An electrophysiological comparison of convergent and divergent strabismus in the cat: electrical and visual activation of single cortical cells *J Neurophysiol*; **49**: 238-53

Fregnac Y, Imbert M (1978) Early development of visual cortical cells in normal and dark reared kittens: relationship between orientation selectivity and ocular dominance *J Physiol*; **278**: 27-44

Fregnac Y, Imbert M (1984) Development of neuronal selectivity in primary visual cortex of cat. *Physiol Rev*; **64**: 325-434

Galuske RA, Kim DS, Castern E, Thoenen H, Singer W (1996) Brain-derived neurotrophic factor reverses experience-dependent synaptic modifications in kitten visual cortex. *Eur. J. Neuros*; **8**: 1554-1559

b Galuske RA, Kim DS, Castern E, Singer W (1996) Differential effects of neurotrophins on ocular dominance plasticity in developing and adult cat visual cortex. *Eur J Neurosci*; **12**: 3315-30

Geinisman Y, Detoledo-Morrell L, Morrell F, Persina, Beatty MA (1996) Synapse restructuring associated with the maintenance phase of hippocampal long-term potentiation *J comp Neurol*; **368**: 413-23

Ghose GM, Roe AW, Ts'o DY (1994) Features of functional organisation within the primate V4. *Sco. Neuros. Abstr*, **20**: 350(10) 840

Giffin F, Mitchell, DE (1978) The rate of recovery of vision after early monocular deprivation in kittens. *J Physiol*; **274**: 511-37

Godecke I, Bonhoeffer T (1996) Development of identical orientation maps for the two eyes without common visual experience. *Nature*; **379**: 251-4

Godecke I, Kim DS, Bonhoeffer T, Singer W (1997) Development of orientation preference maps in area 18 of kitten visual cortex. *Eur J Neurosci*; **9**: 1754-62

Gorin G (1982) *History of ophthalmology*. Wilmington: Publish or Perish

Gosh A, Sahtz CJ (1992) Involvement of subplate neurons in the formation of ocular dominance columns. *Science*; **255**: 1441-3

Grinvald A, Lieke E, Frostig RD, Gilbert CD, Wiesel TN, (1986) Functional architecture of cortex revealed by optical imaging of intrinsic signals. *Nature*; **324**: 361-4

Gu QA, Bear MF, Singer W (1989) Blockade of NMDA-receptors prevents ocularity changes in kitten visual cortex reversed monocular deprivation. *Brain Res Dev Brain Res*; **47**: 281-8

Guillery, R.W, Stelzner DJ (1970), The differential effects of unilateral lid closure upon the monocular and binocular segments of the dorsal lateral geniculate nucleus in the cat. *J Comp Neurol*; **139**: 413-21.

Guillery, R.W. (1972) Binocular competition in the control of geniculate cell growth *J.Comp. Neurology* **144** 177-130

Gutig R, Aharonov R, Rotter S, Sompolinsky H (2003) Learning input correlations through the nonlinear temporally asymmetric Hebbian plasticity. *J. Neurosci*; **23**: 3697-714

Hancock PJ, Baddeley RJ, Smith LS (1992) The principal components of natural images. *Network*; **3**: 61-70

Harwerth RS, Smith EL 3rd, Okundaye OJ (1983) Oblique effects, vertical effects and meridional amblyopia in monkeys. *Exp Brain Res*; **53**: 142-50

Harwerth RS, Smith EL 3rd, Duncan GC, Crawford ML, von Noorden GK (1986) Multiple sensitive periods in the development of the primate visual system. *Science*; **232**: 235-8

Hata Y, Stryker MP (1994) Control of thalamocortical afferent arrangements by postsynaptic activity in developing visual cortex. *Science*; **265**: 1732-1735

Hata Y, Tsumoto T, Stryker MP (1999) Selective pruning of more active afferents when cat visual cortex is pharmacologically inhibited. *Neuron*; **22**: 375-381

Hebb DO (1949) *Organization of Behaviour*. Wiley, New York

Hendrickson AE, Hunt SP, Wu J-Y (1981) Immunochemical localisation of glutamic acid decarboxylase in monkey striate cortex. *Nature*; **292**: 605

Hess RF, Campbell FW, Greehalgh T (1978) On the nature of the neural abnormality in human amblyopia; neural aberrations and neural sensitivity loss. *Pflugers Arch*; **377**:201-7

Hess RF, Holiday IE (1992) The spatial localisation deficit in amblyopia. *Vision Res*; **32**: 1319-39

Hill, DK, Keynes RD (1949) Opacity changes in stimulated nerve. *J Physiol*; **108**: 278-281

Hoffsummer F, Wolf F, Geisel T, Lowel S and Schmidt K (1996) Sequential bifurcation and dynamic rearrangement of columnar patterns during cortical development. In Bower JM (ed), *Computational Neuroscience. Trends in Research* Academic press, San Diego pp 197-202

Hogan D, Berman, NE (1992) The development of neuropeptide Y immunoreactive neurons in cat visual cortical areas. *Brain Res Dev Brain Res*; **67**: 343-369

Hogan D, Berman NE (1994) The development of parvalbumin and calbindin-D28k immunoreactive interneurons in kitten visual cortical areas. *Brain Res Dev Brain Res*; **77**: 1-21

Horton JC, Hubel DH, (1981) Regular patchy distribution of cytochrome oxidase staining in primary visual cortex of macaque monkey. *Nature*; **292**: 762-764

Horton JC (1984) Cytochrome oxidase patches:a new cytochitectonic feature of monkey visual cortex. *Philos. Trans. R. Soc. Lond*; **304**: 199-253

Horton JC, Hocking DR (1996) an adult-like pattern of ocular dominance columns in striate cortex of newborn monkeys prior to visual experience. *J Neurosci*; **16**: 1791-1807

Houzel JC, Milleret C, Innocenti G (1994) Morphology of callosal axons interconnecting areas 17 and 18 of the cat. *Eur J Neurosci*; **6**: 898-917

Hubel DH (1959) Single unit activity in striate cortex of unrestrained cats. *J. Physiology* **147**: 226-238

Hubel DH, Wiesel TN (1962) Receptive fields, binocular interaction and functional architecture in the cat's visual cortex. *J Physiol*; **160**: 106-154

Hubel DH, Wiesel TN (1963) Receptive fields of cells in striate cortex of very young, visually inexperienced kittens. *J Neurophys*; **26**: 994-1002

Hubel DH, Wiesel TN (1965), Binocular interaction of striate cortex of kittens reared with artificial squint. *J Neurophys*; **28**: 1041-1059

Hubel, D.H. & Wiesel, T.N. (1968), Receptive fields and functional architecture of monkey striate cortex. *J Physiol*; **1** 215-43

Hubel DH, Wiesel TN (1969), Anatomical demonstration of columns in the monkey striate cortex, *Nature*; **221 (182)**: 747-50

Hubel DH, Wiesel TN (1970) The period of susceptibility to the physiological effects of unilateral eye closure in kittens. *J Physiol*; **206**: 419-436

Hubel DH, Wiesel TN (1972) Laminar and columnar distribution of geniculo-cortical fibres in the macaque monkey. *J comp. Neurol*; **146**: 421-450

Hubel DH, Wiesel TN (1974) Uniformity of monkey striate cortex: a parallel relationship between field size, scatter, and magnification, factor. *J Comp. Neurol*; **158**: 295-305

Hubel DH, Wiesel TN (1977) Functional architecture of macaque monkey visual cortex. *Proc. R Soc*; **198**: 1-59

Hubel DH, Wiesel TN, LeVay S (1977) Plasticity of ocular dominance columns in monkeys striate cortex. *Phil. Trans. R. Soc. London*; **278**: 377-409

Hubel DH, Wiesel TN, Stryker MP (1978) Anatomical demonstration of orientation columns in macaque monkey. *J Comp Neurol*; **177**: 361-380

Hubel DH (1988) Eye, brain and vision. New York: WH Freeman

Hubener M, Shoham D, Grinvald A, Bonhoeffer T (1997) Spatial relationships among three columnar systems in cat area 17. *J Neurosci*; **17**: 9270-9284

Huang YY, Bach ME, Lipp HP, et al (1996) Mice lacking the gene encoding tissue-type plasminogen activator show a selective interference with late-phase long-term potentiation in both Schaffer collateral and mossy fiber pathways. *Proc Natl Acad Sci USA*; **93**: 8699-704

Huang ZJ, Kirkwood A, Pizzorusso T, Porciatti V, Morales B, Bear MF, Maffei L, Tonegawa S (1999) BDNF regulates the maturation of inhibition and the critical periods of plasticity in mouse visual cortex. *Cell*; **98**: 739-55

Husi H, Grant SG (2001) Proteomics of the nervous system. *TINS*; **24**: 259-266

Hyvarinen A, Oja E (1996) A fast fixed-point algorithm for independent component analysis. *Int Jour. Neural systems*; **7**: 671-687

Ikeda H, Tremain KE (1979) Amblyopia occurs in retinal ganglion cells in cats reared with convergent squint without alternating fixation. *Exp Brain Res*; **35**: 559-82

Innocenti GM, Frost DO (1980) The development of visual callosal connections in the absence of visual experience or of the eyes. *Exp. Brain Res*; **39**: 365-75

Innocenti GM (1986) Postnatal development of corticocortical connections. *Ital J Neurol Sci*; **Suppl 5**: 25-8

Intrator N, Cooper LN (1992) Objective function formulation of the BCM theory of cortical plasticity: statistical connections, stability conditions. *Neural networks*; **5**: 3-17

Jacobson SG, Ikeda H (1979) Behavioural studies of spatial vision in cats with convergent squint: is amblyopia due to arrest of development? *Exp Brain Res*; **34**: 11-26

Jacobson SG, Mohindra L, Held R (1983) Monocular visual form deprivation in human infants. *Doc Ophthalmol*; **55**: 199-211

Jobis FF, Keizer JH, LaManna JC, Rosenthal MJ (1977) Reflectance spectrophotometry of cytochrome aa₃ in vivo. *J Appl Physiol Respir. Environ. Exercise. Physiol*; **43**: 858-872

Johnson F, Hohmann SE, Distefano PS, Bottjer SW (1997) Neurotrophins suppress apoptosis induced differentiation of an avian motor-cortical region. *J Neurosci*; **17**: 2101-2111

Jovanovic JN, Czernik AJ, Fienberg AA, Greengard P, Sihra TS (2000) Synapsins as mediators of BDNF-enhanced neurotransmitter release. *Nat Neurosci*; **3**: 323-9

Kaczmarek L, Kossut M, and Skangiel-Kramska J (1997) Glutamate receptors in cortical plasticity: molecular and cellular biology. *Physiol Rev*; **77**: 217-255

Kafitz KW, Rose CR, Thoenen H, Konnerth A (1999) Neurotrophin-evoked rapid excitation through TrkB receptors. *Nature*; **401**: 918-21

Kalil RE, Spear PD, Langsetmo A (1984) Response properties of striate cortex neurons in cats raised with divergent or convergent strabismus. *J Neurophysiol*; **52**: 514-37

Kandel E, Schwartz J, Jessel TM (1991) Principles of neural science (4th ed). McGraw-Hill/Appleton and Lange

Kaschube M, Wolf F, Geisel T, Lowel S (2002) Genetic influence on quantitative features of neocortical architecture. *J Neurosci*; **22**: 7206-17

Kaschube M, Wolf F, Puhmann, Rathjen S, Schmidt KF, Geisel T, Lowel S (2003) The pattern of ocular dominance columns in cat primary visual cortex: intra – and interindividual variability of column spacing and its dependence on genetic background. *Eur J Neurosci*; **18**: 3251-66

Katz LC, Callaway EM (1992) Development of local circuits in mammalian visual cortex. *Annu Rev Neurosci*; **15**: 31-56

Kaye M, Mitchell DE, Cynader M (1982) Depth perception eye alignment and cortical ocular dominance of dark-reared cats. *Dev Brain Res*; **15**: 204-207

Kim DS, Bonhoeffer T (1994) Reverse occlusion leads to a precise restoration of orientation preference maps in visual cortex. *Nature*; **370**: 370-2

Kim DS, Duong TQ, Kim SG (2000), High-resolution mapping of iso-orientation columns by fMRI. *Nat Neurosci*; **3**: 164-9

Kind PC (1999) Cortical plasticity: Is it time for a change? *Current biology*; **9**: R640-R643

Kind PC, Mitchell DE, Blakemore C, Bonhoeffer T, Sengpiel F (2002) Correlated binocular activity guides recovery from monocular deprivation. *Nature*; **416**: 430-3

Kiopes L, Kiper DC, O'keefe LP, Cavanaugh JR, Movshon JA (1998) Neuronal correlates of amblyopia in the visual cortex of macaque monkeys with experimental strabismus and anisometropia. *J Neurosci*; **18**: 6411-24

Kirkwood A, Lee HK, Bear MF (1995) Co-regulation of long-term potentiation and experience-dependent synaptic plasticity in visual cortex by age and experience. *Nature*; **375**: 328-331

Kirkwood A, Rioult MC, Bear MF (1996) Experience dependent modification of synaptic plasticity in visual cortex. *Nature*; **381**: 526-8

Kleinschmidt A, Bear MF, Singer W (1987) Blockade of "NMDA" receptors disrupts experience-dependent plasticity of kitten striate cortex. *Science*; **238**: 355-8

Komatsu Y, Tomyama K, Maeda J, Sakaguchi H (1981) Long-term potentiation investigated in a slice preparation of striate cortex of young kittens. *Neurosci Lett*; **26**: 269-74

Krahe TE, Medina AE, Ramoa AS (2004) Recovery from the effects of a brief period of monocular deprivation does not require new protein synthesis Program No. 156.14.2004 *Abstract Viewer/Itinerary Planner*. Washington, DC: Society for Neuroscience 2004. Online

Kraut MA, Arezzo JC, Vaughan HG Jr. (1985) Intracortical generators of the flash VEP in monkeys. *Electroencephalography and Clinical Neurophysiology*; **62**: 300-312

Krug K, Akerman CJ, Thompson ID (2001) Responses of neurones in neonatal cortex and thalamus to patterned visual stimulation through the naturally closed lids. *J Neurophysiol*; **85**: 1436-43

Kwong KK, Belliveau JW, Chesler DA, Goldberg IE, *et al* (1992) Dynamic magnetic resonance imaging of human brain activity during primary sensory stimulation. *Proc Natl Acad Sci USA*; **89**: 5675-9

Law CC, Cooper LN (1994) Formation of receptive fields in realistic visual environment according to the Bienenstock, Cooper and Munro (BCM) theory. *Proc Natl Acad Sci USA*; **91**: 7797-801

Lein ES, Hohn A, Shatz CJ (2000) dynamic regulation of BDNF and NT-3 expression during visual system development. *J. comp. Neurol*; **420**:1-18

- LeVay S, Guilbert CD (1976) Laminar patterns of geniculocortical projection in the cat. *Brain Res*; **113**: 1-19
- LeVay S, Stryker MP, Shantz CJ (1978) Ocular dominance columns and their development in layer IV of the cat's visual cortex: A quantitative study *J.Comp. Neuro*; **179**: 223-244
- LeVay S, Stryker MP (1979) The development of ocular dominance columns in the cat. *Soc Neurosci. Symp*; **4**: 83-98
- LeVay S, Wiesel TN, Hubel DH (1980) The development of ocular dominance columns in normal and visually deprived monkeys *J. Comp Neurol*; **191**: 1-51
- Levi DM, Harwerth RS (1978) Contrast evoked potentials in strabismic and anisometric amblyopia. *Invest Ophthalmol Vis Sci*; **17**: 571-5
- Liao DS, Mower AF, Neve RL, Sato-Bigbee C, Ramoa AS (2002), Different mechanisms for loss and recovery of binocularity in the visual cortex. *J. Neurosci*; **22**: 9015-23
- Liao DS, Krahe TE, Prusky GT, Medina AE, Ramoa AS (2004) Recovery of cortical binocularity and orientation selectivity after the critical period for ocular dominance plasticity. *J Neurophysi*; **92**: 2113-21
- Linsker R (1986) From basic network principles to neural architecture (series). *Proc Natl Acad Sci USA*; **83**: 7508-7512
- Liu Y, Shouval H (1994) Localised principal components of natural images – an analytic solution. *Network*; **5.2**: 317-325
- Livingston MS (1995) Oscillatory firing and interneuronal correlations in squirrel monkey striate cortex. *J Neurophysiol*; **75**: 2467-85

Livingston MS, Nori S, Freeman DC, Hubel DH (1996) Stereopsis and binocularity in the squirrel monkey. *Vision Res*; **35**: 345-54

Löwel S, Singer W (1987) The pattern of ocular dominance columns in flat-mounts of the cat visual cortex. *Exp Brain Res*; **68**: 661-6

Löwel S, Bischof H-J, Leutenecker B, Singer W (1988) Topographic relations between ocular dominance and orientation columns in the cat striate cortex. *Exp. Brain. Res*; **71**: 33-46

Löwel S, Singer W (1992) Selection of intrinsic horizontal connections in the visual cortex by correlated neuronal activity. *Science*; **255**: 209-12

Löwel S, Singer W (1993) Monocularly induced 2-deoxyglucose patterns in the visual cortex and lateral geniculate nucleus of the cat:II. Awake animals and strabismic animals. *Eur J Neurosci*; **5**: 857-69

Löwel S (1994) Ocular dominance column development: strabismus changes the spacing of adjacent columns in cat visual cortex. *J Neurosci*; **13**: 7451-68

Löwel S, Schmidt KE, Kim DS, Wolf F, Hoffsummer F, Singer W, Bonhoeffer T (1998) The layout of orientation and ocular dominance domains in area 17 of strabismic cats. *Eur J Neurosci*; **10**: 2629-43

MacKay DJC, Miller KD (1994) The role of constraints in Hebbian learning. *Neural computation*; **6**:100-126

Maisonpierre PC, Belluscio L, Friedman B, Alderson RF, Wiegand SJ, Furth ME, Lindsay RM, Yancoulos GD, (1990) NT-3, BDNF, and NGF in the developing rat nervous system: parallel as well as reciprocal patterns of expression. *Neuron*; **4**: 501-9

Malach R, Ebert R, Van Sluyters RC (1984) Recovery from effects of brief monocular deprivation in the kitten. *J Neurophysiol*; **51**: 538-51

Malach R, Van Sluyters RC (1989) Strabismus does not prevent recovery from monocular deprivation: a challenge for simple Hebbian models of synaptic modification. *Vis Neurosci*; **3**: 267-73

Markram H, Lubke J, Frotscher M, Sakmann B (1997) Regulation of synaptic efficacy by coincidence of post-synaptic Aps and EPSPs. *Science*; **275**: 213-215

Marty, S Berzaghi MdaP, Berninger B (1997) Neurotrophins and activity-dependent plasticity of cortical interneurons. *TINS*; **20**: 198-202

Maurer D, Lewis T, Brent H, Levin A (1999) Rapid improvements in the acuity of infants after visual input. *Science*; **286**: 108-110

Menon RS, Ogawa S, Kim SG, Ellermann JM, Merkle H, Tank DW, Ugurbil K (1992) Functional brain mapping using magnetic resonance imaging. Signal changes accompanying visual stimulation. *Invest Radiol*; Suppl **2**:S47-53

Miller KD, Keller JB, Stryker MP (1989) Ocular dominance column development: analysis and simulation. *Science*; **245**: 605-15

Miller KD (1992) Development of orientation columns via competition between ON and OFF center inputs. *Neuroreport*; **3**: 73-6

Miller KD (1994) A model for the development of simple cell receptive fields and the ordered arrangement of orientation columns through activity-dependent competition between on-and off-center inputs *J Neurosci*; **14**: 409-441

Miller KD (1996) Synaptic economics: competition and cooperation in synaptic plasticity. *Neuron*; **17**: 371-4

Mitchell DE, Cynader M, Movshon JA (1977) Recovery from the effects of monocular deprivation in kittens. *J Comp Neurol*; **176**: 53-64

Mitchell DE (1981) Sensitive periods in visual development. In: *The development of perception:Psychobiological Perspectives*. Edited by RN Aslin, JR Alberts, MR Petersen. New York:Academic, vol 2. p3-43

Mitchell DE, Murphy KM, Kaye MG (1984) The permanence of the visual recovery that follows reverse occlusion of monocularly deprived kittens. *Invest. Ophthalm. Vis Sci*; **25**: 908-917

Mitchell DE, Timney B (1984) Postnatal development of function in the mammalian visual system. In *Handbook of physiology*, section I: *The nervous system*, 3 part 1. Sensory processes (ed. I. Darian-Smith) pp 507-555 Bethesda: American Physio Soc

Mitchell DE (1988) The extent of visual recovery from early monocular or binocular deprivation in kittens. *J Physiol*; **395**: 639-60

Mitchell D (1991) The long term effectiveness of different regimes of occlusion on recovery from early monocular deprivation in kittens. *Philos Trans R Soc Lond B Biol Sci*; **333**: 51-79

Mitchell DE, Gingras G (1998) Visual recovery after monocular deprivation is driven by absolute, rather than relative, visually evoked activity levels. *Current Biology*; **8**: 1179-1182

Mitchell DE (2001) Initial recovery of vision after early monocular deprivation in kittens is faster when both eyes are open. *Proc Natl Acad Sci USA*; **98**: 11662-7

Mitchell DE, MacKinnon S (2002) The present and potential impact of research on animal models for clinical treatment of stimulus deprivation amblyopia. *Clin. Exp. Optom*; **85**: 5-18

Mitchell DE, Kind PC, Sengpiel F, Murphy K (2003) Brief daily periods of binocular vision prevent deprivation-induced acuity loss. *Curr Biol*; **13**: 1704-8

Moseley MJ, Fielder AR, Irwin M, Jones HS, Auld RJ (1997) Effectiveness of occlusion therapy in ametropic amblyopia: a pilot study. *Br J Ophthalmol*; **81**: 956-61

Movshon JA, Blakemore C (1974) Functional reinnervation in kitten visual cortex. *Nature*; **251**: 504-5

Movshon JA (1976) Reversal of the physiological effects of monocular in the kitten's visual cortex *J. Physiol*; **261**: 125-175

Movshon JA, Dursteler MR (1977) Effects of brief periods of unilateral eye closure on the kitten's visual system. *J Neurophysiol*; **40**: 1255-65

Mower GD, Burchfiel JL, Duffy FH (1982) Animal models of strabismic amblyopia: physiological studies of visual cortex and the lateral geniculate nucleus. *Brain Res*; **281**: 311-27

Mower GD, Caplan CJ, Christen WG, Duffey FH (1985) Dark rearing prolongs physiological but not anatomical plasticity of the cat visual cortex. *J Comp. Neur*; **235**: 448-466

Mower AF, Liao DS, Nestler EJ, Neve RL, Ramoa AS (2002), cAMP/Ca²⁺ response element binding protein function is essential for ocular dominance plasticity. *J Neurosci*; **22**: 2237-45

Muller CM, Griesinger CB (1998) Tissue plasminogen activator mediates reverse occlusion plasticity in visual cortex. *Nat Neurosci*; **1**: 47-53

Murphy KM, Mitchell DE (1986) Bilateral amblyopia after a short period of reverse occlusion in kittens. *Nature*; **323**: 536-538

Murphy KM, Mitchell DE (1987) Reduced visual acuity in both eyes of monocularly deprived kittens following a short or long period of reverse occlusion. *J Neurosci*; **7**: 1526-1536

Murphy KM, Jones DG, Van sluyters RC (1995) Cytochrome oxidase blobs in the cat primary visual cortex. *J. Neurosci*; **15**: 4196-4208

Murphy KM, Jones DG, Mitchell DE (2002) Recovery of visual acuity and NMDA expression following monocular deprivation, Program No. 760.10. 2002, *Abstract Viewer/Itinerary Planner*. Washington, DC: Society for Neuroscience 2002. CD-ROM

Mustari M, Cynader M (1981) Prior strabismus protects kitten cortical neurons from the effects of monocular deprivation. *Brain Res*; **211**: 165-170

Nass MN, Cooper LN (1975) A theory for the development of feature detecting cell in visual cortex. *Biol Cybern*; **19**: 1-18

Nase G, Weishaupt J, Stern P, Singer W, Monyer H, (1999) Genetic and epigenetic regulation of NMDA receptor expression in the rat visual cortex. *Eur J Neurosci*; **11**: 4320-6

Obermayer K, Blasdel GG (1993) Geometry of orientation and ocular dominance columns in monkey striate cortex. *J Neurosci*; **13**: 4114-4129

Oja E (1982) Simplified neuron model as a principal component analyzer *Math biol*; **15**: 267-273

Olshausen BA, Field DJ (1996) Emergence of simple-cell receptive field properties by learning a sparse code for natural images. *Nature*; **381**: 607-9

Olson CR, Freeman RD (1978) Monocular deprivation and recovery during sensitive period in kittens. *J Neurophysiol*; **41**: 65-74

Olson CR, Freeman RD (1980) Profile of the sensitive period for monocular deprivation. *Exp Brain Res*; **39**: 17-21

Oxford English Dictionary <http://dictionary.oed.com>

Packwood J, Gordon B (1975) Stereopsis in normal domestic cat, Siamese cat, and cat raised with alternating monocular occlusion. *J Neurophys*; **38**: 1485-1499

Padnick LB, Linsenmeier RA (1999) Properties of the flash visual evoked potential recorded in the cat primary visual cortex. *Vision Res*; **39**: 2833-40

Penn AA, Riquelme PA, Feller MB, Shatz CJ (1998) Competition in Retinogeniculate patterning driven by spontaneous activity. *Science*; **279**: 2108-2112

Perez R, Glass L, Shaler RJ (1975) Development of specificity in the cat visual cortex. *J Math Biol*; **1** : 75

Pham TA, Impey S, Storm DR, Stryker MP (1999) CRE-mediated gene transcription in neocortical neuronal plasticity during the developmental critical period. *Neuron*; **22**: 63-72

Philpot BD, Sekhar AK, Shouval HZ, Bear MF (2001) Visual experience and deprivation bidirectionally modify the composition and function of NMDA receptors in visual cortex. *Neuron*; **29**: 157-169

Pizzorusso T, Fagiolini M, Porciatti V, Maffei L (1997) Temporal aspects of contrast visual evoked potentials in the pigmented rat: effect of dark rearing. *Vision Res*; **37**: 389-95

Poo MM (2001) Neurotrophins as synaptic modulators. *Nat Rev Neurosci*; **2**: 24-32

Pouratian N, Bookheimer SY, O'Farrel AM, Sicotte NL, Cannestra AF, Becker D, Toga AW (2000) Optical imaging of bilingual cortical representations. Case report. *J Neurosurg*; **93**: 676-81

Quinlan EM, Olstein DH, Bear MF, (1999) Bidirectional, experience –dependent regulation of N-methyl-D aspartate receptor subunit composition in the rat visual cortex during postnatal development. *Proc Natl Acad Sci USA*; **96**: 12867-80

b Quinlan EM, Philpot BD, Huganir RL, Bear MF, (1999) Rapid, experience-dependent expression of synaptic NMDA receptors in visual cortex in vivo. *Nat Neurosci*; **2**: 352-7

Rakic P (1976) Prenatal genesis of connections subserving ocular dominance in the rhesus monkey. *Nature*; **261**: 212-234

Rao RP, Sejnowski TJ (2001) Spike-timing-dependent Hebbian plasticity as temporal difference learning. *Neural Comput*; **13**: 2221-37

Rathjen S, Schmidt KE, Löwel S (2002) Two-dimensional analysis of the spacing of ocular dominance columns in normally raised and strabismic kittens

Rauschecker J, Singer W (1982) Binocular deprivation can erase the effects of preceding monocular or binocular vision in kitten cortex. *Brain Res*. **256**: 495-8

Rauschecker JP, Egert U, Kossel A, (1990) Effects of NMDA antagonists on developmental plasticity in kitten visual cortex. *Int J Dev Neurosci*; **8**: 425-35

Reh TA, Constantine-Paton M (1985) Eye-specific segregation requires neural activity in three-eyed *Rana pipiens*. *J Neurosci*; **5**: 1132-43

Reiter HO, Waitzman DM, Stryker MP (1986) Cortical activity blockade prevents ocular dominance plasticity in the kitten visual cortex. *Exp. Brain Res*; **65**: 182-188

Reiter HO, Stryker MP (1988) Neural plasticity without postsynaptic action potentials: less-active inputs become dominant when kitten visual cortical cells are pharmacologically inhibited. *Proc. Natl. Acad. Sci. USA*; **85**: 3623-3627

Reynolds IJ, Bear MF (1991) Effects of age and visual experience on [3H] MK801 binding NMDA receptors in the kitten visual cortex. *Exp Brain Res*; **85**: 611-5

Riddle DR, Lo DC, Katz LC (1995) NT-4 mediated rescue of lateral geniculate neurons from effects of monocular deprivation. *Nature*; **378**: 189-91

Rittenhouse CD, Shouval HZ, Paradiso MA, Bear M (1999) Monocular deprivation induces homosynaptic long-term depression in visual cortex. *Nature*; **397**: 347-350

Roberts EB, Meredith MA, Ramoa AS, (1998) Suppression of NMDA receptor function using antisense DNA block ocular dominance plasticity while preserving visual responses. *J Neurophysiol*; **80**: 1021-32

Roelfsema PR, Koing P, Engel AK, Sireteanu R, Singer W (1994) Reduced synchronisation in the visual cortex of cats with strabismic amblyopia. *Eur J Neurosci*; **6**: 1645-55

Roy C, Sherrington C (1890) On the regulation of the blood supply of the brain. *J Physiol*; **11**: 85-108

Ruthazer ES, Baker GE, Stryker MP (1999) Development of organisation of ocular dominance bands in primary visual cortex of the sable ferret. *J Comp Neurol*; **407**: 151-65

Sala R, Viegi A, Rossi FM, Pizzorusso T, Bonanno G, Raiteri M, Maffei L (1998) Nerve growth factor and brain-derived neurotrophic factor increase neurotransmitter release in the rat visual cortex. *Eur J Neurosci*; **10**: 2185-91

Schmidt KE, Kim DS, Singer W, Bonhoeffer T, Lowel S (1997) Functional specificity of long range intrinsic and interhemispheric connections in the visual cortex of strabismic cats. *J Neurosci*; **17**: 5480-92

Schrader LA, Perrett SP, Ye L, Friedlander MJ (2004) Substrates for coincidence detection and calcium signalling for induction of synaptic potentiation in the neonatal visual cortex. *J Neurophysiol*; **91**: 2747-64

Schroeder CE, Tenke CE, Givre SJ, Arezzo JC, and Vaughan HG Jr. (1991) Striate cortical contribution to the surface-recorded pattern-reversal VEP in the alert monkey. *Vision Research*; **31**: 1143-1157

Sejnowski TJ (1977) Storing covariance with nonlinearly interacting neurons. *J Math Biol*; **4**: 303-21

Sengpiel F, Blakemore C, Kind PC, Harrad R (1994) Interocular suppression in the visual cortex of strabismic cats. *J Neurosci*; **14**: 6855-71

Sengpiel F, Godecke I, Stawinski P, Hubener M, Lowel S, Bonhoeffer T (1998) Intrinsic and environmental factors in the development of functional maps in cat visual cortex. *Neuropharm*; **37**: 607-21

Sengpiel F, Stawinski P, Bonhoeffer T (1999) Influence of experience on orientation maps in cat visual cortex. *Nat Neurosci*; **2**: 727-32

Shatz CJ, Lindstrom S, Wiesel TN, (1977) The distribution of afferents representing the rights and left eyes in the cat's visual cortex. *Brain Res.*; **131**: 103-16

Shatz CJ, Stryker MP (1978) Ocular dominance in layer IV of the cat's visual cortex and the effects of monocular deprivation. *J Physiol*; **281**:267-283

Shatz CJ, Luskin MB (1986) The relationship between the geniculocortical afferents and their cortical target cells during development of the cat's primary visual cortex. *J Neurosci*; **6**: 3655-68

Sherman SM (1972) Development of interocular alignment in cats. *Brain Res*; **37**: 187-203

Sherman SM (1979) Functional development of geniculocortical pathways in normal and amblyopic vision. *Trans Ophthalmol Soc UK*; **99(3)**: 357-62

Sherman SM, Spear PD (1982) Organisation of visual pathways in normal and visually deprived cats. *Physiol Rev*, **62**: 738-855

Shoham D, Hubener M, Schulze S, Grinvald A, Bonhoeffer T (1997) Spatio-temporal frequency domains and their relation to cytochrome oxidase staining in cat visual cortex. *Nature*; **385**: 529-533

Shoham D, Grinvald A (2001) The cortical representation of the hand in macaque and human area S-I: high resolution optical imaging. *J Neurosci*; **21**: 6820-35

Shouval H, Intrator N, Law CC, Cooper LN (1996) Effects of binocular cortical misalignment on ocular dominance and orientation selectivity. *Neural computation*; **8**: 1021-1040

Shouval H, Liu Y (1996) Principal component neurons in a realistic visual environment. *Network*; **7**: 501-515

Sillito AM, Kemp JA, Blakemore C (1981) The role of GABAergic inhibition in the cortical effects of monocular deprivation. *Nature*; **291**: 318-20

Simmers AJ, Ledgeway T, Hess RF, McGraw PV (2003) Deficits to global motion processing in human amblyopia. *Vis Res*; **43**: 729-38

Singer W, von Gruenau M, Rauschecker J (1979) Requirements for the disruption of binocularity in the visual cortex of strabismic kittens. *Brain Res*; **171**: 536-40

b Singer W, von Grunau M, Rauschecker J (1980) Functional amblyopia in kittens with unilateral exotropia I. Electrophysiological assessment. *Exp Brain Res*; **40**: 294-304

Sireteanu R, Fronius M (1981) Naso-temporal asymmetries in amblyopic vision: consequence of long-term interocular suppression. *Vision Res* **21**: 1055-1063

Sireteanu R, Fronius M, Singer W (1981) Binocular interaction in the peripheral visual field of human squint and anisometropic amblyopes. *Vision Res*; **21**: 1065-1074

Sloper JJ, Headon MP, Powell TP (1984) Simultaneous hypertrophy of cells related to each eye in the lateral geniculate nucleus of the infant monkey following short-term reverse suture. *Brain Res*; **317**: 295-7

Smith EL, Yuzo M, Chino JN, Han Cheng, Crawford MLJ, Harwerth RS (1997) Residual binocular interactions in the striate cortex of monkeys reared with abnormal binocular vision. *Amer Physio Soc*; **May 21**: 1353-1362

Snider WD, Lichtman JW (1996) Are neurotrophins synaptotrophins? *Mol Cell Neurosci*. **7**: 433-442

Snyder A, Shapley R (1979) Deficits in the visual evoked potentials of cats as a result of visual deprivation. *Exp Brain Res*; **37**: 73-86

Song S, Miller KD, Abbott LF (2000) Competitive Hebbian learning through spike-timing-dependent synaptic plasticity. *Nat Neurosci*; **3**: 919-926

Speed HD, Morrone MC, Burr DC (1991) Effects of monocular deprivation on the development of visual inhibitory interactions in kittens. *Vis Neurosci*; **7**: 335-43

Spekeijse H, Wagner HG, Wolbarsht ML (1972) Spectral and spatial coding of ganglion cell responses in goldfish retina. *J Neurophysiol*; **1**: 73-86

Stellwagen D, Shatz CJ (2002) An instructive role for retinal waves in the development of retinogeniculate connectivity. *Neuron*; **33**: 357-67

Stent GS (1973) A physiological mechanism for Hebb's postulate of learning *Proc Natl Acad Sci USA* **70**: 977-1001

Stryker MP (1981) Late segregation of geniculate afferents to the cat's visual cortex after recovery from binocular impulse blockage. *Soc Neurosci*; **6**: 2117-2133

Stryker MP, Harris WA (1986) Binocular impulse blockade prevents the formation of ocular dominance columns in cat visual cortex. *J Neurosci*; **6**: 2117-2133

Sur M, Humphrey AL, Sherman SM (1982) Monocular deprivation affects X - and Y-cell retinogeniculate terminations in cats. *Nature*; **300**: 183-5.

Swindale NV (1980) A model for the formation of ocular dominance stripes
Proc. R. Soc. Lond; **208**: 243-264

Swindale NV (1981) Absence of ocular dominance patches in dark reared cats *Nature*
290: 332-333

Swindale NV, Vital-Durand F, Blakemore C (1981) Recovery from monocular deprivation in the monkey. III Reversal of anatomical effects in the visual cortex.
Proc. R. Soc; **213**: 453-450

Taha S, Hanover JL, Silva AJ, Stryker MP (2002) Autophosphorylation of alpha CaMKII is required for ocular dominance plasticity. *Neuron*; **36**:483-91

Theonen H (1995) Neurotrophins and neuronal plasticity. *Science*; **270**: 593-8

Thulborn KR, Waterton JC, Matthews PM, Radda GK (1982) Oxygenation dependence of the transverse relaxation time of water protons in whole blood at high field. *Biochim Biophys Acta*; **714**: 265-70

Tieman SB, Tumosa N (1983) 2-deoxyglucose demonstration of the organisation of ocular dominance in areas 17 and 18 of the normal cat. *Brain Res*; **267**: 35-46

Toga AW, Cannestra AF, Black KL (1995) The temporal/spatial evolution of optical signals in human cortex. *Cereb Cortex*; **5**: 561-5

Trachtenberg JT, Trepel C, Stryker MP (2000) Rapid extragranular plasticity in the absence of thalamocortical plasticity in the developing primary visual cortex. *Science*; **287**: 2029-32

Trachtenberg JT, Stryker MP (2001) Rapid anatomical plasticity of horizontal connections in the developing visual cortex. *J Neurosci*; **21**: 3476

Trepel C, Duffy KR, Pegado DV, Murphy KM (1998) Patchy distribution of NMDAR1 subunit immunoreactivity in developing visual cortex. *J Neurosci*; **18**: 3404-15

Ts'o DY, Frostig RD, Lieke EE, Grinvald A (1990) functional organisation of primate visual cortex revealed by high resolution optical imaging. *Science*; **249**: 417-420

Ts'o DY, Gilbert CD, Wiesel TN (1991) Orientation selectivity of and interactions between color and disparity subcompartments in area V2 of macaque. *Soc. Neurosci. Abstr*; **17**: 431(7) 1089

Ts'o DY, Roe AW, Shey J (1993) Functional connectivity within V1 and V2: Patterns and dynamics. *Soc Neurosci. Abstr*; **19**: 618(3) 1490

Turrigiano GG, Nelson SB (2004) Homeostatic plasticity in the developing nervous system. *Nature reviews Neurosci*; **5**: 97-107

Tusa RJ, Palmer LA, Rosenquist AC, (1978) The retinotopic organisation of area 17 (striate cortex) in the cat. *J Comp Neurol*; **177**: 213-35

van Ooyen A (2001) Competition in the development of nerve connections: a review of models. *Network*; **12**: R1-47

van Rossum MC, Bi GQ, Turrigiano GG (2000) Stable Hebbian learning from spike timing –dependent plasticity. *J Neurosci*; **20**: 8812-21

Van Sluyters RC (1978) Reversal of the physiological effects of brief periods of monocular deprivation in the kitten. *J Physiol*; **284**: 1-17

Van Sluyters RC, Levitt FB (1980), Experimental strabismus in kittens. *J Neurophysiol*; **43**: 686-697

Van Sluyters RC, Levitt FB (1983) Experimental strabismus in the kitten *J. Neurophysi*; **43**: 686-699

Von Bartheld CS, Byers MR, Williams R, Bothwell M (1996) Anterograde transport of neurotrophins and axodendritic transfer in the developing visual system. *Nature*; **379**: 803-833

Von Grunau MW, Singer W (1980) Functional amblyopia in kittens with unilateral exotropia II Correspondence between behavioural and electrophysiological assessment. *Exp brain Res*; **40**: 305-10

von der Malsburg C (1973) Self-organisation of orientation sensitive cells in the striate cortex. *Kybernetik*; **14**: 85-100

von der Malsburg CH, Willshaw DJ (1976) A mechanism for providing continuous neural mappings: Ocularity dominance stripes and ordered retino-tectal projections *Exp. Brain. Res.(suppl)*; **1**: 463-469

Von Noorden GK (1990) *Binocular vision and ocular motility* St Louis: CV Mosby

Wang G, Tanaka K, Tanifuji M (1994) Optical imaging of functional organization in macaque inferotemporal cortex. *Soc. Neurosc. Abst*; **20**: 138(10) 316

Wickelgren-Gordon B (1972) Some effects of visual deprivation on the cat superior colliculus. *Invest Ophthal*; **11**: 460-467

Wiesel TN, Hubel DH (1963) Single-cell responses in striate cortex in kittens deprived of vision in one eye. *J Neurophysiol*; **26**: 1003-1017

Wiesel TN, Hubel DH (1965) Extent of recovery from the effects of visual deprivation in kittens. *J Neurophysiol*; **28**: 1060-1072

b Wiesel TN, Hubel DH (1965) Comparison of the effects of unilateral and bilateral eye closure on cortical unit responses in kittens *J Neurophysiol*; **28**: 1029-1040

Weliky M, Katz LC (1999) Correlational structure of spontaneous neuronal activity in the developing lateral geniculate nucleus *in vivo*. *Science*; **285**: 599-604

Weliky M (2000) Correlated neuronal activity and visual cortical development *Neuron*; **27**: 427-30

Willshaw DJ, von der Malsburg (1976) How patterned neural connections can be set up by self-organisation. *Proc R Soc Lond B Biol Sci*; **194**: 431-45

Wong EH, Levi DM, McGraw PV (2001) Is second-order spatial loss in amblyopia explained by the loss of first-order spatial input? *Vis Res*; **41**: 2951-60

Woodruff G, Hiscox F, Thompson JR, Smith LK (1994) Factors affecting the outcome of children treated for amblyopia. *Eye*; **8**(pt 6): 627-31

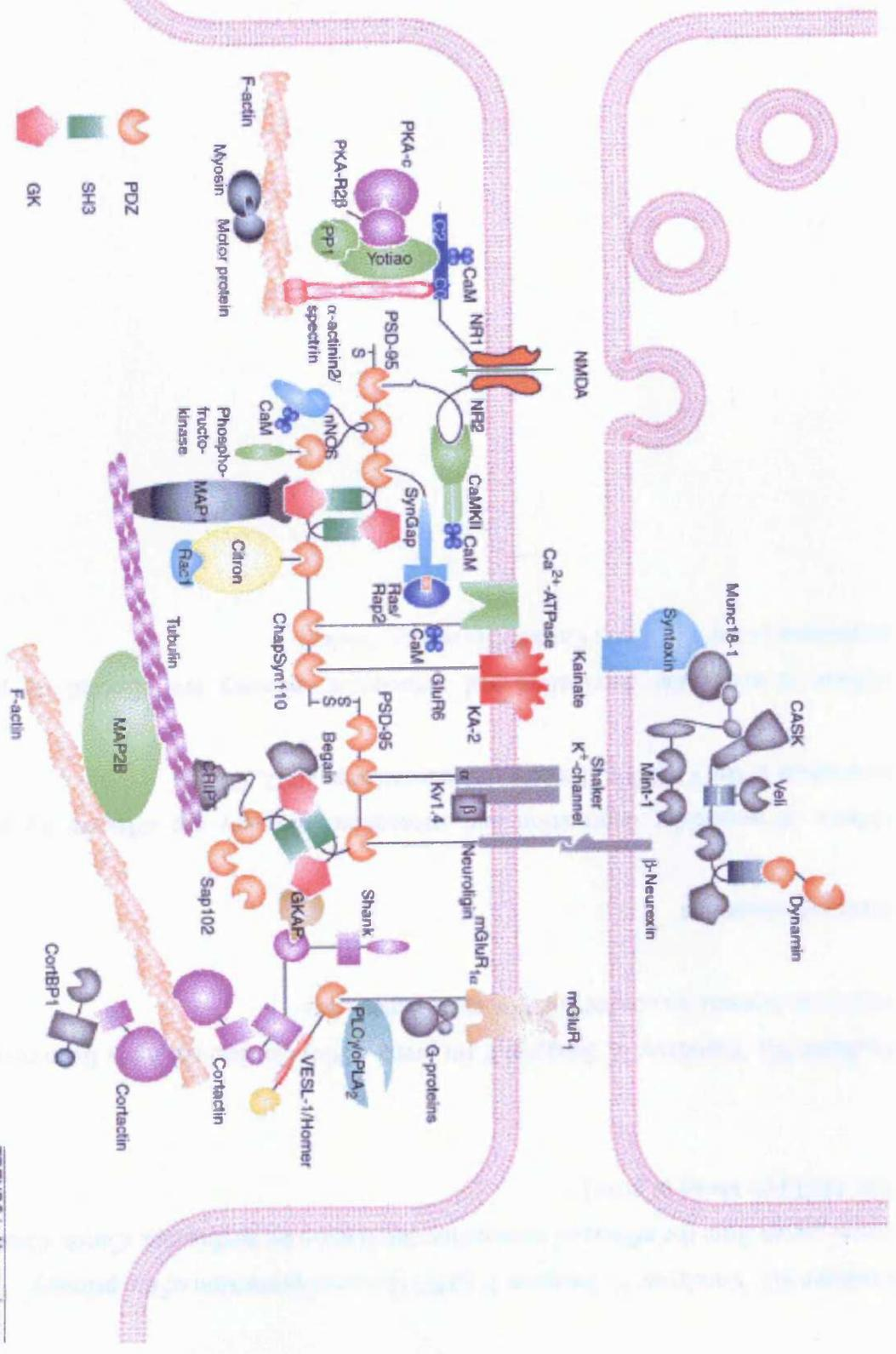
Woods RP, Cherry SR, Mazziotta JC (1992) Rapid automated algorithm for aligning and reslicing PET images. *J Comput Assist Tomogr*; **16**: 620-33

Yinon U, Auerbach E, Blank M, Friesenhausen J (1975) The ocular dominance of cortical neurons in cats developed with divergent and convergent squint. *Vis. Res*; **15**: 1251-1256

Yinon U (1976) Age dependence of the effect of squint on cells in kittens visual cortex. *Exp. Brain. Res* **26**: 151-157

Figure Ap II (i) Presumed assembly of proteins found in the NMDA receptor complex (From Husi and Grant 2001)

Abbreviations; CaM, calmodulin; CaMKII, calcium calmodulin kinase II; MAP, microtubule associated protein; mGluR, metabotropic glutamate receptor; nNOS, neuronal nitric oxidase synthase; NR1, NMDAR receptor subunit 1; PLA, phospholipase A; PLC phospholipase C; PKA, protein kinase A; PP1, proein phosphatase 1; PSD-95, post synaptic density 95.



PUBLICATIONS

Faulkner SD, Vorobyov V, Sengpiel F (2005) Limited protection of the primary visual cortex from the effects of monocular deprivation by strabismus, *Cereb. Cortex*, Feb 16 [Epub ahead of print]

Faulkner SD, Vorobyov V, Sengpiel F (in prep.- 2004) Cortical recovery from reverse occlusion depends on concordant binocular experience.

Oral presentations

Effects of monocular deprivation and subsequent recovery are effected by prior strabismus in cat V1 (2002) Society of Neuroscience 2002, Florida

Effects of monocular deprivation and subsequent recovery are effected by prior strabismus in cat V1 (2002) Cardiff University, Wales

